



Australian Government
Geoscience Australia

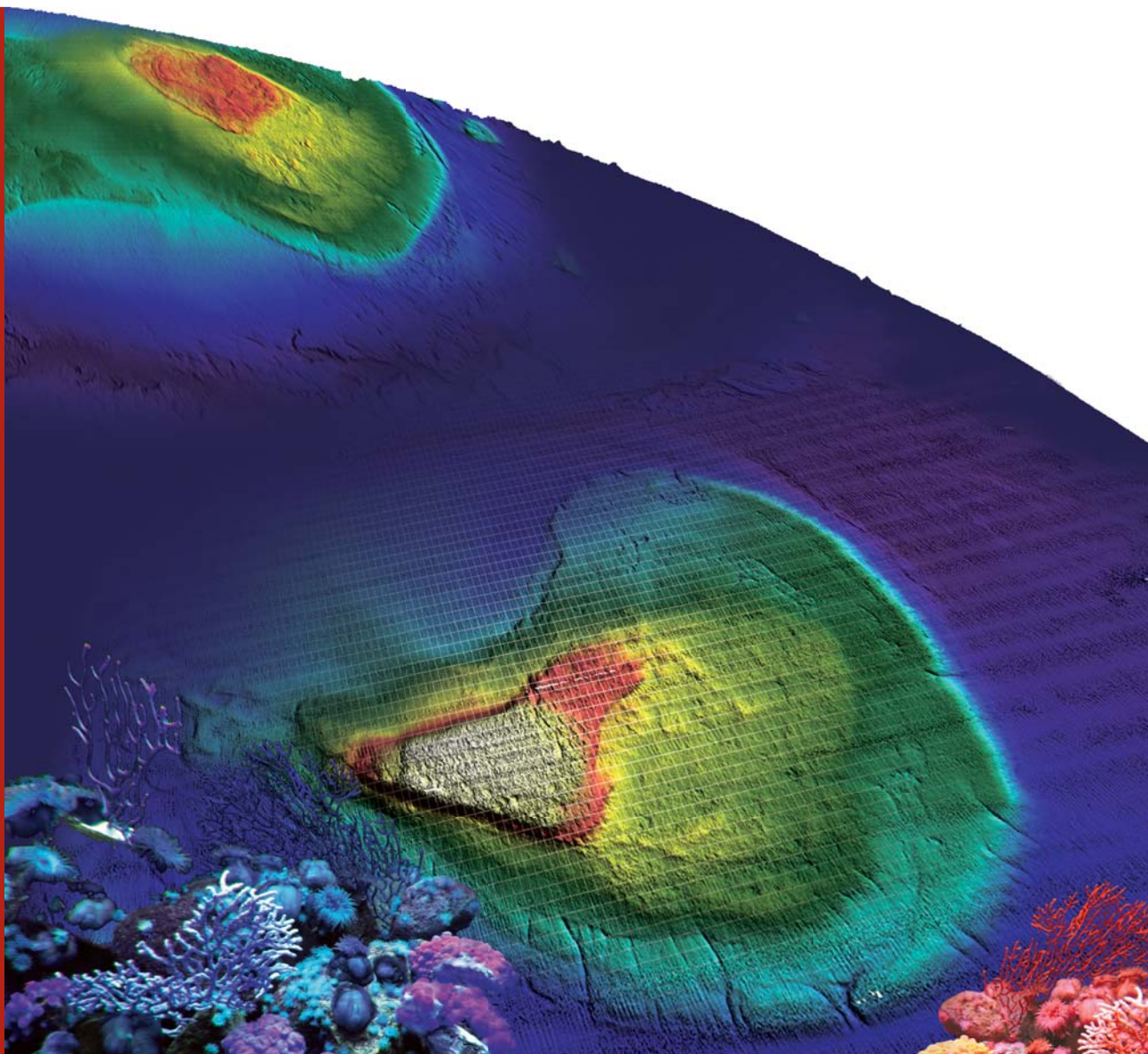
Submerged coral reefs and benthic habitats of the southern Gulf of Carpentaria:

Post-Survey Report - GA Survey 276, RV *Southern Surveyor*

*Peter T. Harris, Andrew Heap, John Marshall, Mark Hemer, James Daniell,
Alison Hancock, Cameron Buchanan, Laura Sbaffi, David Brewer, and Don Heales*

Record

2007/02



Submerged coral reefs and benthic habitats of the southern Gulf of Carpentaria: Post-Survey Report - GA Survey 276, RV *Southern Surveyor*

Geoscience Australia
Record 2007/02

by

Peter T. Harris¹, Andrew Heap¹, John Marshall¹, Mark Hemer¹, James Daniell¹, Alison Hancock¹, Cameron Buchanan¹, Laura Sbaffi¹, David Brewer², and Don Heales²

1. Marine and Coastal Environment Group, Geoscience Australia, GPO Box 378, Canberra ACT 2601
2. CSIRO Marine Laboratories, 233 Middle Road, Cleveland Qld 4163



Australian Government

Geoscience Australia

Department of Industry, Tourism & Resources

Minister for Industry, Tourism & Resources: The Hon. Ian Macfarlane, MP

Parliamentary Secretary: The Hon. Bob Baldwin, MP

Secretary: Mark Paterson

Geoscience Australia

Chief Executive Officer: Dr Neil Williams

© Commonwealth of Australia, 2007

This work is copyright. Apart from any fair dealings for the purpose of study, research, criticism, or review, as permitted under the *Copyright Act 1968*, no part may be reproduced by any process without written permission. Copyright is the responsibility of the Chief Executive Officer, Geoscience Australia. Requests and enquiries should be directed to the **Chief Executive Officer, Geoscience Australia, GPO Box 378 Canberra ACT 2601**.

Geoscience Australia has tried to make the information in this product as accurate as possible. However, it does not guarantee that the information is totally accurate or complete. Therefore, you should not solely rely on this information when making a commercial decision.

ISSN 1448-2177

ISBN 978-1-921236-12-9 (Hardcopy & CD-ROM)

ISBN 978-1-921236-11-2 (WEB)

GeoCat # 65073

Bibliographic reference: Harris, P.T., Heap, A., Marshall, J., Hemer, M., Daniell, J., Hancock, A., Buchanan, C., Brewer, D., Heales, D. (2006) Submerged coral reefs and benthic habitats of the southern Gulf of Carpentaria: Post-Survey Report GA Survey 276, RV Southern Surveyor. Geosciences Australia Record 2007/02, 134 pp.

Contents

Acknowledgements	vi
Executive Summary	vii
Chapter 1. Introduction.....	1
1.1 VOYAGE OBJECTIVES	3
1.2 VOYAGE TRACK	3
1.2.1 Sampling results.....	3
Chapter 2. Acoustic Data	5
2.1 MULTIBEAM SWATH SONAR RESULTS.....	5
2.1.1 Area A.....	8
2.1.2 Area B.....	8
2.1.3 Areas C and D.....	9
2.1.4 Area E.....	9
2.1.5 Area F.....	9
2.2 TOPAS SUB-BOTTOM PROFILER RESULTS	10
2.3 METHODS FOR DETERMINING ACOUSTIC FACIES	10
2.4 DESCRIPTIONS OF ECHO-TYPES AND CORRELATIONS WITH BATHYMETRY	12
2.4.1 Area A.....	12
2.4.2 Area B.....	14
2.4.3 Area C.....	15
2.4.4 Area D.....	17
2.4.5 Area E.....	17
2.4.6 Area F.....	17
Chapter 3. Meteorology and Oceanography	21
3.1 METEOROLOGY	21
3.1.1 Methods.....	21
3.1.2 Results.....	21
3.2 OCEANOGRAPHY	21
3.2.1 CTD Deployments	21
3.2.1.1 Water Mass Properties.....	21
3.2.1.2 Transmissometer Profiles of Suspended Sediments	24
3.2.1.3 Composition of material retained on the filter papers	27
3.2.2 Underway Data	29
3.2.3 Details of Mooring Deployments.....	29
3.2.4 Data Processing.....	33
3.2.5 Data Recovery.....	34
3.2.5.1 283/Stn6CM1 – BRUCE 1	34
3.2.5.2 283/Stn7CM2 & 276/Stn20CM3 – ADCP (Angus, son of BRUCE)	34
3.2.5.3 Stn3CM2 – BRUCE-2.....	34
3.2.6 Preliminary Data Analysis	34
3.2.6.1 Statistics	34
3.2.6.2 Sea Level.....	34
3.2.7 Currents.....	35
3.2.8 Bedload Transport Estimates	36
3.2.9 Results of Instrument Deployments	37
3.2.9.1 Statistics for Station 6CM1	37
3.2.9.2 Statistics for Station 21CM4	37
3.2.9.3 Statistics for Station 7CM2	37
3.2.10 Sea Level and Surface Wave Data	38
3.2.10.1 Station 1CM6	38

3.2.10.2 Station 21CM4	40
3.2.10.3 Station 7CM2	43
3.2.11 Current Measurements	46
3.2.11.1 Station 6CM1	46
3.2.11.2 Station 21CM4	50
3.2.11.3 Station 7CM2	53
3.2.12 Bedload Transport Estimates	59
3.2.12.1 Station 6CM1	59
3.2.12.2 Station 21CM4	59
3.2.12.3 Station 7CM2	59
Chapter 4. Underwater Drilling Results	63
4.1 INTRODUCTION	63
4.1.1 Description of the Underwater Drill	63
4.1.2 Core Descriptions and Logging	65
4.2 LITHOLOGICAL ANALYSIS OF DRILL CORES	65
4.2.1 Uranium-Series Ages	66
4.2.1.1 Analytical Methods	72
4.2.1.2 Uranium-series Dating Results	73
4.2.2 REEF R1	73
4.2.2.1 Core 276/01RD01	73
4.2.2.2 Core 276/02RD02	75
4.2.2.3 Core 276/03RD03	76
4.2.2.4 Core 276/10RD04	76
4.2.2.5 Core 276/11RD06	76
4.2.2.6 Core 276/12RD07	76
4.2.2.7 Discussion of Cores from Reef R1	77
4.2.3 REEF R2	77
4.2.3.1 Core 276/13RD08	77
4.2.3.2 Core 276/14RD09	79
4.2.4 REEF R3	80
4.2.4.1 Core 276/15RD11	81
4.2.4.2 Core 276/16RD12	81
4.2.4.3 Discussion – Reefs R2 & R3	81
4.2.5 REEF R4	81
4.2.5.1 Core 276/22RD14	83
4.2.5.2 Core 276/23RD15	83
4.2.5.3 Core 276/24RD16	84
4.2.5.4 Core 276/25RD17	84
4.2.5.5 Core 276/26RD18	84
4.2.5.6 Core 276/27RD19	85
4.2.5.7 Core 276/28RD20	85
4.2.5.8 Core 276/29RD21	85
4.2.5.9 Core 276/30RD22	85
4.2.5.10 Core 276/31RD23	86
4.2.5.11 Core 276/32RD24	86
4.2.5.12 Discussion – Reef R4	86
4.2.6 REEF R5	88
4.2.6.1 Core 276/50RD31	88
4.2.6.2 Core 276/52RD32	89
4.2.6.3 Core 276/53RD33	89
4.2.6.4 Core 276/57RD34	90
4.2.6.5 Core 276/58RD35	90
4.2.6.6 Core 276/59RD36	91
4.2.6.7 Core 276/60RD37	91
4.2.6.8 Core 276/61RD38	91
4.2.6.9 Core 276/62RD39	91
4.2.6.10 Core 276/63RD40	92
4.2.6.11 Core 276/65RD41	92

4.2.6.12 Core 276/67RD42	92
4.2.6.13 Core 276/68RD43	92
4.2.6.14 Discussion – Reef R5	92
4.2.7 Reef R6	94
4.2.7.1 Core 276/34RD26	94
4.2.7.2 Core 276/43RD27	94
4.2.8 Reef R7	95
4.2.8.1 Core 276/45RD28	95
4.2.8.2 Core 276/46RD29	96
4.2.8.3 Core 276/49RD30	97
4.3 DISCUSSION OF REEF DRILLING RESULTS	99
4.3.1 Hardground	99
4.3.2 Boundstone/Bafflestone	99
4.3.3 Solution Unconformity and Framework	100
4.4 BRYOMOL REEF – CORE 276/17RD13	102
Chapter 5. Biological description of submerged reefs and benthic habitats	104
5.1 INTRODUCTION	104
5.2 MATERIALS AND METHODS	104
5.2.1 Benthic sled	104
5.2.2 Underwater Video Camera	105
5.2.3 Sediment grab	106
5.3 PRELIMINARY RESULTS	107
5.3.1 Benthic Sled	107
5.3.2 Sediment grabs	108
5.3.3 Underwater Video	108
5.4 PROPOSED SAMPLE ANALYSES AND REPORTING	109
Chapter 6. Discussion	110
6.1 SUBMERGED CORAL REEFS IN NORTHERN AUSTRALIA	110
6.2 WATER DEPTHS OF SUBMERGED REEFS	111
6.3 FUTURE RESEARCH	112
References Cited	113
Appendix 1. Scientific Party	117
Appendix 2. List of stations and activities completed on Survey 276	118
Appendix 3. Voyage Narrative	127
Appendix 4. Drill Core Logs	133
Appendix 5. Photographs of Drill Cores	133
Appendix 6. Petrographic Descriptions	133
Appendix 7. Thin Section Photomicrographs	133
Appendix 8. Underwater Videos	133

Acknowledgements

The authors wish to thank Captain Ian Taylor and the crew of the RV *Southern Surveyor* for their assistance in collecting the data contained in this report. Thanks also to the staff in the Sedimentology laboratory at Geoscience Australia and to Prof. Malcolm McCulloch and the laboratory staff of the Research School of Earth Sciences, Australian National University, for their work on Uranium-Thorium dating of our drill-core samples. The report was improved by reviews of an earlier draft provided by Dr Lynda Radke and David Ryan. This report is published with permission of the Chief Executive Officer, Geoscience Australia.

Executive Summary

In 2003, Geoscience Australia discovered three large patch reefs in the southern Gulf of Carpentaria (GA Survey 238; SS-03/2004; Harris et al., 2004). The submerged platform reefs (R1, R2 and R3) are located east of Mornington Island and appear to have been formed when sea level was ~30 m below its present position, however as the ship did not come prepared with a drill-core sampler, the sub-surface composition of the reefs was not determined. The submerged platforms support live hard corals in many locations and their discovery raised the question of the possibility of widespread reef occurrence in that region. Survey 276 was designed to deliver some answers to these questions.

The current survey used rotary drilling of reefs R1, R2 and R3 which recovered coral material from 8 sites. Multibeam sonar bathymetry and rotary drill cores were collected over two sections (R4 and R5) of a large (>100 km long) submerged platform that extends westwards from Mornington Island. The platform exhibits a Karst erosion surface, exhibiting drainage and depressions with raised rims, overprinting relict reef-growth geomorphic features. Reef growth features include raised rims, spur and groove reef front and elevated back-reef mounds. Other platform reefs were mapped in the south-western Gulf (R6 and R7) and in the Arafura Sea (R8). Rotary drilling has confirmed the coral reef composition of these features.

Preliminary assessments of the recovered drill cores indicate that reef growth has persisted in the region for several glacial cycles, extending over at least the past 120,000 years. Dating of Holocene corals by the U/Th method demonstrates that a phase of rapid (1-2 m per kyr) reef growth occurred at most sites between 9 and 7 kyr before present, with zero or much reduced growth rates occurring after 7 kyr ago. Although coral growth occurs in many areas, the production of carbonate has not been sufficient to build the reef-tops upwards to the present sea level. The observations of live corals, but low carbonate production rates, are consistent with a “catch-up” reef growth pattern, in which the upper surfaces of the reefs are submerged 20 to 30 m below present sea level, with isolated local reef-tops having reached to within 18 m of the sea surface. An analysis of the hypsometry of the reef surfaces indicates that platform surfaces at all sites (R1 to R8) are confined to two narrow depth intervals, centred at 26.8 ± 1 m and 30.7 ± 0.3 m. The good correspondence of hypsometric peaks indicates regionally significant phases of carbonate deposition during a prolonged, Pleistocene sea level still stand.

This voyage has proved that the southern Gulf of Carpentaria contains a previously unknown major coral reef province in Australia. The reefs support locally diverse and luxuriant coral growth. From a management perspective, the slow rates of coral growth point to the need for protection of these reef systems because of their limited capacity to recover from natural or human-induced disturbances.

Chapter 1. Introduction

Coral reefs are best known in Australia from the Great Barrier Reef and Ningaloo Reef complexes in Queensland and Western Australia. Smaller reef complexes such as the Houtman Abrolhas Reefs in Western Australia (Collins et al., 1996) and Ashmore Reef on the North West Shelf, have been documented, but generally few modern coral reefs have been documented in Australia outside of these regions.

In 2003, scientists from Geoscience Australia discovered, mapped and sampled three platform reefs in the southern Gulf of Carpentaria (Harris et al., 2004; Fig. 1.1A). Based on their geomorphology, they are clearly reefal limestone platform reefs that appear to have been formed when sea level was ~30 m below its present position, such as are commonly found in the Great Barrier Reef (eg. Harris and Davies, 1989). Due to the 30 m depth of their platforms, these features may be classified as “submerged” reefs in the context of Macintyre (1972), since they appear to have established themselves in relation to pre-existing sea levels. The coral limestone buildups are underlain by acoustic basement features, which also exhibit positive relief as seen in sparker seismic profiles. Repeated submergence of these reefs during sea level oscillations through the Quaternary is apparently associated with coral growth and the deposition of carbonate, as indicated by the series of 3-4 lateral ridges that can be seen along the margin of platform reef R1 (Fig. 1.1B). The fact that these reefs support live hard corals in many locations is, furthermore, evidence of a “catch-up” growth strategy (in the context of Neuman and Macintyre, 1985) relative to post-glacial sea level rise. This growth strategy involves slow reef growth rates following submergence of the reef pedestal after sea level rise, and is in contrast to “keep-up” growth strategy where the rate of vertical reef growth is comparable to the rate of sea level rise.

The Carpentaria reefs have not been killed off by warm, or overly turbid, waters. A live specimen of *Turbinaria* (plate coral) was dredged from one station and live hard corals were also seen in underwater video at 7 other stations (Harris et al., 2004; Fig. 1.1B). Another platform located at 30m depth adjacent to the northern end of Mornington Island shows clear evidence of weathering, forming a distinctive pock-marked, Karst limestone bank. Weathered limestone cobbles dredged from this bank are composed of bryozoans and molluscs (a Bryomol reef; Fig. 1.1A). Hence, there exists a diversity of reef types present in the region, whose range and distribution can only be established by further seabed mapping and characterisation surveys.

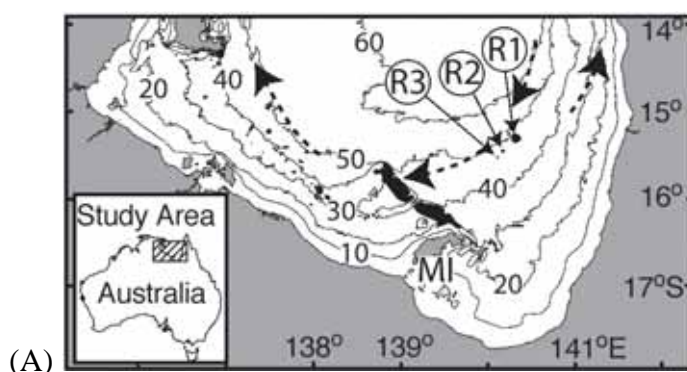


Figure 1.1 (A) Location map showing bathymetry of the Gulf of Carpentaria and the location of submerged reefs R1, R2 and R3 (from Harris et al., 2004). Arrows indicate the direction of residual water circulation during SE trade winds (Wolanski, 1993). Other submerged platforms, that may also be coral reefs, are shown in black. Note the large platform extending westward from Mornington Island (MI).

A recent study of benthic biota in the Gulf by Hill et al. (2002) combined historical datasets to predict the spatial distribution of species richness and some benthic community types as functions of physical variables. For many community types, variables such as average oxygen concentration, variability in oxygen concentration, variability in nitrate concentration, average temperature, and proportion of sand are important predictors of α -diversity, community structure and biomass indicating the potential importance of both geology and oceanography for an understanding of Gulf benthos.

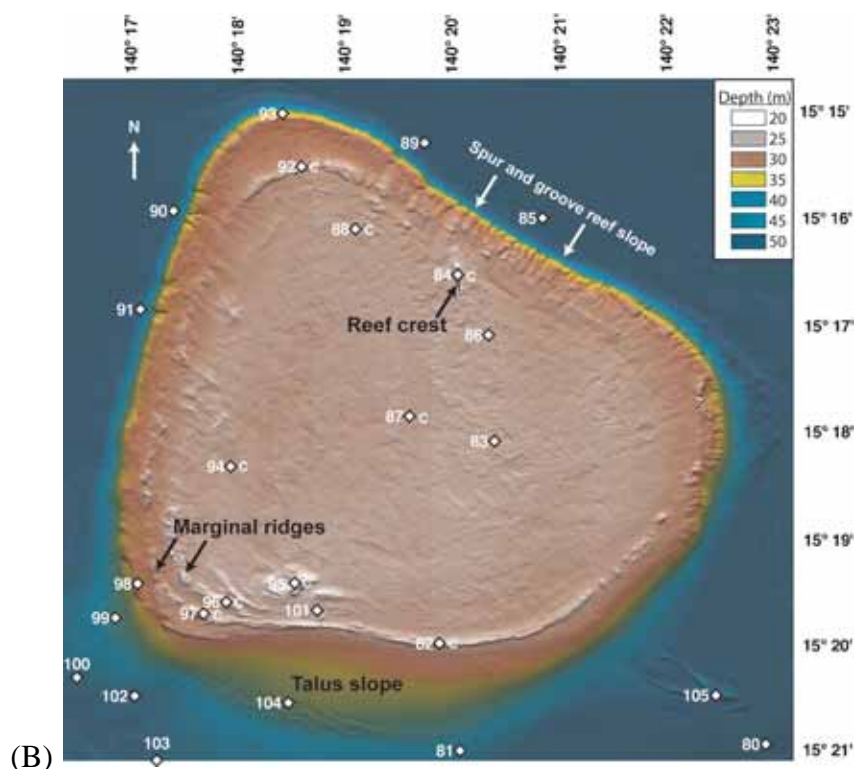


Figure 1.1 (B) Detailed colour bathymetry map of reef R1 (from Harris et al., 2004), showing typical patch reef geomorphology. Mapping was carried out using a Reson™ 240 kHz multibeam sonar system and data gridded at 10 m resolution. Survey lines were spaced at 100 to 150 m and adjusted according to water depth to provide 100% coverage at a ~3 m horizontal resolution. C indicates stations where live corals were seen using underwater video.

Much of our knowledge of the benthic fauna of the Gulf is derived from soft-bottom communities. However, many areas of rocky seabed (untrawlable grounds; Hill et al., 2002) are known to exist in the southern Gulf and based on the results of Survey 238, many of these rocky features may be submerged coral reef platforms (Fig. 1.1B). In Australia, there is a need for such studies of benthic habitats and major sedimentation processes for the purposes of regional marine planning, designing representative systems of marine protected areas, and marine environmental management. Hence, a primary goal of the survey was to identify and characterise rocky reef-type substrates, and their associated biological communities in the southern Gulf.

Throughout the late Quaternary, the Gulf of Carpentaria has been repeatedly submerged and exposed by fluctuating sea level (Fig. 1.2). During times of low sea-level, the Gulf contained a lake with an outlet channel to the Arafura Sea. When the Arafura sill (-55 m depth) was breached by rising sea level, the Gulf became a brackish to marine environment. Recent studies of the late-Quaternary history of the Gulf have shown that this repeated exposure and submergence has been recorded in the sediments, which show basin-wide sea-level/lake-level changes from evidence of sedimentology, foraminifers, ostracods, pollen, and geochemistry (Chivas et al., 2001). The newly discovered reefs provide a further sea level indicator, in

addition to the sill-depth of the Gulf, since radiometric dating of fossil corals will provide a constraint on times when sea level was at or above –30 m water depth. Hence, a further scientific objective of the proposed cruise will be to sample and date relict reefal sediments to attempt to provide more accurate indicators of past sea levels and their time of occurrence.

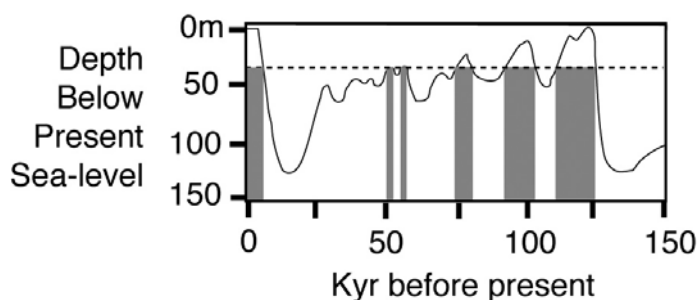


Figure 1.2. Global eustatic sea level curve for the past 150,000 years (after Chappell and Shackleton, 1986). Shaded areas mark the time intervals when sea level was <30 m (indicated by horizontal dashed line) below present position. This accounts for 28% of the past 150kys, when reefs could grow in the Gulf of Carpentaria at the depth ranges observed.

1.1 VOYAGE OBJECTIVES

The hypothesis we are testing is that “the growth of coral reefs has been widespread in the Gulf of Carpentaria throughout the late Quaternary, particularly when sea level was around 30 m below its present position, resulting in numerous submerged catch-up reefs in the southern Gulf”. The objectives of the survey were as follows:

1. To acquire drill core samples from suspected submerged coral reefs to confirm their coral composition and provide material suitable for radiometric dating
2. To collect multibeam sonar and sub-bottom profile information from other bathymetric mounds in the southern Gulf to ascertain their geomorphic nature
3. To collect biological samples and underwater video records of the seafloor in order to document the benthic communities and fauna associated with the submerged reef features; and
4. Collect data on water properties, currents and suspended sediments to document the modern reef habitats and their environments.

1.2 VOYAGE TRACK

GA Survey 276 started in Weipa on 23-03-05. The names of the science party and crew are listed in [Appendix 1](#). After testing of multibeam sonar equipment, the ship transited to the first drill sites on a submerged coral reef (R1 in [Fig. 1.1A](#)). Drilling continued on reefs R1, R2 and R3 before the ship sailed to a site located off the eastern side of Mornington Island ([Fig. 1.1A](#)). Drilling was completed on this site at 0700 hrs on Easter Sunday, 27th March (see Voyage Narrative, below, for a discussion of the daily activities). A further 6 areas were explored and investigated in the southern Gulf of Carpentaria and in the Arafura Sea (Areas A, B, C, D, E and F; see [Fig. 1.3](#)). Activities included recovery and deployment of current meters, multibeam swath mapping, underwater video, water column sampling and seafloor sampling. Different activities were carried out in specific study areas as described below. The ship arrived in Darwin on 13th April after 22 days at sea.

1.2.1 Sampling results

The sampling program completed operations at 72 stations. A full listing of all operations completed, with coordinates and water depths, is provided in [Appendix 2](#). A discussion of the

operations is provided in the Chief Scientists Narrative Log in [Appendix 3](#). Operations are summarised in Table 1.1

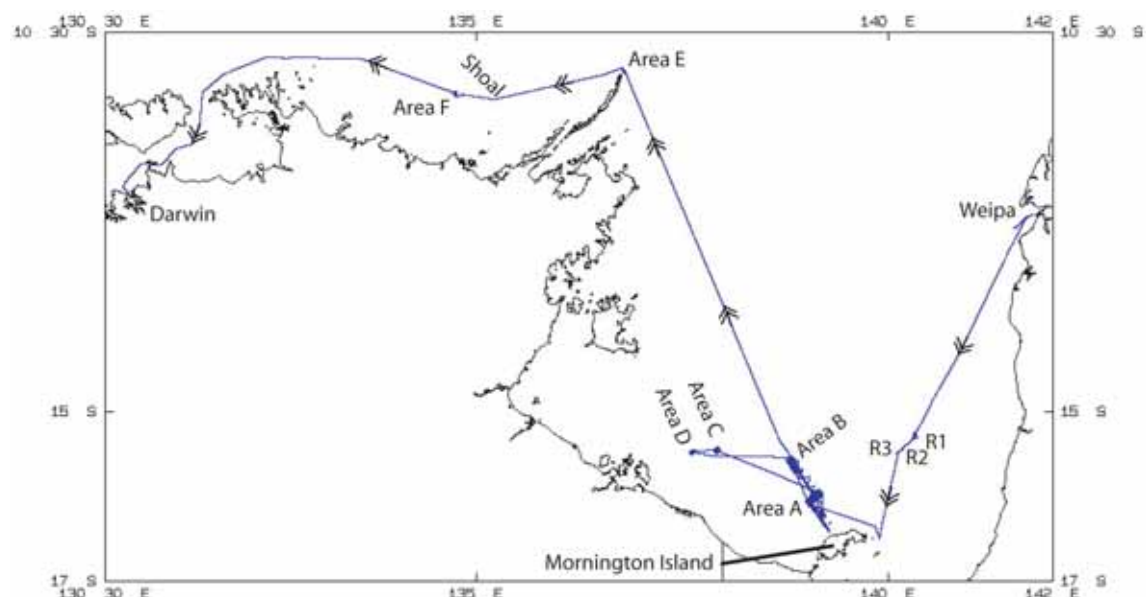


Figure 1.3 Track of the RV *Southern Surveyor* during GA survey 276 of the southern Gulf of Carpentaria. The total voyage track covered 6,925 km from Weipa to Darwin.

Table 1.1 Sampling operations completed on Survey 276.

67	Underwater cameras
43	Rotary Drill Cores
39.03	Metres of core
60	CTD's
120	Filter papers of surface and bottom water samples
43	Rock Dredges
63	Smith McIntyre Grabs

In addition to the operations summarised in Table 1.1, the BRUCE and ADCP instrument frames were successfully recovered at the start of the voyage, redeployed and then recovered again at the end of the voyage. Some highlights of the sampling results are described in the Chief Scientists Narrative ([Appendix 3](#)).

Chapter 2. Acoustic Data

2.1 MULTIBEAM SWATH SONAR RESULTS

Two multibeam sonar systems were used on the survey; the ship's Simrad EM-300 30 kHz system, plus a Reson 8101 240 kHz system. Although there were some initial problems with the Reson system, we eventually had both systems running in parallel. This has enabled some comparative studies of the two systems to be carried out which will be reported in detail in later post-survey reports. In general, the two systems provided good quality data in the 20-50 m depth range in which we were working. There is little difference apparent in bathymetry grids where a grid spacing of 5 to 10 m was used. At finer grid spacings (< 5 m), however, the higher frequency of the Reson system provided better resolution data in comparison with the EM-300, which tended to look a bit more "grainy" than the Reson data. For most mapping purposes, therefore, we conclude that the ship's EM-300 system will provide useful, good-quality products (especially at >10 m grid spacing) in shallow water conditions as encountered on this survey (i.e. in 20 to 50 m water depth).

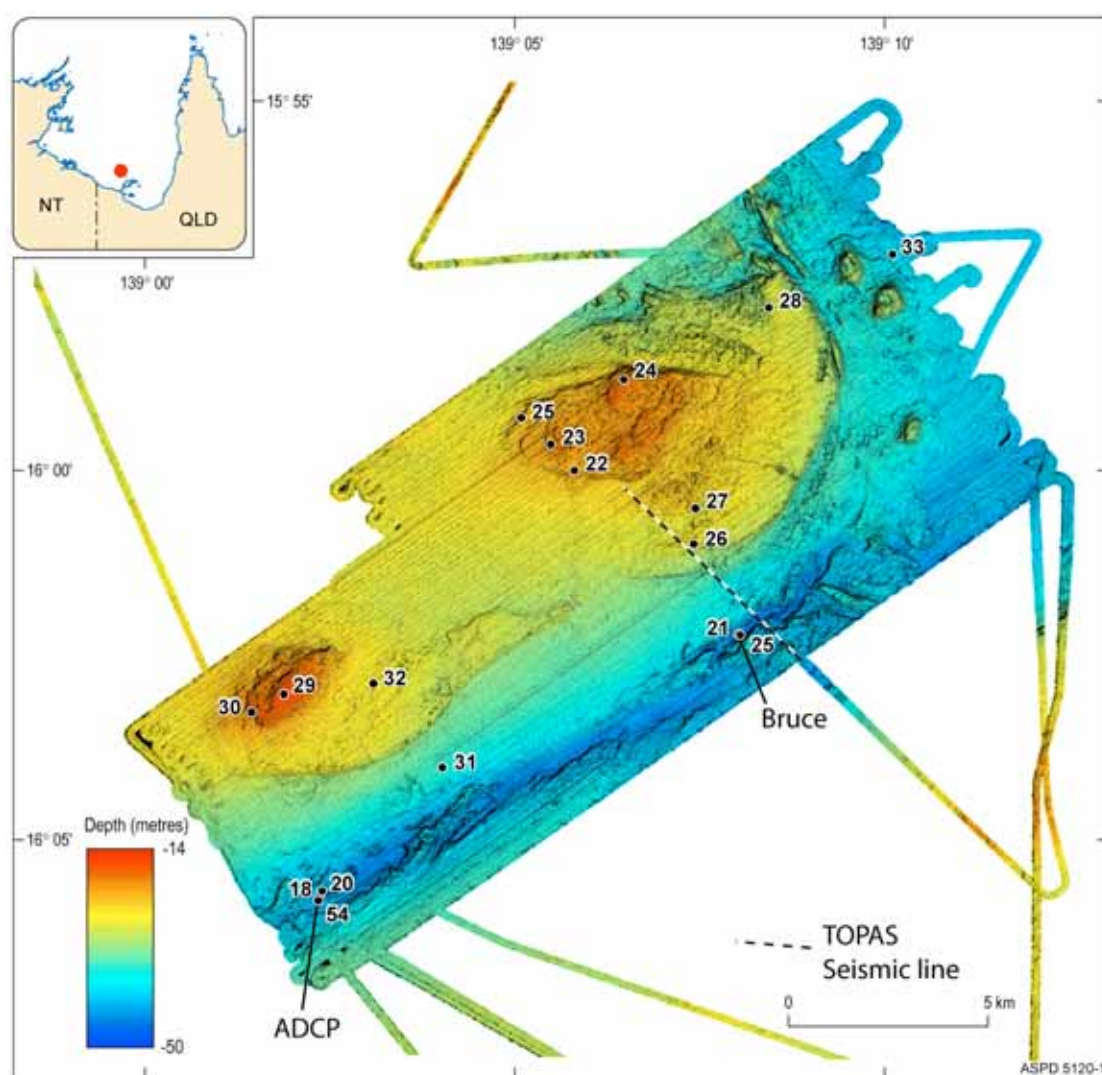


Figure 2.1. Bathymetric image of Area A, showing the locations of sample sites, the two current meters (ADCP and Bruce) and the location of a Topas seismic line shown in [Figure 2.6](#).

Multibeam surveys were carried out at 6 locations (Areas A, B, C, D, E and F). In general, the Topas sub-bottom profiler was run at the same time as the two swath mappers, so the line

km of data collected applies to both the multibeam and sub-bottom profiler data sets. A list of the separate survey areas with the line km of data collected in each area is listed in Table 2.1.

Table 2.1: Geophysical survey line kilometres completed on Survey 276.

Survey Area	Line km run	Figure No.
Area A	1540	2.1
Area B	1520	2.2
Area C	240	2.3
Area D	260	2.4
Area E	73	2.5
Area F	170	2.6

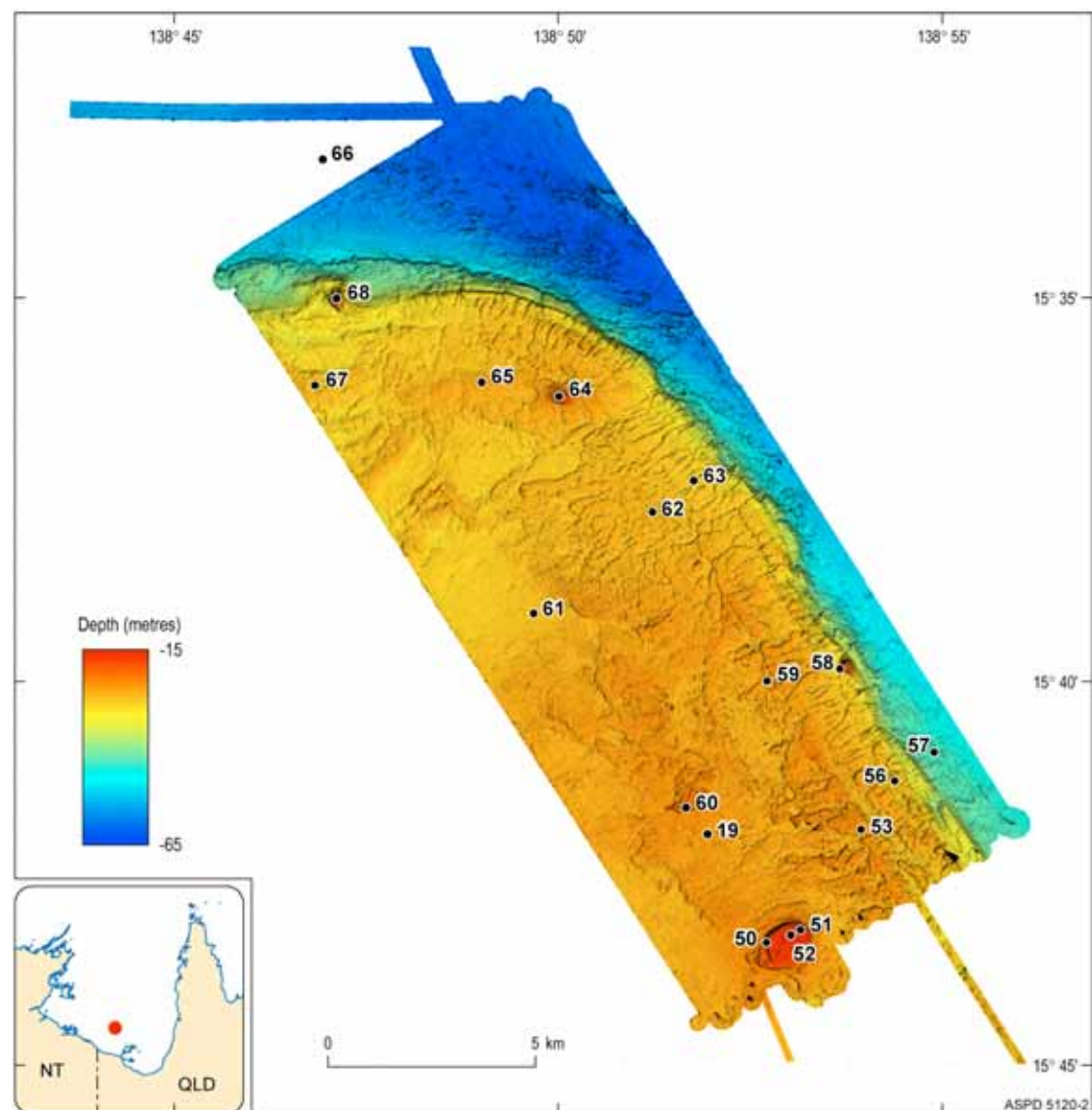


Figure 2.2. Bathymetric image of Area B, showing the locations of sample sites. The Bruce current meter was recovered at Station 19.

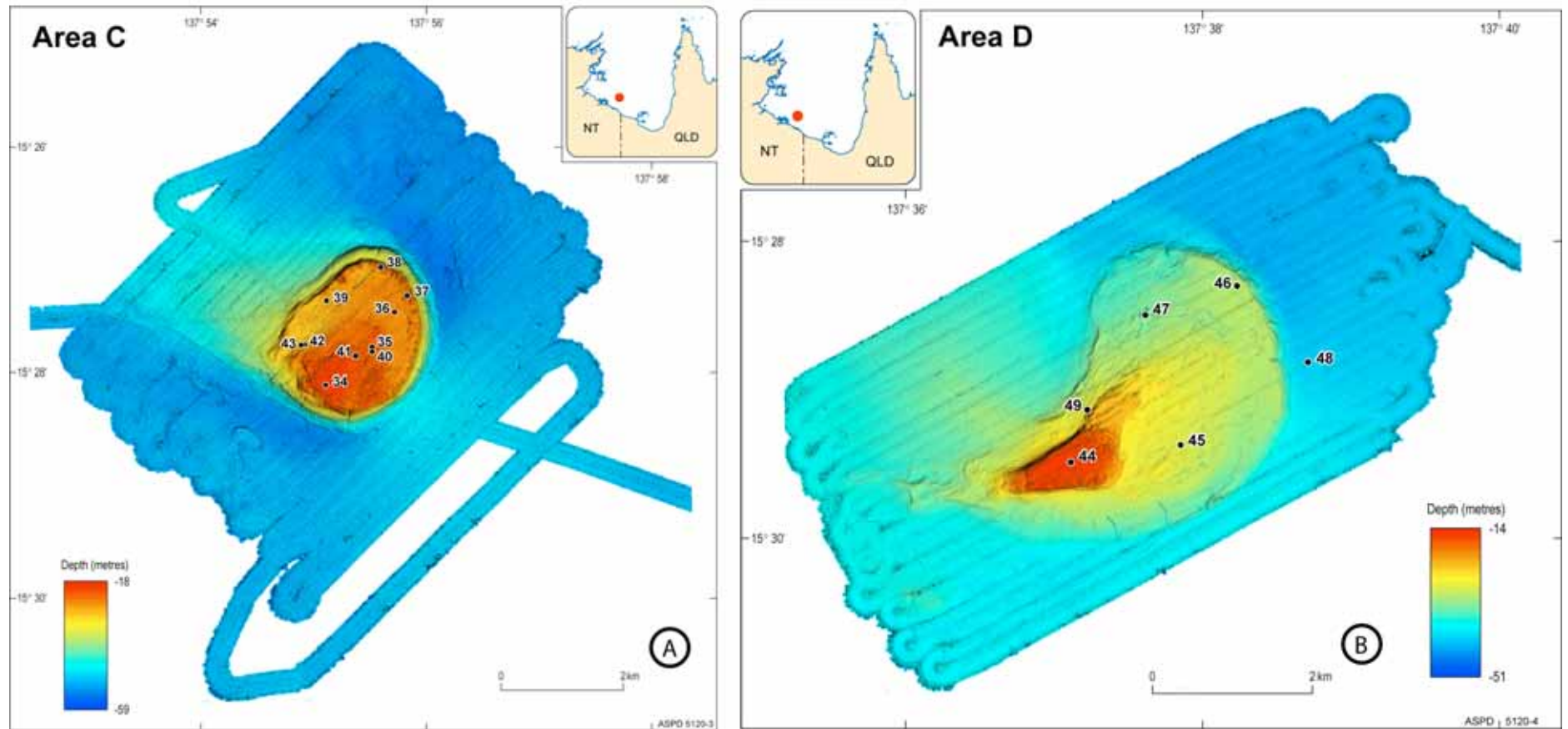


Figure 2.3. (A) Bathymetric image of Area C; and (B) Bathymetric image of Area D. The images show locations of sample sites. These two platform reefs both have sediment talus slopes extending to the WNW, streaming away from their leeward sides. Transport of sediment off the reef flats and onto these talus slopes is most likely to be the result of tropical cyclones.

2.1.1 Area A

Area A is the south-eastern end of the elongate platform that extends north-westwards from Mornington Island. Area A includes the locations of the two re-deployed current meters (ADCP and Bruce; Fig. 2.1). The area is characterised by elongate ridges, spur and groove platform margins and Karst doline features. The adjacent channel exhibits localised depressions that appear to have been formed by local tidal currents. The overall appearance is of widespread erosion and the features all appear rounded and muted, in comparison with the previously-mapped platform reefs (Fig. 2.1). This reef platform is referred to as Reef R4 elsewhere in this report.

2.1.2 Area B

Area B includes the north-western end of the same elongate platform that extends north-westwards from Mornington Island. This reef platform is referred to as Reef R5 elsewhere in this report. It is also characterised by elongate ridges forming an oval-shaped rim along the platform margin, spur and groove incision into the platform margins and Karst doline and fluvial-erosion features. Four areas of active reef growth have formed dome-shaped reefs that rise up to within <20 m of the sea surface (red spots on Fig. 2.2). The largest of these is nearly 1 km in diameter and is located on the southern edge of the mapped area (Fig. 2.2). The Bruce current meter frame was moored on the southern edge of this site.

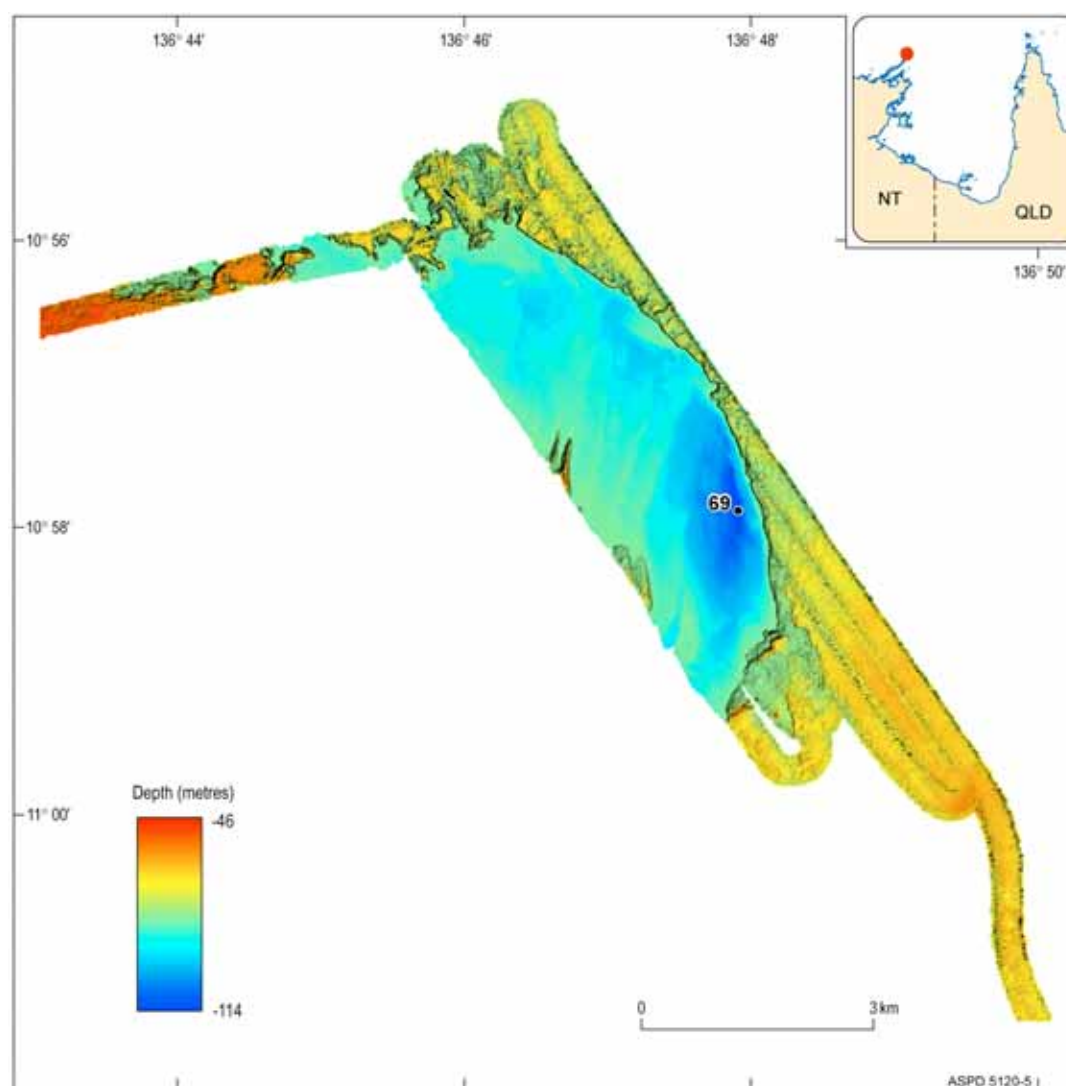


Figure 2.4. Bathymetric image of Area E, showing the locations of sample site 69. At 114 m water depth, this site is the deepest location in the Gulf of Carpentaria surveyed to date.

2.1.3 Areas C and D

Areas C and D are both small platform reefs located 200 km to the west of Mornington Island. They are two of approximately 50 such bathymetric banks that occur in this region of the Gulf. Their reef-geomorphology and character is exhibited by the occurrence of spur and groove margins, raised rim, central platform with localised reef build-up and karst erosion features (Fig. 2.3A and B). These reef platforms are referred to as Reefs R6 and R7 elsewhere in this report.

2.1.4 Area E

Area E is a tidally-scoured depression on the seafloor located directly north of Cape Wessel, at the northern end of the Wessel Islands (Fig. 2.4). Tidal scour is suggested by the closed bathymetric contours and the curved shape of the depression which is aligned with the main orientation of tidal flow across the area. The depression is up to 114 m in water depth, and it is therefore the deepest point within the Gulf of Carpentaria. Biologically, its significance may be as the home to a population of hammerhead sharks, although none were seen in our underwater video records from the area.

2.1.5 Area F

Area F is another small platform reef; it was one of two bathymetric shoals that can be seen in the nautical charts for this area. One of the shoals turned out not to exist at the indicated location. The presence of this second reefal shoal (Fig. 2.5) is significant because it points to the prospect of others like it existing in the Arafura Sea region. A recent analysis of geomorphic features on the Australian continental margin (Harris et al., 2003) identified several banks and rocky pinnacles in the area – our identification of a submerged reef in this area points to the possibility that some or all of these other bathymetric features may be submerged coral reefs.

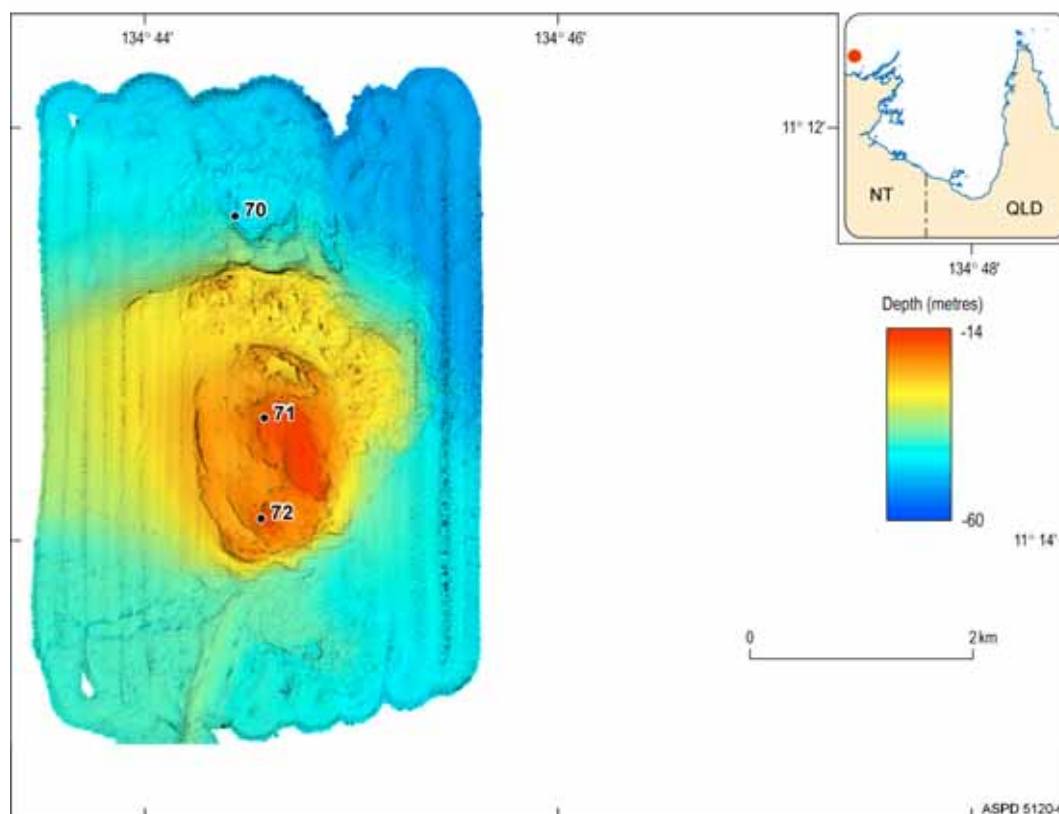


Figure 2.5. Bathymetric image of Area F, showing the locations of sample sites. Note the sediment talus slope extending to the west, streaming away from the leeward side of the reef.

2.2 TOPAS SUB-BOTTOM PROFILER RESULTS

As noted above, the Topas sub-bottom profiler was run throughout the voyage at the same time as the multibeam sonar; hence these two data sets are complementary. The Topas system gave good results in the shallow waters of the survey areas and was operated in Ricker mode at all times. There was no occurrence of interference between the Topas and either of the two multibeam systems being operated.

Sub-bottom profiler results were mixed: excellent results were obtained in areas of soft sediment deposits on the seafloor surrounding the reef platforms. In particular, images from talus slope deposits located on the flanks of all platform reefs that we examined were collected by the Topas system (talus slope deposits are also apparent in the multibeam images; [Figs 1.1B](#), [2.3A](#), [2.3B](#) and [2.5](#)). Good penetration was also obtained from some of the relict fluvial, cut and fill deposits that were mapped in Area A ([Fig. 2.6](#)).

In contrast, the limestone reef surfaces were acoustically opaque to the frequency and power of the Topas system and minimal sub-surface information was obtained (eg. [Fig. 2.6](#)). The main reef platform in Area A was also subjected to seismic profiling using a towed sparker system, but again the results did not yield sub-surface information. The lack of any sub-surface information being represented in the seismic data could be explained by either massive bedding within reefs and/or low seismic penetration associated with hard-reflective upper surfaces to the reef features.

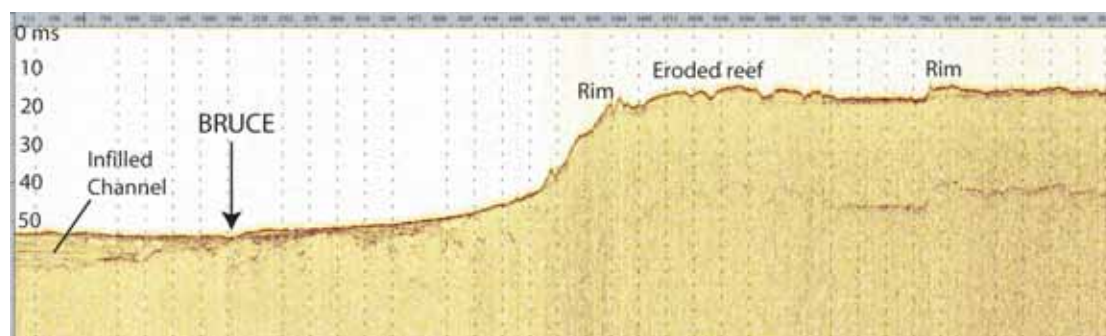


Figure 2.6. Example of Topas sub-bottom profile data collected across a reef and submarine valley in Area A (see [Fig. 2.1](#) for location of the line). The location of the BRUCE current meter site is indicated.

2.3 METHODS FOR DETERMINING ACOUSTIC FACIES

Acoustic facies mapping was undertaken for areas A, B, C, D, E and F. The acoustic response of the surface sediments recorded by the Topas sub-bottom profiler (echo-sounder) was interpreted based on Damuth (1980) classification schemes. The resultant acoustic map layer is available to ground truth against data collected in the area.

Echo-sounders and sub-bottom profilers were developed primarily to measure water depth and image the sub-surface structure of the seabed, respectively. However, these instruments can additionally provide data on changes in seafloor reflectivity (relative hardness of the bottom) and topography (relative bed roughness). Depending on the stratum type and the weather conditions sub-bottom profilers can penetrate and return an image of the sub-stratum up to around 100 m below the seafloor. However, more commonly substrata depths of tens of metres are imaged. Different echo-characters form through the interaction between ocean bottom and echo-pulse. Seafloor geology affects the echo-returns by the type, layering, structure and topography. Additional information such as sediment samples are needed to define the echo-types in terms of regional sedimentary and geological processes.

Acoustic remote sensing of the seafloor is a particularly useful mapping technique in sensitive benthic environments such as coral reefs because the technique is non-destructive (has no known impact on biota). Acoustic mapping is a convenient technique for areas with existing

data, which has been routinely, collected on ships echo-sounders. With careful groundtruthing and comparison with other data types, acoustic facies may be used as a proxy for seafloor geology. It provides an additional thematic layer to be used in conjunction with other datasets in regional marine planning.

Damuth (1980) developed a classification system for paper-based 12 and 3.5 kHz echograms. Survey 276 collected digital records, which were interpreted on-screen using the same visual descriptive methods. Damuth classified seafloor echo-character based on parameters of clarity, continuity of echo and seafloor morphology ([Table 2.2](#)).

Type I – distinct echoes

Type II – indistinct – prolonged

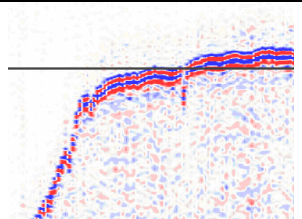
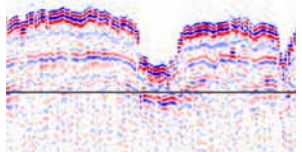
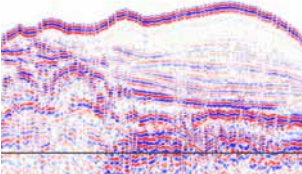
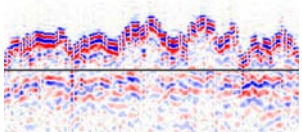
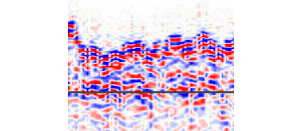
Type III – indistinct – hyperbolae

These were further sub-divided based on presence/absence of sub-bottom reflectors, extent of prolongation and relationship of hyperbolae to the seafloor. Type III echo-characters were not identified from this survey.

A Topas PS18 parametric sub-bottom profiler was used to collect data on survey 276. The Topas system is designed for high spatial resolution sub-bottom profiling. A difference frequency signal generated by two high frequency signals centred on 18 kHz is used by the system. Topas sub-bottom profilers are capable of subsurface penetration of more than 150 m in water depths of 1000 m with a range resolution of 30 cm or more depending on substrate type. Penetration performance is dependant on sediment character, water depth and transmitted signature.

Echo characteristics were identified along sub-bottom profiler lines, their positions noted and the information was recorded in an Excel spreadsheet. The profiles were viewed from SEG Y format using the software SeisVu (Areas A & B) and SeiSee (Areas C, D, E & F). The information was then transferred from the Excel spreadsheet to line coverages in ArcInfo, which were mapped spatially using ArcView and ArcGis. Polygons were projected around the line based interpretation with reference to the swath bathymetry images.

Table 2.2. Five echo-type classifications (after Damuth, 1980), with descriptions and examples from the Gulf of Carpentaria.

Type	Classification	Description	Example
IA	Distinct	Sharp, continuous echo with no sub-bottom reflectors - single seafloor reflector (SR)	
IB	Distinct	Sharp, continuous parallel sub-bottom reflectors (SBR)	
IC	Distinct	Sharp, continuous with non-conformable sub-bottom reflectors	
IIA	Indistinct – prolonged	Semi-prolonged with intermittent sub-bottom reflectors	
IIB	Indistinct – prolonged	No sub-bottom reflectors	

2.4 DESCRIPTIONS OF ECHO-TYPES AND CORRELATIONS WITH BATHYMETRY

2.4.1 Area A

The acoustic facies mapped across area A correlated with the complex and variable bathymetry imaged by the swath (Figure 2.7). As shown in Figure 2.7, type IC was the most dominant echo-type mapped covering around $\frac{2}{3}$ of the area. Type IA covers around $\frac{1}{4}$ of the area. Types IIA and IIB occur in minor areas, with type IB covering very minor patches of type IB. Echo-types with sub-bottom reflectors (SBR), IC, IIA and IB, covered of the area (Fig. 2.8). Bathymetric highs to some extent correlated with type IA. A clear boundary was mapped on the eastern edge of a bathymetric high in the central north. Three small bathymetric highs in the north east also correlated with type IA. Further correlations between bathymetry and acoustic facies were difficult to determine.

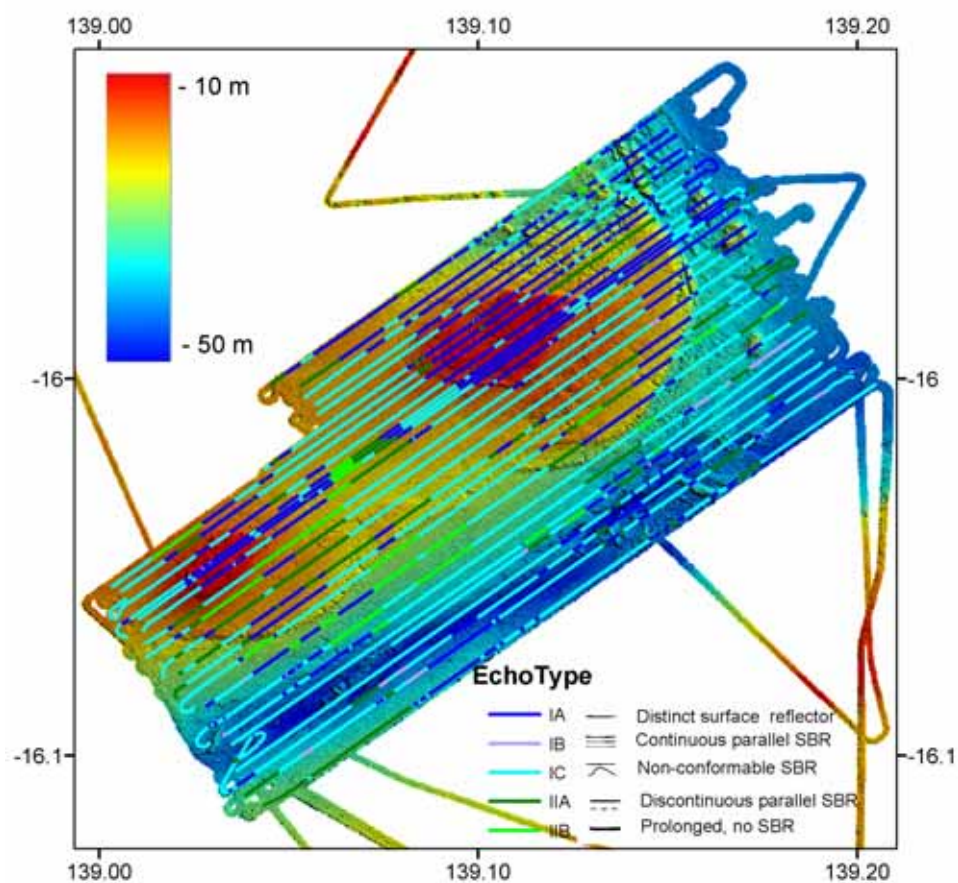


Fig 2.7. Area A, echo-type mapped along line displayed with bathymetric imagery.

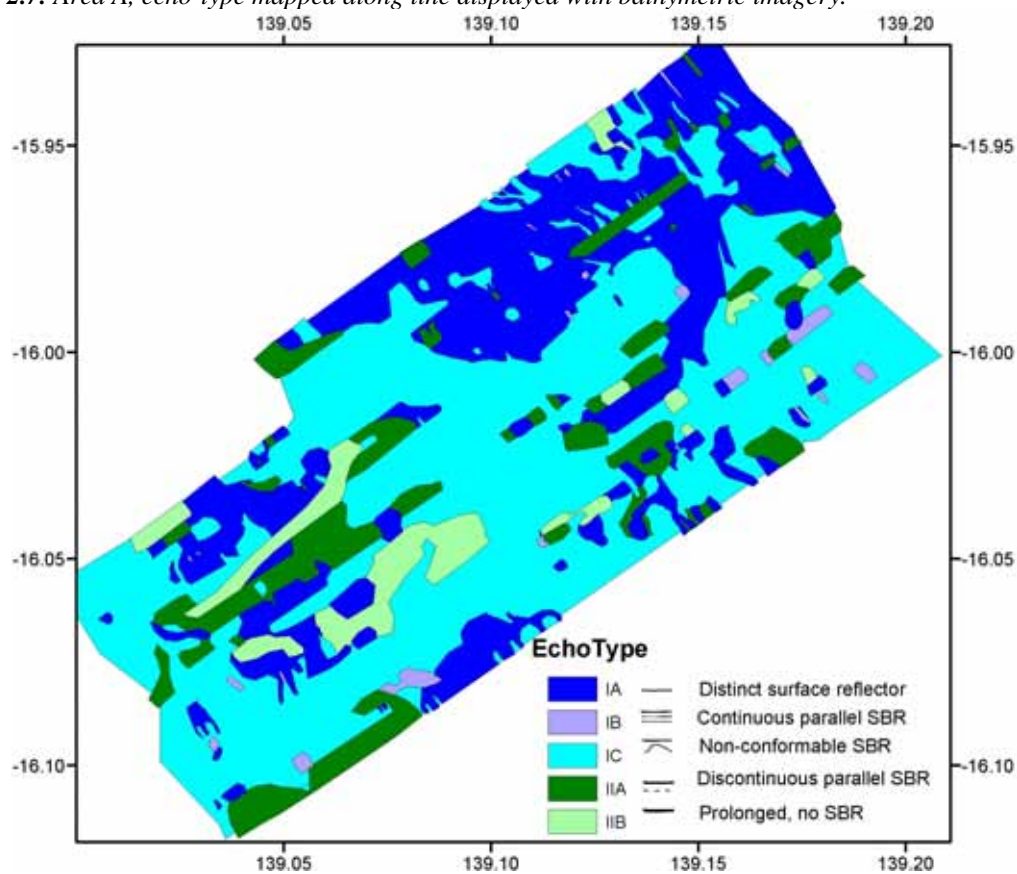


Fig 2.8. Area A, echo-type polygons map.

2.4.2 Area B

Acoustic facies mapped in Area B were variable and complex across the broad north-west trending bathymetric high that covered most of area B (Fig. 2.9). Type IC covered 1/3 of the area and types IA and IIA of the area each (Fig. 2.10). Minor areas of types IB and IIB were mapped. No clear correlations between bathymetry and echo-type were determined. Exceptions include a small bathymetric high in the south and central north that correlated with type IA. Figure 2.10 shows that echo-types with SBR were dominant. Echo types with a single seafloor reflector (SR), IA, covered 1/4 of the area in patches to the west and east. Prolonged echo-types, IIB, were only present in minor areas.

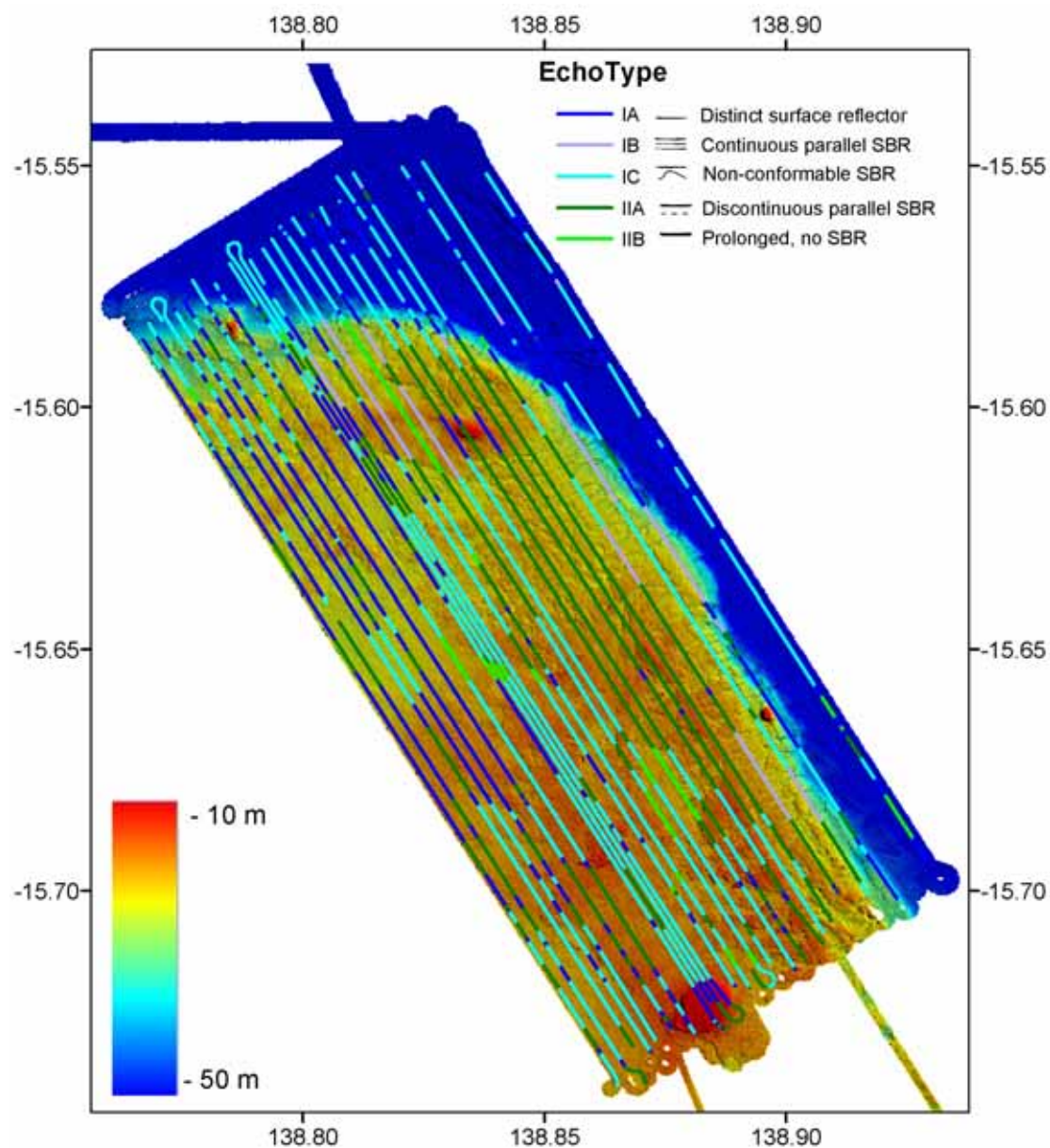


Fig. 2.9. Area B, echo-type mapped along line displayed with bathymetric imagery.

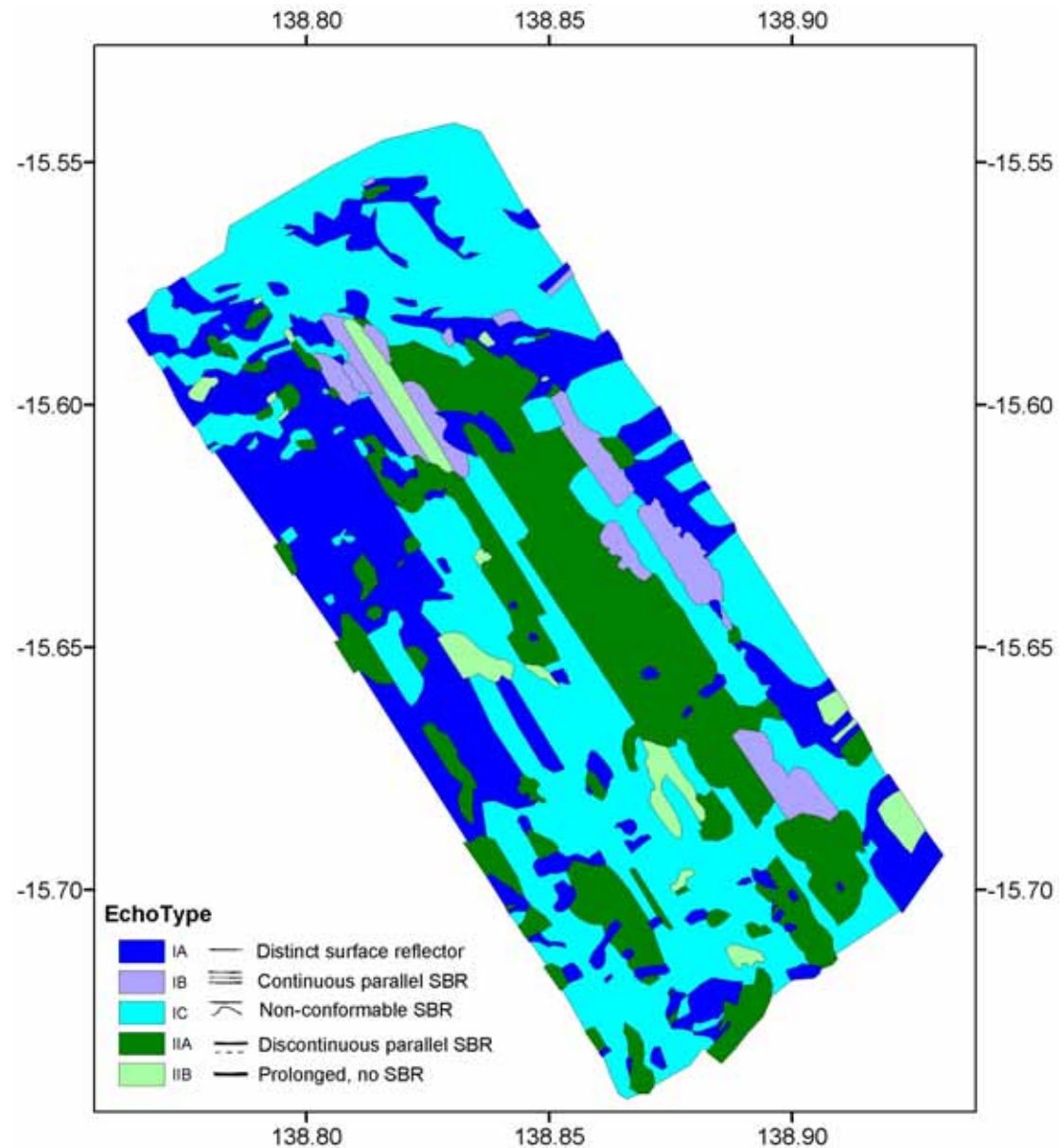


Fig. 2.10. Area B, echo-type polygons map.

2.4.3 Area C

Area C was a simple area comprised of a single circular bathymetric high. As shown in [Figure 2.11](#), the central bathymetric high platform correlated with echo-type IIB. The surrounding slope correlated with type IA and the deeper areas correlated with type IC. The prolonged echo types were found on top of the bathymetric high, whereas types with a single seafloor reflector were found on the slope. Types with sub-bottom reflectors were found in the deeper surrounds ([Fig. 2.12](#)).

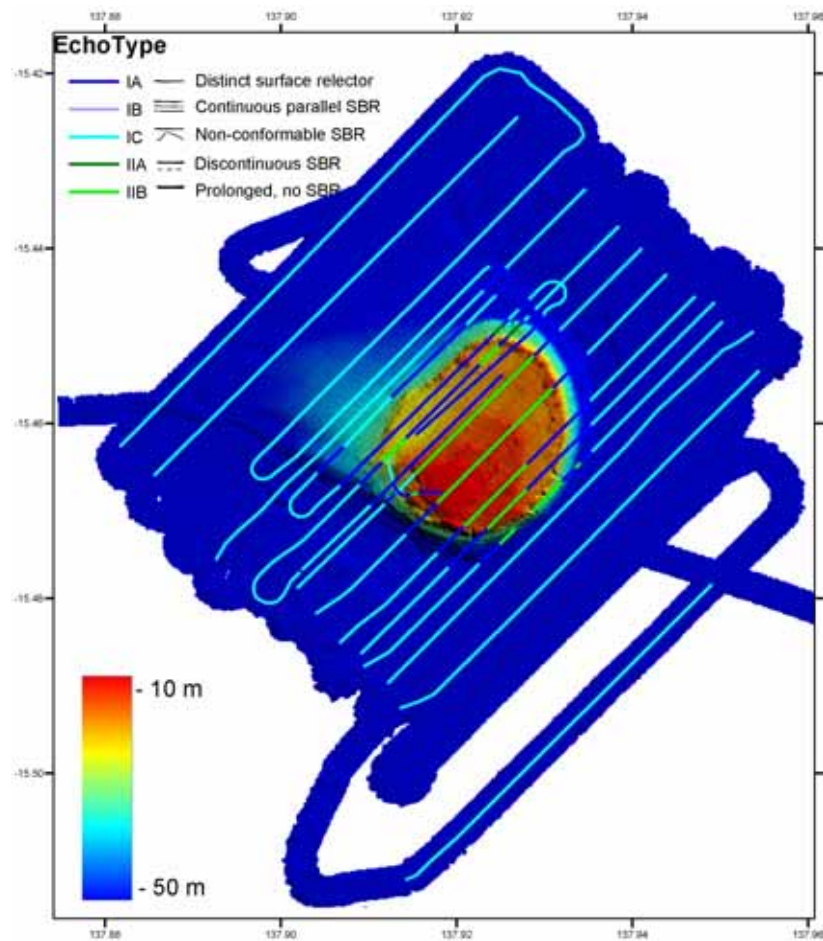


Fig. 2.11. Area C, echo-type mapped along line displayed with bathymetric Imagery.

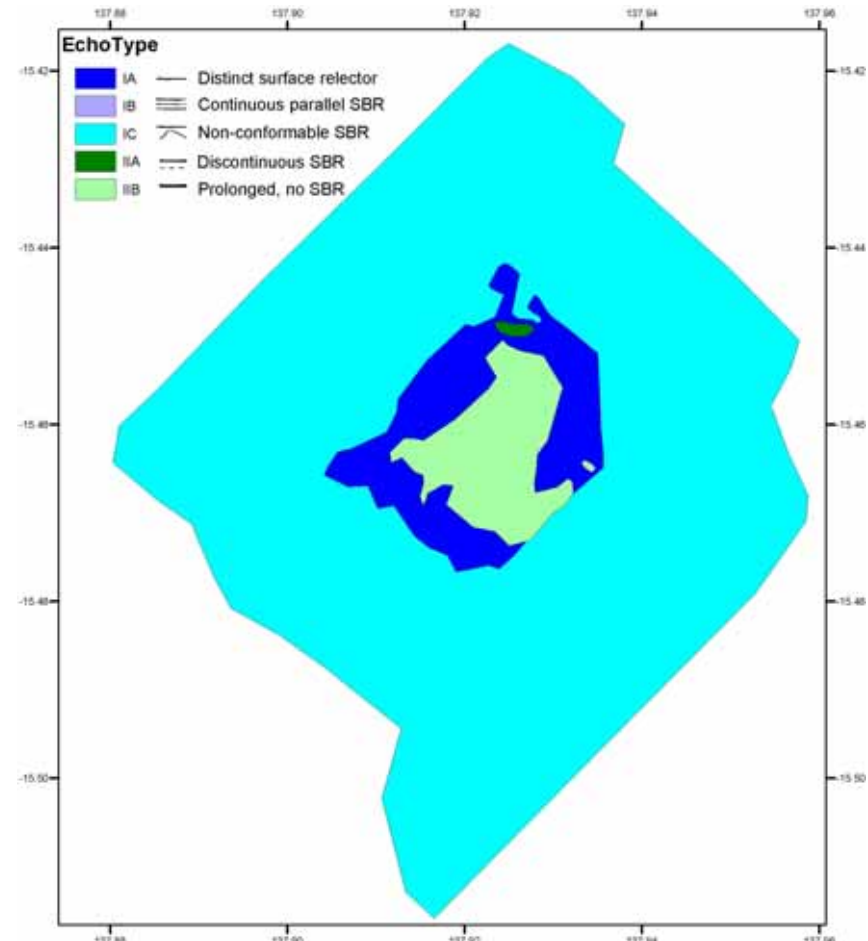


Fig 2.12. Area C, echo-type polygons map.

2.4.4 Area D

Area D is an elongated northeast southwest trending bathymetric high with a broad eastern terrace. [Figure 2.13](#) shows that echo type IA correlated with the bathymetric high and slope, covering about 1/3 of the area. Type IC was found both on the deeper surrounding area, on the slope to the west, the terrace to the east. Type IC represented about 2/3 of the area. Minor areas of types IIA and IIB were mapped. Echo-types with sub-bottom reflectors occurred both in the deeper areas and an area on the western terrace. Echo-types with a single seafloor reflector were mapped on the slope, high and two areas to the northeast ([Fig. 2.14](#)).

2.4.5 Area E

Area E is a rugged, elongate bathymetric depression, with a steep northern wall and elongate gullies leading to the east and west out of the depression. [Figure 2.15](#) shows that type IC (a SBR echo-type) was mapped predominantly in the south east with patches to the north, covering about 1/3 of the area. Type IA (a SR echo-type) was mapped to the north with a smaller patch to the south, covering in total about 2/3 of the area ([Fig. 2.16](#)). A minor patch of IIB (a prolonged echo-type) was mapped in the centre of the area. In general correlations were difficult to determine between bathymetry and acoustic facies. Although some edge boundaries were obvious, for example in the south the boundary between IC and IA correlates with a sharp bathymetry boundary.

2.4.6 Area F

Area F is a single circular bathymetric high with a rugged terrace to the north east and a broad slope to the west. [Figure 2.17](#) shows echo-type IC (a SBR echo-type) covered 2/3 of the area. This correlated to the deeper surrounding bathymetry and western slope and two areas on the central bathymetric high. Type IA (a SR echo-type), covered 1/3 of the area and was mapped on the bathymetric high, north eastern terrace and a deeper area to the south west ([Fig. 2.18](#)).

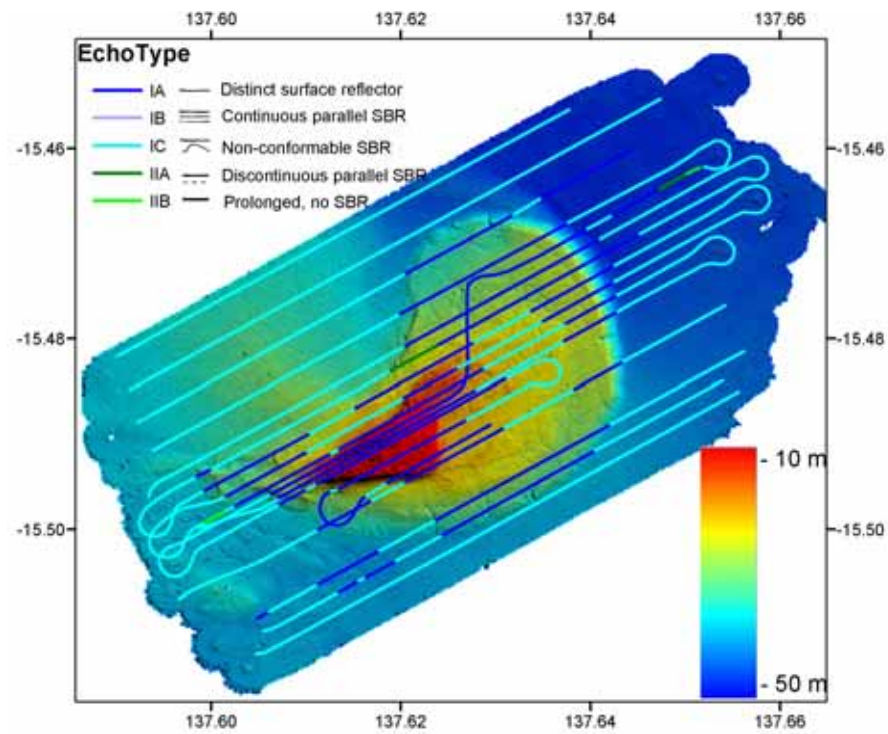


Fig. 2.13. Area D echo-type mapped along line displayed with bathymetric imagery.

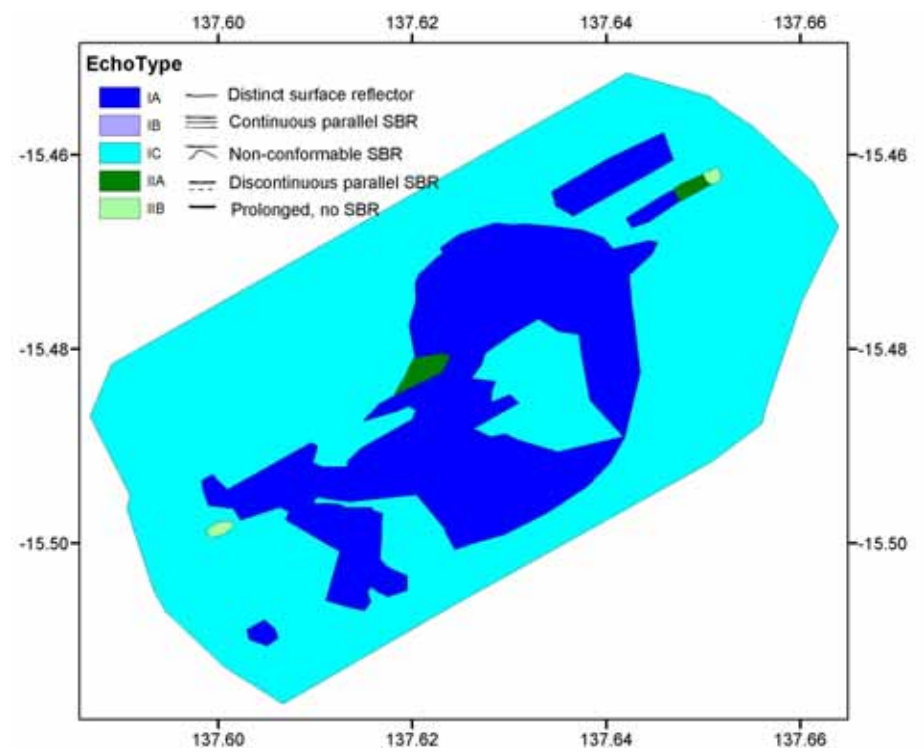


Fig. 2.14. Area D, echo-type polygons map.

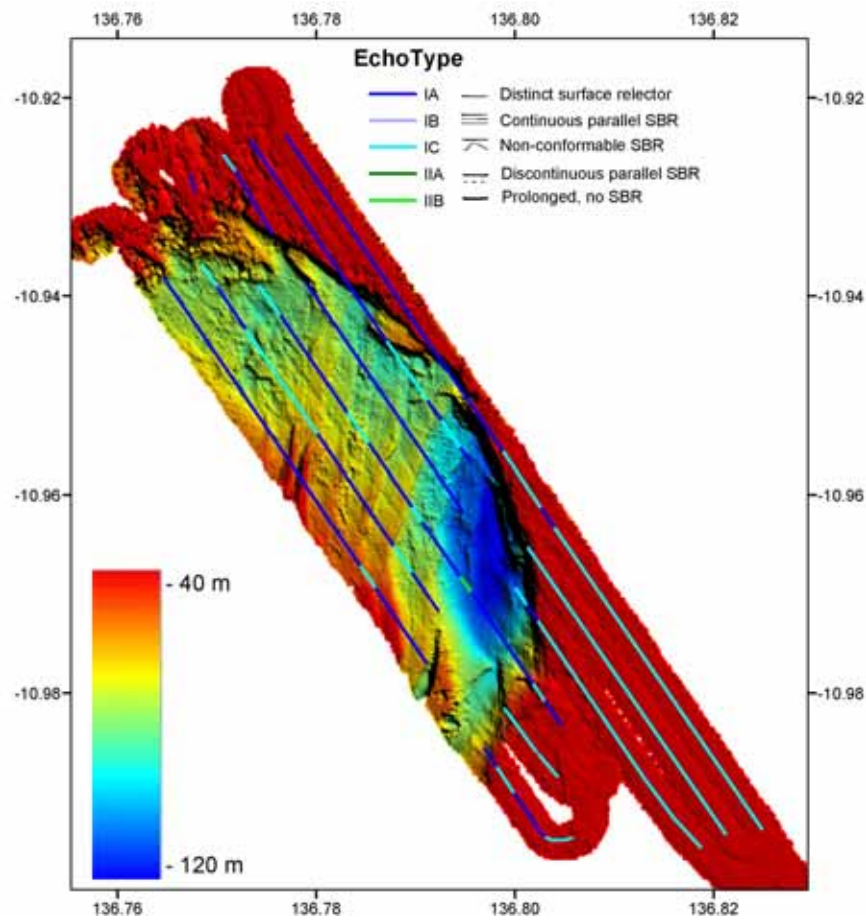


Fig. 2.15. Area E, echo-type mapped along line displayed with bathymetric imagery.

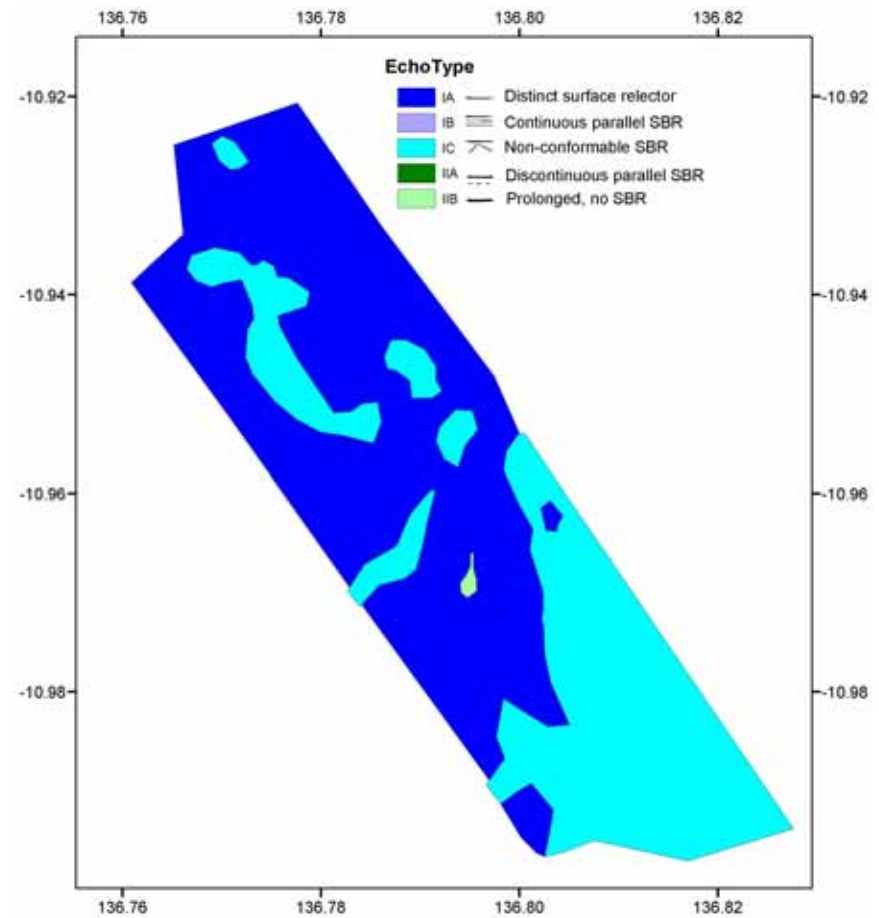


Fig. 2.16. Area E echo-type polygons map.

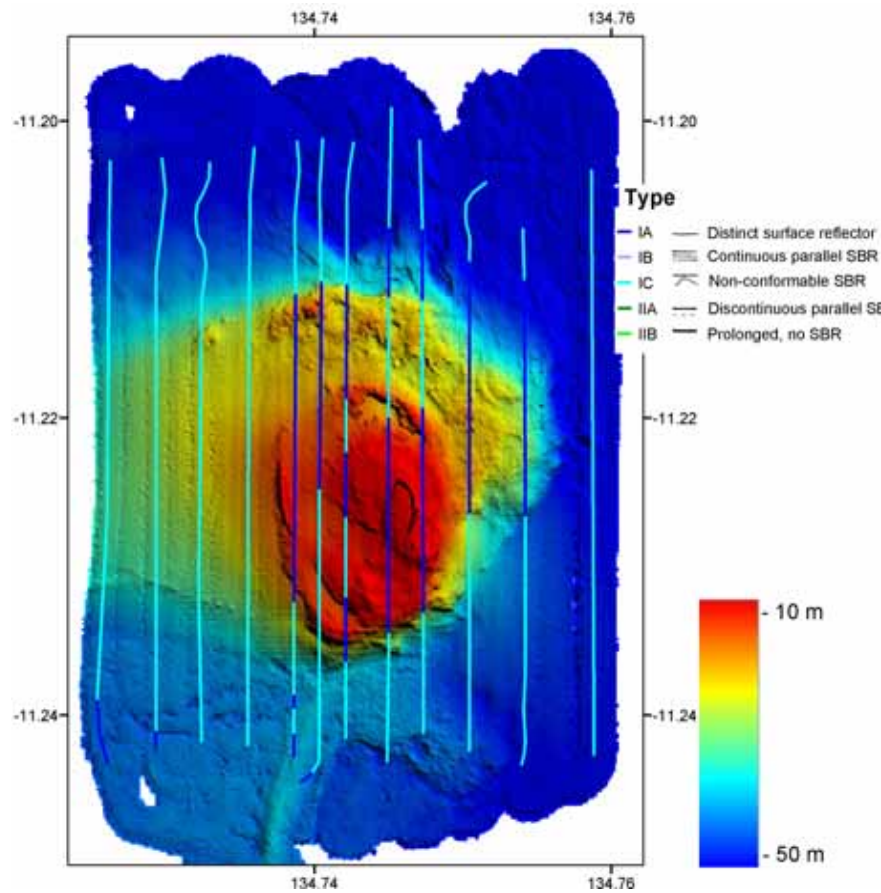


Fig. 2.17. Area F, echo-type mapped along line displayed with bathymetric imagery.

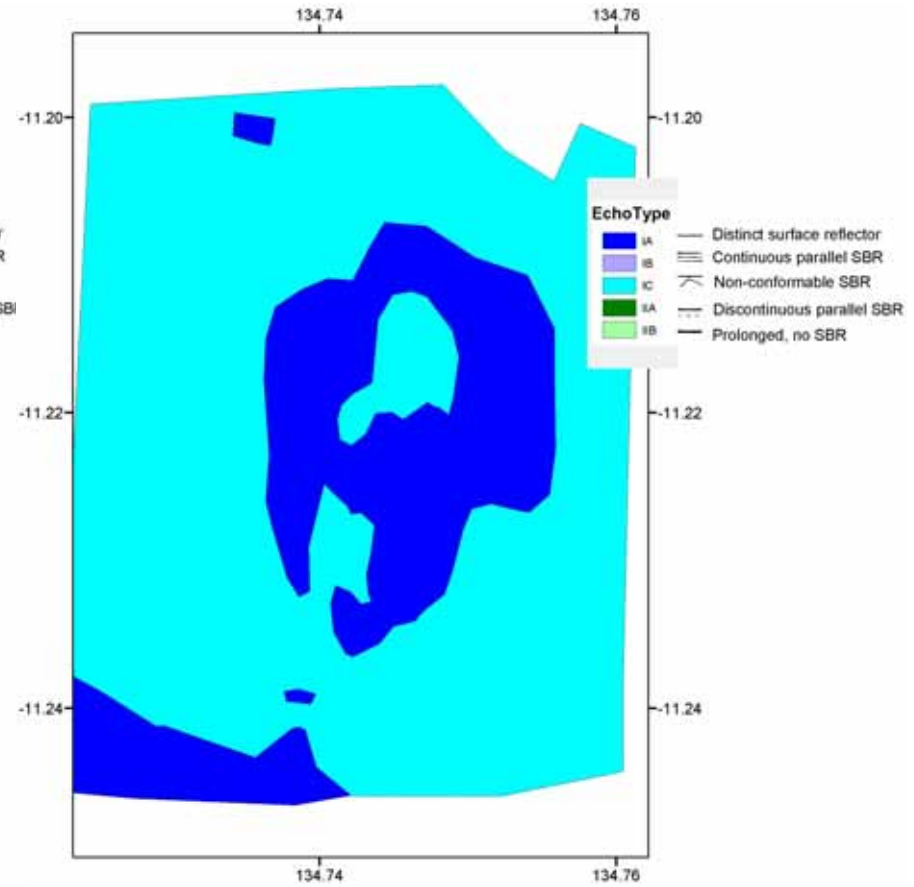


Fig. 2.18. Area F echo-type polygons map.

Chapter 3. Meteorology and Oceanography

3.1 METEOROLOGY

3.1.1 Methods

The RV *Southern Surveyor* has an on board meteorological log which records Atmospheric temperature, relative humidity, mean and gusting wind speeds and direction, and atmospheric pressure. These logs are available electronically post-survey from the National Facility website.

The ship log has been obtained for both S283 (SS0305) and S276 (SS0405), as both of these surveys covered the period of the current meter deployments.

3.1.2 Results

[Figure 3.1](#) displays the meteorological conditions for the 49 day period from the commencement of Survey 283 to the end of Survey 276. It should be noted that the meteorological conditions are recorded aboard vessel, and consequently they contain both spatial and temporal variability. For the purposes of this report, spatial variability is ignored. Data is recorded every 10 seconds. However for this report, it has been re-sampled at hourly intervals. The record commences at 0325 hrs 23-Feb-2005 GMT (DOY 53.166), and continues until 2225hrs 12-Apr-2005 GMT (DOY 101.94).

For the period of the two surveys, wind speed was typically of the order of 10-15 knots. However, the wind velocities contain a diurnal signal. During survey 283, greater wind speeds were typically experienced in the early hours of morning (local time), before the sun had risen. However, during survey 276, daily maximum wind speeds were generally experienced late morning (local time) after the sun had risen until approximately 11am (local time).

At approximately DOY 70, Cyclone Ingrid passed through the Gulf of Carpentaria. This resulted in the most significant weather event during the two surveys, with wind speeds in excess of 35 knots, atmospheric temperature dropping 4 degrees from approximately 30dC to ~ 26dC. Atmospheric pressure dropped to 1003 hPa, and a noticeable increase in relative humidity from ~ 70% to ~90% was associated with the passage of Ingrid. The wind direction data obtained from the underway dataset was particularly noisy, and has not been included in the analysis.

Temperature has a relatively strong diurnal signal, with magnitude of approximately 2dC. A strong diurnal signal is also observed in the atmospheric pressure, with magnitude of approximately 4 hPa. Humidity displays a similar diurnal signal variation with a magnitude of approximately 5-10%.

3.2 OCEANOGRAPHY

3.2.1 CTD Deployments

3.2.1.1 Water Mass Properties.

Fifty-eight CTD deployments were completed, from the 7 key areas (R1, R2 and R3, Mornington Reef, Area B, Area C, Area D, Area E and Area F) with details listed in [Table 3.2](#). The CTD model was a Seabird-SBE911-Plus and it was deployed at each location with recordings taken from between 1m below the sea surface to 1m above the sea floor.

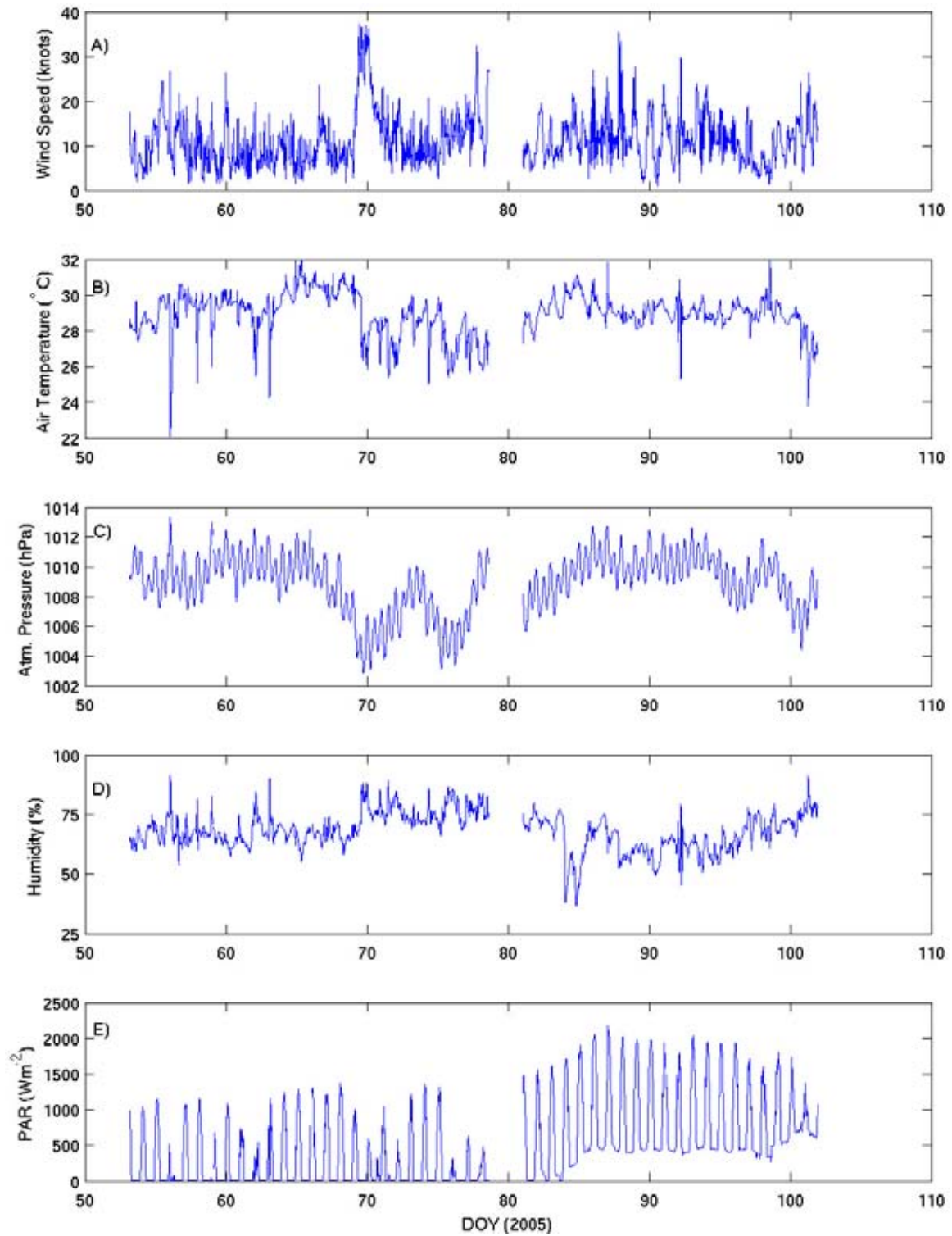


Figure 3.1. Time-series of raw meteorological data from the FRV *Southern Surveyor* for the period of surveys 283 and 276. a) wind speed, b) air temperature, c) Atmospheric pressure, d) Relative humidity, and e) PAR – light sensor.

Table 3.1 Raw meteorological statistics from underway data obtained from FRV Southern Surveyor for the period of Surveys 283 and 276.

FIRST RECORD GMT (2005)	LAST RECORD GMT (2005)	SAMPLING INTERVAL	WIND SPD MEAN WIND SPD STD WIND SPD MAX	TEMP MIN TEMP MEAN TEMP MAX	PRES MIN PRES MEAN PRES MAX	HUMIDITY MIN HUMIDITY MEAN HUMIDITY MAX	PAR MIN PAR MEAN PAR MAX
0325 23-Feb	2225, 12 April	Hourly	11.23 kts 5.69 36.15	25.33°C 28.98 32.07	1002.9 hPa 1008.9 1013.3	37.6 % 68.0 91.4	3.0 uE/m2 480.2 2091.1

The lowest salinities are recorded in the region of R1, R2 and R3 (Fig. 3.2). In this region, a relatively uniform salinity profile is observed (Fig. 3.3) with salinities of approximately 34.05‰ (parts per thousand) measured on the practical salinity scale (PSS). Highest salinities are recorded in Areas C and D in the southwest portion of the Gulf of Carpentaria, with relatively uniform salinity profiles of over 34.6‰. Generally, salinity profiles are relatively uniform, however some vertical structure is observed in Area B (halocline observed at 10, 20 and 35 m in 3 casts with salinity ranging from 34.45‰ in the surface mixed layer, up to 34.55‰ in the bottom layer), and in one cast on the Mornington Reefs (no sharp halocline, but a steady salinity gradient ranges from 34.3‰ to 34.7‰ in 42 m water depth).

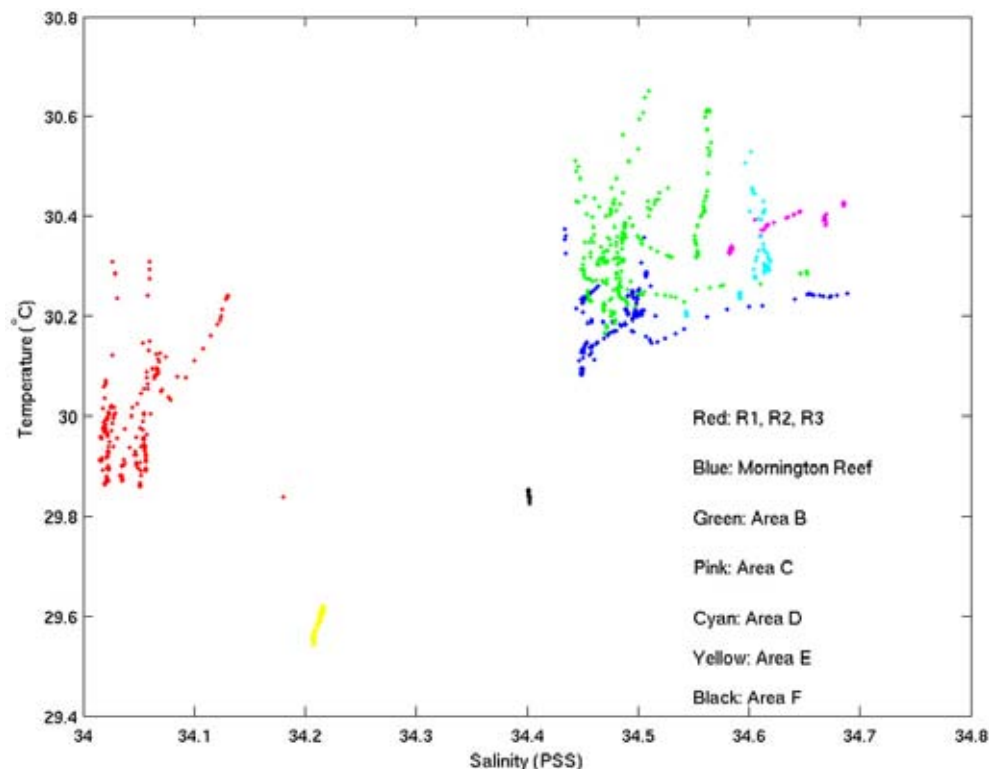


Figure 3.2. Temperature-salinity plot of all CTD data collected on survey. Different colours represent different regions as marked.

Lowest temperatures are observed in the CTD casts of Area E and F (Fig. 3.2). Temperature profiles are relatively uniform in these Areas with values of approximately 29.6°C and 29.8°C respectively.

Water properties of regions Mornington Reefs and Areas B, C and D display similar properties with salinities in the range of 34.45‰ to 34.7‰ and temperature in the range of 30.2 to 30.6°C. The Mornington Reef region is the coolest of the 4 regions with temperatures less than 30.3°C.

3.2.1.2 Transmissometer Profiles of Suspended Sediments

Suspended sediment concentrations measured by the transmissometer during the CTD casts were calibrated by the filtration of surface and near-bed water samples (Table 3.2). Area E had the highest surface and near-bed suspended sediment concentration. Areas C and F also had mean suspended sediment concentrations in excess of 0.01 g/l.

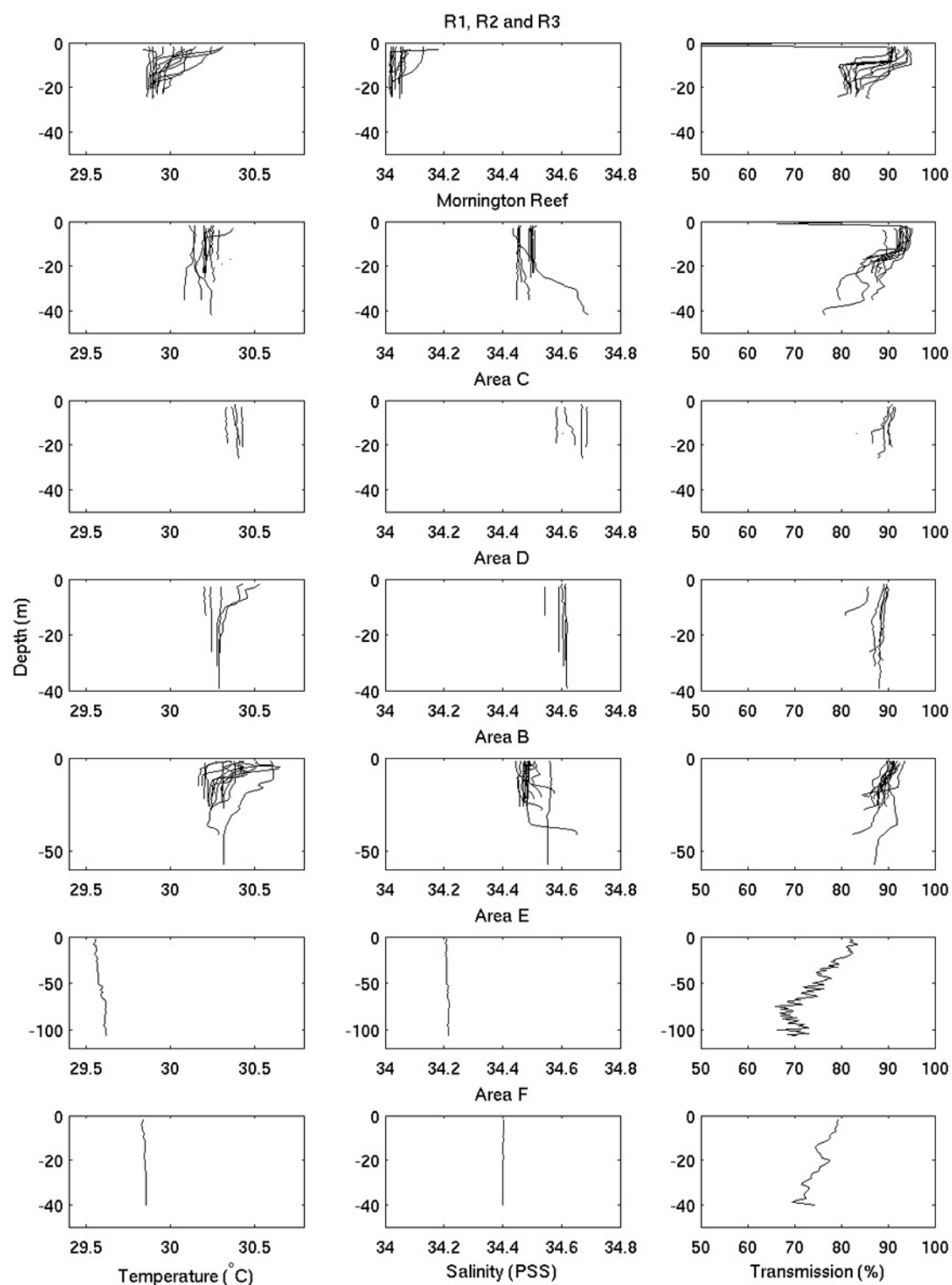


Figure 3.3. Plots of temperature, salinity and transmissivity versus depth for all (~60) CTD profiles taken on survey in Areas R1R2R3, Mornington Reef, Area B, C, D, E and F.

Table 3.2. List of CTD stations from Survey 276, and suspended sediment concentrations (SSC) measured by filtration of surface (top) and near-bed (bot) water samples.

STN	OP	SAMPLE CSIRO NO.		SSC TOP (G/L)	SSC BOT (G/L)
1	CTD	1	1	0.0107	0.0113
2	CTD	2	2	0.0114	0.01
3	CTD	3	3	0.0051	0.0098
4	CTD	4	4	0.0107	0.0112
5	CTD	5	5	0.005	0.005
6	CTD	6	6	0.0042	0.0049
7	CTD	7	7	0.0036	0.0046
8	CTD	8	9	0.0046	0.0044
9	CTD	9	10	0.004	0.0044
13	CTD	10	11	0.0107	0.0112
14	CTD	11	12	0.0124	0.0121
15	CTD	12	13	0.0049	0.0049
16	CTD	13	14	0.0043	0.0043
17	CTD	14	15	0.0114	0.0113
18	CTD	15	16	0.0103	0.0121
21	CTD	16	17	0.0045	0.0038
22	CTD	17	19	0.0112	0.0113
23	CTD	18	20	0.0049	0.0054
24	CTD	19	21	0.0058	0.0048
25	CTD	20	22	0.0037	0.0046
26	CTD	21	23	0.0048	0.0049
27	CTD	22	24	0.0112	0.0095
28	CTD	23	25	0.0109	0.0098
29	CTD	24	27	0.0107	0.0112
30	CTD	25	30	0.0089	0.0106
31	CTD	26	31	0.0043	0.004
32	CTD	27	33	0.0037	0.0042
33	CTD	28	34	0.0096	0.0083
35	CTD	30	35	0.0112	0.0122
36	CTD	31	36	0.0113	0.0108
37	CTD	32	38	0.0115	0.0112
38	CTD	33	39	0.0102	0.0107
39	CTD	34	40	0.0111	0.0109
41	CTD	36	42	0.0102	0.0115
46	CTD	37	44	0.0113	0.0101
47	CTD	38	45	0.0048	0.0057
48	CTD	39	46	0.0039	0.0042
49	CTD	40	47	0.0042	0.0042
50	CTD	41	51	0.0053	0.0048
51	CTD	42	52	0.0109	0.0113
53	CTD	43	53	0.011	0.0094
54	CTD	44	55	0.004	0.0048
55	CTD	45	56	0.0035	0.0044
56	CTD	46	57	0.0034	0.0044
57	CTD	47	58	0.0046	0.0058
58	CTD	48	59	0.0044	0.0053
59	CTD	49	60	0.0092	0.0094
60	CTD	50	61	0.0101	0.0079
61	CTD	51	62	0.0099	0.0097
62	CTD	52	63	0.0108	0.011
63	CTD	53	64	0.0058	0.0041
64	CTD	54	65	0.004	0.0029
65	CTD	55	66	0.0035	0.0034
66	CTD	56	67	0.0028	0.0037
67	CTD	57	68	0.0035	0.0032
68	CTD	58	69	0.0091	0.0113
69	CTD	59	70	0.0125	0.0144
70	CTD	60	71	0.0123	0.0125

Table 3.3. Statistics of suspended sediment concentrations measured by filtration. Top and bottom refers to surface and near-bed water-samples taken for the indicate area.

AREA		MEAN G/L	MAX G/L	MIN G/L	SD	NO. PTS.
R1-R3	top	0.0070	0.0124	0.0036	0.0035	13
	Bot	0.0075	0.0121	0.0043	0.0033	13
MReef	top	0.0075	0.0112	0.0037	0.0031	14
	Bot	0.0075	0.0121	0.0038	0.0032	14
AreaB	top	0.0061	0.0110	0	0.0035	16
	Bot	0.0062	0.0113	0	0.0036	16
AreaC	top	0.0111	0.0115	0.0102	0.0005	5
	Bot	0.0112	0.0122	0.0107	0.0006	5
AreaD	top	0.0069	0.0113	0.0039	0.0036	5
	Bot	0.0071	0.0115	0.0042	0.0034	5
AreaE	top	0.0125	0.0125	0.0125	0	1
	Bot	0.0144	0.0144	0.0144	0	1
AreaF	top	0.0123	0.0123	0.0123	0	1
	Bot	0.0125	0.0125	0.0125	0	1

Vertical profiles of transmissivity differ between the 7 areas. In the region of R1, R2 and R3, and on the Mornington Reef, a surface mixed layer of 10-20 m water thickness is present with relatively uniform and clear water. Below this layer, turbidity shows a marked increase. In Area E and F, turbidity is greatest nearest to the seabed, suggesting localised resuspension and advection of bottom sediment are important processes.

Water samples were collected using the ship's CTD rosette and 2.5-litre Niskin bottles. One litre of seawater was filtered through pre-weighted 45µm mesh glass membranes using a vacuum system on board the vessel. The filter papers were then stored in a dry freezer and, on return to the laboratory, were oven dried at 60 C and re-weighted to ± 0.0001 g to obtain the weight of suspended sediments. Suspended sediment concentrations were finally calculated from these weights and the details entered into Geoscience Australia's Marine Sediment Database (MARS). All samples were subsequently visually inspected using a standard binocular microscope to provide an assessment of the type and nature of the particles in suspension.

Suspended sediment concentrations (SSCs) present comparable values at surface and near-bottom, which might indicate very stable oceanographic conditions throughout the water column, at least at the time of the survey. The similarities in concentration between top and bottom parts of the water column (Fig. 3.4), reflects the typically well-mixed conditions and generally low values of SSC. The average SSC is 7.6 mg/l in both surface and bottom sets of samples. Surface samples range from 2.8 to 12.8 mg/l (Fig. 3.5a) while deep samples range from 2.9 to 14.4 mg/l (Fig. 3.5b). Overall, no spatial pattern is evident in the distribution of the SSCs within the Gulf of Carpentaria. Although the Arafura Sea samples had the highest concentrations (276/69CTD59 and 276/70CTD60), the SCC concentrations there were not significantly greater than in the Gulf.

3.2.1.3 Composition of material retained on the filter papers

A distinguishing factor of the water samples collected on Survey 276 is the overall lack of suspended material in them. Diatom spicules and dinoflagellates represent the most abundant organic components by far. Most of the dinoflagellates observed belong to the *Ceratium* family. However, *Cerodinium* sp., *Protoperidinium* sp. and *Warnowia* sp. (chain forming species) are also common.

Specimens of copepods, mostly belonging to the *Euchaeta* family, have been recorded in almost all the samples in varying abundances, from 2/3 specimens in the most western samples to 25/30

specimens in the eastern ones. Small brown wool-like particles have been identified as copepod fecal pellets and represent another very common component of the samples.

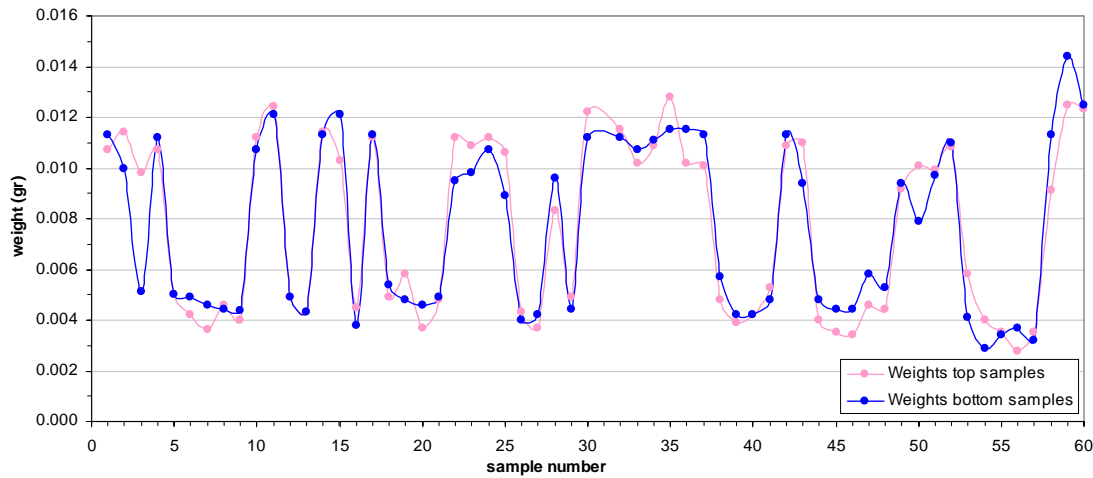


Figure 3.4. Comparison between the weights of the sediments collected through the filtered water samples both at surface and near the sea floor.

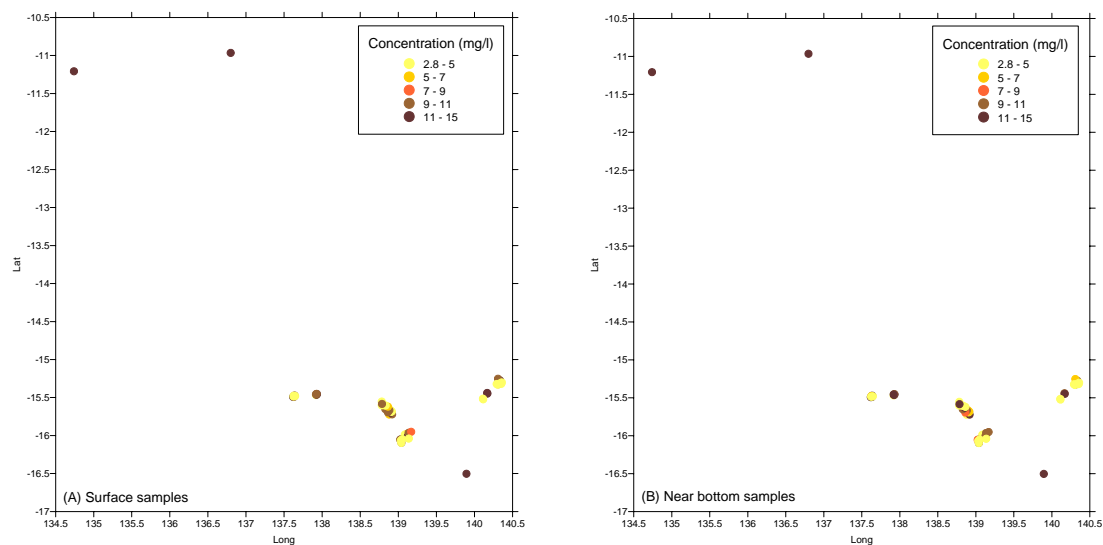


Figure 3.5. (A) Suspended sediment concentrations of water samples collected near the surface; (B) suspended sediment concentrations of water samples collected near the sea floor.

Planktonic foraminifera are extremely rare and have been identified only in few samples with random distribution. They mostly belong to the *Globigerinoides* and *Orbulina* genera and are in their juvenile forms. Some of the samples also present bright green filaments that have been identified as algae. In particular, samples 276/22CTD17 and 276/31CTD26 are very rich in filaments. Samples 276/69CTD59 and 276/70CTD60 are, by far, the richest of the entire survey and are both located in the Arafura Sea. They are the only samples also presenting a few (2/4) specimens of centric diatoms.

The mineralogical content of the samples is also very low, with small particles of quartz, biotite and manganese identified in the southernmost and very shallow samples. In general, the inorganic fraction represents <3% of the total composition of the samples.

Samples collected close to the seabed present very similar compositions and abundances to those of the surface ones. Overall, based on a visual inspection, the size fraction of the material deposited on the near-bottom filter papers is smaller than that from the surface samples. The inorganic content is also higher at depth, although it is very difficult, due to the very small size of the filter papers, to identify the nature of the few minerals observed. As an average value, about 5-10% of the near-bottom samples can be considered to be composed by inorganic particles.

The main organic components of the near-floor samples are, in order of decreasing abundance, diatom spicules, dinoflagellates, copepods, centric diatoms and algae. Almost no foraminifera have been identified in the samples, with the exception of one or two specimens of juvenile benthonic forms in samples 276/13CTD10 (also the richest in terms of copepods content with over 30 specimens) and 276/14CTD11, which presents 2 specimens of *Amphistegina* sp. Gastropods, bivalves, ostracods and other common marine organisms are also absent from the filter papers.

3.2.2 Underway Data

The RV southern surveyor log records surface salinity and temperature at the location of the vessel for the period of deployment.

Figures 3.6 to 3.8 display the spatial and temporal variability of water temperature, salinity and fluorescence as recorded by the underway logger through the course of the survey.

Temperature (Fig 3.6) displays highest values in the south-west of the Gulf of Carpentaria (Areas B, C and D), with values up to 30.7 dC. Lowest temperatures of 29.3 dC are recorded in the deeper waters of the Wessel Deep to the north-west of the Gulf of Carpentaria.

Salinity (Fig 3.7) displays highest values of 34.9 in the southern-most portion of the Gulf off of Mornington Island. Lowest salinities (values less than 31) were recorded on departure from Weipa in the north-east of the Gulf of Carpentaria. Salinity was relatively uniform throughout most of the Gulf with values of approximately 34.

Fluorescence (Fig 3.8) shows a peak in the channel where the current meter moorings were deployed in Area B. Away from this location, fluorescence was relatively low.

3.2.3 Details of Mooring Deployments

The hydrodynamic conditions were recorded with a pair of moorings designed to measure currents, temperature, salinity, and turbidity. Moorings were deployed at two locations during survey 283, recovered at the beginning of survey 276, and recovered again at the end of survey 276. All deployments are described here.

During survey 283, Mooring Stn06CM1 consisted of the Geoscience Australia instrument frame, BRUCE (Benthic Research frame for Underwater sediment Concentration Experiments). BRUCE was deployed on the top of the reef at the north-western end of the reef found in Area B at location 15° 42.024' S, 138° 52.029' E in 26.0 m water depth. The mooring was complete at 1734 26/02/2005 GMT.

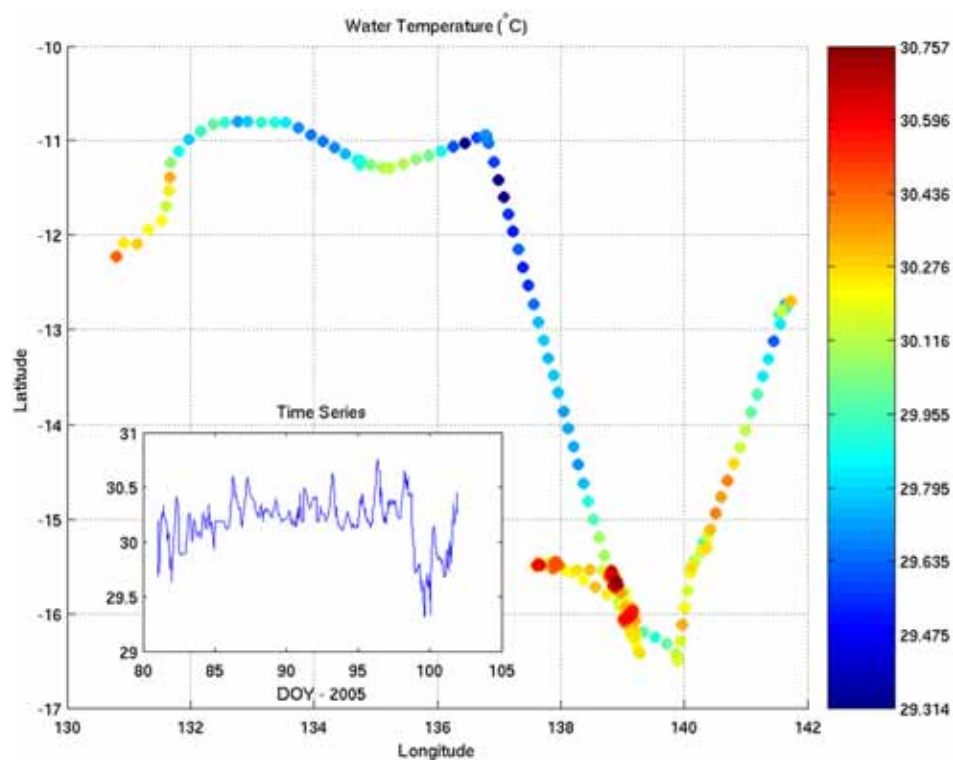


Figure 3.6. Spatial and temporal variability of water temperature (°C) recorded by the surface underway logger during survey 276.

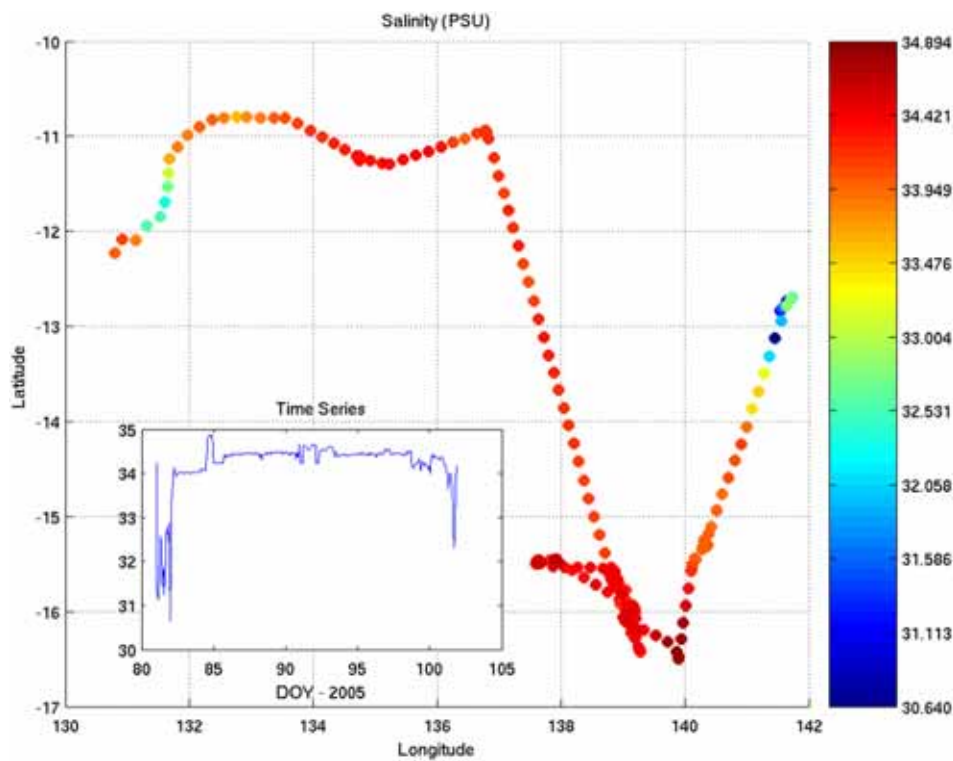


Figure 3.7. Spatial and temporal variability of salinity (as measured on the practical salinity scale) recorded by the surface underway logger during survey 276.

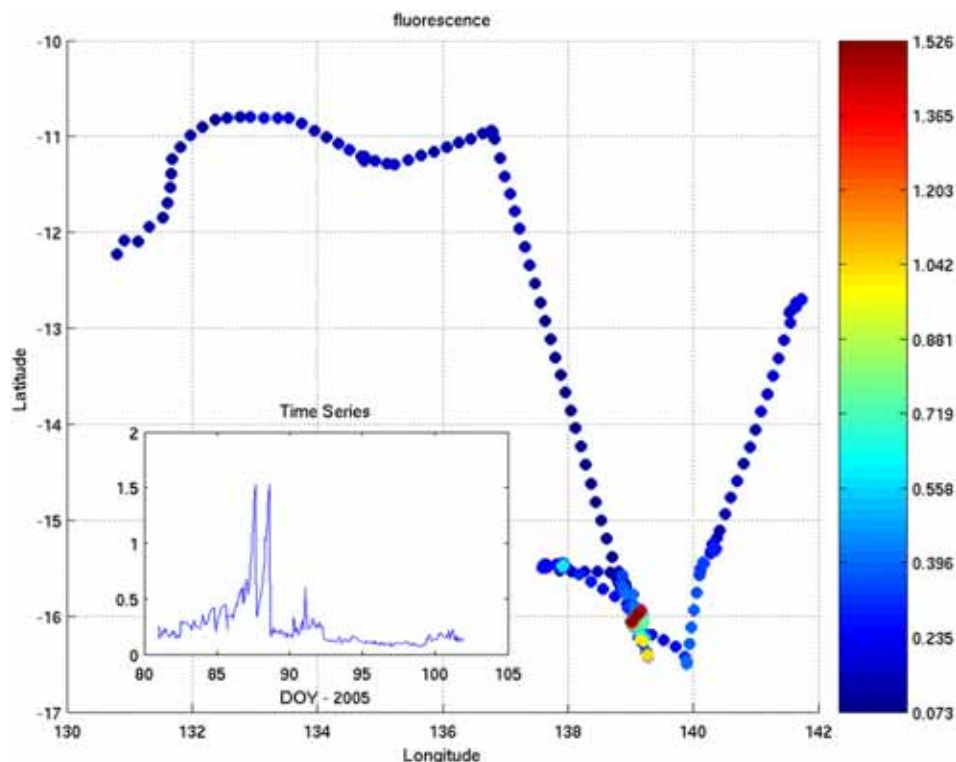


Figure 3.8. Spatial and temporal variability of Fluorescence (dC) recorded by the surface underway logger during survey 276.

BRUCE comprises a 300 kg weighted steel frame equipped with:

- A NortekTM Vector Acoustic Doppler Velocimeter (ADV #N4103). This instrument was positioned to sample at 100 cm above the base of the benthic frame. The vector uses acoustic sampling techniques to measure flow in a remote sampling volume (Nortek, 2000). The instrument was programmed to burst sample every hour for 8 minutes at 8 Hz to record at turbulent time scales. This instrument logs vector components of velocity (east, north and up), pressure and temperature internally to be downloaded on recovery. The Nortek vector (ADV #N4103) contains 82 MB of internal memory ($\sim 2 \times 10^6$ samples).
- A type-B SequoiaTM Laser In-Situ Scattering and Transmissiometry – 100 (LISST-100) transmissometer laser particle sizer (LISST #104579). This instrument was positioned to sample at 27cm above the base of the benthic frame. The LISST measures the scatter of a laser light source to infer the size distribution of suspended matter (Agrawal & Pottsmith, 2000). The LISST was programmed to burst sample for 8 mins at 0.125 Hz at the commencement of the ADV burst (i.e. every hour). The instrument internally logs the scattering at 32 angles; size distribution as concentration ($\mu\text{l/l}$) in 32 log-spaced size bins ranging from 1.25-250 μm ; optical transmission; water depth and temperature, to be downloaded on recovery. The LISST (#104579) contains 2MB of internal memory.
- Two BenthosTM optical backscatter sensors, positioned to sample at 100 cm (OBS #897) and 27 cm (OBS #2167) above the base of the benthic frame. The OBS instruments measure suspended sediment concentration in the water column. These instruments were powered by, sampled at the same rate as, and logged to, the Nortek Vector as “analog inputs” on the Advanced Tab of the Deployment Planning dialog box. The OBS instruments also require calibration before each

deployment. The calibration was carried out using the same procedure as that specified for the LISST-100.

- A Seabird Electronics (SBETM) CTD (CTD #1620) positioned to sample at 27 cm above the base of the benthic frame. The CTD was programmed to be powered by and sample at the same rate as the LISST-100. Temperature and conductivity were logged to the LISST internal memory to be downloaded on recovery.

On deployment, a box core (283/2BC1) was also collected. The mooring was left to be recovered on the following Geoscience Australia survey 276 (SS0405).

Mooring 07CM02 consisted of the Geoscience Australia Acoustic Doppler Current Profiler (Angus, son of BRUCE). The mooring was deployed in the narrow tidal channel located mid-way between the BRUCE mooring site and Mornington Island in Area B at location 16° 5.706' S, 139° 2.418' E in 40.8 m water depth. The mooring was complete at 0138 27/02/2005 GMT.

The Stn7CM2 mooring contained an RD Instruments Workhorse Sentinel 600 kHz ADCP (# 5581). The instrument measures currents from the doppler shift of sound reflected from the water column from two pairs of orthogonal acoustic beams (Gordon, L., 1996). ADCP #5581 contains the following feature upgrades: Mode 5, 8, and 11 high resolution modes; high ping rate mode 12; and waves array upgrade. The instrument contains internal memory of 144 MB. This instrument was programmed to sample in "High Ping-rate Mode 12" to obtain profiles of currents from about 1.2 m above the seabed to near the water surface with measurements spaced 1.2 m apart in the vertical. Mode 12 allows a higher ping rate, allowing more data to be collected, thus improving ensemble average accuracy. Give deployment configuration, the RDI software estimates a standard deviation of velocity estimates of 2.1 cm/s. The instrument was set-up to measure turbulence using the variance method (Lu and Lueck, 1999). RDI's fast-pinging mode 12 was used with a ping rate of 8Hz; velocities were averaged and recorded every second.

No other samples were collected at the time of deployment due to hydraulic difficulties with the winch frame. The mooring was left to be recovered on the following Geoscience Australia survey (SS0405).

During survey 276, Mooring 283/Stn6CM1 was recovered at 0346 27/03/2005 GMT. Data were successfully retrieved from the Nortek Vector, however no data were recorded on the Sequoia LISST. The mooring was moderately fouled with barnacles. The OBS sensors had much growth, however the LISST optics appeared to be clear.

Mooring 283/Stn7CM2 was recovered at 0110 27/03/2005 GMT. It was noted on recovery that the lead weight to be attached to the base of the ADCP to allow free movement in the gimbal was not attached. Data were successfully recovered from the ADCP, however the instrument is noted to have been at an angle for the period of deployment.

The ADCP (Angus, son of BRUCE) was re-deployed in approximately the same location, and consequently will be treated as the same mooring in the following analysis. The precise location of the re-deployment (Mooring 276/20CM3) was at 16° 5.700' S, 139° 2.400' E in 41.2 m. water depth, and was completed at 1744 27/03/2005 GMT. The ADCP was programmed identically, using RDI's fast-pinging mode 12 with a ping rate of 8 Hz, and averages being averaged and recorded every second. At the time of deployment, CTD 276/20CTD15 was also deployed. The mooring was finally recovered at 0123 8/04/2005 GMT. Data were successfully downloaded. At the time of recovery, samples 276/54CTD44, 276/54GR45, and 276/54CAM52 were collected.

BRUCE was re-deployed on survey 276 in a different location to that during survey 283. Consequently, in the following analysis, it is treated as a separate mooring (276/21CM4).

While programming BRUCE for the second deployment, it was discovered that the LISST and Vector were not communicating. It was eventually decided that BRUCE would be deployed without the LISST. Given the Seabird relies upon the LISST for power, and to log data, the Seabird was also not deployed on the second deployment. Cabling to connect the Vector to OBS's only were not available, and consequently, the only instrument to be deployed was the Nortek Vector. The vector was programmed to collect current velocity data at 8 Hz for 8 minutes, every hour on the hour.

The BRUCE frame was re-deployed in the same tidal channel as the ADCP, slightly north east of the ADCP frame at location 16deg 2.213' S, 139deg 8.031' E in 44.8 m. water depth. The mooring was complete at 0447 28/03/2005 GMT. At the time of deployment, samples 276/21CTD16, 276/21GR18, and 276CAM21 were collected. The mooring was recovered at 0400 08/04/2005 GMT. Data recovery were successful. At the time of recovery, sample 276/55CTD45 was collected.

3.2.4 Data Processing

Data processing was carried out using Matlab software. After data were downloaded from the instruments and converted to a readable format, they were carefully checked for instrument malfunctions and then edited. The beginning and end of each data series were truncated and outliers deleted. Short data gaps have typically been left as gaps, having been filled with 'NaN' values where applicable. Data were carefully checked at each stage of processing. After editing, the basic version of the data file includes variables recorded at the basic sampling interval, and a low-pass filtered data file created from the basic version. The low-pass filter essentially removes all fluctuations of periods less than 33 hours. Low-pass filtered data were sub-sampled every 6 hours.

The ADCP's were configured to record data in Beam coordinates. Upon recovery, the ADCP data were transferred to a personal computer using the RD Instruments (www.rdinstruments.com) software. Using the RDITM ADCP software WinADCP, recorded variables East, North, Up, Error and Depth were exported to MATLAB format for times that the Mooring was in the water. Matlab routines were used to check for data quality, flag bad values, and discard bins that were always beyond the water surface.

Also, data were eliminated where correlation (SNR) was <90%. Additional bad data was eliminated using the following criteria:

- Error > 10 cm/s, u, v, w were removed.
- If mid bin depth was higher than the recorded water level (depth), u, v, w were removed.

Some near-surface bins were not discarded. At times of low tide, the side-beam reflection renders this data invalid, so near-surface ADCP data must be interpreted with care. On occasion, the ADCP skips an ensemble record because the data is poor. Data have blank placeholders for the missing ensemble records.

Until more sophisticated methods of cleaning the near-surface data are carried out, judgement will be needed when interpreting surface data.

3.2.5 Data Recovery

3.2.5.1 283/Stn6CM1 – *BRUCE 1*

Mooring Stn1CM1 commenced logging of data on the Nortek Vector at 18:00 26/02/2005 GMT (JD 56.75). The first reading of the instrument after the mooring was complete occurs at 18:00 26/02/2005 (JD 56.75). The last reading to occur before the battery failed on the Nortek occurred at 19:30 23/03/2005 (JD 81.8125). All recordings after this time have also been deleted. The total record length is 25.0625 days.

3.2.5.2 283/Stn7CM2 & 276/Stn20CM3 – *ADCP (Angus, son of BRUCE)*

Mooring Stn7CM2 commenced logging of data on the ADCP at 00:00 28/02/2005 GMT (JD 58.00). The first reading of the instrument after the mooring was complete occurs at 00:00 28/2/2005 (JD 58.00). The last reading to occur before the memory filled on the ADCP was recorded at 15:00 22/03/2005 (JD 80.625). The ADCP was recovered, memory cleared after a data download and re-deployed. Data began recording again at 18:00 27/03/2005 (JD 85.75). The final data record before the ADCP was recovered occurred at 01:00 08/04/2005 (JD 97.0417).

The total record length is 39.0417 days, with data gap of 5.125 days between JD 80.625 and JD 85.75.

3.2.5.3 Stn3CM2 – *BRUCE-2*

Mooring Stn21CM4 commenced logging of data on the Nortek Vector at 02:00 28/03/2005 GMT (JD 86.0833). The first reading of the instrument after the mooring was complete occurs at 05:00 28/3/2005 (JD 86.2083). The first 3 hours of the records have been deleted while the mooring was out of the water. The last reading to occur before the mooring was recovered occurred at 08:00 08/04/2005 (JD 97.333). The total record length is 11.1247 days.

3.2.6 Preliminary Data Analysis

3.2.6.1 Statistics

Raw statistics have been calculated for each variable recorded on each mooring. These include minimum, maximum, mean and standard deviation values of each variable during the entire deployment of each mooring.

3.2.6.2 Sea Level

A pressure record is recorded by each of the instruments listed here:

- the RD Instruments ADCP on which 'depth' is recorded in 'm'. This reading has also been converted to a measurement of water-depth with respect to the sea-bed by adding 0.5 m to the measured reading, representing the height of the ADCP sensors above the seabed.
- the Nortek Vector ADCP. Sea-level is recorded in 'm' above the instrument.

A classical harmonic tidal analysis has been carried out on the sea-level record obtained from each instrument of a mooring using the T_TIDE package in MATLAB (Pawlowicz et al., 2002) and compared. The results of the analysis for the four largest constituents (M2, S2, K1, O1) are presented in the following section.

To determine the nature of the tides at each mooring location, the 'form ratio', $F = (K1+O1)/(M2+S2)$, a measure of the signature based on the relative magnitudes of their main diurnal and semi-diurnal constituents (Pond & Pickard, 2000), has been calculated.

F = 0 to 0.25: semi-diurnal tides.

F = 0.25 to 1.5: mixed, mainly semi-diurnal tides.

F = 1.5 to 3.0: mixed, mainly diurnal tides.

F > 3.0: Diurnal tides.

3.2.7 Currents

Given our interest is in sea-bed processes, processing and analysis of current meter data is focussed on data obtained from the first bin. The ADCP's were configured such that the centre of first bin was 1.2 m above the sensors. This corresponds to approximately 1.7 m above the seabed. To provide an indication of the vertical current profile at each site, data from the nearest bin below lowest tide (i.e., the highest bin with a continuous record), has also been processed, analysed and presented.

At each current meter mooring, the following analyses have been carried out on bottom and 'surface' currents:

1. Progressive vector plots, and determination of the mean residual current during the deployment.
2. Time series plots, to provide an overview of the observations and to determine the mean absolute current speeds during the deployment.
3. Principal axes for both the basic 10-min processed data and the low-passed currents were computed for the entire record and by month. Major and minor axes, orientation, and ellipticity were computed from the east (u) and north (v) current components as:

$$\begin{aligned}\text{major axis} &= [0.5 (UU + VV) + R] / n \}^{(1/2)} \\ \text{minor axis} &= [0.5 (UU + VV) - R] / n \}^{(1/2)} \\ \text{orientation} &= 90^\circ - 0.5 \tan^{-1} [2 UV / (UU - VV)] \\ \text{ellipticity} &= 1 - (\text{minor axis} / \text{major axis})\end{aligned}$$

where

$$\begin{aligned}UV &= \text{Sum}(u*v) - n*U*V \\ UU &= \text{Sum}(u*u) - n*U*U \\ VV &= \text{Sum}(v*v) - n*V*V \\ R &= [(0.5 (UU - VV))^2 + (UV)^2]^{(1/2)}\end{aligned}$$

and U and V are the means of the east and north velocity components, respectively. Sum means sum over the entire data set of n values. The orientation is measured clockwise from true north. 0° is true north, and 90° is east.

4. Scatter plots of the basic processed data and the low-passed currents (subsampling to be 6-hourly) to visually show the distribution of the current speed and direction. Superimposed on the scatter plots are the mean vector current over the entire deployment, and the principal axes of the currents, shown as an ellipse.
5. A tidal analysis of the currents. The following procedure has been followed to determine tidal ellipses of each current record.
 - Read in horizontal velocity time series (u,v)
 - Remove means from both u and v.
 - Determine amplitude and phase of each tidal constituent for u and v components separately using T_TIDE software (Pawlowicz et al., 2002).
 - For each constituent, use the fit amplitudes to construct tidal ellipse parameters using 'tidal_ellipse' package (Xu, 2002) in MATLAB. This provides estimates of:

- the semi-major axis (or maximum current velocity),
- ellipse eccentricity (the ratio of semi-minor to semi-major axis). A negative value indicates that the ellipse is traversed in a clockwise direction,
- Ellipse inclination, or angle between east (x-) and semi-major axis, and
- Phase, the angle that the oppositely rotating circular components must traverse from their initial positions for them to meet.

3.2.8 Bedload Transport Estimates

Although wave and turbulence data will be available at a later date, estimates of bed shear stresses, and hence bedload transport, are currently based on the assumption of a steady flow. Five methods have been used to estimate bedload transport at the site. These include:

- a) Bagnold's bedload equation, modified by Gadd et al. (1978)

$$q = (\beta/\rho_s)(u_{100}-u_{cr})^3,$$

where q is the volume rate of sediment transport per unit width of bed [m^2/s], β has a value of 1.73, as used in the SEDTRANS96 model, outlined in Li and Amos. (2001). The critical velocity for the initiation of bedload transport u_{cr} is obtained from $\tau_{cr} = 0.5\rho f_{cs}u_{cr}^2$, and u_{100} is the current speed measured 100cm above the bed.

- b) The Engelund-Hansen (1967) total load equation. For continental shelf conditions, this equation is modified to (Li and Amos, 2001):

$$q = 0.05u_{100}^2\rho^2 u_*^3/D(\Delta\rho g)^2,$$

where $\Delta\rho = \rho_s - \rho$, and ρ_s is the density of the sediment (For quartz 2650 kgm⁻³), and ρ is the density of seawater. u_* is the skin-friction shear velocity.

- c) The Einstein-Brown bedload equation (Brown, 1950). This equation can be written in the form (Li and Amos., 2001)

$$q=40W_sD(\rho/\Delta\rho gD)^3u_*^{*5}|u_*|,$$

where W_s is the settling velocity.

- d) Yalin bedload equation (Yalin, 1963).

$$q=0.635Du_*[(\tau^*-(1/a)\ln(1+a\tau^*))],$$

where $\tau^* = (\tau_b - \tau_{cr})/\tau_{cr}$, is the normalised shear stress and a is equal to $2.45(\rho/\rho_s)^{0.4}(\tau_{cr}/\Delta\rho gD)^{0.5}$.

- e) Bagnold's bedload equation as modified by Hardisty (1983)

$$q = k1(u_{100}^2-u_{cr}^2) u_{100},$$

u_{cr} is the critical threshold velocity defined in this instance as

$$u_{cr} = 1.226(100D)^{1.29}$$

as outlined by Miller et al. (1977). K_1 is a function of sediment grain size (D) such that:

$$k_1 = (1/6.6 (1000D))^{1.23} \text{ kg m}^{-4} \text{ s}^2$$

It is this bedload transport equation which has been used in all previous Geoscience Australia cruise reports, so is included here for completeness.

For consistency with previous cruise reports, the above estimates of q in units $[\text{m}^2/\text{s}]$ must be multiplied by $1/(10\rho_s)$ to express bedload transport in units g/cm/s .

Grain-size data at each site was unavailable at the time of writing, so a mean grain size, D of 0.0005 m (0.5 mm) has been assumed. Vector Stick plots of Bedload Transport estimates are presented to enable an overview of the main stage of tide at which bedload is important.

3.2.9 Results of Instrument Deployments

3.2.9.1 Statistics for Station 6CM1

Statistics for each of the currents recorded by the Nortek at Stn6CM1 during the entire deployment are displayed in Table 3.4.

Table 3.4. Stn6CM1. Raw current meter velocity statistics. All statistics are in cm/s.

EAST MINIMUM	EAST MEAN	EAST MAXIMUM	EAST STD DEV.
-25.00	-1.71	11.06	6.64
NORTH MINIMUM	NORTH MEAN	NORTH MAXIMUM	N STD DEV.
-23.85	-0.42	20.19	8.70
SPEED MEAN		SPEED MAXIMUM	SPEED STD
10.03		25.33	4.70

3.2.9.2 Statistics for Station 21CM4

Statistics for each of the currents recorded by the Nortek at Stn21CM4 during the entire deployment are displayed in Table 3.5.

Table 3.5. Stn21CM4. Raw current meter velocity statistics. All statistics are in cm/s.

EAST MINIMUM	EAST MEAN	EAST MAXIMUM	EAST STD DEV.
-11.55	1.77	13.06	5.86
NORTH MINIMUM	NORTH MEAN	NORTH MAXIMUM	N STD DEV.
-14.16	0.54	16.02	7.59
SPEED MEAN		SPEED MAXIMUM	SPEED STD
8.93		18.86	3.93

3.2.9.3 Statistics for Station 7CM2

Statistics for each of the currents recorded at the sea-bed and sea 'surface' by the ADCP at Stn7CM2 during the entire deployment are displayed in [Table 3.6](#).

Table 3.6. Stn7CM2. Raw current meter statistics for bed (Bin 1: 2.2 m above seabed) currents and 'surface' currents below lowest tide (Bin 24: 31.5m above bed). All statistics are in cm/s.

BIN	EAST MINIMUM	EAST MEAN	EAST MAXIMUM	EAST STD DEV.
1	-22.64	0.910	19.95	8.25
24	-34.90	-1.67	32.03	10.34
BIN	NORTH MINIMUM	NORTH MEAN	NORTH MAXIMUM	N STD DEV.
1	-18.56	0.72	16.94	7.49
24	-23.48	-1.95	38.49	10.47
BIN	SPEED MEAN		SPEED MAXIMUM	SPEED STD DEV.
1	10.36		23.08	4.26
24	13.41		39.83	6.57

3.2.10 Sea Level and Surface Wave Data

3.2.10.1 Station 1CM6

At Stn1CM6, pressure is recorded by the Nortek. A time-series plot of sea-level recorded by the Nortek is shown in [Figure 3.9](#). Table 3.7 presents the results of the tidal analysis of the sea-level record for the four largest constituents (M2, S2, O1, K1).

Table 3.7. Results from the classical harmonic analysis. Record Length 25.00 days. Start time is 26/02/05 18:00:00. Mean water depth from record is 26.0 m. Phase is with respect to Greenwich Mean Time.

TIDE	FREQUENCY (CPH)	AMPLITUDE (M)	AMP. ERROR (M)	PHASE (DEGREES)	PH. ERROR (DEGREES)
O1	0.0387307	0.3554	0.068	107.67	8.94
K1	0.0417807	0.3333	0.055	184.00	9.31
M2	0.0805114	0.1393	0.056	84.59	5.70
S2	0.0833333	0.0271	0.010	168.70	25.73

The form ratio, F , calculated at Stn6Cm1 is equal to 4.16, indicating that tides are strongly diurnal at the site.

Significant constituents calculated within the tidal analysis, where amplitude of a tidal constituent is greater than the calculated error in amplitude for that constituent, are predominantly in the diurnal and semi-diurnal bands (~ 0.04 and ~ 0.08 cph respectively) ([Fig. 3.9](#)). Some higher frequency constituents are also significant. Tidal phase, presented in [Fig 3.9 C](#) show that the significant constituents generally have small phase errors. The residual time-series after removal of the tidal signal has low amplitudes, indicating that the sea surface signal is almost entirely driven by tidal effects.

Each 8 minute burst obtained every 90 minutes on the Nortek has been used to compute the wave parameters (Tucker and Pitt, 2001). Velocity data components, u, v, w were resampled at 2 Hz so that computation time was decreased. The MATLAB DIWASP functions were used to compute the significant wave height, peak wave period, and the dominant wave direction. The following DIWASP parameters were set:

- # directions in calculation – 180
- # Fourier Transforms in spectral estimation 1024
- # algorithm iterations – 100
- Smoothing enabled
- Direct Fourier Transform method.
- The x-axis direction was set to 270.

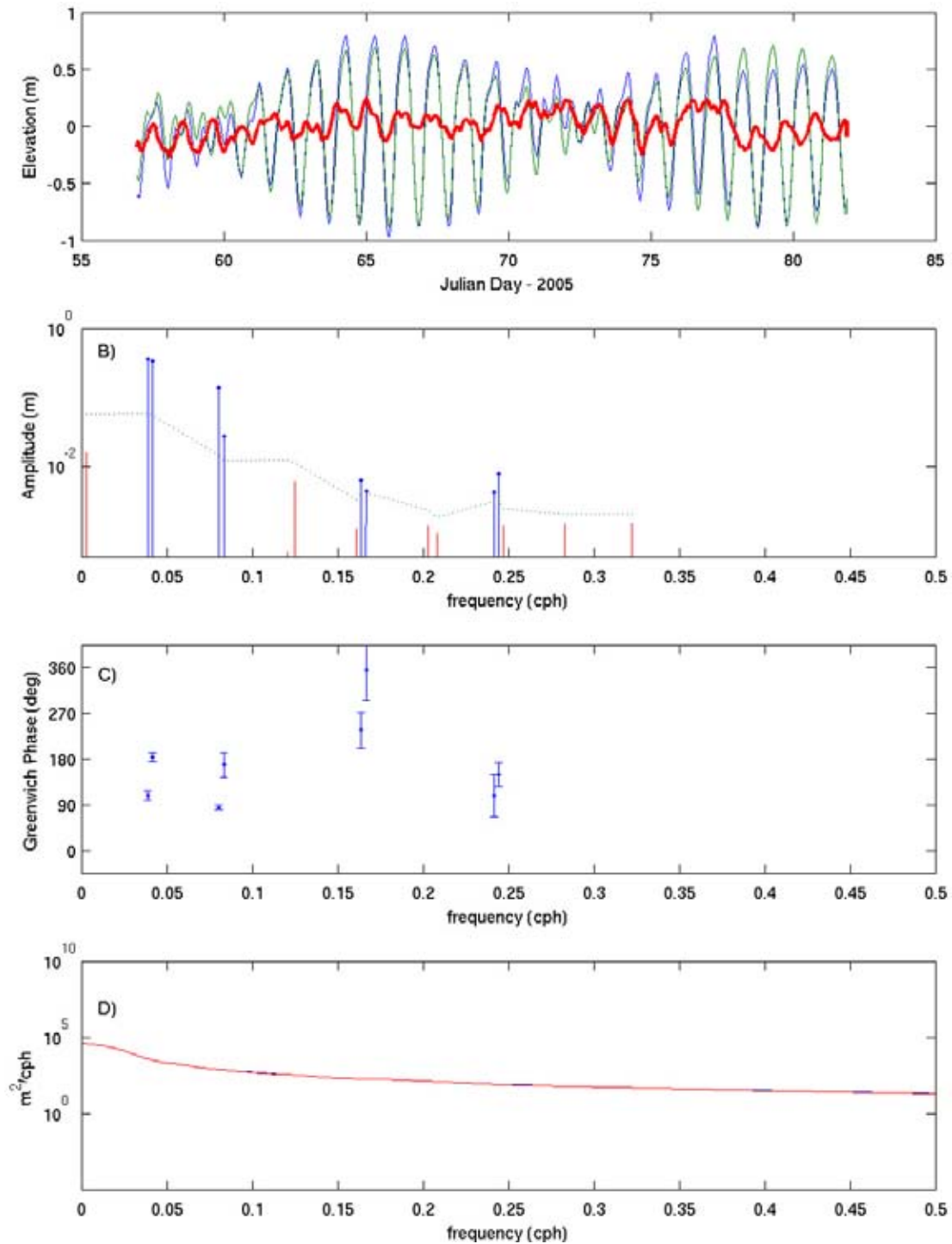


Figure 3.9. Results of classical harmonic analysis of pressure data from Stn6CM1. A) Blue line is Raw Time Series referenced to the mean level in the record, Green line is Tidal prediction from analysis referenced to the mean, Red line is residual time series after removal of the tidal signal; B) Amplitude of all analysed components with 95% significance level (green dashed line). Note frequency dependence. Significant constituents ($amp > amp_err$) are marked with a solid circle; C) Phase of significant constituents with 95% confidence interval; D) Spectral Estimates before and after removal of tidal energy. Blue-line is energy of original time-series, red-line is non-tidal energy.

Figure 3.10 displays the calculated significant wave height (H_s), and the peak wave period (T_p) for the period of deployment. The maximum significant wave height experienced during the course of the survey was 1.63 m on JD 69.18. The peak wave period at during this period was 6.7 s. Statistics of the waves recorded at Stn6CM1 are displayed in Table 3.8.

Table 3.8 Statistics of the waves recorded at Stn6CM1.

	MINIMUM	MEAN	MAXIMUM	STD DEVIATION
H_s (m)	0.07	0.31	1.63	0.24
T_p (s)	3.45	5.49	7.14	0.65

3.2.10.2 Station 21CM4

At Stn21CM4, water pressure was recorded by the Nortek current meter. A time-series plot of sea-level recorded by the Nortek is shown in Figure 3.11. Table 3.9 presents the results of the tidal analysis of the sea-level record for the four largest constituents (M2, S2, O1, K1).

Table 3.9. Results from the classical harmonic analysis. Record Length 10.96 days. Start time is 28/03/05 05:00:00. Mean water depth from record is 46.9 m. Phase is with respect to Greenwich Mean Time.

TIDE	FREQUENCY (CPH)	AMPLITUDE (M)	AMP. ERROR (M)	PHASE (DEGREES)	PH. ERROR (DEGREES)
O1	0.0387307	Record too	Short		
K1	0.0417807	0.4386	0.418	167.14	61.10
M2	0.0805114	0.1386	0.017	86.24	8.25
S2	0.0833333	Record too	Short		

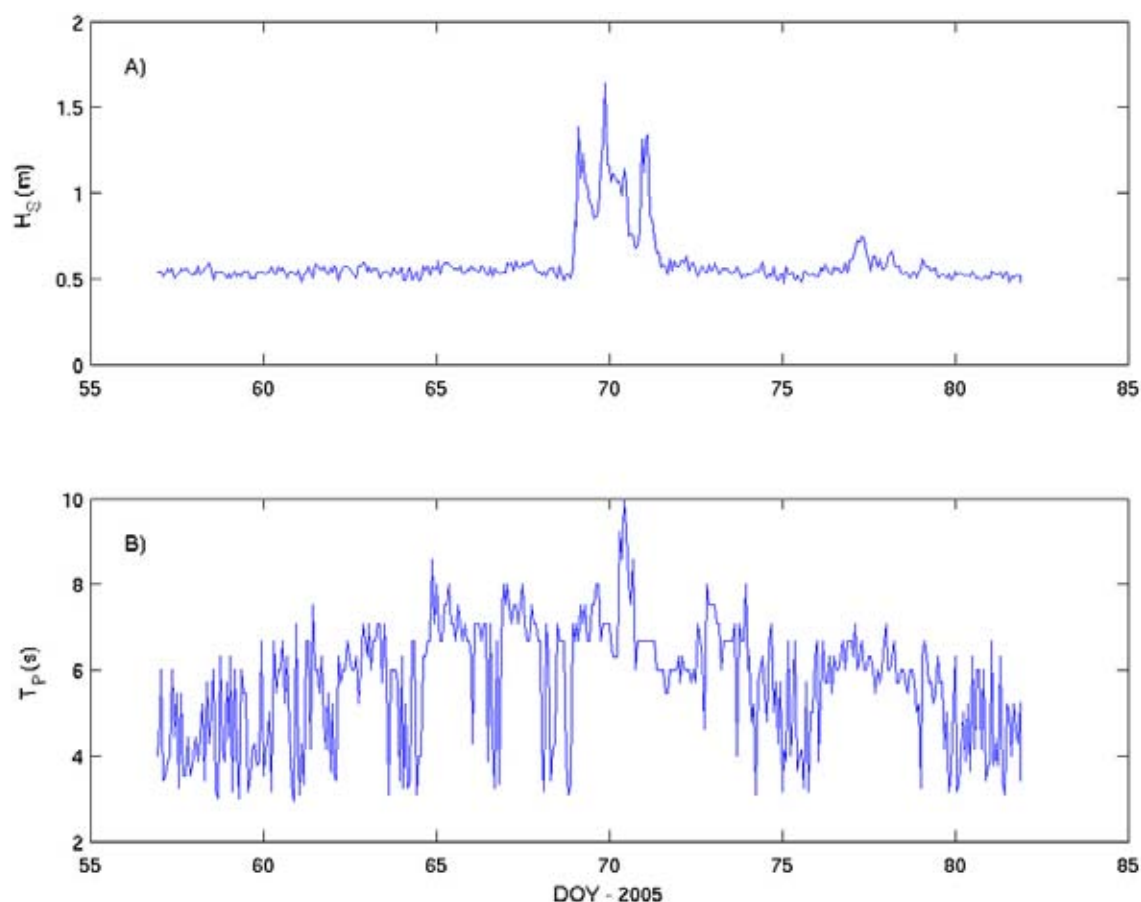


Figure 3.10. Time series of wave statistics recorded at Stn6CM1. A) Significant Wave Height, and B) Peak Wave Period.

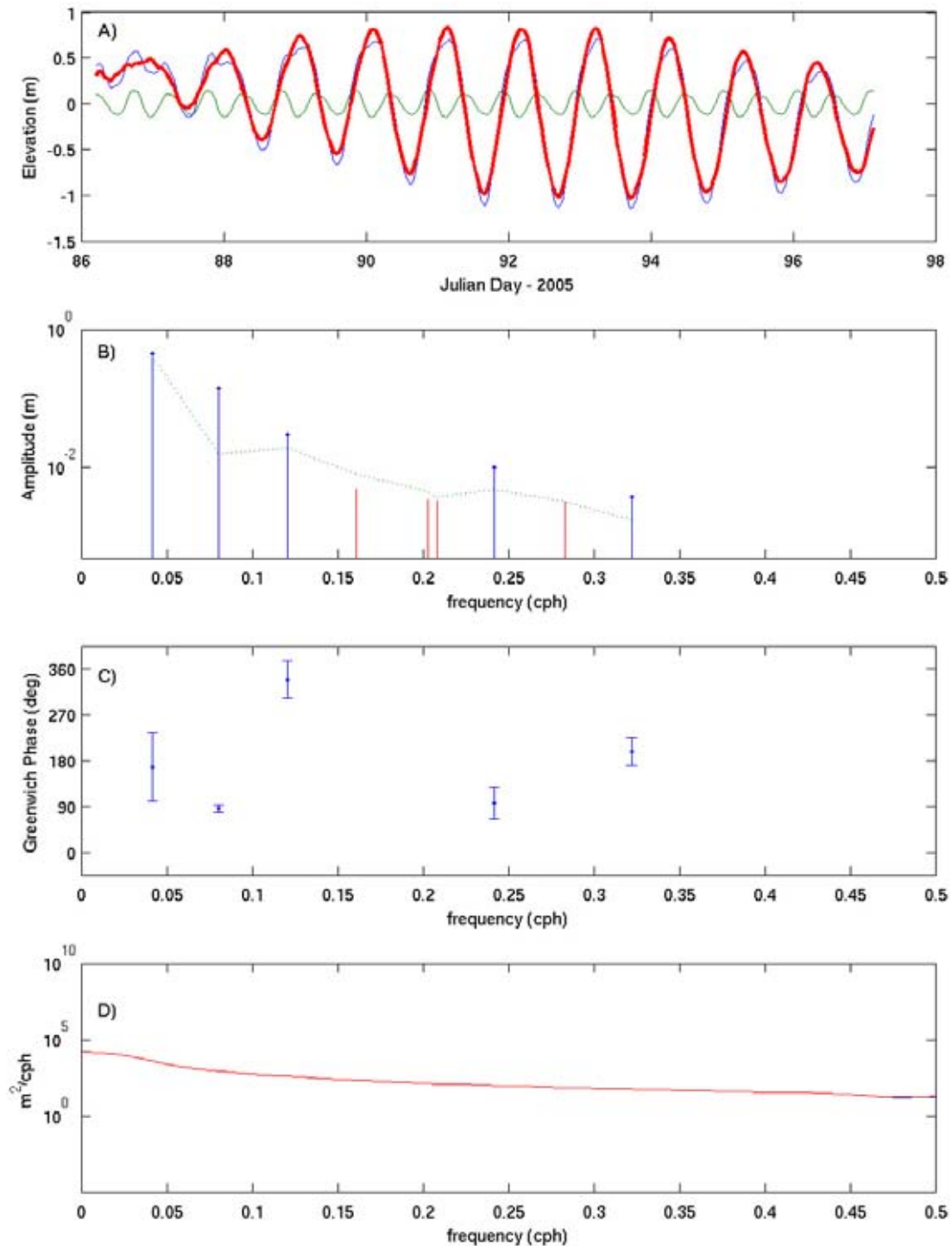


Figure 3.11. Results of classical harmonic analysis of pressure data from Stn21CM4. A) Blue line is Raw Time Series referenced to the mean level in the record, Green line is Tidal prediction from analysis referenced to the mean, Red line is residual time series after removal of the tidal signal; B) Amplitude of all analysed components with 95% significance level (green dashed line). Note frequency dependence. Significant constituents ($amp > amp_err$) are marked with a solid circle; C) Phase of significant constituents with 95% confidence interval; D) Spectral Estimates before and after removal of tidal energy. Blue-line is energy of original time-series, red-line is non-tidal energy.

The form ratio, F , calculated at Stn21Cm4 is equal to 3.16, indicating that tides are diurnal at the site.

Significant constituents calculated within the tidal analysis, where the amplitude of a tidal constituent is greater than the calculated error in amplitude for that constituent, are predominantly in the diurnal and semi-diurnal bands (~ 0.04 and ~ 0.08 cph respectively) (Fig. 3.11 B). Some higher frequency constituents are also significant. Tidal phase, presented in Fig 3.11 C) show that the significant constituents generally have small phase errors. The residual time-series after removal of the tidal signal has low amplitudes, indicating that the sea surface signal is almost entirely driven by tidal effects.

Each 8 minute burst obtained every 90 minutes on the Nortek has been used to compute the wave parameters (Tucker and Pitt, 2001). Velocity data components, u, v, w were resampled at 2Hz so that computation time was decreased. The MATLAB DIWASP functions were used to compute the significant wave height, peak wave period, and the dominant wave direction. The following DIWASP parameters were set:

- # directions in calculation – 180
- # Fourier Transforms in spectral estimation 1024
- # algorithm iterations – 100
- Smoothing enabled
- Direct Fourier Transform method.
- The x-axis direction was set to 270.

Figure 3.12 displays the calculated significant wave height (H_s), and the peak wave period (T_p) for the period of deployment. The maximum significant wave height experienced during the course of the survey was 0.80 m on JD 93.20. The peak wave period at during this period was 6.3 s. Statistics of the waves recorded at Stn21CM4 are displayed in Table 3.10.

Table 3.10. Statistics of the waves recorded at Stn21CM4.

	MINIMUM	MEAN	MAXIMUM	STD DEVIATION
H_s (m)	0.08	0.22	0.80	0.11
T_p (s)	3.85	6.97	10.0	0.87

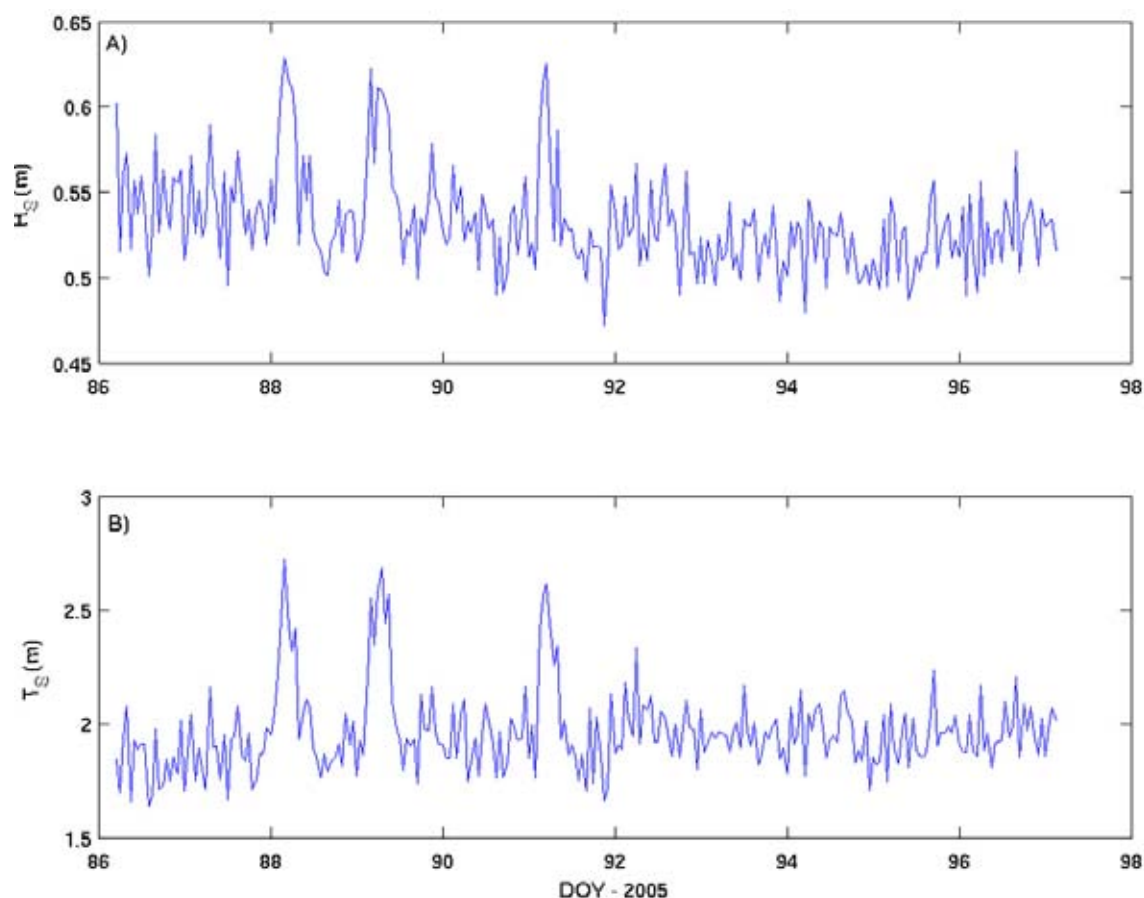


Figure 3.12. Time series of wave statistics recorded at Stn21CM4. A) Significant Wave Height, and B) Peak Wave Period.

3.2.10.3 Station 7CM2

At Stn7CM2, pressure is recorded by the ADCP. A time-series plot of sea-level recorded by the ADCP is shown in Figure 3.13. A slight offset was observed between the sealevel record of the first deployment (Stn7CM2; mean 41.2746 m), and the second deployment (Stn20CM3; mean 40.9857 m). To avoid the effects of this offset on sea level analysis, the second deployment time-series has the mean of the second deployment removed, and the mean of the first deployment added.

Table 3.11 presents the results of the tidal analysis of the sea-level record for the four largest constituents (M2, S2, O1, K1).

Table 3.11. Results from the classical harmonic analysis. Record length is 39.03 days. Start time is 28/02/05 00:00:00. Mean water depth from record is 41.3 m. Phase is with respect to Greenwich Mean Time.

TIDE	FREQUENCY (CPH)	AMPLITUDE (M)	AMP. ERROR (M)	PHASE (DEGREES)	PH. ERROR (DEGREES)
O1	0.0387307	0.4114	0.012	108.37	1.60
K1	0.0417807	0.3662	0.013	182.98	1.98
M2	0.0805114	0.1484	0.006	88.79	2.31
S2	0.0833333	0.0281	0.006	173.75	12.26

The form ratio, F, calculated at Stn7Cm2 is equal to 4.41, indicating that tides are strongly diurnal at the site.

Significant constituents calculated within the tidal analysis, where amplitude of a tidal constituent is greater than the calculated error in amplitude for that constituent, are predominantly in the diurnal and semi-diurnal bands (~ 0.04 and ~ 0.08 cph respectively) (Fig. 3.13 B). Some higher frequency constituents are also significant. Tidal phase, presented in Fig. 3.13 C) show that the significant constituents generally have small phase errors. The residual time-series after removal of the tidal signal has low amplitudes, indicating that the sea surface signal is almost entirely driven by tidal effects.

Each 8 minute burst obtained every 90 minutes on the Nortek has been used to compute the wave parameters (Tucker and Pitt, 2001). Velocity data components, u,v,w were resampled at 2Hz so that computation time was decreased. The MATLAB DIWASP functions were used to compute the significant wave height, peak wave period, and the dominant wave direction. The following DIWASP parameters were set:

- # directions in calculation – 180
- # Fourier Transforms in spectral estimation 1024
- # algorithm iterations – 100
- Smoothing enabled
- Direct Fourier Transform method.
- The x-axis direction was set to 270.

Figure 3.14 displays the calculated significant wave height (H_s), and the peak wave period (T_p) for the period of deployment. The analysis has resulted in a noisy wave record at the site. This is likely a result of the settings in DIWASP which could be improved in a more thorough analysis. The maximum significant wave height experienced during the course of the survey was 2.30 m on JD 87.96. The peak wave period at during this period was 2.94 s. Statistics of the waves recorded at Stn7CM2 are displayed in Table 3.12.

Table 3.12. Statistics of the waves recorded at Stn7CM2.

	MINIMUM	MEAN	MAXIMUM	STD DEVIATION
H_s (m)	1.26	1.86	2.30	0.15
T_p (s)	2.00	3.52	9.09	1.50

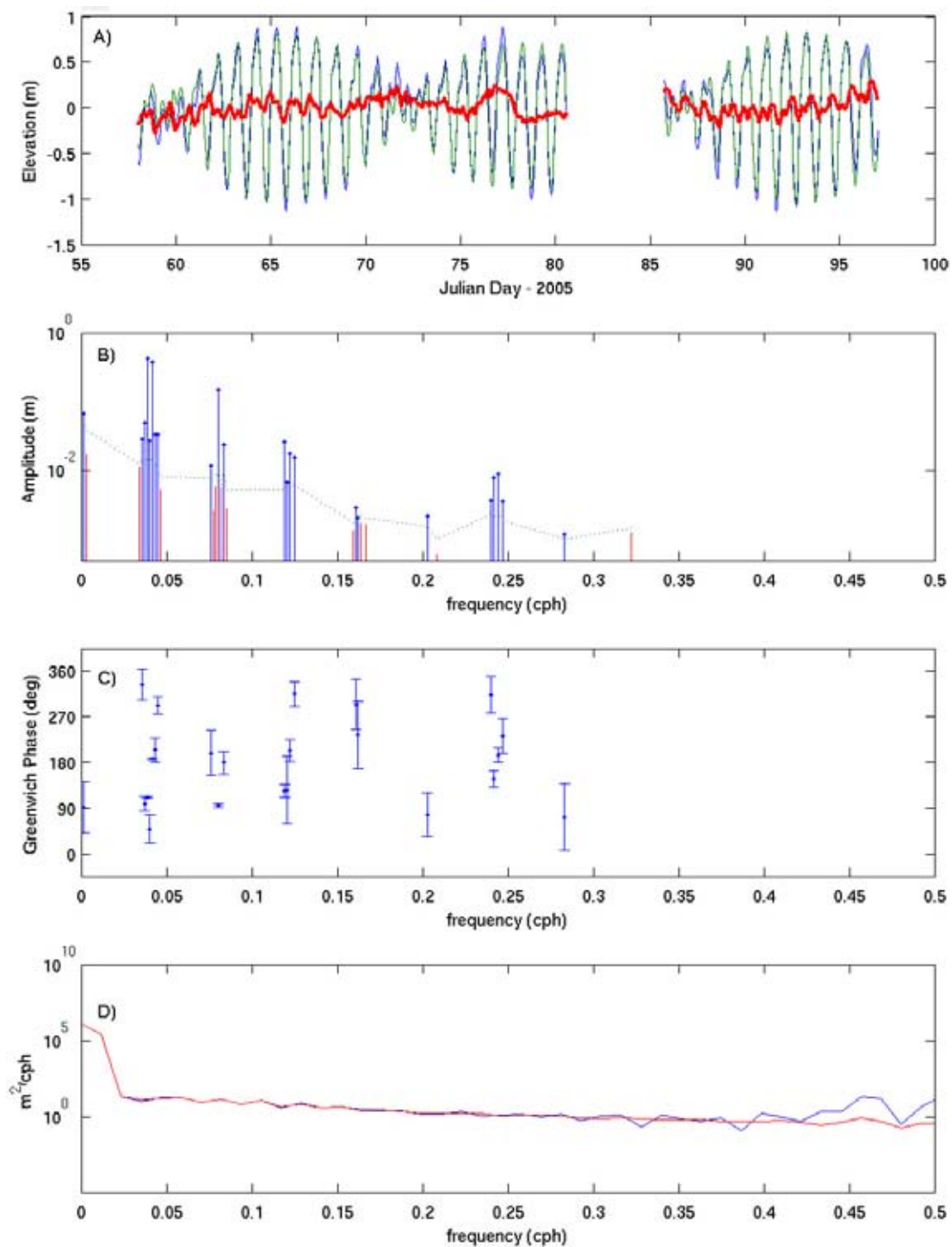


Figure 3.13. Results of classical harmonic analysis of pressure data from Stm7CM2. A) Blue line is Raw Time Series referenced to the mean level in the record, Green line is Tidal prediction from analysis referenced to the mean, Red line is residual time series after removal of the tidal signal; B) Amplitude of all analysed components with 95% significance level (green dashed line). Note frequency dependence. Significant constituents ($amp > amp_err$) are marked with a solid circle; C) Phase of significant constituents with 95% confidence interval; D) Spectral Estimates before and after removal of tidal energy. Blue-line is energy of original time-series, red-line is non-tidal energy.

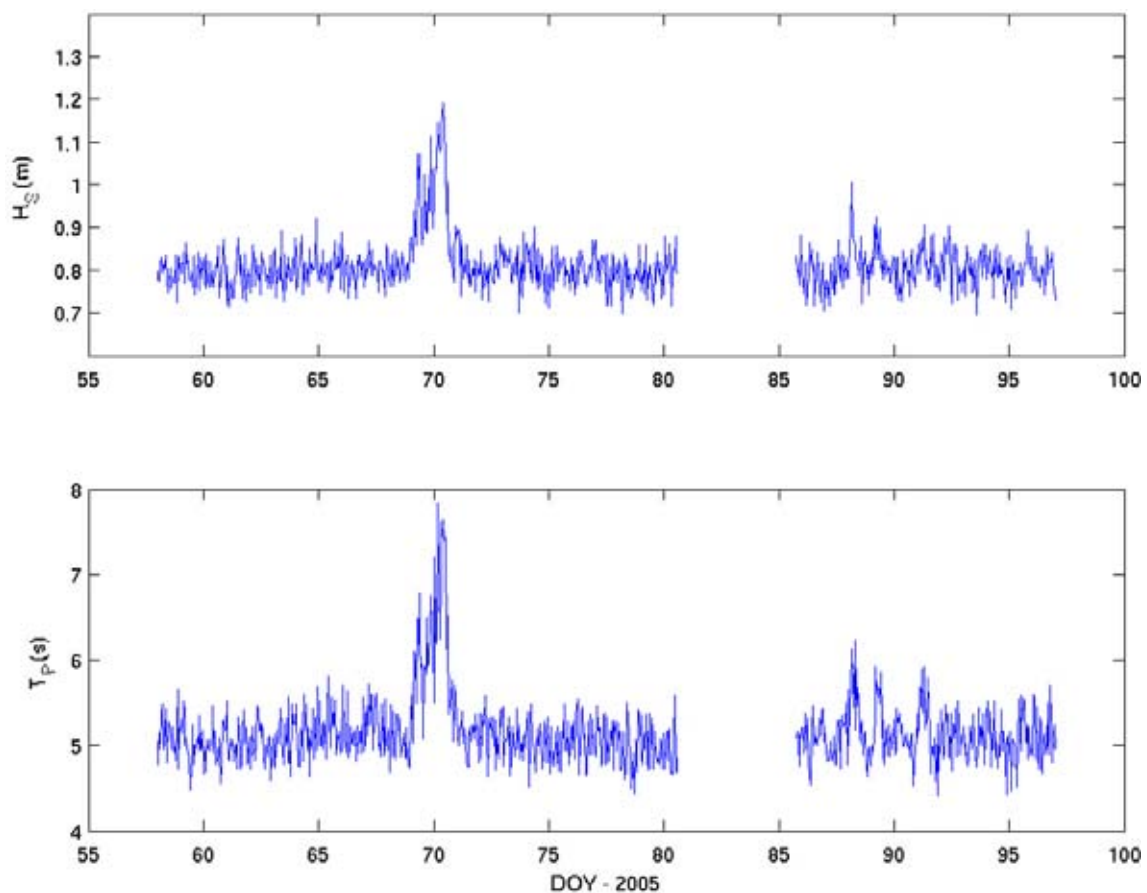


Figure 3.14. Time series of wave statistics recorded at Stn6CM1. A) Significant Wave Height, and B) Peak Wave Period, and C) Peak Wave Direction.

3.2.11 Current Measurements

3.2.11.1 Station 6CM1

A progressive vector plot for each of the bed currents, and that at the top of the water column are shown in [Figure 3.15](#) and time-series plots are shown in [Figure 3.16](#). Note that missing data does not contribute to calculated displacement. Given surface data contains a lot of missing data, the displacement is not comparable to currents at the seabed.

Time series of low-pass filtered current meter data Stn6Cm1 are show in [Figure 3.17](#). [Table 3.13](#) displays the principal axes for both the processed data and the low-passed currents for currents recorded at 1 m above the seabed.

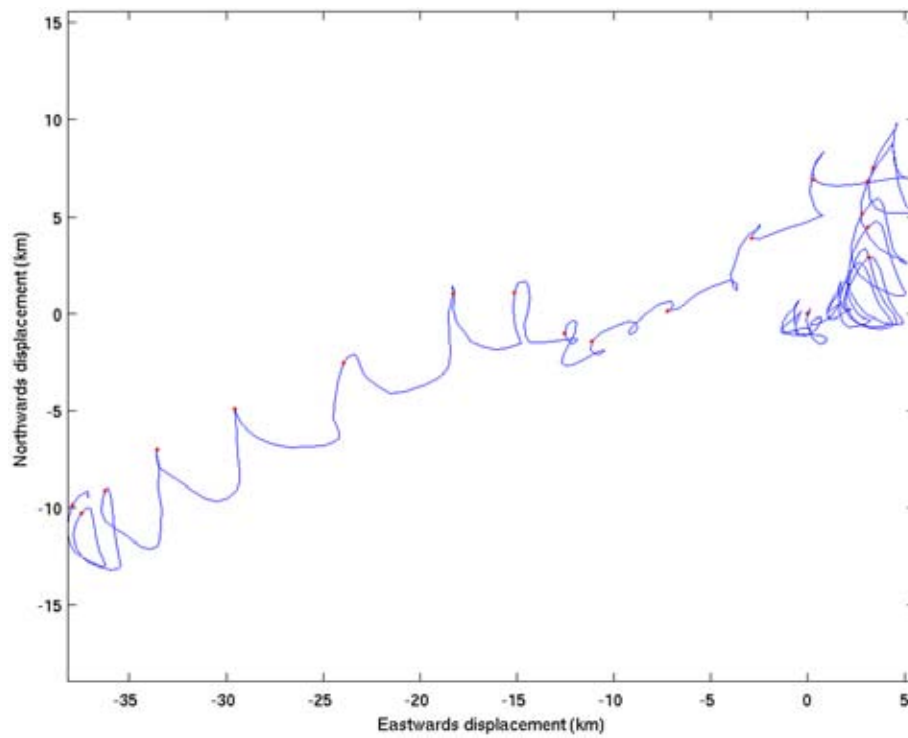


Figure 3.15. *Stn1CM6 current meter progressive vector plot obtained from data recorded. The origin of the plot corresponds to the location of the Stn2CM7 mooring. Dots indicate the beginning of each 24 hour period.*

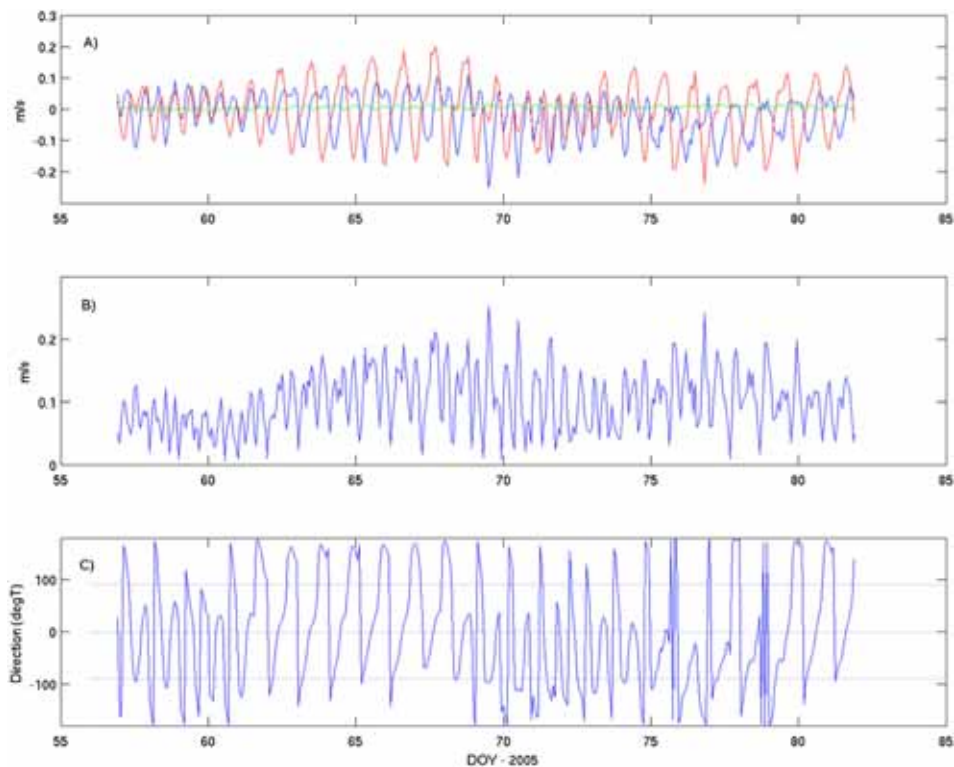


Figure 3.16. *Stn1CM6 current meter time-series obtained from data. A) Time series of East (Blue), North (Red), and Up (Green) velocity components B) Time series of absolute current speed, C) Time series of current direction.*

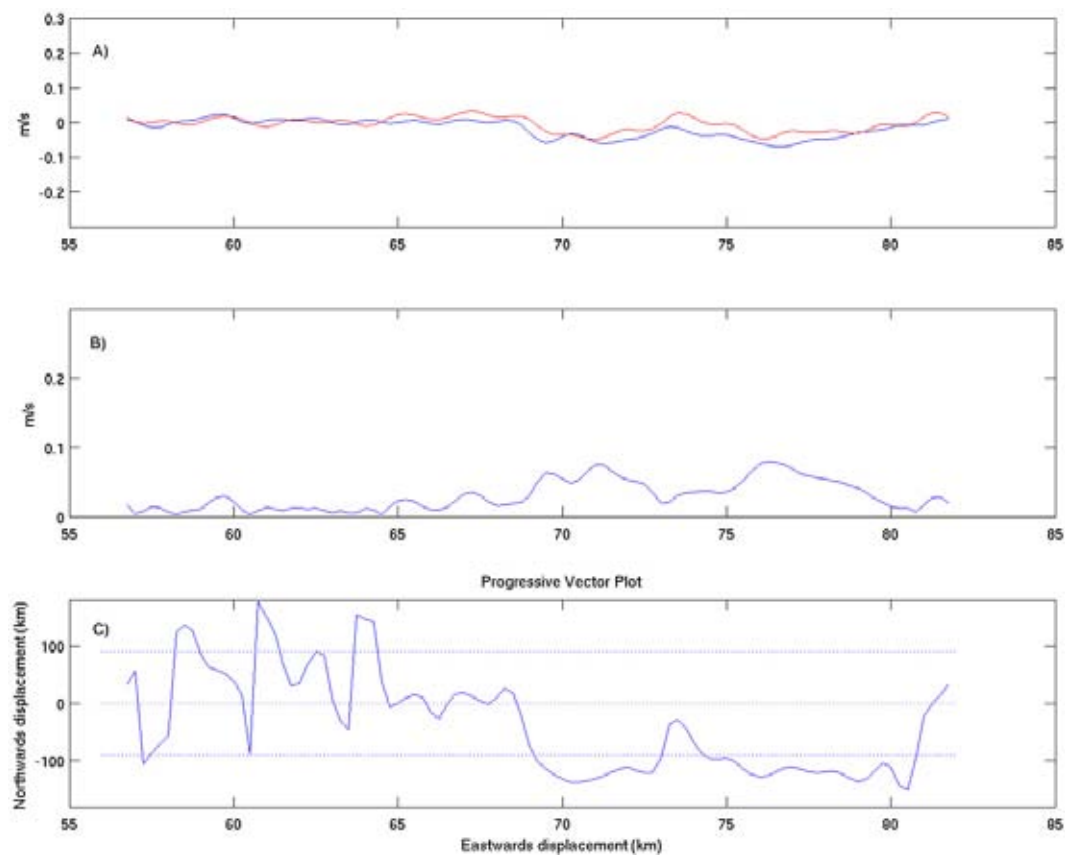


Figure 3.17. *Stn1CM6 Low-Pass Filtered current meter time-series obtained from data recorded. A) Time series of East (Blue), North (Red), and Up (Green) velocity components B) Time series of absolute current speed, C) Time series of current direction.*

Table 3.13. Station 6CM1. Principal axes of currents for currents at sea-bed and sea 'surface'. LP, indicates from Low Pass filtered record.

	1 M ABOVE SEABED
Major-	8.70
Minor -	6.64
Orient -	0.4312
Ellip	0.2374
Major – LP	3.13
Minor – LP	1.04
Orient – LP	-127.71
Ellip – LP	0.6674

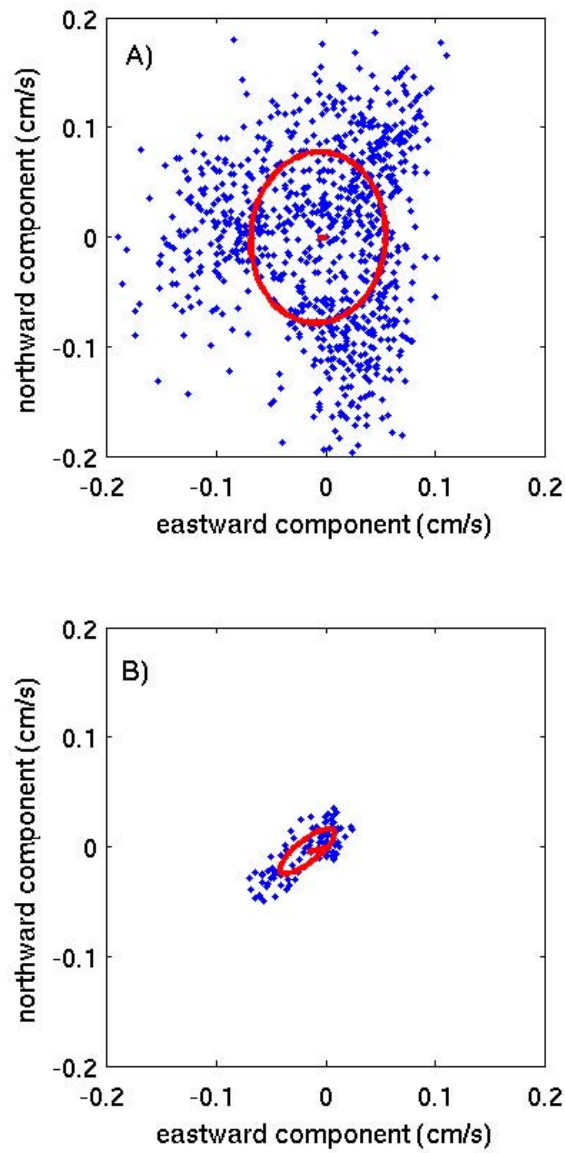


Figure 3.18. *Stn6CM1* scatter plots with the mean current vector (origin zero), and the ellipse of the principal axes of currents superimposed. The ellipse is centred upon the mean current vector: A) displays scatter plots of the basic 90-min processed current data from 1 m above the seabed; B) displays scatter plots of the low-pass filtered current data from 1 m above the seabed.

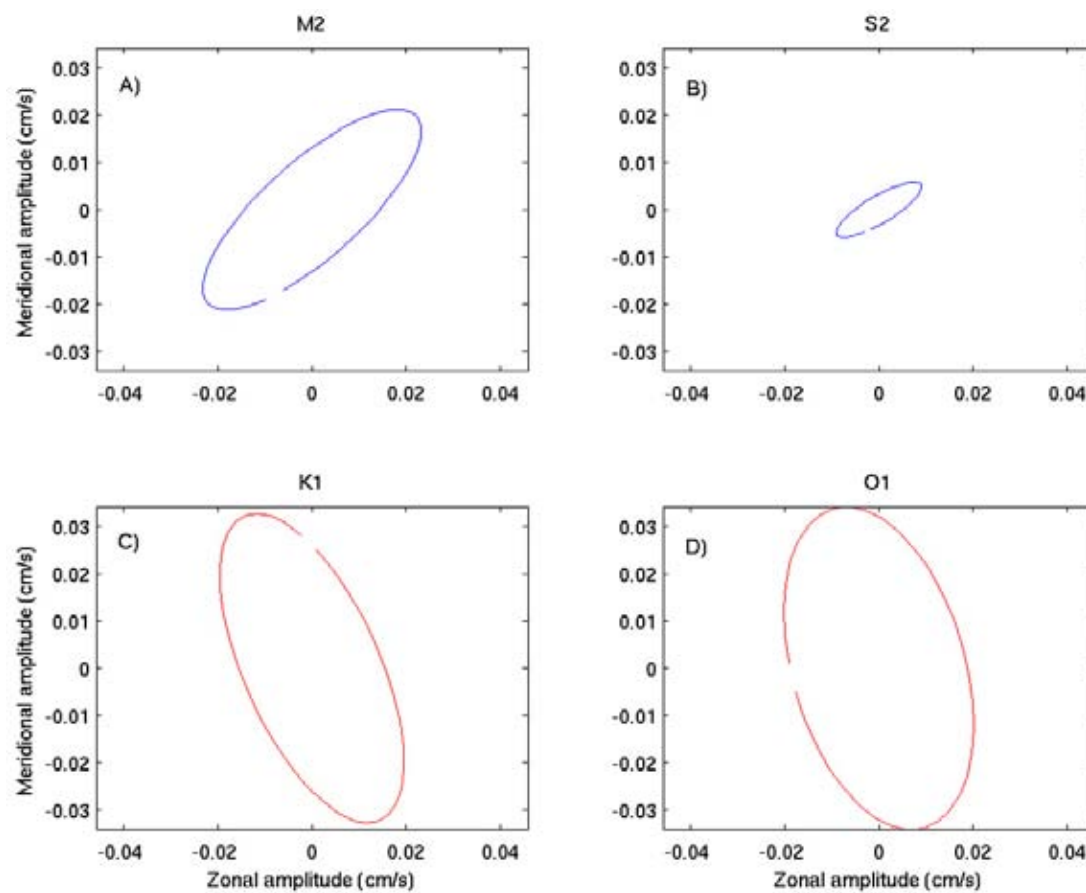


Figure 3.19 Tidal ellipse parameters for the four major constituents (M2, S2, K1, O1) are listed in Table 3.14 for the Stn6CM1 Mooring. Red indicates that the ellipses are travelled clockwise.

Table 3.14. Tidal Ellipse parameters of bed and surface currents from Mooring Stn6CM1.

CONSTITUENT	SEMI-MAJOR AXIS (CM/S)	ECCENTRICITY	INCLINATION (DEGREES)	PHASE (DEGREES)
M2	6.62	0.354	43.12	180.14
S2	2.78	0.280	32.50	55.73
K1	7.89	-0.390	113.51	213.15
O1	7.42	0.514	213.15	229.23

3.2.11.2 Station 21CM4

A progressive vector plot for each of the bed currents, and that at the top of the water column are shown in Figure 3.20. Note that missing data does not contribute to calculated displacement. Given surface data contains a lot of missing data, the displacement is not comparable to currents at the seabed. Time series of currents are shown in Figure 3.21. Table 3.15 displays the principal axes for both the processed data and the low-passed currents for currents recorded at 1 m above the seabed.

The principal axes for both the processed data and the low-passed currents for currents recorded at 1 m above the seabed are listed in Table 3.15.

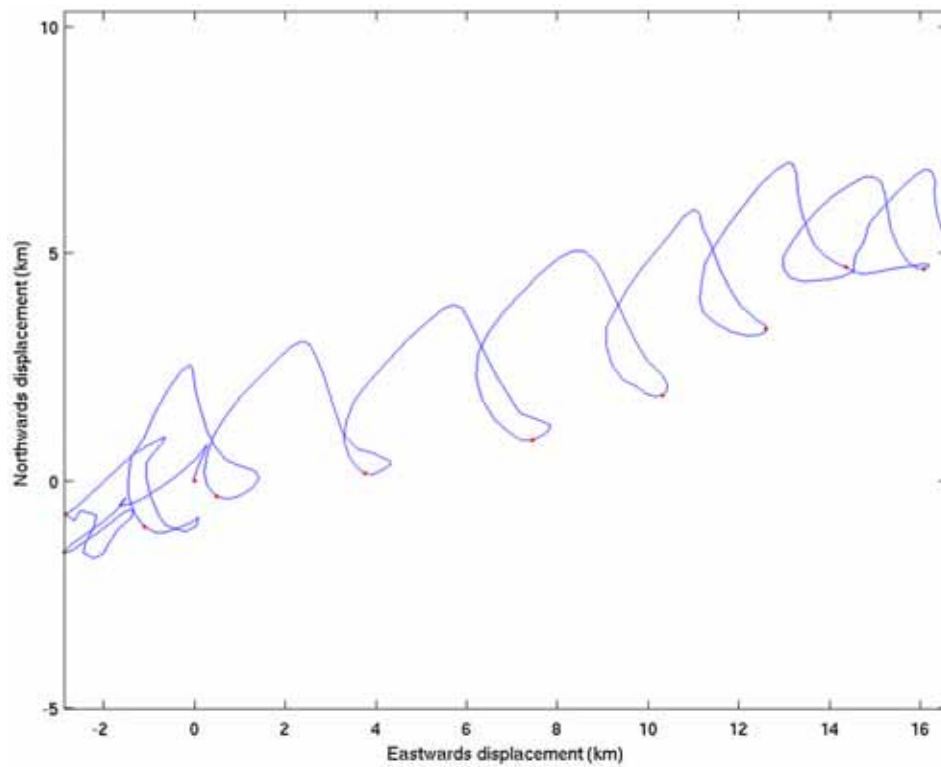


Figure 3.20. *Stn21CM4 current meter progressive vector plot obtained from data recorded. The origin of the plot corresponds to the location of the Stn21CM4 mooring. Dots indicate the beginning of each 24 hour period.*

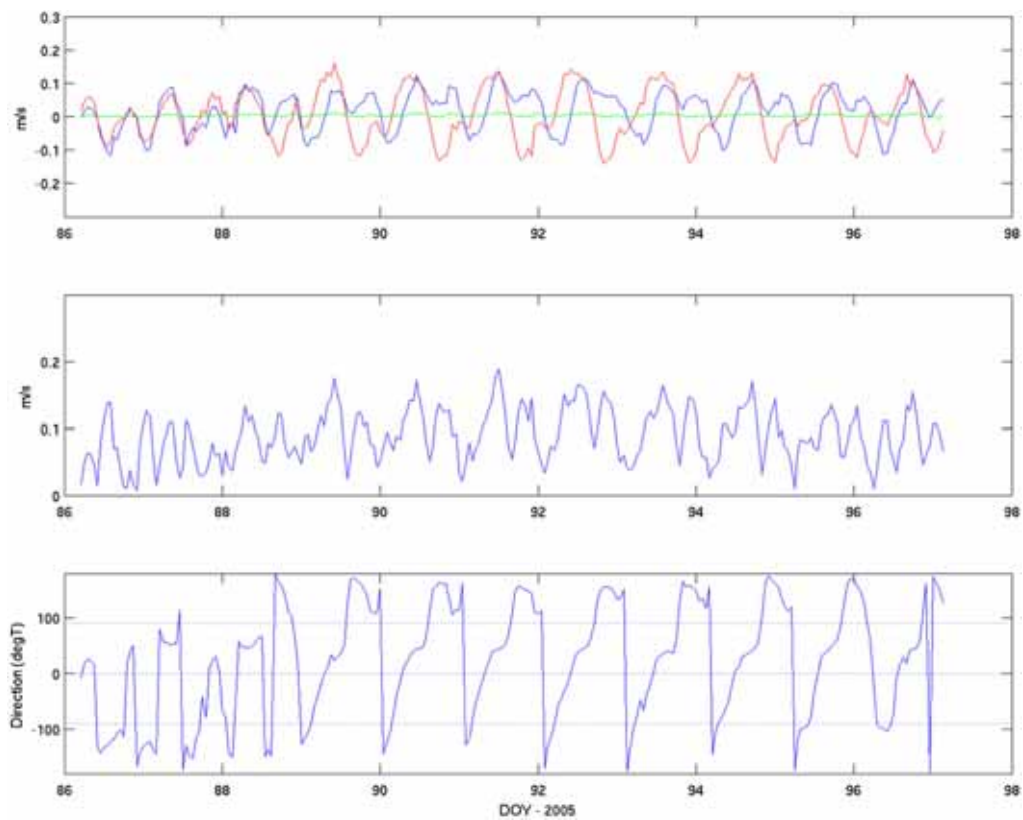


Figure 3.21. *Stn21CM4 current meter time-series obtained from data. A) Time series of East (Blue), North (Red), and Up (Green) velocity components B) Time series of absolute current speed, C) Time series of current direction.*

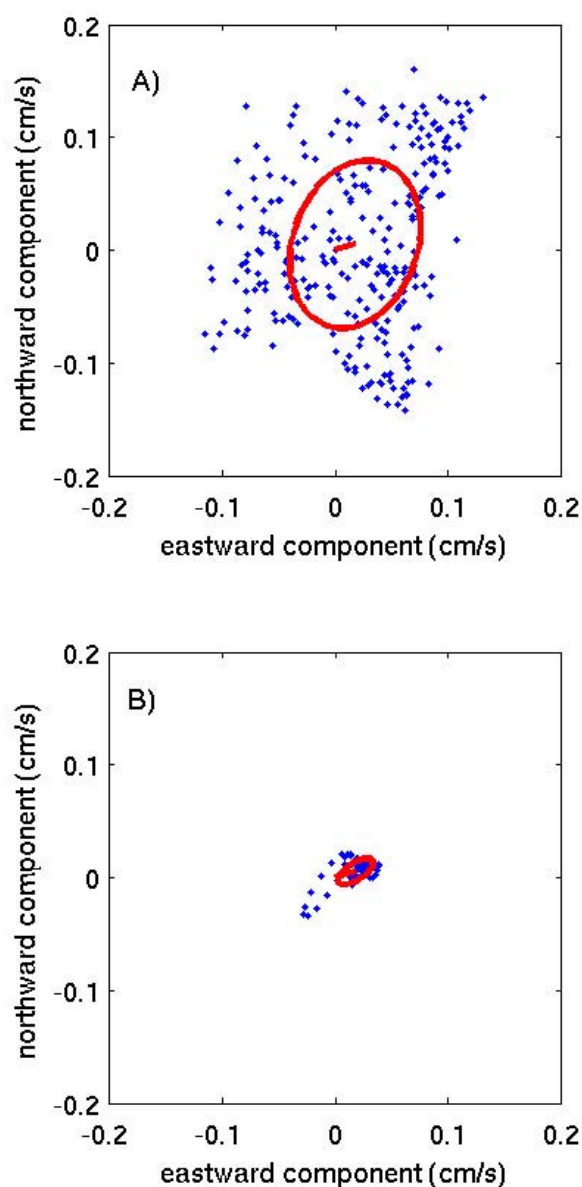


Figure 3.22. *Stn21CM4* scatter plots with the mean current vector (origin zero), and the ellipse of the principal axes of currents superimposed. The ellipse is centred upon the mean current vector: A) displays scatter plots of the basic 90-min processed current data from 1 m above the seabed; B) displays scatter plots of the low-pass filtered current data from 1 m above the seabed.

Table 3.15. Station 21CM4. Principal axes of currents for currents at sea-bed and sea 'surface'. LP, indicates from Low Pass filtered record.

	1 M ABOVE SEABED
Major-	7.79
Minor -	5.60
Orient -	18.63
Ellip	0.2810
Major – LP	6.55
Minor – LP	4.21
Orient – LP	-7.14
Ellip – LP	0.3569

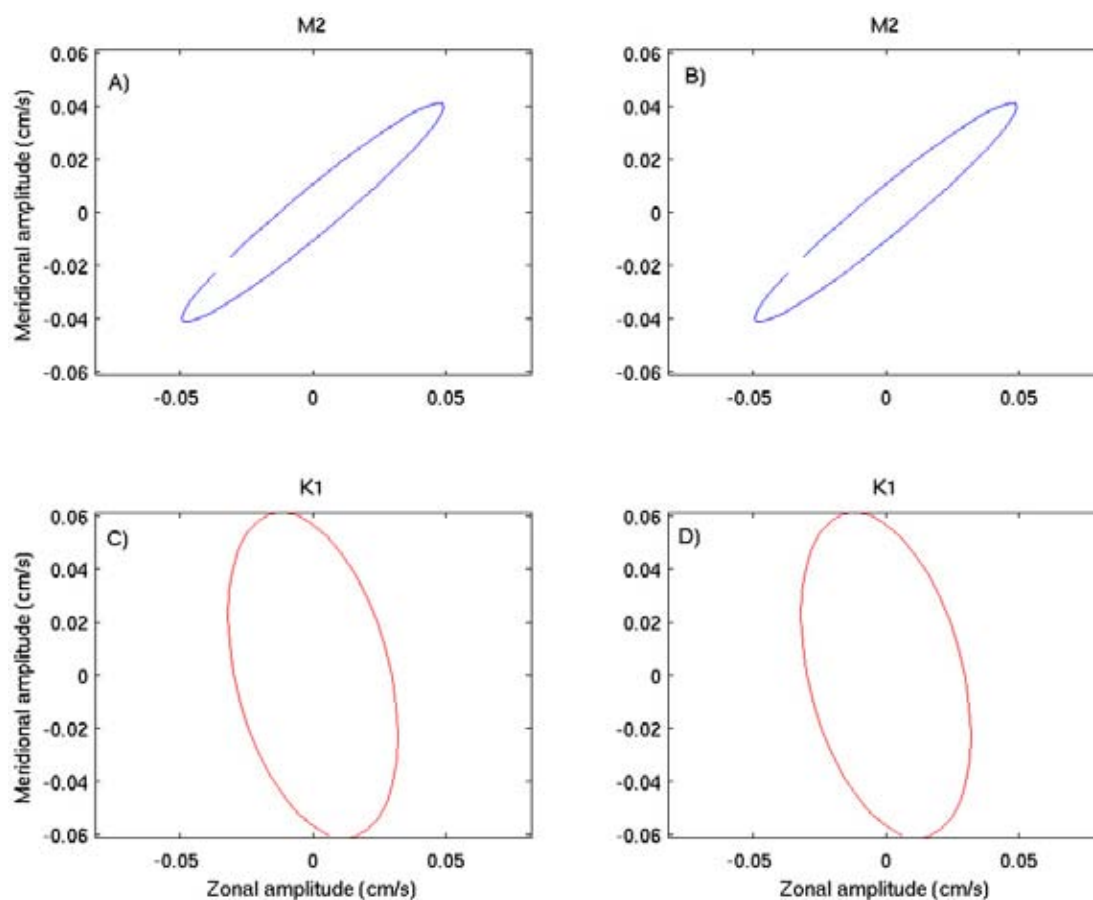


Figure 3.23 Tidal ellipse parameters for the four major constituents (M2, S2, K1, O1) are listed in Table 3.16 for the Stn21CM4 Mooring. Red indicates that the ellipses are travelled clockwise.

Table 3.16. Station 6CM1. Tidal ellipse parameters of bed and surface currents from Mooring 21CM4.

CONSTITUENT	SEMI-MAJOR AXIS (CM/S)	ECCENTRICITY	INCLINATION (DEGREES)	PHASE (DEGREES)
M2	6.38	0.131	39.83	14.79
S2				
K1	6.31	-0.459	103.96	119.38
O1				

3.2.11.3 Station 7CM2

A progressive vector plot for each of the bed currents, and that at the top of the water column are shown in Figure 3.24. Note that missing data does not contribute to calculated displacement. Time series plots of near bed and surface currents are shown in Figure 3.25 and 3.26, respectively.

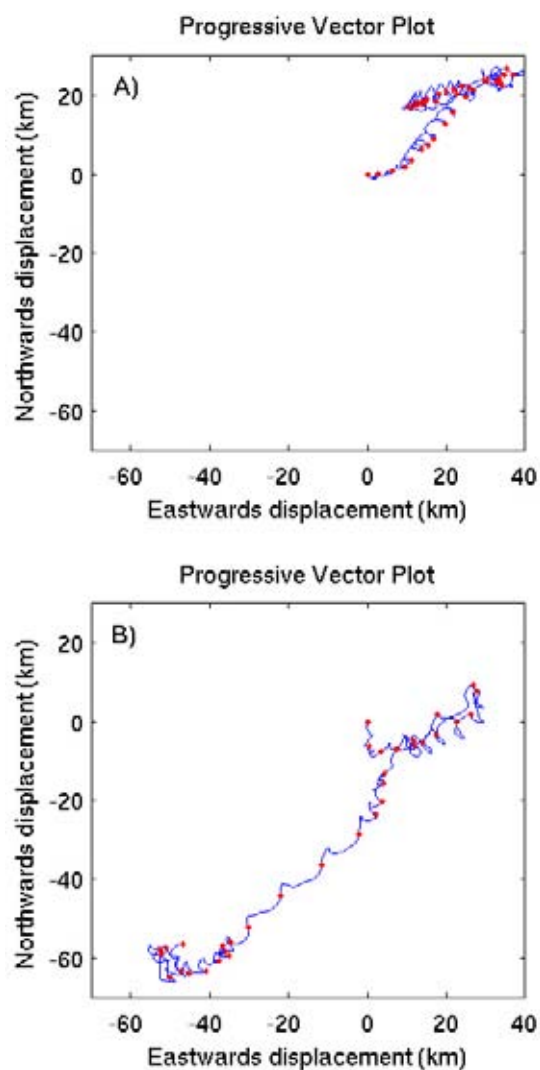


Figure 3.24. *Stn7CM2* current meter progressive vector plot obtained from data recorded in a) bin 1 (2.5 m above seabed), b) bin 24 (31.5 m above seabed). The origin of the plot corresponds to the location of the *Stn7CM2* mooring. Dots indicate the beginning of each 24 hour period.

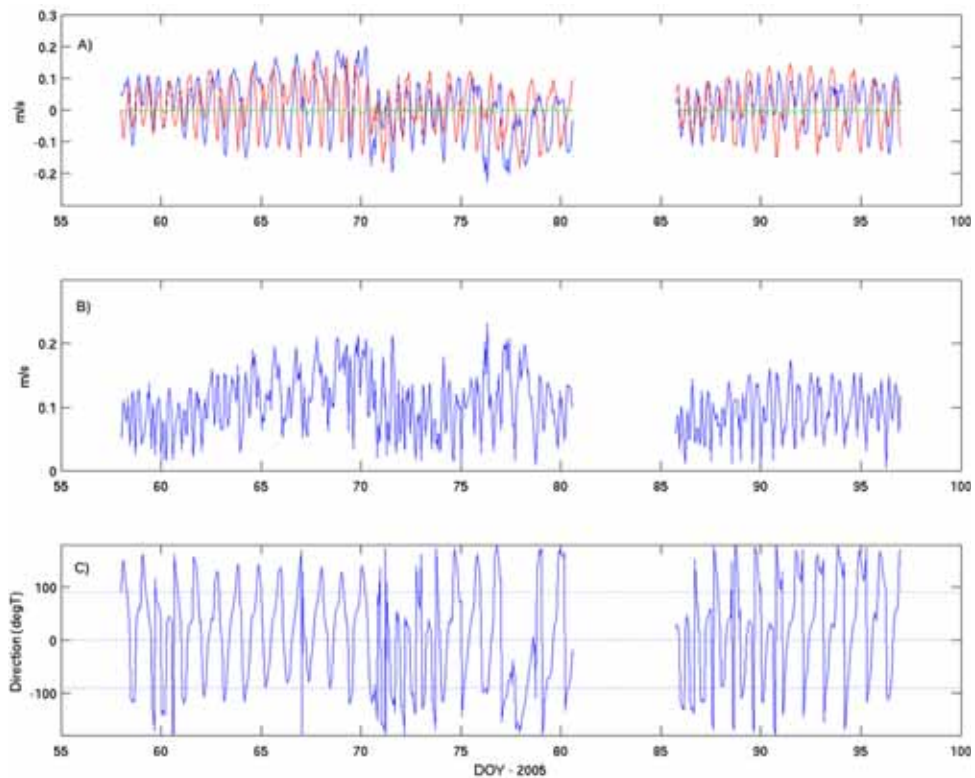


Figure 3.25. Stn7CM2 current meter time-series obtained from data recorded in bin 1 (2.2 m above seabed). A) Time series of East (Blue), North (Red), and Up (Green) velocity components B) Time series of absolute current speed, C) Time series of current direction.

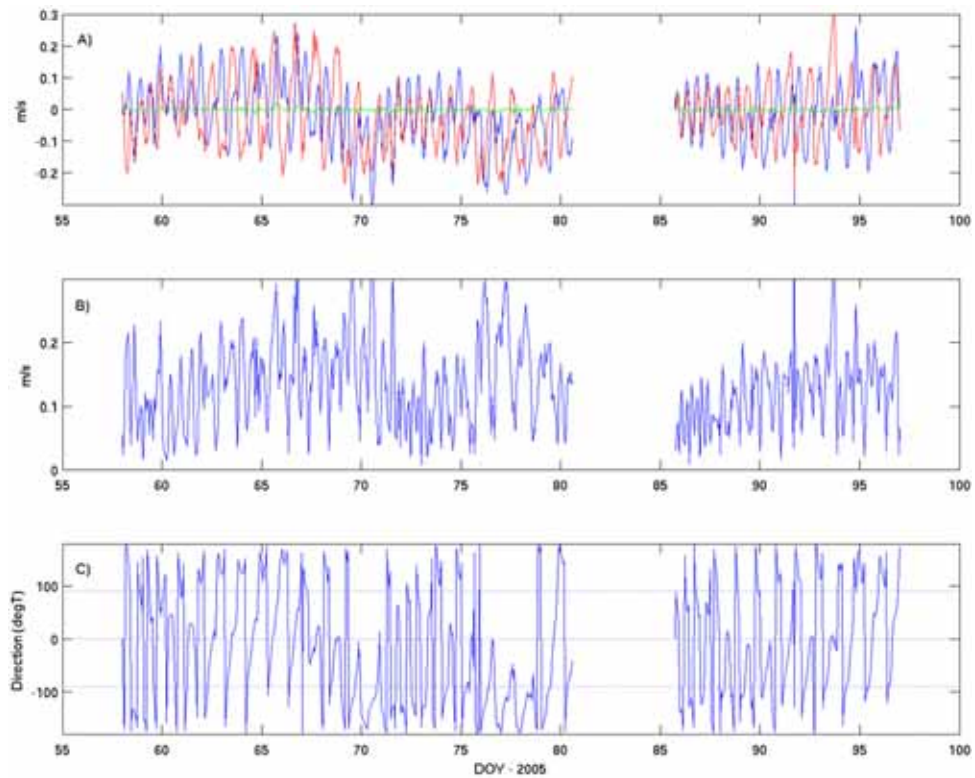


Figure 3.26. Stn7CM2 current meter time-series obtained from data recorded in bin 24 (31.5 m above seabed). A) Time series of East (Blue), North (Red), and Up (Green) velocity components B) Time series of absolute current speed, C) Time series of current direction.

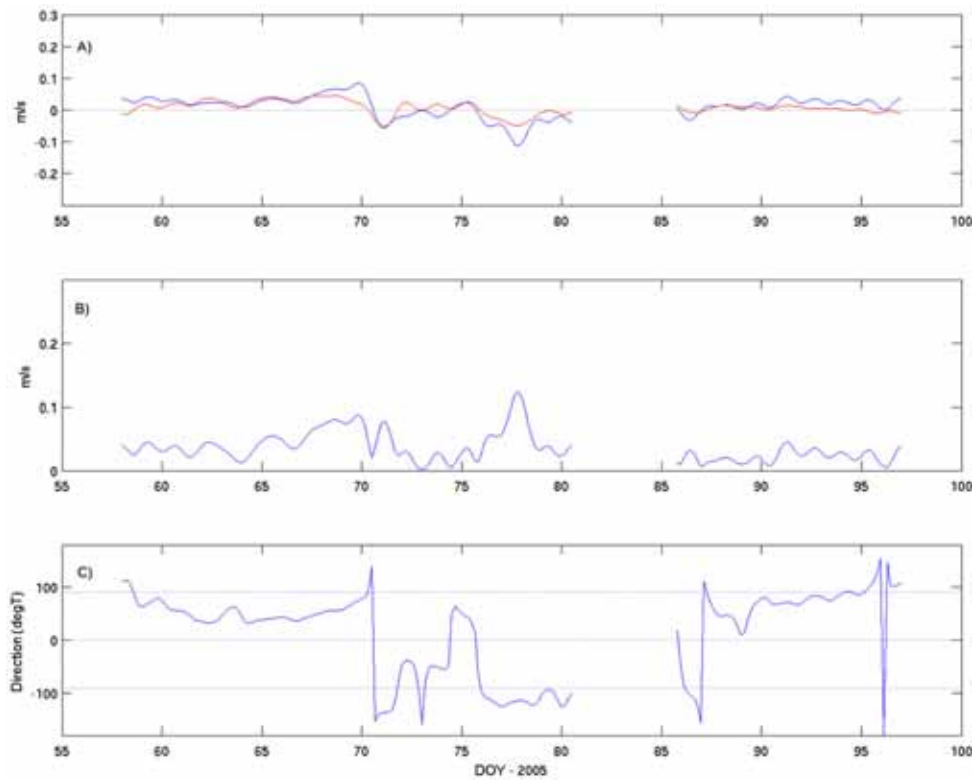


Figure 3.27. Stn7CM2 Low-Pass Filtered current meter time-series obtained from data recorded in bin 1 (2.2 m above seabed). A) Time series of East (Blue), North (Red), and Up (Green) velocity components B) Time series of absolute current speed, C) Time series of current direction.

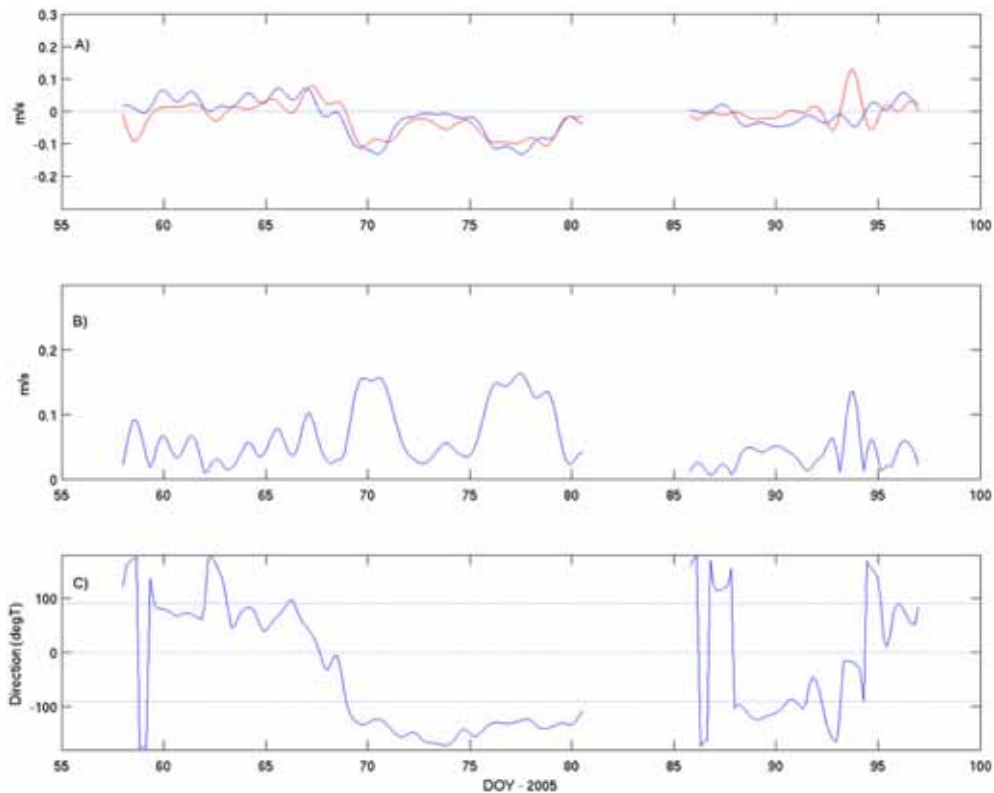


Figure 3.28. Stn7CM2 Low-Pass Filtered current meter time-series obtained from data recorded in bin 24 (31.5 m above seabed). A, B and C as in Fig 3.27.

Table 3.17 displays the principal axes for both the processed data and the low-passed currents for currents recorded in bin 1 (2.2 m above the bed), and bin 24 (31.5 m above the seabed = surface).

Table 3.17. Station 7CM2. Principal axes of currents for currents at sea-bed and sea ‘surface’. LP, indicates from Low Pass filtered record. Statistics in cm/s. MAB = meters above seabed.

	BIN 1 – 2.2 MAB	BIN 24 – 31.5 MAB – SURFACE
Major-	8.10	10.32
Minor -	6.50	9.09
Orient -	-121.66	-47.97
Ellip	0.1980	0.1192
Major – LP	3.66	5.09
Minor – LP	1.21	1.72
Orient – LP	-118.14	-103.10
Ellip – LP	0.6683	0.6631

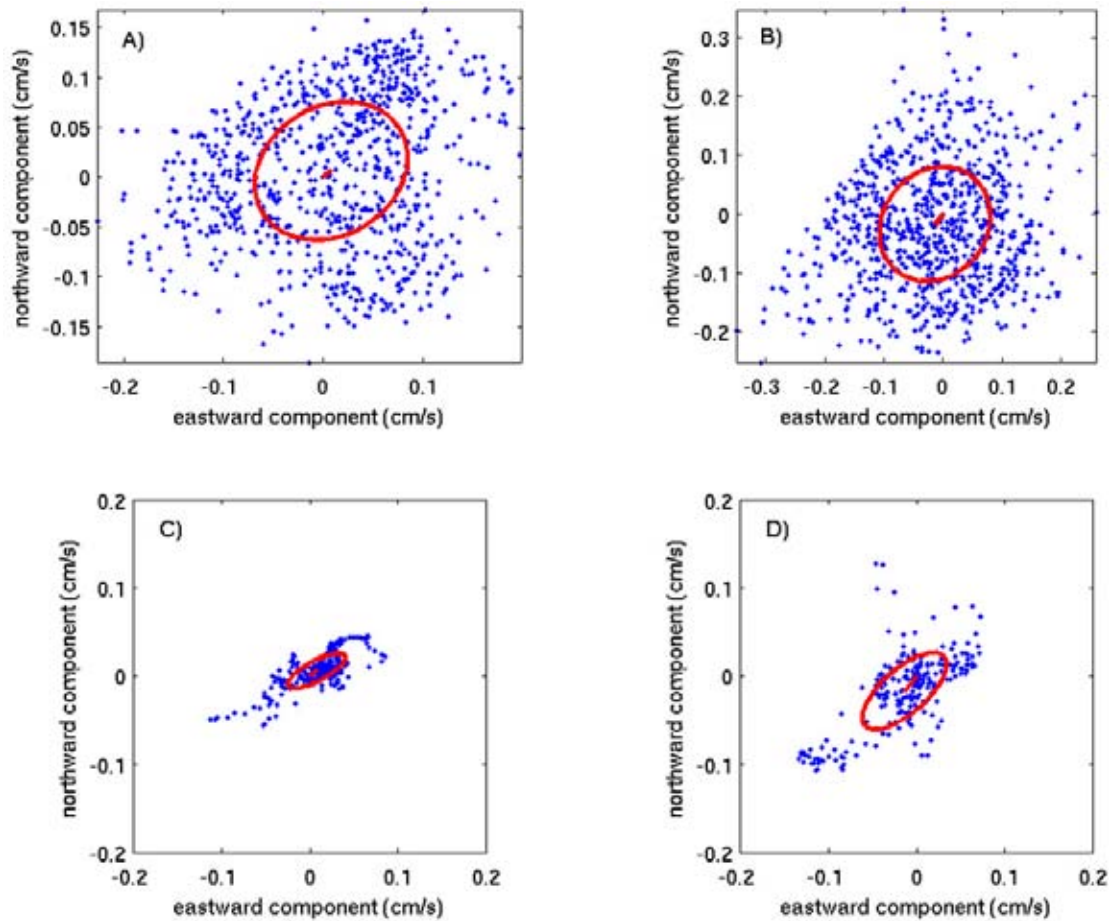


Figure 3.29. *Stn7CM2* scatter plots with the mean current vector (origin zero), and the ellipse of the principal axes of currents superimposed. The ellipse is centred upon the mean current vector: A) displays scatter plots of the basic 10-min processed current data from bin 1 (2.2 mab); B) displays scatter plots of the basic 10-min processed current data from bin 24 (31.5 mab); C) displays scatter plots of the low-pass filtered current data from bin 1 (2.2 mab); D) displays scatter plots of the low-pass filtered current data from bin 24 (31.5 mab).

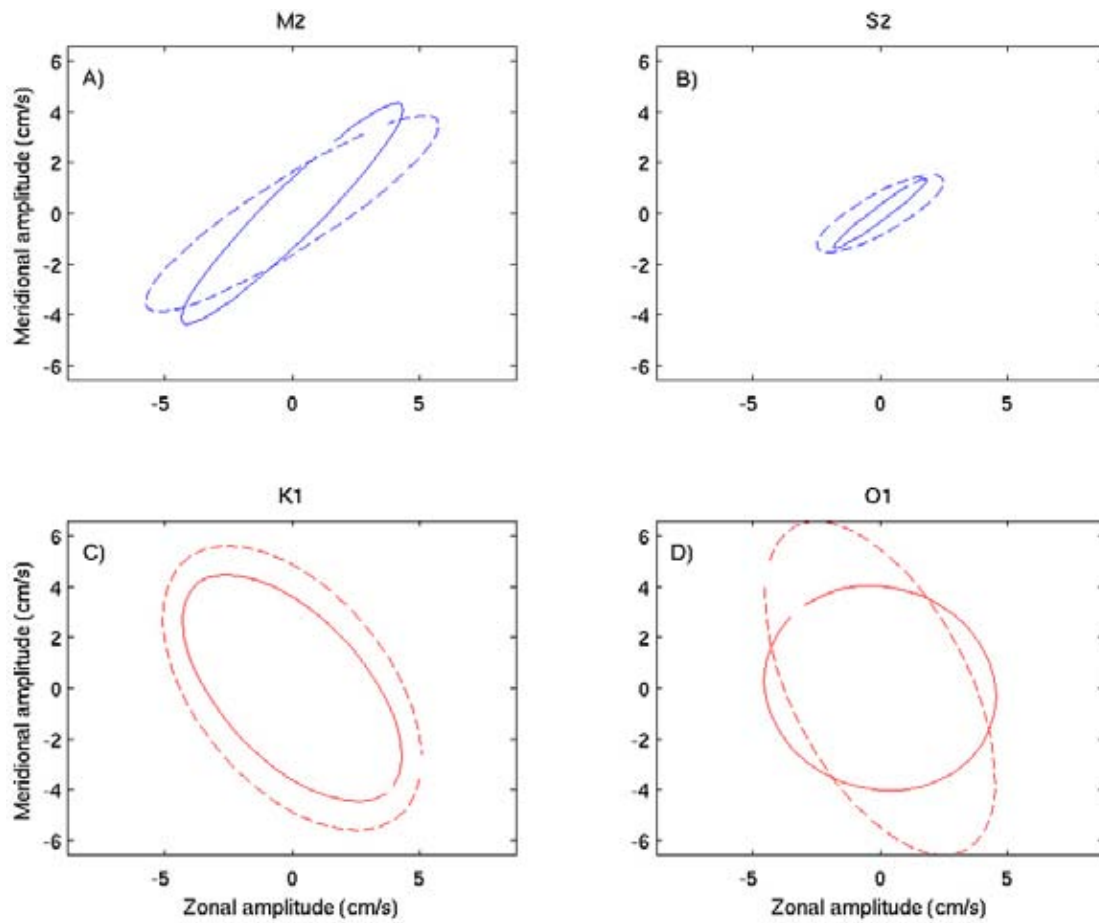


Fig 3.30 Tidal ellipse parameters for the four major constituents (M2, S2, K1, O1) are listed in Table 3.18 for the station 4CM3, for each of the bed currents (bin 1), and from the 'surface' currents (bin 24). Red indicates that the ellipses are travelled clockwise, dashed lines indicate surface (bin 24) ellipses.

Table 3.18. Stn7CM2. Tidal Ellipse parameters of bed and surface currents from Mooring Stn4CM3.

BIN	CONSTITUENT	SEMI-MAJOR AXIS (CM/S)	ECCENTRICITY	INCLINATION (DEGREES)	PHASE (DEGREES)
1	M2	7.31	0.1844	45.86	284.99
	S2	2.62	0.0168	39.06	286.68
	K1	7.07	-0.4247	133.78	187.29
	O1	6.22	0.7023	160.19	311.83
24	M2	8.15	0.1745	32.42	305.30
	S2	3.92	0.2122	25.58	300.68
	K1	8.32	-0.5308	135.46	207.93
	O1	7.84	-0.5571	116.39	12.82

3.2.12 Bedload Transport Estimates

3.2.12.1 Station 6CM1

Table 3.19 lists the calculated total bedload and direction at Station 6CM1 for the entire deployment using each of the defined formulations. Vector stick plots are plotted for bedload for each method in Figure 3.31.

Table 3.19. Total bedload and direction at Station 6CM1 for the entire deployment using each of the defined formulations.

	BAGNOLD (GADD ET AL., 1978)	ENGELUND- HANSEN	EINSTEIN- BROWN	YALIN	BAGNOLD (HARDISTY, 1983)
Q – Ave. (10^{-5} g cm $^{-1}$ s $^{-1}$)	0.0	4.50	0.345	450.0	0.0
Q - total (10^3 g cm $^{-1}$)	0.0	0.03	0.002	1.56	0.0
Dirn (° True)	NA	-126.9	-128.09	-97.68	NA

3.2.12.2 Station 21CM4

Table 3.20 lists the calculated total bedload and direction at Station 21CM4 for the entire deployment using each of the defined formulations. Vector stick plots are plotted for bedload for each method in Figure 3.32.

Table 3.20. Total bedload and direction at Station 21CM4 for the entire deployment using each of the defined formulations.

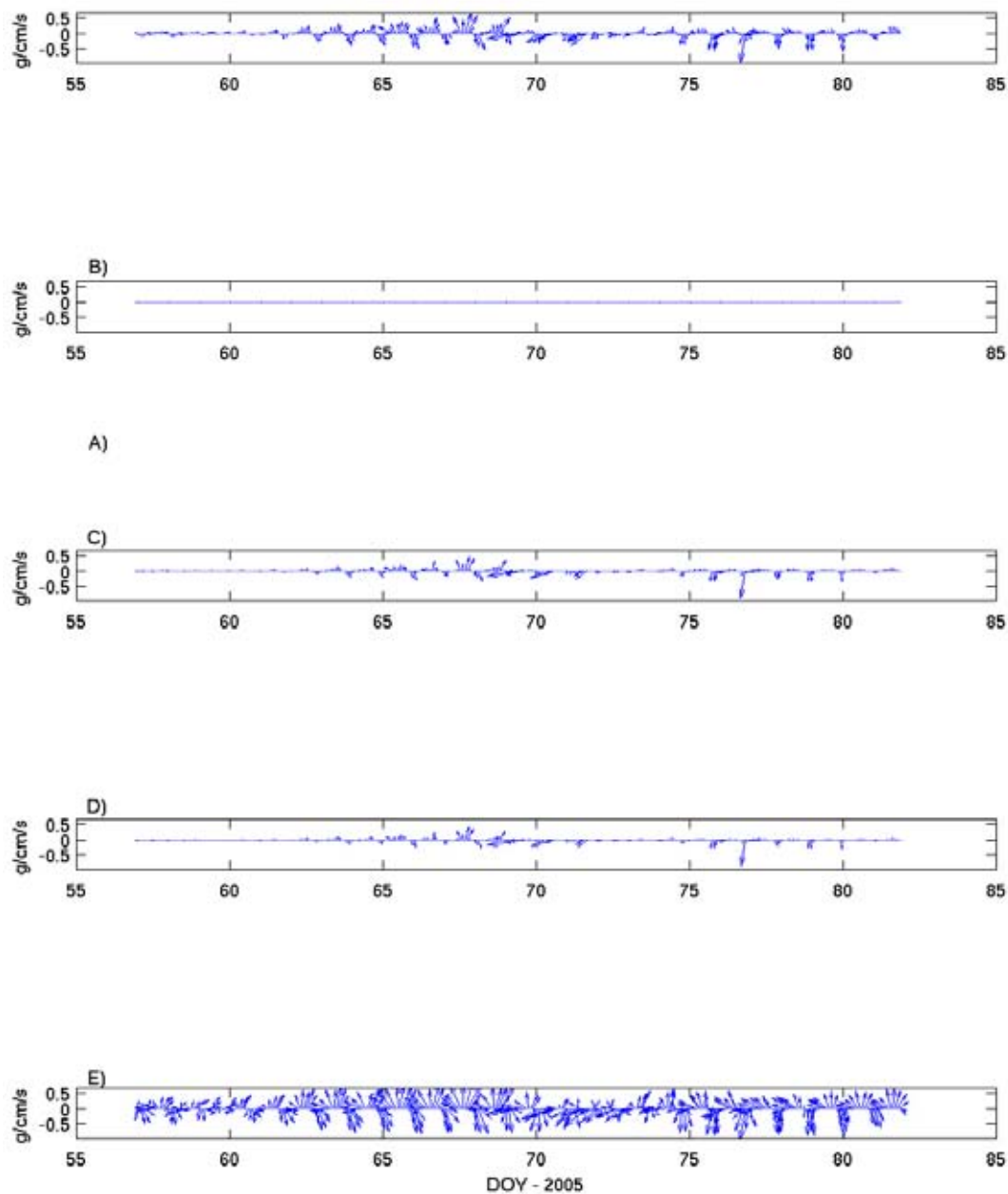
	BAGNOLD (GADD ET AL., 1978)	ENGELUND- HANSEN	EINSTEIN- BROWN	YALIN	BAGNOLD (HARDISTY, 1983)
Q – Ave. (10^{-5} g cm $^{-1}$ s $^{-1}$)	0.0	2.02	0.123	432.1	0.00
Q - total (10^3 g cm $^{-1}$)	0.0	0.092	0.0063	7.30	0.0
Dirn (° True)	NA	53.91	51.84	78.67	NA

3.2.12.3 Station 7CM2

Table 3.21 lists the calculated total bedload and direction at Station 7CM2 for the entire deployment using each of the defined formulations. Vector stick plots are plotted for bedload for each method in Figure 3.33.

Table 3.21. Total bedload and direction at Station 7CM2 for the entire deployment using each of the defined formulations.

	BAGNOLD (GADD ET AL., 1978)	ENGELUND- HANSEN	EINSTEIN- BROWN	YALIN	BAGNOLD (HARDISTY, 1983)
Q – Ave. ($10^{-5} \text{ g cm}^{-1} \text{ s}^{-1}$)	0.0	4.00	0.287	470.0	0.00
Q - total (10^3 g cm^{-1})	0	17.5	1.23	1468.4	0
Dirn ($^{\circ}$ True)	NA	69.70	69.09	46.34	NA

**Figure 3.31.** Vector stick plots of bedload transport at Stn6CM1, as calculated using a) Bagnold (Gadd et al., 1978), b) Engelund Hansen, c) Einstein-Brown, d) Yalin, e) Bagnold (Hardisty, 1983).

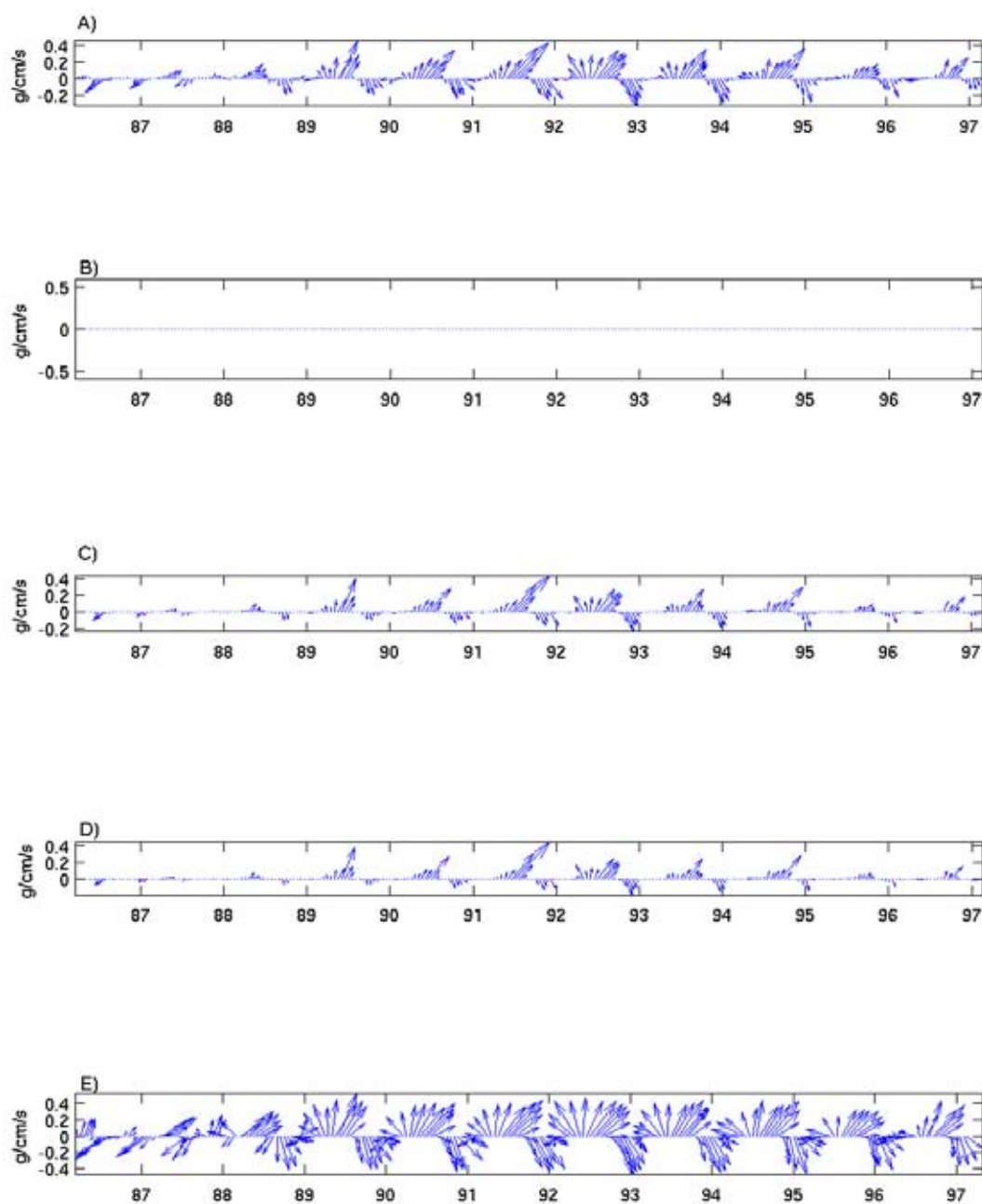


Figure 3.32. Vector stick plots of bedload transport at Stn6CMI, as calculated using a) Bagnold (Gadd *et al.*, 1978), b) Engelund Hansen, c) Einstein-Brown, d) Yalin, e) Bagnold (Hardisty, 1983).

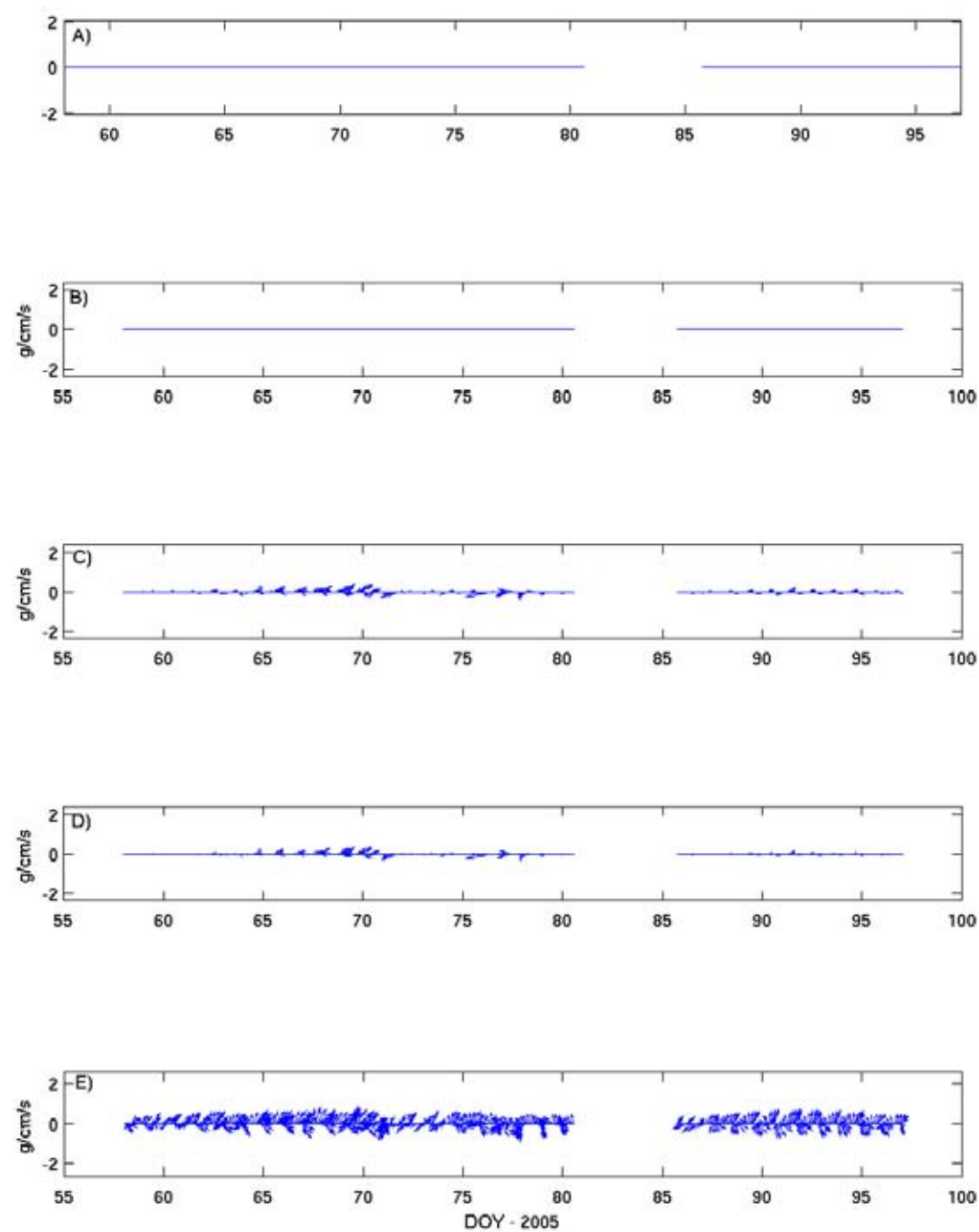


Figure 3.33. Vector stick plots of bedload transport at Station 7CM2, as calculated using a) Bagnold (Gadd et al., 1978), b) Engelund Hansen, c) Einstein-Brown, d) Yalin, e) Bagnold (Hardisty, 1983).

Chapter 4. Underwater Drilling Results

4.1 INTRODUCTION

During survey 276 rotary drilling was carried out at 43 sites (Table 4.1) at all seven of the reefs sites mapped during the survey (reefs R4 to R7; see Fig. 4.1). Drill cores were also collected from reefs R1, R2 and R3 that had been previously documented (see Chapter 1). Cores from these first 3 reefs (R1-R3) recovered coral material and confirmed the coral reef composition of these features, as well as of the large platform reefs located west of Mornington Island (Reefs R4 and R5) and two additional patch reefs mapped further towards the west near the Sir Edward Pellew Island Group (Reefs R6 and R7). Drilling was also carried out at one site on a bryozoan-mollusc (BRYOMOL) carbonate platform located to the east of Mornington Island (Fig. 4.1).

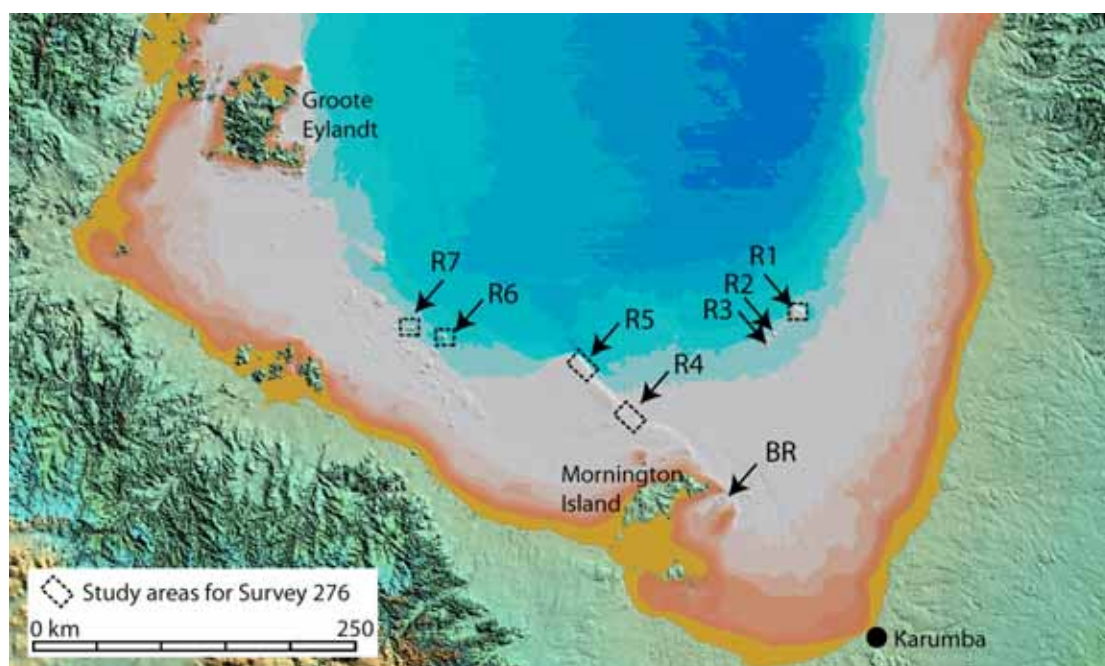


Figure 4.1 Bathymetric map of the southern Gulf of Carpentaria showing the locations of reefs R1 to R7 that were drill targets during survey 276. The location of the BRYOMOL reef (BR) drill target is also indicated.

4.1.1 Description of the Underwater Drill

Drilling was carried out using a portable rotary drill, equipped with a diamond cutting bit and water-pumping system. Seawater was pumped from a ship-board water pump down an umbilical cable to the drill tower (Fig. 4.2), where it passed down a cavity in the core barrel (between the liner and outside core barrel) before exiting via small outlets in the cutting bit. Flushing was continuous throughout the drilling operations to keep the drill bit clear of debris.

The overall weight of the drill is around 2,000 kg, and hydraulic legs could be raised or lowered to level the drill frame and to put pressure on/off of the drill cutter during drill operations. Rotation of the drill at speeds of around 30 RPM was powered by another hydraulic motor located at the top of the core barrel. The drill speed and hydraulic systems were all operated remotely from a control panel on board the ship. Stopping and starting of the drill during the operations was sometimes found to break the drill free from obstructions and improved drill penetration. Sensors on the derrick monitored the depth of vertical drill penetration into the seabed.

The drill is capable of taking up to 3.0 m length of core in water depths up to 50 m. Core recovery varied from 0.10 to 2.55 m (Fig. 3.3), with a total recovery of 39 m and an average recovery of 0.93 m (see table 4.1).

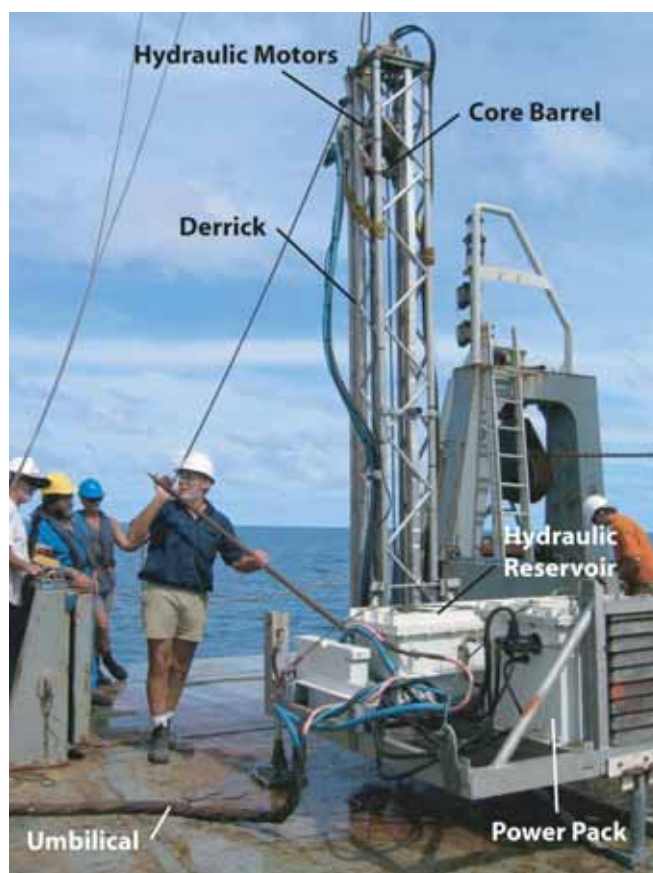


Figure 4.2. Photograph of the Geoscience Australia rotary drill, used on Survey 276. The drill was operated at water depths of up to 44 m and a maximum core length of 2.55 m was recovered.

Technical specifications of the Geoscience Australia drill are as follows:

Power unit on rig:	Electric motor-driven hydraulic power pack.
Control:	24 volt industrial hydraulic control from panel.
Monitoring:	Video camera, industrial proximity sensors.
Hydraulic pressure:	0 to 1800 psig.
Power for Drill Rig:	415 volt 3 phase 32 amp 50Hz circuit.
Power for Water Pump:	415 volt 3 phase 32 amp 50Hz circuit.
Water for Water Pump:	Self priming to a height of 3 metres.
Folded Mast:	W 2000mm x L 4500mm x H 1700mm.
Vertical Mast:	W 2000mm x L 2000mm x H 4700mm.
Weight:	2000 kg.
Lifting Height:	6 metres under A-frame for deployment. (lower A-frame clearances can be used with special deployment techniques).
Drill Barrel:	NMLC triple tube.
Core Diameter:	50 mm.
Hole Diameter:	75.7 mm.
Core Length:	3000 mm.
Core Bit:	7/9 3 step 25 ct N00D bit.

Size:	75 mm diameter x 70 metres long x 170 kg.
Power Cable:	3 phase power cable, 32 amp.
Control Cable:	Treotham rubber sheathed A07 27 x 1.5.
Water Hose:	19 mm chemical 300 psi.
Video Cable:	3 x coaxial cables x 75 ohm.

The rig is lowered over the side of the ship using the A-frame and with the mast in the vertical position (Fig. 4.2). When on the sea floor the drill rig is levelled and the operator then commences drilling, with drill speed and water pressure being varied to suit the conditions. The position of the drill barrel and the depth of penetration are monitored by the video camera, and drilling continues until either no further penetration can be achieved or the barrel achieves full penetration. The drilling procedure normally lasted around 45 minutes, although bottom time varied depending on the conditions. Up to 900 kg of pull out force can be exerted on the drill barrel during extraction, with or without rotation. Once back on board, the mast is lowered and the core extracted from the drill barrel.

4.1.2 Core Descriptions and Logging

In the laboratory the cores were split, and one half was kept as an archive while the other was used for analysis. The archive half was described in detailed core logs (Appendix 4). The cores were photographed and the digital image archived (Appendix 5). The reef-limestone cores were classified using a modification of the original Dunham (1962) classification, along with depositional textures described by Embry and Klovan (1971). For clarification, a brief description of each category is given below:

- Mudstone*: mud (<62 µm)-supported fabric with <10% sand-size grains.
- Wackestone*: mud-supported fabric with >10% sand-size grains.
- Packstone*: grain-supported (62-2000 µm) fabric with intergranular mud.
- Grainstone*: grain-supported fabric with no mud.
- Floatstone*: matrix-supported fabric with grains >2000 µm in size.
- Rudstone*: grain-supported fabric with grains >2000 µm in size.
- Bafflestone*: formed by organisms that trap sediment.
- Boundstone*: components organically bound during deposition.
- Framestone*: formed by organisms which build a rigid framework.
- Coral*: Discrete colonies or parts thereof that consist entirely of scleractinian corals.

The core logs, as well as showing the textural/depositional classification also show the position of, and value of, any age determinations, the position of the solution unconformity (i.e. the boundary between the Holocene and Pleistocene sections), and, in places, selected photographs of pertinent parts of the core (Appendix 5). During the core description process, samples were designated for both thin section and/or X-ray diffraction (XRD) analysis. With the latter, only corals in good condition were selected because they eventually would be required for dating.

A total of 169 thin sections were prepared for petrographic analysis. Petrographic descriptions were carried out on each thin section (Appendix 6) and photomicrographs taken where appropriate (Appendix 7).

A total of 55 samples were submitted to the Department of Marine and Earth Sciences, Australian National University for mineralogical determination using X-ray diffraction (XRD). The results of these analyses are presented in Table 4.2.

4.2 LITHOLOGICAL ANALYSIS OF DRILL CORES

In this section a description of each core is provided, with data derived from the visual core log descriptions (Appendix 4), core photographic images (Appendix 5), thin section descriptions

(Appendix 6), thin section descriptions photomicrographs (Appendix 7), mineralogical determination derived from X-ray diffraction analyses (XRD; Table 4.2), and uranium-series age determinations (Table 4.3).

Where possible, each core is divided into a Holocene and Pleistocene Section. The division is usually based on a combination of age, XRD, lithology and diagenesis. However, in a few cores the division is not as clear-cut, usually because of a lack of XRD data and/or age determination, or poor resolution of diagenetic features. The boundary between the two is usually marked by a solution unconformity.

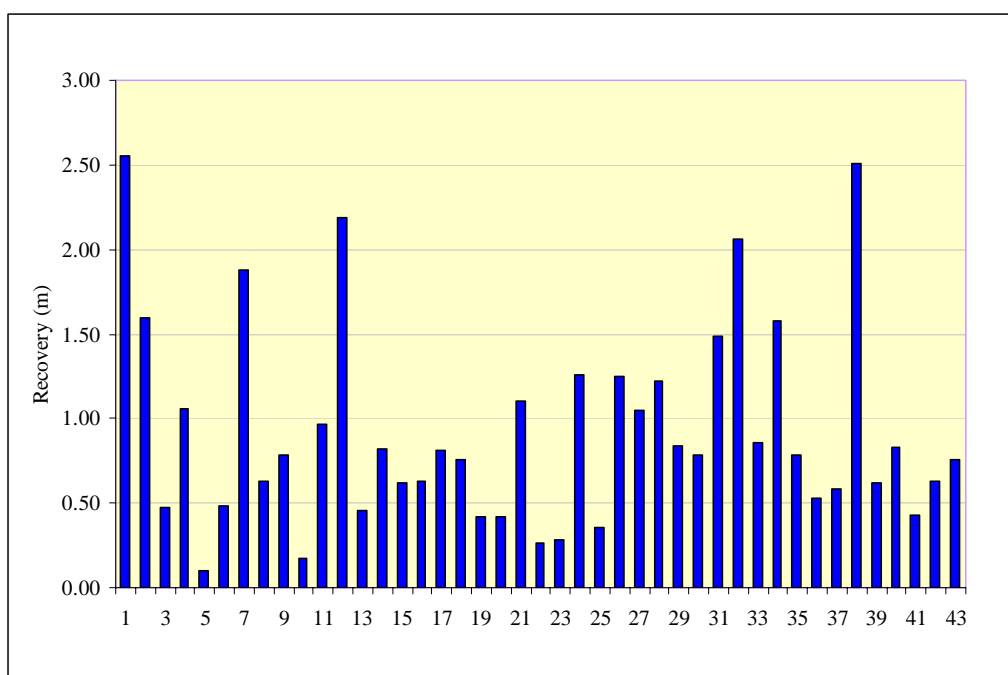


Figure 4.3. Histogram showing the relative lengths of drill cores obtained during survey 276.

4.2.1 Uranium-Series Ages

Out of the 55 coral samples analysed by XRD, a total of 17 were chosen for U-series dating on the basis of their >95% aragonite mineralogy. These samples were broken up into small 5-10 gm sub-samples and underwent further cleaning using dentist tools to remove any undetected contamination. The cleaned samples then underwent various chemical procedures, as described below, and were analysed for their uranium and thorium isotopic composition using the Thermo Finnegan “Neptune” multi-collector inductively coupled plasma mass spectrometer (MC-ICPMS) at the Research School of Earth Sciences, Australian National University. In addition, another 5 samples whose coral structure was intact, but whose mineralogy was mainly calcite, were analysed for exploratory purposes and to constrain minimum ages for the cores.

Table 4.1. List of drill core samples obtained during survey 276. The coordinates of the drill sites, water depth of sites plus length of drill core (penetration) are also listed.

SAMPLE ID	REEF DRILLED	LAT DEG	LAT MIN	LONG DEG	LONG MIN	PENETRATION (M)	WATER DEPTH (M)
276/01RD01	R1	-15	17.74	140	19.475	2.50	26.80
276/02RD02	R1	-15	16.522	140	20.143	1.60	26.40
276/03RD03	R1	-15	15.146	140	18.484	0.47	30.80
276/10RD04	R1	-15	19.247	140	17.45	1.06	26.40
276/11RD05	R1	-15	19.365	140	18.572		23.20
276/11RD06	R1	-15	19.332	140	18.604	0.48	23.20
276/12RD07	R1	-15	19.758	140	18.231	1.88	26.40
276/13RD08	R2	-15	26.358	140	9.967	0.63	29.20
276/14RD09	R2	-15	26.874	140	10.185	0.78	26.40
276/15RD10	R3	-15	30.879	140	6.629		30.80
276/15RD11	R3	-15	30.879	140	6.629	0.97	30.40
276/16RD12	R3	-15	31.401	140	6.846	2.19	20.20
276/17RD13	BR	-16	30.163	139	53.663		27.60
276/22RD14	R4	-16	0.053	139	5.799	0.82	23.60
276/23RD15	R4	-15	59.653	139	5.495	0.62	22.00
276/24RD16	R4	-15	58.777	139	6.496	0.63	19.60
276/25RD17	R4	-15	59.299	139	5.093	0.81	23.60
276/26RD18	R4	-16	1.002	139	7.44	0.76	25.60
276/27RD19	R4	-16	0.518	139	7.447	0.42	25.20
276/28RD20	R4	-15	57.8	139	8.101	0.42	29.60
276/29RD21	R4	-16	3.037	139	1.883	1.10	18.40
276/30RD22	R4	-16	3.28	139	1.458	0.26	20.00
276/31RD23	R4	-16	4.027	139	4.027	0.28	27.20
276/32RD24	R4	-16	2.897	139	3.102	1.26	26.40
276/33RD25	R4	-15	57.085	139	10.112		38.00
276/34RD26	R6	-15	28.105	137	55.123	1.25	19.20
276/43RD27	R6	-15	27.77	137	54.885	1.05	29.60
276/45RD28	R7	-15	29.36	137	37.885	1.22	29.20

SAMPLE ID	REEF DRILLED	LAT DEG	LAT MIN	LONG DEG	LONG MIN	PENETRATION (M)	WATER DEPTH (M)
276/46RD29	R7	-15	28.303	137	38.234	0.84	31.60
276/49RD30	R7	-15	29.139	137	37.416	0.78	25.60
276/50RD31	R5	-15	43.408	138	52.722	1.49	19.20
276/52RD32	R5	-15	43.312	138	53.037	2.06	16.40
276/53RD33	R5	-15	41.929	138	53.953	0.86	25.20
276/57RD34	R5	-15	40.952	138	54.923	1.58	44.00
276/58RD35	R5	-15	39.836	138	53.679	0.78	30.40
276/59RD36	R5	-15	40.017	138	52.829	0.53	26.40
276/60RD37	R5	-15	41.645	138	51.665	0.58	24.80
276/61RD38	R5	-15	39.088	138	49.729	2.51	29.20
276/62RD39	R5	-15	37.803	138	51.237	0.62	27.60
276/63RD40	R5	-15	37.14	138	51.815	0.83	30.80
276/65RD41	R5	-15	36.119	138	49.031	0.43	26.00
276/67RD42	R5	-15	36.117	138	46.949	0.63	29.60
276/68RD43	R5	-15	35.009	138	47.119	0.76	24.00

Table 4.2. X-ray Diffraction (XRD) Results from drill core samples.

SAMPLE NUMBER	LAB NO.	SCAN	CALCITE	ARAGONITE	HALITE	QUARTZ	ERROR	CHI ²
			wt%	wt%	wt. %	wt. %	wt. %	1-sigma
276 01RD01/39-40	1	A21064	<0.2	99.8			0.1	2.00
276 01RD01/84-85	2	B5002	major	trace				
276 02RD02/140-141	3	A21065	major	trace				
276 02RD02/105-106	4	A21066	major	trace				
276 02RD02/95-96	5	A21067	major	trace				
276 02RD02/150-151	6	B5004	major	trace				
276 10RD04/84-85	7	B5003	major	trace				
276 12RD07/34-35	8	B5005		100.0				
276 12RD07/52-53	9	B5006	0.3	98.3	1.3		0.2	1.25
276 12RD07/94-95	10	A21068	17.1	82.9			0.4	1.97
276 13RD08/37-38	11	A21069	<0.8	99.2			0.2	1.98
276 14RD09/28-29	12	B5007	0.4	99.6			0.2	1.62
276 16RD12/200-201	13	A21070	<0.3	99.2	0.5		0.1	1.57
276 16RD12/124-125	14	B5008	<0.3	99.7			0.1	1.62
276 16RD12/19-20	15	A21071		100.0				
276 16RD12/176-177	16	B5009	1.2	98.7			0.2	1.61
276 16RD12/90-91	17	A21072	<0.3	99.7			0.1	1.99
276 16RD12/60-61	18	B5010	1.3	97.8	0.09		0.3	1.17
276 23RD15/14-15c	19	B5011	100.0					
276 25RD17/74-75	20	A21073	major	trace				
276 26RD18/31-32	21	B5012	1.2	98		0.8	0.4	1.58
276 29RD21/79-80	22	A21074	major	trace				
276 34RD26/123-124	23	A21075	<.7	97.7	0.8	0.9	0.2	1.98
276 34RD26/57-58	24	B5013	0.7	99.3			0.1	1.57
276 34RD26/108-109	25	A21076	<0.4	99.6			0.3	2.09
276 34RD26/10-11	26	B5014	0.6	99			0.2	1.59
276 34RD26/30-31	27	A21077	<0.2	99.3		0.6	0.1	1.93
276 43RD27/15-16	28	B5015	1.7	98.3			0.2	1.53
276 45RD28/44-45	29	A21078	1	98.4		0.6	0.2	1.90
276 46RD29/79-80	30	B5016	major	trace				
276 46RD29/25-26	31	B5017	major	trace				
276 46RD29/63-64	32	A21081	major	trace				
276 49RD30/50-51	33	B5018	31.9	67			0.4	1.67
276 49RD30/78-79	34	A21082	4.6	95.4			0.8	2.02
276 49RD30/20-21	35	B5019	<0.3	99.7			0.2	1.59
276 50RD31/146-147	36	A21083	major	trace				
276 50RD31/9-10	37	B5020	major	trace				
276 50RD31/27-28	38	B5021	major	trace				
276 50RD31/87-88	39	A21084	major	trace				
276 50RD31/127-128	40	A21085	major	trace				
276 52RD32/199-200	41	B5022	major	trace				
276 52RD32/25-26	42	B5023	major	trace				
276 52RD32/52-53	43	B5024	major	trace				
276 52RD32/109-110	44	A21087	major	trace				
276 52RD32/152-153	45	A21088	major	trace				
276 53RD33/61-62	46	A21089		100.0				
276 53RD33/50-51	47	A21090	1.3	98.2	0.6		0.1	1.62
276 53RD33/12-13	48	A21091	3.3	95.8		0.8	0.3	2.03
276 58RD35/15-16	49	A21092	1.5	98		0.5	0.3	1.75
276 58RD35/75-76	50	A21093	100.0					
276 59RD36/21-22	51	A21094	21.8	78.2			0.7	2.03
276 60RD37/53-54	52	A21095	<0.2	99.8			0.2	2.08
276 62RD39/35-36	53	A21096	3.0	94.6		2.4	0.2	2.13

SAMPLE NUMBER	LAB NO. SCAN		CALCITE	ARAGONITE	HALITE	QUARTZ	ERROR	CHI ²
			wt%	wt%	wt. %	wt. %	wt. %	1-sigma
27669RD43/28-29	54	A21097	1.5	98.5			0.5	1.89
27668RD43/58-59	55	A21098	0.2	99.2		2.06	0.2	2.06

Table 4.3. Uranium-series Ages of Corals from Drill Core Samples

Core Number	Mineralogy ^a	U (ppm)	²³⁰ Th (ppt)	²³² Th (ppb)	d ²³⁴ U ₀ (‰) ^b	²³⁰ Th/ ²³⁸ U	²³⁰ Th/ ²³² Th	Age (kyr)	d ²³⁴ U _T (‰) ^b
276/01RD01/39-40cm	arag. (99.8%)	2.8	4.26	7.58	146.7 ± 0.9	0.09480 ± 0.00035	105	9.367 ± 0.036	150.7 ± 0.9
276/01RD01/84-85cm	calc. (major*)	1.8	25.01	58.23	111.7 ± 1.1	0.86984 ± 0.00350	81	158.500 ± 1.400	175.1 ± 1.6
276/12RD07/52-53cm	arag. (98.3%)	2.4	3.85	3.45	145.0 ± 1.6	0.09744 ± 0.00054	209	9.650 ± 0.056	149.0 ± 1.6
276/12RD07/94-95cm	calc. (17.1%)	2.0	24.05	3.88	118.2 ± 1.1	0.74103 ± 0.00162	1163	114.930 ± 0.480	163.7 ± 1.5
276/13RD08/37-38cm	arag. (99.2%)	3.2	5.13	13.2	145.9 ± 1.5	0.09877 ± 0.00041	73	9.784 ± 0.044	150.0 ± 1.5
276/14RD09/28-29cm	arag. (99.6%)	2.7	3.93	0.25	145.9 ± 1.2	0.09065 ± 0.00061	2895	8.950 ± 0.061	149.6 ± 1.2
276/16RD12/19-20cm	arag. (100%)	2.1	2.89	0.31	148.0 ± 1.4	0.08506 ± 0.00038	1753	8.359 ± 0.040	151.6 ± 1.4
276/16RD12/90-91cm	arag. (99.7%)	2.0	2.82	1.93	148.0 ± 1.6	0.08679 ± 0.00037	274	8.535 ± 0.040	151.6 ± 1.6
276/16RD12/176-177cm	arag. (98.7%)	3.2	4.9	1.26	145.9 ± 1.1	0.09540 ± 0.00045	728	9.436 ± 0.048	149.9 ± 1.1
276/23RD15/14-15cm	calc. (100%)	1.0	8.68	6.19	124.0 ± 1.9	0.56022 ± 0.00163	263	73.870 ± 0.360	152.9 ± 2.3
276/26RD18/31-32cm	arag. (98.0%)	3.6	5.83	4.73	145.5 ± 0.5	0.09953 ± 0.00054	231	9.870 ± 0.055	149.7 ± 0.5
276/34RD26/10-11cm	arag. (99.0%)	2.5	1.13	0.23	147.1 ± 1.1	0.02756 ± 0.00029	937	2.643 ± 0.028	148.2 ± 1.1
276/34RD26/123-124cm	arag. (97.7%)	2.3	1.29	10.32	146.8 ± 1.0	0.03480 ± 0.00035	23	3.349 ± 0.037	148.2 ± 1.1
276/43RD27/15-16cm	arag. (98.3%)	4.2	5.03	42.05	145.8 ± 1.2	0.07419 ± 0.00037	22	7.270 ± 0.038	148.8 ± 1.2
276/45RD28/44-45cm	arag. (98.4%)	3.5	5.46	15.28	147.4 ± 1.0	0.09770 ± 0.0043	67	9.661 ± 0.046	151.5 ± 1.0
276/46RD29/63-64cm	calc. (major)	3.0	28.15	26.82	118.5 ± 1.4	0.58349 ± 0.00764	197	78.900 ± 1.500	148.2 ± 1.8
276/49RD30/78-79cm	arag. (95.4%)	2.7	4.44	14.32	146.7 ± 1.1	0.09987 ± 0.00047	58	9.892 ± 0.048	150.8 ± 1.1
276/52RD32/52-53cm	calc. (major)	2.5	21.09	15.87	123.1 ± 1.9	0.51302 ± 0.00136	249	65.490 ± 0.285	148.3 ± 2.2
276/53RD33/61-62cm	arag. (100%)	3.2	4.17	9.95	147.1 ± 1.1	0.08152 ± 0.00051	79	8.000 ± 0.051	150.5 ± 1.0
276/58RD35/15-16cm	arag. (98.0%)	3.6	4.49	26.92	147.0 ± 1.0	0.07809 ± 0.00046	31	7.657 ± 0.047	150.2 ± 1.0
276/60RD37/53-54cm	arag. (99.8%)	2.9	4.53	10.12	149.7 ± 0.8	0.09739 ± 0.00052	84	9.610 ± 0.053	153.8 ± 0.8
276/62RD39/35-36cm	arag. (94.6%)	3.2	5.54	73.36	147.2 ± 1.0	0.10666 ± 0.00057	14	10.590 ± 0.058	151.7 ± 1.0

^a arag. = aragonite; calc. = low-Mg calcite; major = >90%^b $\delta^{234}\text{U}_0$ = measured value; the initial value $\delta^{234}\text{U}_T = \delta^{234}\text{U}_0 e^{\lambda_{234} T}$; where T = age (in years) and $\lambda^{234} = 2.835 \times 10^{-6} \text{ yr}^{-1}$

4.2.1.1 Analytical Methods

The chemical separation procedures for U-Th analyses used here are basically a refined version of the chemical separation procedure of Lou et al. (1997), with the coral being dissolved in HNO₃, followed by the addition of a mixed ²²⁹Th-²³³U spike. The U and Th fractions are extracted and almost completely separated using a micro ion exchange column of TRU spec resin with a combination of 0.1M HCl + 0.02M HF to collect the Th fraction, followed by 0.1M HCl + 0.3M HF to collect the U fraction. The U and Th solutions are introduced separately into the ICPMS with an APEX desolvator fitted with a free-aspirating, low-flow Teflon PFA nebuliser. Desolvation is achieved by heating the spray chamber, followed by chilling of the helical stage of the flow path. A standardised set of plasma operating conditions is used which remain constant over each analytical session.

A rigorous cleaning procedure is utilised in the sample introduction system. This consists of a combination of multi-step 2% HNO₃, 0.05% HF, and 1% Triton surfactant injections. Careful monitoring of blanks and possible spectral interferences is always essential in MC-ICPMS and this is especially the case for measuring the extremely low abundances of ²³⁰Th.

Th and U isotope measurements are performed in four sequential steps (Table 4.4), utilising the high abundance energy filter (RPQ) in the central channel. The RPQ gives a substantially improved abundance sensitivity of better than 0.2 ppm in the mass region of interest and, hence, tailing corrections are minimal. The isotopes ²²⁹Th and ²³⁰Th are each measured in the central ion counter (with RPQ) concurrently with ²³²Th in a Faraday cup (L2) and ²³⁸U in Faraday cups (cups H3 and H4), taking advantage of multi-collection measurements in reducing errors from beam instabilities. The isotope ²³⁴U is also measured in the ion counter concurrently with ²³⁸U, ²³⁵U, ²³³U and ²³²Th in Faraday cups (cups H2, H1, L1, L2). Mass fractionation corrections for ²²⁹Th/²³⁰Th, ²²⁹Th/²³²Th, ²³⁴U/²³⁸U and ²³³U/²³⁸U ratios are undertaken using the naturally occurring ²³⁵U and ²³⁸U measured simultaneously in Faraday cups. The concentrations of ²³⁰Th and ²³⁸U are determined using the enriched ²²⁹Th and ²³³U tracers respectively. Backgrounds on the Th masses due to tailing effects are eliminated by utilisation of the RPQ, and are more than adequately accounted for by a single baseline measurement at mass 229.4. This mass position was chosen to minimise the possibility of non-integer interferences, particularly those that occur in the mass region of 230.5-231.0. Although the ²³⁰Th/²³⁸U ratio can be successfully determined from this Th protocol, the measurement of ²³⁴U/²³⁸U is not optimal, as it relies on an SEM/Faraday gain measured with greater uncertainty introduced by the use of the RPQ. For this reason, the ²³⁴U/²³⁸U is measured in a separate U protocol (Table 4.4).

Table 4.4. Faraday cup configuration for Th and U analysis with an axial SEM ± RPQ

	INTEGRATION TIME (SECS)	L2	L1	AXIAL SEM	H1	H2	H3	H4
RPQ on								
Th Step 1	12 x 6	232	233	234	235	238		
Th Step 2	12 x 12		230			238		
Th Step 3	12 x 12		229				238	
Th Step 4	12 x 6			229.4				
RPQ off								
U Step 1 12 x 8			234.5					
U Step 2 12 x 12		232	233	234	235	238		
U Step 3 12 x 8			233.5					

Although ²³⁴U/²³⁸U ratios can in principal be directly measured using only faraday cups (Anderson et al., 2004; Bernal et al., 2002) this requires large ion beams of ²³⁸U (300-500 V) which is not generally applicable. The approach adopted here is to measure ²³⁴U on an ion counting system, simultaneously

with ^{233}U , ^{235}U and ^{238}U on the Faraday array. This approach is shown in [Table 4.4](#) (step 2) and requires cross calibration of the gain of the SEM relative to the Faraday system.

4.2.1.2 Uranium-series Dating Results

The results of the U-series age determinations are shown in [Table 4.3](#) in order of sequence of core number and depth in the core. For the aragonite corals, the majority were $\geq 98\%$ aragonite, while only 3 samples were less (97.7, 95.4 and 94.6%; [Table 4.3](#)). The calcite corals were nearly all 100% calcite. One coral (276/01RD07/94-95cm) had 17.1% calcite. This was the only coral analysed that had a mixed mineralogy.

The aragonite corals have a uranium content of 2.0 to 4.2 ppm, which falls within the usual range of uranium values for scleractinian corals.

4.2.2 REEF R1

This reef is the largest (72 km²; Harris et al., 2004) and most easterly of the free standing drowned reefs that form part of the southern Gulf region ([Fig. 4.1](#)). A total of seven holes (cores 1-7) were drilled on the broad platform on top of the reef ([Fig. 4.4](#)). Cores ranging from 0.1 to 2.5 m were recovered from water depths of 23.2 to 30.8 m. Holes 2, 4 and 7 were all drilled in a water depth of 26.4 m, on the top of the slightly raised (0.5 m) rim that is present around a large part of the reef perimeter, whereas hole 1 was drilled in the centre of the platform in a water depth of 26.8 m. Holes 5 and 6 were drilled on the top of a smaller raised platform at the southern end of the reef in a water depth of 23.2 m. Hole 3 was drilled in 30.8 m of water on the northern end of what appears to be a lower platform that skirts the edge of the main reef. This reef edge platform appears to be common around some of the other reefs as well (see Figure 3 of Harris et al. (2004).

4.2.2.1 Core 276/01RD01

Holocene Section (0-0.56 m): The top 10 cm of the core is iron-stained and encrusted by coralline algae and sepolids, and the matrix is mainly filled by micrite. In addition there are at least three generations of borings by bivalves and sponges which have been filled by micrite cement (RD01; Fig. G-00110). This can be interpreted as a hardground, whereby there has been no accretion beyond this point, and the limestone has undergone intense action by endoliths.

The remainder of the Holocene section consists of a corallgal framestone (see core log; [Appendix 4](#)), but which varies from coral to algal boundstone. The algal boundstone consists of crustose coralline algae, serpulids, vermetid gastropods, encrusting foraminifera and bryozoans, bivalves in an Mg-calcite micrite cement. The crustose coralline algae are quite distinctive, in that they are genera that consist of a thin thallus (RD01; Fig. G-00043) in comparison to say the more typical reef-type coralline algae which tend to be quite massive. While this may be a boundstone, on the whole, it is the micrite that cements the rock.

Towards the base of the section (at 0.4 m) there is a large polyp coral (*Goniopora* sp.). The coral is partly encrusted by a thin layer of coralline algae. XRD results indicate that the cleaned sample is aragonite, and this gave an age of 9367 ± 36 years ([Table 4.3](#)).

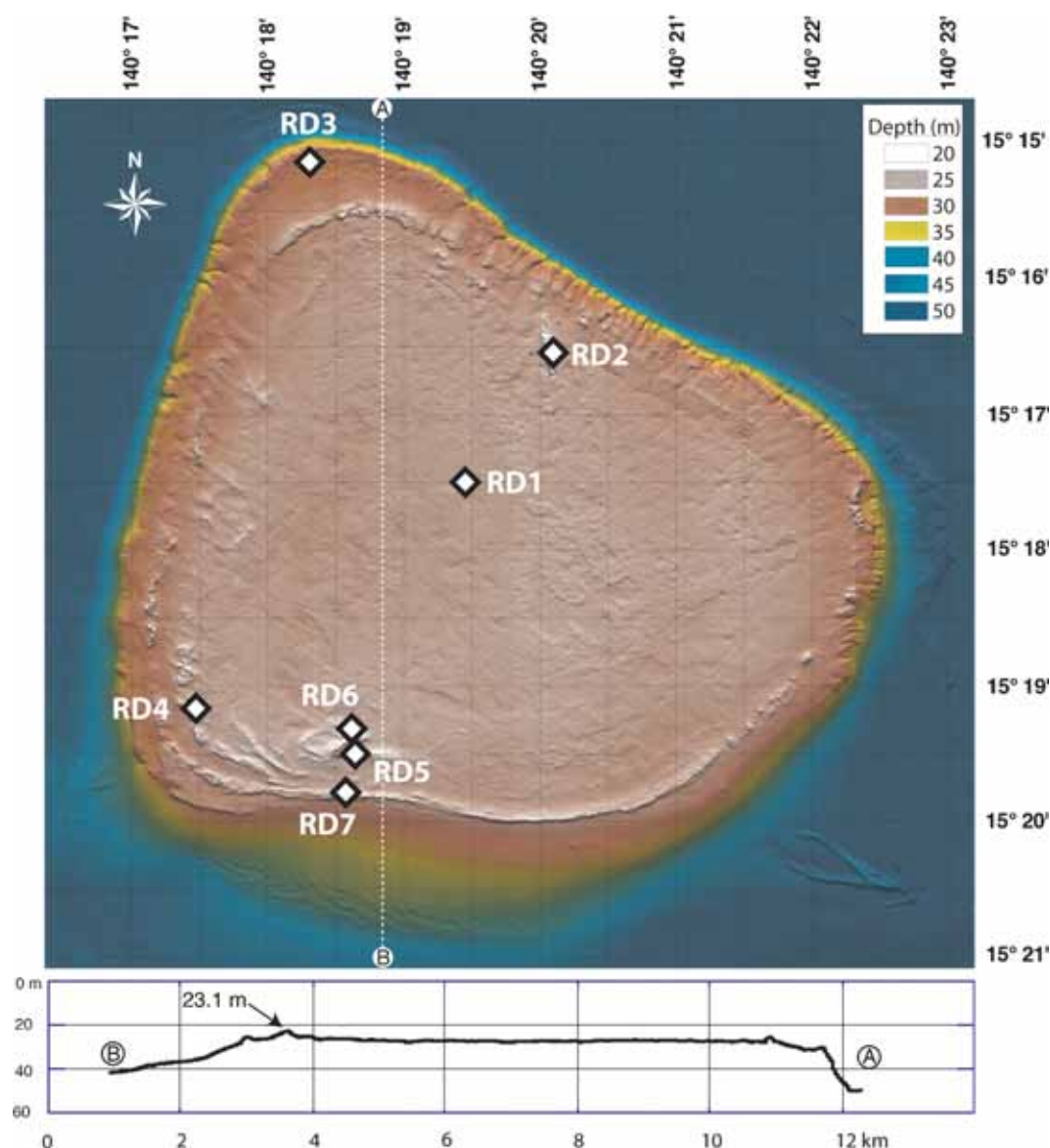


Figure 4.4 Location of drill sites on Reef R1 in relation to false-colour bathymetry. A bathymetric profile across the reef top illustrates the total relief of Reef R1 is around 20 m.

Pleistocene Section (0.56-2.50 m): A solution unconformity occurs at 0.56m between the overlying early Holocene coral above and a light grey to greyish black mudstone below (see core log; [Appendix 4](#)). The black mudstone is vuggy, but the vugs do not appear to be caused by dissolution of skeletal particles because of their irregular outlines. One clue as to their identity is the presence of calcite needle and microspar cements (RD01; Fig. G-00048), and what is interpreted here as alveolar structure. These features suggest that some, if not all, of the vugs have been formed by rootlets, and as such it is a form of calcrete. Some vugs are even thin string-like features that are suggestive of root hairs (RD01; Fig. G-00051). The only obvious cement is fairly fine sparry calcite. Most of it tends to occur within the vugs, but there are rare occurrences of skeletal fragments that show replacement by calcite cement. This also would indicate that the rock is pre-Holocene.

What is essentially a framestone extends to 0.95 m, below which is a vuggy packstone that extends to the bottom of the core. The framestone consists of leached aragonite elements (corals etc) which have been filled by sparry calcite cement, which becomes more coarsely crystalline with depth. Here, the

skeletal outlines are poorly defined as a result of extensive neomorphism and dissolution/precipitation. Both fabric selective and cross-cutting textures are evident, indicating both freshwater vadose (above the water table) and meteoric-phreatic (below the water table) environments of diagenesis (RD01; Fig. G-00003). The underlying vuggy packstone is fairly uniform in fabric and texture throughout its length (see core photo; [Appendix 5](#)). No corals or coralline algae are evident, and the major allochems appear to be encrusting foraminifera and/or bryozoans, together with some bivalve fragments. There is evidence of widespread dissolution, with mouldic porosity developed and which is sometimes filled by sparry calcite cement. With depth, the amount of sparry calcite cement increases, until much of the porosity is considerably reduced. Here, both grains and cement are sometimes made up of a single calcite crystal or, more commonly, cross-cutting mosaics are present (RD01; Fig. G-00042). This indicates that the environment of diagenesis was essentially meteoric-phreatic.

The pre-Holocene section has undergone extensive diagenesis as a result of subaerial exposure, with phreatic diagenesis being pervasive, resulting in replacement of everything (including pores!) by coarsely crystalline calcite. However, reefal framework makes up the minority of this section. The majority of the section contains no identifiable corals or coralline algae, so it is more likely that this section was a lagoon facies rather than reef framework. This would fit in with the location of the core at the very centre of Reef 1 ([Fig. 4.4](#)).

4.2.2.2 Core 276/02RD02

Holocene Section (0-0.33m): This is primarily a rudstone/boundstone, with coral and other skeletal particles encrusted by coralline algae, particularly in the top 13cm. The top is heavily iron-stained, particularly the micrite matrix, although the staining is very patchy, with, say, some skeletal chambers filled with iron-rich micrite and adjacent chambers filled with ordinary micrite. Elsewhere there is evidence of phosphate deposition, with banded iron/phosphate deposits forming a late-stage cement in places (RD02, G-00113 & G-00114; [Appendix 5](#)). Because the rock is Holocene in age (i.e. corals and molluscs are still aragonite), the question is how has the top become so iron-stained? It too seems to represent an hiatal surface, similar to that observed in Core RD01. The presence of iron/phosphate deposits, although rare, could point to a hardground where iron, possibly from terrigenous sources has become enriched over time. The phosphate is probably from sea water, but it too, has gradually been adsorbed onto the hydrated iron oxides precipitated as part of the hardground. Where the limestone is more of a boundstone, the crustose coralline algae has been bored by bivalves (the shells of which are still present) and sponges. This particular coralline algae (*Lithophyllum* sp.?) is very knobbly and forms an interconnected, but open, framework that has been partly filled (25%) by a semi-lithified lime mud. Apart from the coralline algae, there are serpulids, vermetid gastropods and bivalves.

Pleistocene Section (0.33-1.60 m): A solution unconformity is present at 0.33m which is the junction between the rudstone/boundstone and a somewhat dirty grainstone (see core log; [Appendix 4](#)). The latter shows some laminations in the top 10cm, and there are signs of soil development, which include red iron-rich inclusions. Below that is a fairly pristine coral with no internal sediment or cement, but the original aragonite has been completely replaced by calcite. The calcite crystals are large and at the top show a fabric selective mosaic, indicating neomorphism in a vadose environment, whereas with depth the calcite fabrics are indicative of a phreatic environment.

The position of this core towards the outer northern rim of the reef indicates a thin veneer of Holocene boundstone that may have been deposited in a relatively high energy environment. Comparison with other ages from Reef 1 would suggest that this was deposited in the early Holocene soon after sea level overtopped the reef. The underlying massive coral is obviously pre-Holocene from the calcitic mineralogy, but it does suggest that it was an actively growing part of the reef during this period (last interglacial?).

4.2.2.3 Core 276/03RD03

Holocene? Section (0-0.47 m): This is a type of core where it is difficult to tell whether it is Holocene or older (see core log; [Appendix 4](#)). The corals in the framestone are still aragonite and there is a fair amount of acicular aragonite cement (both inter and intraskeletal) present (RD03, G-00128; [Appendix 7](#)). However, there are also suggestions that leaching is taking place, with mouldic porosity evident, and in thin section the corals appear to be undergoing a process of “micritisation” (RD03, G-00129; [Appendix 7](#)). There are also signs of pedogenesis and the framestone has a red discolouration that seems typical of many of the late Pleistocene limestones encountered elsewhere. However, no signs of calcite were detected. Besides the coral, the core contains a baffestone that consists of crustose coralline algae and serpulid worm tubes in a blackish-grey wackestone matrix (see core photo; [Appendix 5](#)). This is similar to the boundstone/bafflestone described in the other cores, which would suggest that the core is Holocene in age.

4.2.2.4 Core 276/10RD04

Holocene Section (0-0.86 m): The top of the Holocene section (0-0.24 m; see core log; [Appendix 4](#)), like many other of the cores, is a hardground which consists of a bored and infilled rudstone containing fragments of iron-stained serpulids, corals and molluscs. This hiatal surface suggests that no reef growth has occurred on this site for some time, and ties in with an early Holocene growth phase, as seen from U/Th age determinations in cores 1 and 7. The rudstone grades down to a weathered coralline algal/serpulid baffestone towards the base. The remainder of the Holocene section (0.24-0.86 m) consists of the same algal/serpulid baffestone, but is less weathered.

Pleistocene Section (0.86-1.06 m): The solution unconformity is marked here by the first appearance of calcite (as determined by XRD and thin section examination). The rudstone (see core log; [Appendix 4](#)) contains fragments (1-2 cm diam) in a muddy matrix. The fragments consist mainly of coral, with some coralline algae and serpulids, in a micrite matrix that fills both skeletal pores and interskeletal voids.

4.2.2.5 Core 276/11RD06

This is a relict biogenic rudstone that consists of bored and encrusted coral fragments in an unconsolidated grainstone/packstone matrix. The section is assumed to be Holocene, but there is no XRD or thin section evidence to back this up.

4.2.2.6 Core 276/12RD07

Holocene Section (0 to ~0.80 m): Again, the top part of the core (0-20 cm) appears to be a hardground, consisting of an iron-stained and coralline algal encrusted rudstone (see core log; [Appendix 4](#)). Beneath this is a 34 cm length of coral (in three pieces) with thin grey lithified crusts on parts of the coral's exterior, and bored by molluscs (*Lithophaga* sp.), sponges and polychaetes. The XRD results show this sample to be 98-100% aragonite. However, some of the coral pores are filled with internal sediment. From the XRD results it can only be assumed that this too is mostly aragonite and probably was deposited soon after the coral. The base of the coral gave a U/Th age of 9650 ± 56 ([Table 4.3](#)). This, plus, the age from RD01 of 9367 ± 36 , indicates that Reef 1 began growing during the earliest Holocene, presumably soon after rising sea level overtopped the reef rim.

Between 0.54 and 0.88 m the lithology consists of a boundstone/bafflestone, consisting of white serpulids and coralline algae in a dark grey to black fine-grained matrix (see core log; [Appendix 4](#)), similar to that reported from other cores from this reef. At about 0.80 m there is a subtle change, only detected in thin section, where the algal boundstone becomes a skeletal wackestone. What is unusual here is that the boundstone appears not to have been subaerially exposed, whereas the wackestone is full of sparry calcite cement (mainly filling secondary porosity) (RD07, G-00142; [Appendix 7](#)). This then represents the actual Holocene/Pleistocene boundary, but with no direct evidence of calcrete formation.

Pleistocene Section (0.80?-1.88 m): While the actual depth to the solution unconformity cannot be determined, it seems that anything below 0.82 m is definitely pre-Holocene. A coral, possibly a faviid, occurs between 0.88 and 0.96 m (see core log; [Appendix 4](#)), and while the XRD results on the cleaned sample for dating indicate that it is 83% aragonite, the thin section shows that at least 50% of the coral is now calcite. The aragonite sections of the coral show signs of selective leaching, whereas the calcite part is largely neomorphic. The U-series age of $114,930 \pm 480$ can only be seen as a minimum age, because of the 17% calcite in the dated sample. However, it does confirm that the section is at least late Pleistocene.

The lithology between 0.96 and 1.29 m is a boundstone/packstone with some layers of coralline algae and serpulids(?) in a weathered, sometimes iron-stained matrix. In contrast to the one in Core 4, there is more filling of intercoralline cavities, but this has been affected by later dissolution (or secondary porosity). Sparry calcite cement is fairly common, both as an inter- and an intra-skeletal fill. Most of the iron staining is patchy, but mainly occurs within the micrite cement (RD07, G-00137; [Appendix 5](#)). Quartz grains (20-100 μm) are present in the matrix, but they are relatively uncommon ($\approx 2\%$).

The boundstone/packstone gradually develops into a packstone, which also shows signs of weathering and iron-staining (RD07, G-00138; [Appendix 7](#)). While it is mostly fine-grained, some coral fragments are present towards the base. The corals have been neomorphosed to calcite, whereas, in places, the intraskeletal pores have been lined or filled with sparry calcite cement (RD07, G-00139; [Appendix 7](#)).

4.2.2.7 Discussion of Cores from Reef R1

A composite of the drill logs for Reef R1 is shown in [Figure 4.5](#). All drill holes recovered Holocene material, and four holes penetrated into Pleistocene limestone. In the latter cores the solution unconformity is shown to occur within a narrow depth range (26.7-27.3 m). In cores where the solution unconformity is present, the Holocene reef varies in thickness between 0.33 and 0.86 m. The two Holocene uranium-series ages from this reef show fairly tight timing, with an age of 9367 ± 36 years for RD01 and 9650 ± 65 years for RD07 ([Table 4.3](#)). Because the age for RD07 occurs where coral starts to replace a coralline algal bafflestone, it is assumed that this is time of initial coral growth; occurring first on the slightly raised rims and then, soon after, within the centre of the platform. The thickness of the Holocene reef suggests that growth, while widespread and initiating almost as soon as sea level overtopped the reef platform, was short lived.

4.2.3 Reef R2

This reef is located about 25 km to the south west of Reef R1 ([Fig. 4.1](#)). The surrounding sea floor at 45-50 m depth rises to 18 m on the shallowest part of the platform. The platform is roughly circular with two distinct levels, one at about 30 m and the other around 27 m. The shallower platform is located to the south ([Fig. 4.6](#)) and forms a ridge at 24 m and a peak in the south at 18-20 m (Heap et al., 2006). Two holes were drilled on the top of the reef (see [Fig. 4.6](#)); hole 8 on the northern margin in a water depth of 29.2 m, and hole 9 on the northern edge of the higher platform at a depth of 26.4 m. Core recovery was 0.63 and 0.78 m respectively.

4.2.3.1 Core 276/13RD08

Holocene Section (0-0.40 m): This is a heavily bored, coral/algal floatstone cum framestone that has been filled by cemented internal sediment and iron stained. As with the tops of cores described from reef R1, the association appears to represent a hardground (see core log; [Appendix 4](#)). Quartz comprises about 6-8% and some of it is reasonably coarse (medium sand size). Some quartz grains have rims that form ooids (RD08, G-00147; [Appendix 7](#)). They appear to be iron-rich, but their exact mineralogy is unknown.

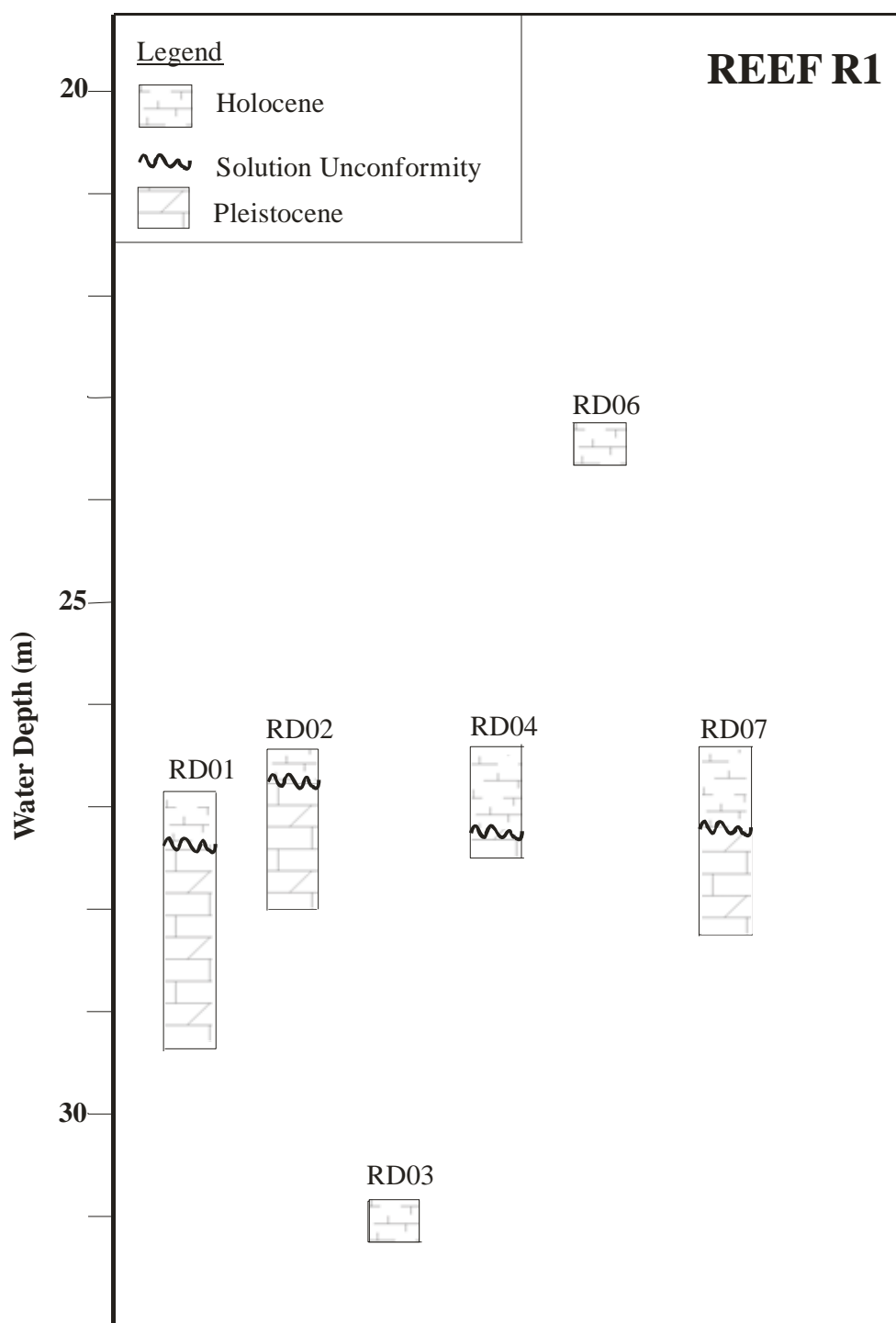


Figure 4.5. Composite core log for Reef R1 showing position and lithology of drill holes in relation to water depth.

Beneath the hardground is a framestone consisting of fragments of platy and branching corals in a grainstone matrix (see core log; [Appendix 4](#)). XRD and thin section examination show that the corals are aragonite, and there is some infill of pores by internal sediment. A coral from the base of the section gave a U/Th age of 9784 ± 44 ([Table 4.3](#)).

Pleistocene Section (0.40-0.63 m): A solution unconformity occurs at 0.40 m. This was identified by the presence of calcite in thin sections below this depth. The section consists of a friable, cemented, floatstone consisting of coralline algae and serpulids in a weathered partly iron-stained packstone matrix.

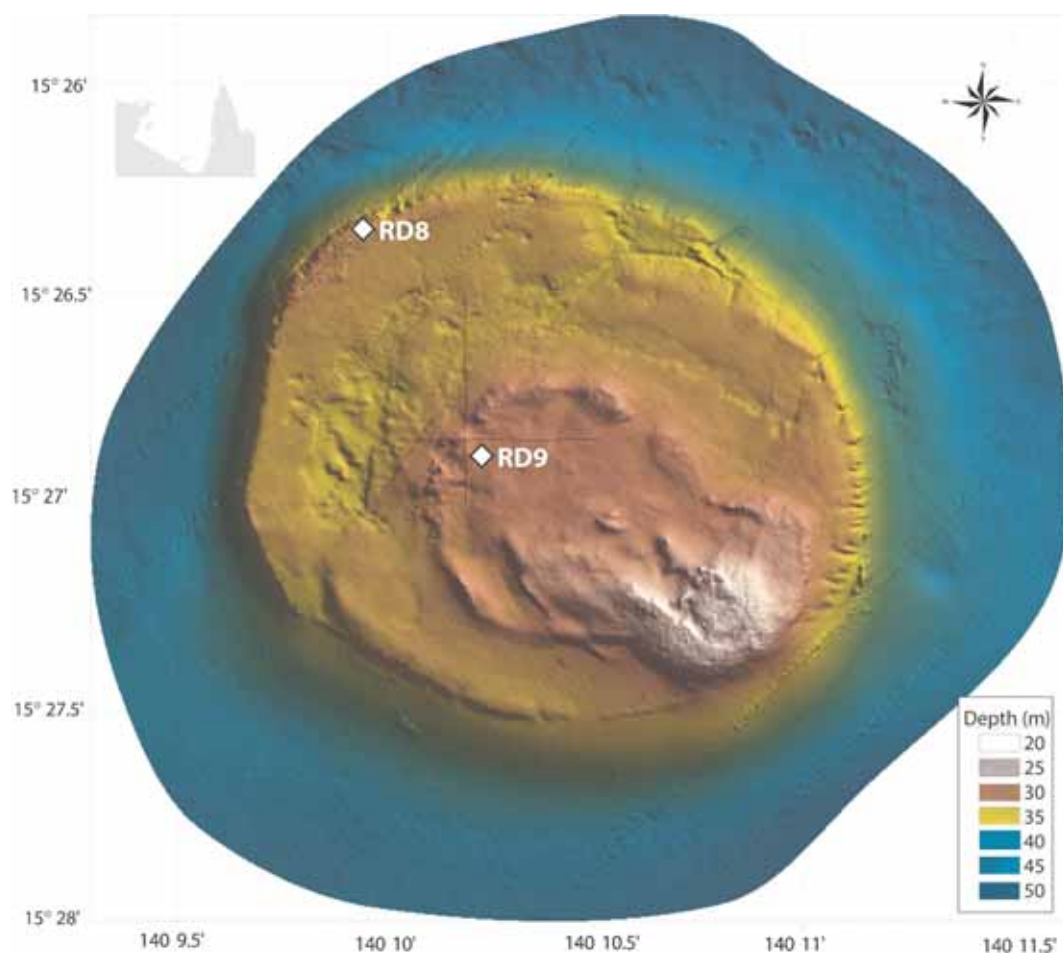


Figure 4.6 Locations of drill core sites on reef R2.

4.2.3.2 Core 276/14RD09

Holocene Section (0-0.78 m): The top of the core (0-0.20 m; see core log; [Appendix 4](#)) has all the appearances of a hardground, consisting of an iron-stained, heavily bored rudstone made up of fragments of coral, coralline algae and molluscs in a grainstone matrix. Directly below is an *in-situ* coral (*Acropora* sp.?) with some mollusc borings and lithified crusts on top. The coral has a large proportion (60%) of its pores filled with internal sediment. The amount of infill, which consists of silt-size skeletal material in a micrite matrix, is unusual because the XRD results show 99% aragonite. Either the cemented internal sediment was removed during cleaning or nearly all the infill, even the micrite cement, is aragonite. This coral gave a U/Th age of 8950 ± 61 , which is in the same range as ages from Reef 1 and Core 8 ([Table 4.3](#)), so it is considered to be reasonably reliable.

Further down the core (0.54-0.78 m) is the distinctive boundstone/bafflestone (see core photo; [Appendix 4](#)) seen in the other cores which consists of branching coralline algae (*Lithophyllum* sp.) and vermetid gastropods in a dark grey matrix. The presence of aragonitic allochems and aragonite cement indicates that it is Holocene (RD09, G-00149; [Appendix 5](#)). An unusual feature is the presence of rounded silt-size black grains (RD09, G-00149; [Appendix 5](#)), which have been observed in the matrix of some of the other boundstone/bafflestones. In the example shown here, the grains occur as a late stage geopetal fill (after aragonite cement) within the chambers of a vermetid gastropod. This would be in keeping with the premise that the coralline algal/vermetid boundstone had already been deposited before it started to trap the silt-size matrix. The mineralogy of these grains is unknown, but it could suggest that it is these that are imparting the darker colour to the matrix.

4.2.4 REEF R3

This reef forms the third and smallest of the chain that extends southwest of Reef R1 ([Fig. 4.1](#)). The platform is oval-shaped and has two distinct levels, similar to Reef R2, but at ≈ 30.1 m and at ≈ 18 -20 m (Heap et al., 2004). The shallower platform is located to the south ([Fig. 4.7](#)). Two holes were drilled on the reef (see [Fig. 4.7](#)); hole 11 on the seaward edge of the deeper platform in a water depth of 30.4 m, and hole 12 on the higher platform at a depth of 20.2 m. Core recovery was 0.97 and 2.19 m respectively.

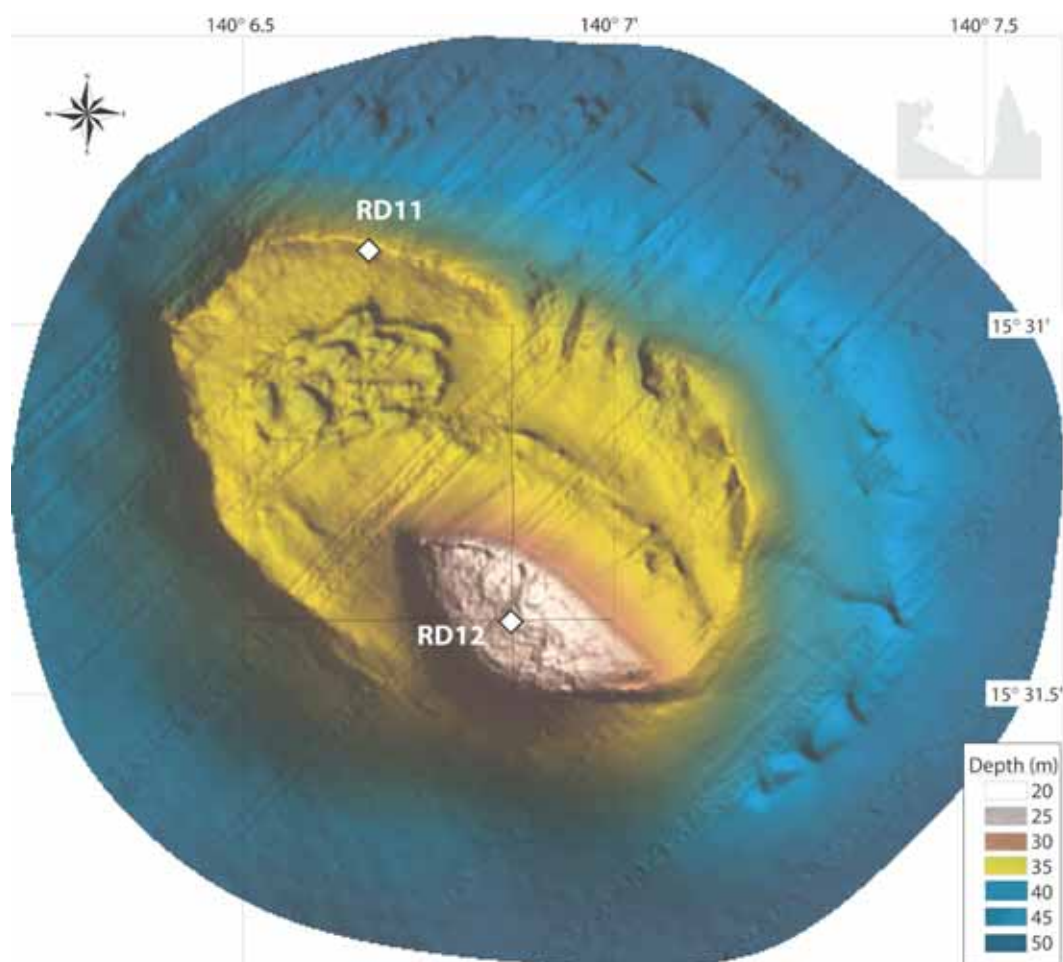


Figure 4.7 Locations of drill core sites on reef R3.

4.2.4.1 Core 276/15RD11

Holocene Section (0-0.19? m): Reddish-grey unconsolidated rudstone, consisting of fragments of corals and molluscs, with some carbonate sand. Because the material is mainly uncemented it has been designated as Holocene, although there is not direct evidence, such as mineralogy, to support this.

Pleistocene Section (0.19?-0.97 m): The total section consists of a reddish stained, high quartz (10-20%), porous (30-40%) packstone with abundant sparry calcite cement. While the core itself is markedly reddish (see core photo; [Appendix 5](#)), the amount of iron staining seen in thin section is not that apparent, although it does exist. Much of the porosity is secondary, and, apart from a few large fragments of coral and coralline algae, there is only a vague hint of skeletal material in either hand specimen or thin section.

4.2.4.2 Core 276/16RD12

Holocene Section (0-2.19? m): The majority of the core is a framestone consisting mainly of branching and platy corals, predominantly species of *Acropora* and *Pocillopora*, and with a 37 cm head of *Porites* sp. near the base (see core log and photo; [Appendix 5](#)). Parts of the framework have been encrusted by coralline algae and bored, mainly by bivalves and sponges, with filling of the larger borings by uncemented internal sediment. Grey discolouration of parts of the coral is evident, and there are some thin lithified crusts.

While the corals look fairly fresh and unaltered, in thin section some centres of calcification are darker and wider than normal, often surrounded by an aureole of partially leached? trabeculae that show up slightly brown in transmitted light (RD12, G-00021; [Appendix 7](#)). While this was originally thought to represent pre-Holocene material, the three ages on this core ([Table 4.3](#)) confirm that it is Holocene. The three ages of 8359 ± 40 at 20 cm, 8535 ± 40 at 90 cm, and 9436 ± 48 years at 176 cm indicate that this particular Holocene reef section (the longest drilled) was growing at rates of 0.95 to 4.0 m kyr^{-1} .

4.2.4.3 Discussion – Reefs R2 & R3

A composite of the drill logs for Reefs R2 and R3 is shown in [Figure 4.8](#). The Holocene/Pleistocene boundary was detected in cores 8 and 11, with Holocene thicknesses of 40 and 19 cm respectively. Holes 9 and 12 recovered only Holocene material; the 2.19 m section in hole 12 is the thickest recovered in the entire area. It is noticeable that this relatively thick sequence occurs on the shallowest part of reef R3, although there appears to be no relationship between water depth and age. The five Holocene uranium-series ages from these reefs are similar to the ages from Reef R1, suggesting that coral growth began soon after the tops of the platforms were flooded.

4.2.5 REEF R4

While this is referred to as a reef, it is more of a carbonate platform that has two reef-like shallow areas on top ([Fig. 4.9](#)). This reef is located on the seaward edge of a large platform that extends for about 100 km to the northwest of Mornington Island ([Fig. 4.1](#)). Reef R4 occurs on the southern edge, while Reef R5 is present to the north ([Fig. 4.1](#)). On the eastern side of Reef R4 the sea floor rises from 45-50 m to 18 m onto the shallowest part of the platform. The platform is divided into two “high” areas that are reef-shaped, and which occur at 18-25 m water depth, while between them is a deeper platform at 25-30 m. Five holes (RD14-17, and RD19) were drilled on the northern high, while two holes (RD21-22) were drilled on the southern high ([Fig. 4.9](#)). In addition, three holes were drilled on the deeper platform (RD18, 20 and 24), while another two holes (RD23 and RD25) were drilled in deeper water. For the 12 drill holes, core recovery varied from 0.26-1.26 m ([Fig. 4.2](#)).

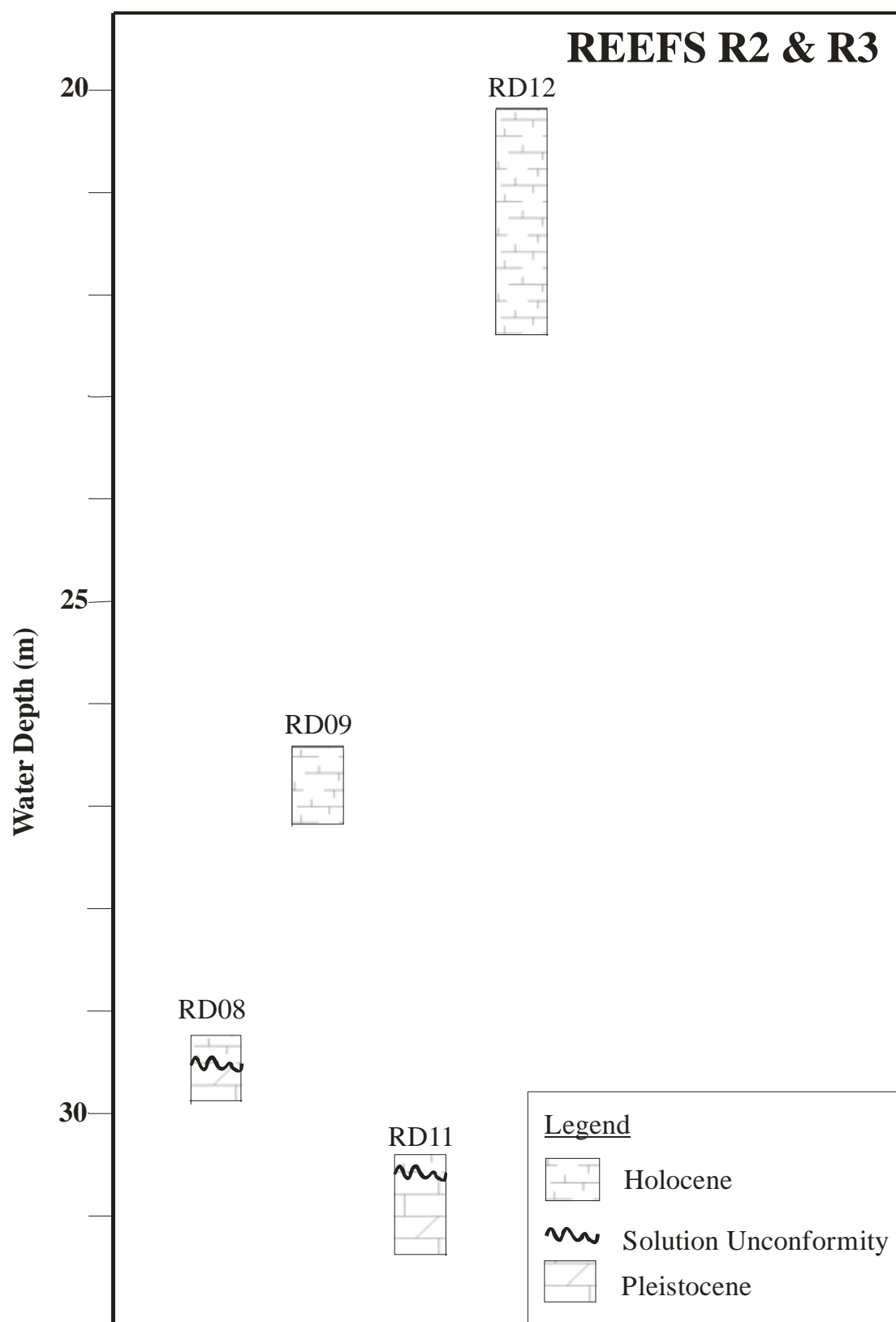


Figure 4.8. Composite core log for Reefs R2 & 3 showing the position and lithology of drill holes in relation to water depth.

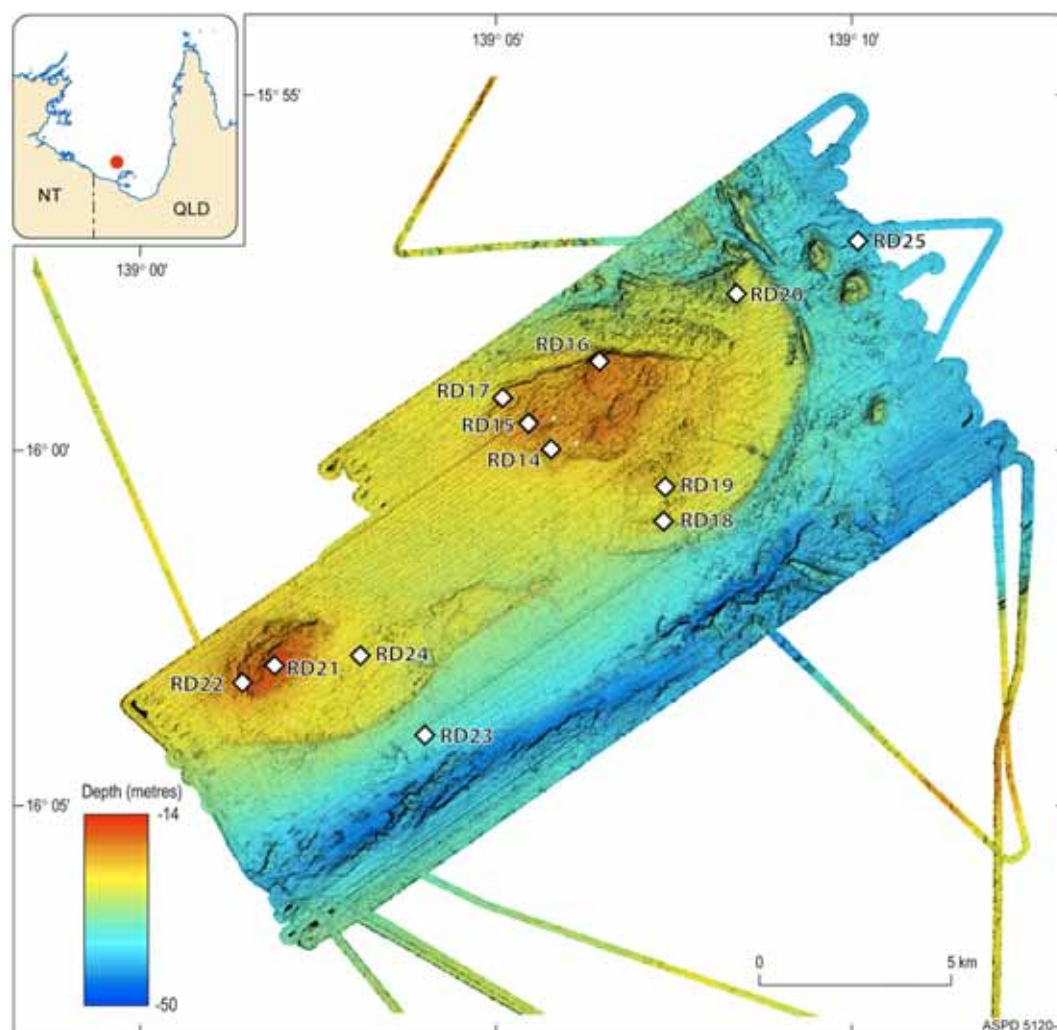


Figure 4.9 Locations of drill core sites on reef R4.

4.2.5.1 Core 276/22RD14

Pleistocene Section (0-0.82 m): This core consists of a reddish-stained packstone, similar to that in core 11 (see core photo; [Appendix 5](#)) consisting of scattered coral fragments in a skeletal matrix overlying a grey, unconsolidated floatstone, consisting of large fragments of coral in a packstone matrix (see core log; [Appendix 4](#)). The two appear to be reasonably identical in thin section, consisting of corals (calcite), coralline algae, molluscs, quartz (10-15%), and forams in a mixed sparite and micrite cement, except the lower unit shows no signs of iron-staining.

4.2.5.2 Core 276/23RD15

Pleistocene Section (0-0.62 m): The unconsolidated rudstone (see core log; [Appendix 4](#)) at the top of the core (0-0.24m) consists of iron-stained fragments of bored coral and other skeletal material. The corals are now calcite and have pore linings of sparry calcite cement. The coral has been converted to calcite as a result of neomorphism, but the neomorphic calcite (apart from being slightly darker in transmitted light) is similar in crystal size to the sparry calcite cement. A calcite coral near the top of the core gave a U-series age of $73,870 \pm 360$ years ([Table 4.3](#)), which, again, must be treated as a minimum age, in lieu of its mineralogy.

The iron staining is considered to be a result of weathering of the exposed surface of the rudstone during subaerial diagenesis. Beneath (0.24-0.47 m) is a floatstone consisting of fragments of branching coral in a greyish packstone matrix (see core log; [Appendix 4](#)). The base of the core is an

iron-stained framestone, consisting mainly of coral, but with some coralline algae and molluscs. In thin section it is noticeable that there are also abundant benthic forams (RD15, G-00155; [Appendix 5](#)).

4.2.5.3 Core 276/24RD16

Pleistocene Section (0-0.63 m): The top of the core consists of a beige to slightly reddish, well cemented packstone that contains some larger skeletal fragments. Below this is reddish coloured unconsolidated rudstone. The base of which is distinctly iron-stained. The amount of iron-staining in this core indicates that it has undergone prolonged subaerial exposure.

4.2.5.4 Core 276/25RD17

Pleistocene Section (0-0.62 m): The top 13 cm consists of a floatstone that has undergone extensive pedogenesis, mainly in the form of root moulds. Directly beneath this soil horizon is a friable to unconsolidated packstone that contains some gravel-size skeletal fragments. In addition, it contains numerous rounded, granule-size intraclasts which consist of skeletal fragments (e.g. coral) or iron-rich micrite (with quartz) (RD17, G-00158; [Appendix 7](#)). These occur in a benthic foram, quartz (up to 15%), micrite matrix and a later sparry calcite cement. The rounded nature of the intraclasts suggests that they have been transported or formed in a high energy environment. The presence of very large (granule-size) quartz grains also suggest that they are an *in situ* and not transported by fluvial or aeolian processes. One possibility is that they are a littoral deposit formed from the weathered remnants of the platform itself.

The rest of the core consists of a heavily iron stained framestone?, that consists of skeletal particles in a reddish brown matrix (see core photo; [Appendix 5](#)). The corals have all been neomorphosed to calcite and vadose conditions are indicated by fabric selective crystal mosaics that now make up the original coral skeleton. This contrasts with the finer, clearer sparry calcite cement that is widespread; lining/filling both coral pores and cavities/borings (RD17, G-00025 & G-00026; [Appendix 7](#)). There is a fair amount of internal sediment infill, particularly within borings and interskeletal cavities. The internal sediment consists of silt-size quartz and skeletal fragments (including sponge chips) in a dark (in transmitted light) micrite cement. The quartz grains are subangular and range in size from fine silt to fine sand (moderate to poorly sorted). While most of this infill appears to be now calcite, the combination of the quartz grains with the skeletal material that is set in what was once Mg-calcite cement indicates that the quartz was introduced while the reef was still growing (marine) and not after it was subaerially exposed (RD17, G-00027; [Appendix 7](#)).

4.2.5.5 Core 276/26RD18

Holocene Section (0-0.35 m): The top half of the Holocene section consists of a somewhat iron stained unconsolidated gravel, consisting of fragments of corals and molluscs. This is underlain by a skeletal limestone in a sand/mud matrix (unconsolidated). At the base of the Holocene section is a slightly bored and infilled coral fragment. This is an aragonite coral with about 20% of pores containing some internal sediment (plus quite a lot of quartz grains; see RD18, G-00030; [Appendix 5](#)). There is a fair amount of discolouration of the coral (in transmitted light). This does not involve the centres of calcification necessarily, but occurs elsewhere within the trabeculae, and is not brownish, but nearly black (RD18, G-00029; [Appendix 5](#)). This type of discolouration may be a result of partial dissolution. However, the XRD results show the coral to be aragonite and it gave an age of 9870 ± 55 years ([Table 4.3](#)).

Pleistocene Section (0.35-0.76 m): The solution unconformity has been placed at 0.35 m, although beneath that is a reworked limestone gravel in a muddy matrix whose age is uncertain. The majority of the Pleistocene section is a corallgal framestone with cavities filled with iron-stained internal sediment. Sparry calcite cement has infilled the moulds of some allochems as well as filling some cavities (both inter- and intraskeletal). The primary micrite matrix contains silt-size quartz, silt-size

internal sediments (now calcite), and small benthic forams. The less common second generation micrite is iron-stained and contains coarser (sand-size) quartz grains.

4.2.5.6 Core 276/27RD19

Holocene Section (0-0.28 m): The top 12 cm of this core consists of iron-stained uncemented rubble that presumably forms part of a hardground or hiatal surface. Beneath that are unconsolidated and tightly packed limestone clasts in a carbonate sand matrix. It is possible that the limestone clasts are pre-Holocene, but there is no thin section or XRD to confirm this. A reasonably fresh looking coral is present at 0.24m.

Pleistocene Section (0.28-0.42 m): The solution unconformity (see core log; [Appendix 4](#)) has been placed at 0.28 on the basis of the sequence directly below it being angular limestone pebbles that could be the source of the limestone clasts observed near the base of the Holocene section. Deeper in the core the clasts are mud supported and the matrix is iron-stained.

4.2.5.7 Core 276/28RD20

Holocene Section (0-0.19 m): This is an iron-stained, quartz-rich packstone that also contains skeletal fragments in a micrite matrix (see core log; [Appendix 4](#)). The quartz grains vary from silt to coarse sand, and from angular to well-rounded. Some quartz grains have rims that appear to be superficial ooids (RD20, G-00173; [Appendix 7](#)), but it is not certain if the rims are carbonates or iron oxides (at this stage they are considered to be carbonate, but they do have a reddish colour under crossed polarisers). Skeletal particles are variable, mainly mollusc fragments (often heavily bored and filled) and benthic forams. However, there are also some rare coral and coralline algal fragments. Heavily iron-stained and rounded intraclasts are fairly common also. These are either quartz-rich or carbonate. The presence of allochems with their original mineralogy and acicular aragonite cement indicates that the packstone is Holocene.

Pleistocene Section (0.19-0.42 m): The solution unconformity is placed at 0.19 m where the quartz-rich packstone is replaced down core by a wackestone consisting of limestone clasts in a muddy matrix (see core log; [Appendix 4](#)).

4.2.5.8 Core 276/29RD21

Pleistocene Section (0-1.10 m): This core consists predominantly of a coral framework (see core log; [Appendix 4](#)) consisting mainly of branching and platey corals which have some cavity fill. The top 9 cm shows a large boring(?) that has extensive iron staining (see core photo; [Appendix 5](#)), but beneath that it appears to be totally free of iron, and the corals are relatively pristine (although they are now calcite). The corals are completely neomorphosed to calcite, with fabric selective (freshwater vadose) fabrics towards the top and cross cutting fabric (RD21, G-00174 & 175; [Appendix 7](#)), indicative of a freshwater phreatic environment of diagenesis, throughout the rest of the core. Many of the corals have their pores filled with what was originally a marine micritic cement. In other pores there is a thin layer of micrite cement followed by small crystals of sparry calcite cement, which have then been enveloped within the larger calcite crystals (RD21, G-00174; [Appendix 7](#)). Quartz is a relatively minor constituent (<5%), is mainly silt-size, and occurs in both coral pores and boring fill.

4.2.5.9 Core 276/30RD22

Holocene Section (0-0.26 m): The age of this core is unknown because no age determinations or thin sections are available. However because it consists of mainly unconsolidated gravel (see core log; [Appendix 4](#)), it is assumed to be Holocene. While the top of the core is iron-stained, this is likely to be a result of no growth of the platform, forming the hiatal surface present at the top of many of the other cores.

4.2.5.10 Core 276/31RD23

The age of this core from the deeper front of the platform is not apparent from the core description (see core log; [Appendix 4](#)). The core log shows a mottled oxidised packstone containing abundant serpulids as well as other skeletal fragments in a muddy sandy matrix overlying a greyish wackestone, coated by a mottled mud. The upper part may be comparable to the coralline algal/serpulid boundstone/bafflestone described in some of the other cores (e.g. cores 3 and 4; see core logs; [Appendix 4](#)), in which case it is likely to be Holocene.

4.2.5.11 Core 276/32RD24

Pleistocene Section (0-1.26 m): The top 28 cm consists of a coral rudstone, consisting of pieces of framework along with rounded corals fragments. It is difficult to determine if this is Pleistocene or not from the core log, but it is considered to be a weathered product of the underlying sequence, which is definitely pre-Holocene. This underlying unit is a framestone with iron staining in the top part of the unit (see core log; [Appendix 4](#)). It consists essentially of a branching coral framework, which has been completely neomorphosed to calcite together with abundant sparry calcite cement and micrite pore fill. Vadose conditions are indicated by a fabric-selective crystal mosaic. Between the corals is a somewhat iron-stained skeletal packstone, with allochems (now calcite) in a mainly micrite cement. From various lines of evidence, this appears to have originally been a framestone that was filled by silt-size internal sediments and marine micrite cement, as well as bored several times by a variety of endoliths, with the borings becoming filled with micrite cemented internal sediments, and finally subaerially exposed (vadose). After that there was infill of both primary and secondary porosity by sparry calcite cement. Several generations of sparry calcite precipitation can be delineated by iron-rich layers (RD24, G-00176; [Appendix 7](#)), suggesting that the iron oxides were introduced into the limestone at various stages during its exposure above sea level.

The lower part of the core consists of what appears to be a framestone. It consists of branching corals in a mud supported matrix. The limestone has a somewhat weathered look (see core photo; [Appendix 5](#)) and is iron-stained. It is very different from the framestone towards the top of the core. This is verified by thin section examination which shows a heavily iron-stained quartz/skeletal packstone as the matrix, with some large quartz grains (up to coarse sand-size) in a mainly micrite matrix. Rounded intraclasts are also iron-stained and fairly common. The only other discernable skeletons are benthic forams. The abundance of quartz and its much larger grainsize indicates that this was deposited in a different environment from the framestone unit above it. It tends to resemble the Pleistocene framework in core 18 and possibly the Holocene section in core 20.

4.2.5.12 Discussion – Reef R4

A composite of the drill logs for Reef R4 is shown in [Figure 4.10](#), representing the northern and southern “highs” respectively. What these show is that there is very little Holocene material present, and of the seven holes drilled in the shallower areas (RD14-19 and RD 21) five had no Holocene reef at all; these also happened to be the shallowest holes (18.0-23.5 m). This more or less diminishes the amount of Holocene reef growth on this part of the platform, with a maximum recorded Holocene reef thickness of only 0.35 m. However, the one Holocene age from the platform of 9870 ± 55 again shows that reef growth commenced as soon as the platform was initially flooded, but that it ceased soon after.

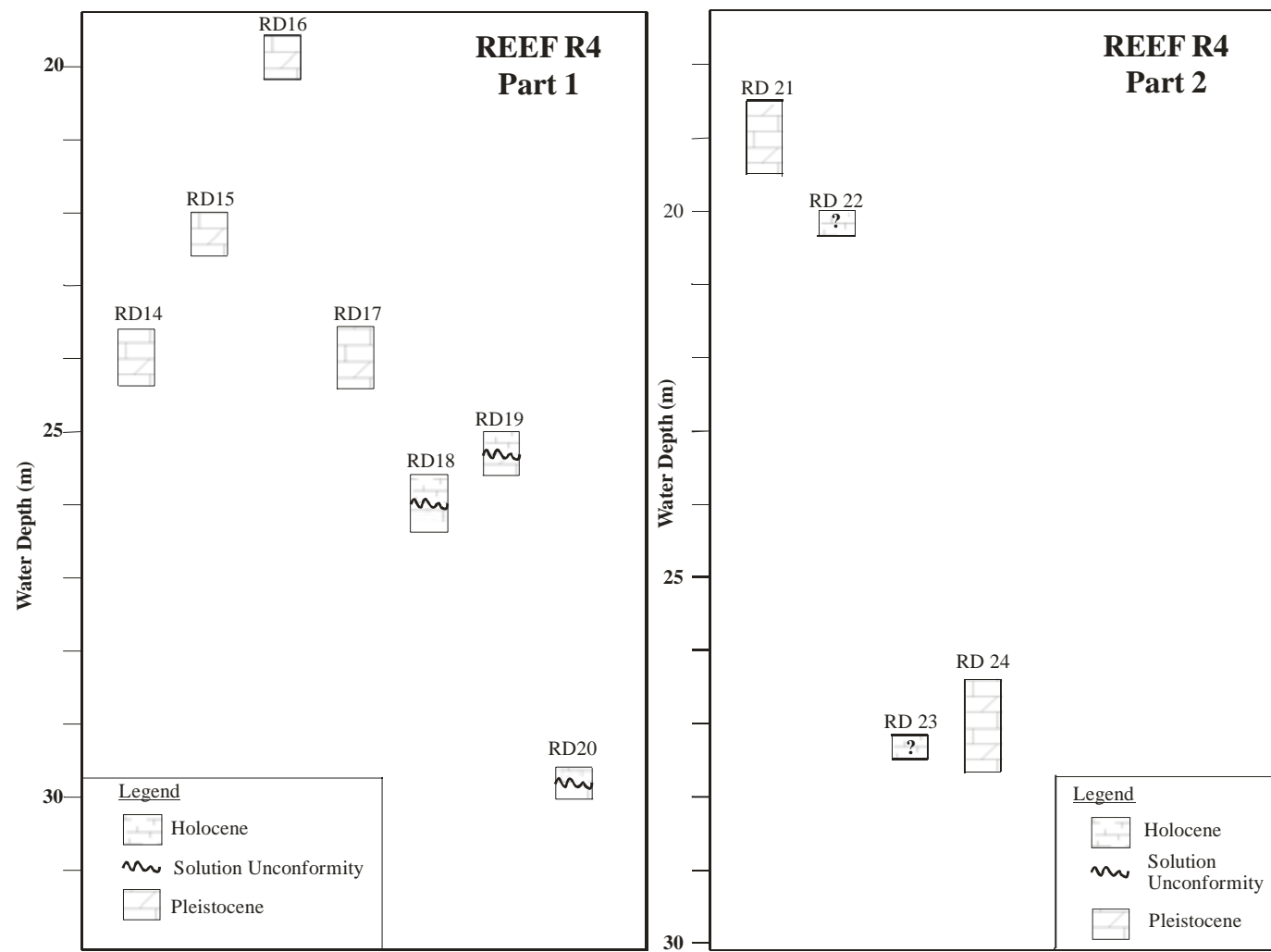


Figure 4.10. Composite core log for Reef R4 showing the position and lithology of drill holes in relation to water depth.

4.2.6 REEF R5

As with reef R4, this “reef” forms the northern part of the carbonate platform that extends northwest from Mornington Island (Fig. 4.1). On the eastern side of Reef R5 the sea floor rises from 45-50 m onto the main platform at depths of 25-30 m, and reaching a minimum depth of 16 m at the southern end (Fig. 4.11). Twelve holes (RD31-33, and RD35-43) were drilled on the platform, while one hole (RD34) was drilled off the platform in a water depth of 44 m. Recovery for all 13 drill holes varied from 0.43-2.51 m (Fig. 4.2).

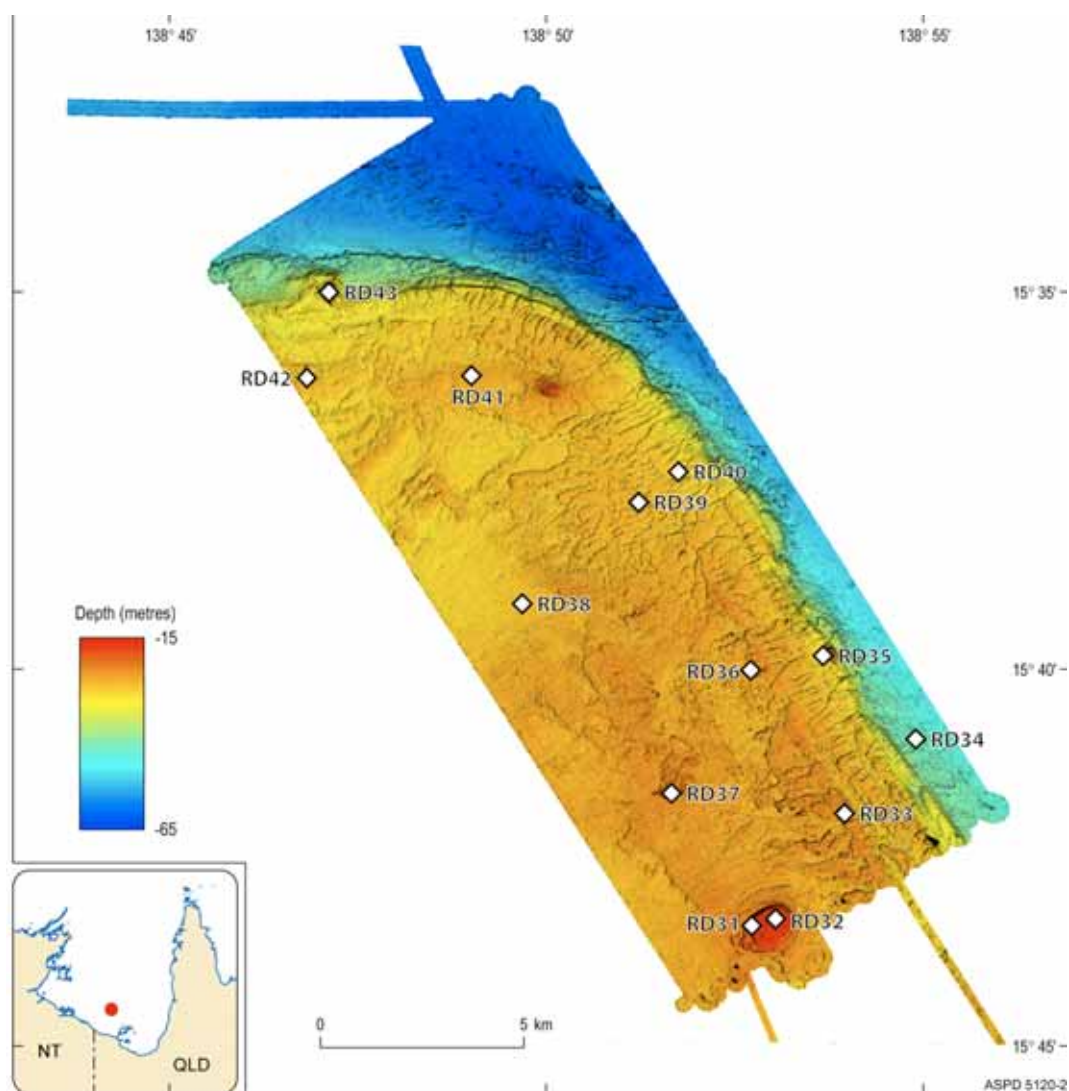


Figure 4.11. Locations of drill core sites on reef R5.

4.2.6.1 Core 276/50RD31

Pleistocene Section (0-1.49 m): The top of the core (see core log; Appendix 4) consists mainly of a skeletal packstone/wackestone with some larger coral pieces incorporated. The corals are neomorphosed to calcite and there is some fine pore lining by calcite cement. The packstone/wackestone consists of larger benthic foraminifera (*Amphistigina* sp?, *Marginopora vertebralis*; RD31, G-00061; Appendix 7), plus fragments of benthic forams, echinoid spines, corals and quartz with some patches of micrite. The limestone has around 40% porosity and is mainly cemented by sparry calcite between grain boundaries. Because they are originally Mg-calcite, most of the forams are intact, whereas original aragonite allochems have been neomorphosed to calcite.

Quartz grains make up about 5-10% of the constituents. Their grain size ranges from silt to medium sand, while shape is angular to rounded (RD31, G-00063; [Appendix 7](#)).

The lower part of the core is a calcitic coral/algal framestone with interskeletal cavities often filled by cemented internal sediment (see core log and core photo; [Appendix 5](#)). The corals consist of species of *Porites* and *Acropora* that have undergone neomorphism in a subaerial vadose environment. The corals have been encrusted by coralline algae, with cavities and borings filled or partly filled with original micrite cemented internal sediment and some secondary lime mud. Quartz is relatively minor (<5%) compared to the overlying packstone/wackestone.

4.2.6.2 Core 276/52RD32

Pleistocene Section (0-2.06 m): The top of the core consists of a fairly massive coral with some encrustation by coralline algae on top (see core log; [Appendix 4](#)). The coral has been bored mainly by sponges and bivalves, and while some are filled, it by is unconsolidated lime mud. The top half of the coral is somewhat iron-stained. Thin section examination shows that the coral has been neomorphosed to calcite and XRD results ([Table 4.2](#)) show that it is 100% calcite (as is the rest of the core).

The next sequence (0.37-1.05 m; see core log; [Appendix 4](#)) consists of what could be described as either a packstone with several large corals incorporated or a sediment filled framestone. These branching corals (*Acropora* sp.?) have been transformed to calcite mainly as a result of neomorphism, but there are also some examples of solution/reprecipitation. Many of the coral pores are lined by a thin (50µm) layer of micrite cement, which is most probably marine in origin. In parts of the coral, where dissolution is stronger than neomorphism, the micrite forms a thick “micrite envelope” after which the dissolution voids are filled with clear, sparry calcite cement RD32, G-00072; [Appendix 7](#)). A calcitic coral at a depth of 0.52 m gave a minimum age of $65,490 \pm 285$ years ([Table 4.3](#)).

The sediment filling the cavities between the larger branching corals consists of a highly porous (>50%) foram-rich packstone with some vestiges of an original coral structure. The packstone consists of large benthic forams, molluscs, coralline algae and quartz in a sparry calcite cement, and is similar to the packstone at the top of core 31.

Below 1.05 m the sequence is more obviously a framestone, with corals such as *Porites* sp. and *Acropora* sp. predominating, and the base of the core is a massive *Acropora* sp. (see core log; [Appendix 4](#)). The corals have all been neomorphosed to calcite and most examples in thin section show the coral is now made up of large calcite crystals which envelop both the coral and surrounding pores (RD32, G-00069; [Appendix 5](#)), an indication of a subaerial phreatic environment of diagenesis.

4.2.6.3 Core 276/53RD33

Holocene Section (0-0.86 m): The top of this coral framestone, consists of at least three generations of iron-stained lime mud/internal sediment, and also contains about 15% of fine sand- to silt-size quartz (RD33, G-00076; [Appendix 7](#)). An age of 8000 ± 51 years ([Table 4.3](#)) for a coral at 0.62 m and the preservation of original aragonite skeletons indicates that the entire core is Holocene, so the presence of so much quartz at the very top of this core is significant.

Directly beneath this is a highly altered coral (aragonite), which has pores often fringed by aragonite cement or filled with Mg-calcite micrite cemented internal sediments. The top of the coral is thinly encrusted by coralline algae. Below this is a 35 cm long *Porites* sp. At the top of the coral there is about 20% infill by cemented internal sediments, whereas the remainder is fairly pristine.

The base of the core (see core log; [Appendix 4](#)) consists of fragments of encrusted coral and gravel, which are slightly dark grey in colour. In thin section this shows up as a heavily bored and infilled framestone that has at least 2 generations of borings and at least 2 generations of internal sediment

fill. Most noticeable is the presence of abundant sponge chips in this section (RD33, G-00081; [Appendix 5](#)) which, while very common as an internal sediment elsewhere (e.g. GBR), is relatively rare in the Gulf cores. Quartz is also quite common and ranges from fine silt to coarse sand. The original skeletal elements, such as corals and molluscs (or rather what's left of them after extensive boring and infill), are aragonite.

4.2.6.4 Core 276/57RD34

Pleistocene Section (0-1.58 m): This core (see core log; [Appendix 4](#)) is off the reef platform in 44 m of water ([Fig. 4.11](#)). The core is very unusual, having a chocolate brown skeletal grainstone at the top and a fairly stiff pale coloured mudstone with some iron-staining at the base (see core photos; [Appendix 5](#)). The grainstone is made up predominantly of coarsely crystalline calcite cement which has filled both skeletal moulds (originally aragonite) and matrix. Skeletal particles are either neomorphosed to calcite (aragonite allochems) or preserve their skeletal structure (Mg-calcite allochems). The calcite cement crystals are euhedral and either equant or elongate, with well defined crystal (bi-pyramidal) terminations where they project into voids (RD34, G-00083 & G-00091; [Appendix 7](#)). Quartz is fairly common (up to 15% in places) and occurs in all shapes and sizes. The iron-staining within the grainstone comes from several sources. Some of the most iron-rich phases are in the form of rounded intraclasts which consist of angular quartz of various sizes in a haematite? matrix (RD34, G-00101; [Appendix 7](#)). The intraclasts can be up to pebble size, and since many of them do not appear to contain any carbonate, it suggests that they may be a result of pedogenesis. The intraclasts have been deposited, together with individual quartz grains, within interskeletal cavities and later cemented by calcite. While the intraclasts are obvious, most of the iron staining is more discrete, occurring along crystal boundaries (RD34, G-00085 & G-00086; [Appendix 7](#)) as well as in patches. Some of the haematite? occurs as discrete grains (RD34, G-00083; [Appendix 7](#)). The deposition of iron oxides along calcite crystal boundaries suggests that it took place in a subaerial environment and that it was a periodic rather than a continuous process.

4.2.6.5 Core 276/58RD35

Holocene Section (0-0.18 m): The thickness of the Holocene section is only 18 cm here and at 0.16m a coral gave a U/Th age of 7657 ± 47 years ([Table 4.3](#)). The solution unconformity is marked by a fairly pristine but bored coral overlying a weathered looking limestone. The thin Holocene sequence basically rules out any real attempt at reef colonisation here; from the age and the thickness it seems that the coral was an individual colony, such as those seen in some of the video footage from this reef.

Pleistocene Section (0.18-0.78 m): This consists of a framestone (see core log; [Appendix 4](#)), consisting mainly branching corals or fragments of branching corals, along with some encrustation and sediment fill. The corals have a somewhat weathered look and there are indications of iron staining. The corals have been completely converted to calcite and many of the pores are filled with calcite cement. In the interskeletal cavities both articulate and crustose coralline algae tend to dominate, with lesser amounts of benthic forams, quartz and other minor skeletal elements, in a sparry calcite cement. In places, only coralline algae, benthic forams and micrite envelopes are the only observable features, with all the aragonite allochems being dissolved. Elsewhere, the micrite envelopes have been filled by sparry calcite cement (RD35, G-00161; [Appendix 7](#)). It is noticeable that there are two sparite textures. The most common is a coarse (50-200µm) cement that is predominantly interskeletal, but does fill solution moulds or what were originally skeletal chambers in aragonite shells. The less common is a much finer (almost microspar) that appears to mainly fill some chambers and what appear to be burrows or borings (RD35, [Appendix 5](#), G-00162). Quartz grains make up about 8%. Some secondary (later) infill is present in some cavities. It consists of quartz grains in a yellowish (in transmitted light), microcrystalline matrix/cement(?).

4.2.6.6 Core 276/59RD36

Pleistocene Section? (0-0.53 m): The top of the core (see core log; [Appendix 4](#)) consists of a loosely packed coral floatstone, the top half of which is slightly weathered and iron-stained. Between 0.34 and 0.43 m there is a corallgal framestone with some sediment fill and a thin lithified crust on top. The base of the core is a rudstone, consisting of coarse coral gravel in a tightly packed granule-size shell grit.

4.2.6.7 Core 276/60RD37

Holocene Section (0-0.58 m): The core is confirmed as Holocene from a U-series age of 9610 ± 53 ([Table 4.3](#)) from the base of the core (see core log; [Appendix 4](#)). Apart from the coral at the base, most of the core is made up fragments of coral, coralline algae and molluscs in a coarse skeletal sand matrix.

4.2.6.8 Core 276/61RD38

Pleistocene Section (0-2.51 m): The top of the core (see core log; [Appendix 4](#)) consists of a coarse, fawn coloured, well cemented grainstone with larger fragments of molluscs and corals, as well as coralline algae, benthic forams, and smaller fragments of corals and molluscs in a predominantly sparry calcite cement. The top of the grainstone is iron-stained and quartz-rich (20%), whereas this grades down to 5% near the base.

The middle section of the core (see core log; [Appendix 4](#)) consists of highly weathered granule- to cobble-size, angular fragments of reef rock, the outer edges of which have been coated with iron oxides. In some respects the clasts appear to be shattered (see core photo 1; [Appendix 5](#)). The limestone appears to have undergone a fair amount of diagenesis as evidenced by a slightly marbled look in places. The limestone is a combination of corals and often quartz-rich packstone/wackestones. The corals tend to be heavily bored and have undergone diagenesis in both vadose and phreatic environments. What is of interest is that the borings have been filled by silt-size internal sediments and sand-size quartz grains in a micrite cement, which would have been indicative of a submarine cement, presumably Mg-calcite. While it is not that obvious in thin section, where the colour is masked to some extent by the opaqueness (in transmitted light) of the micrite, in hand specimen this boring fill is of an ochre colour. This suggests that the iron-staining occurred while the coral was still in the marine environment and that the red clay (along with the quartz grains) was being deposited simultaneously as the internal sediment and the cement. The packstone/wackestone consists of quartz (3-20%), benthic forams, and coralline algae, in an iron-rich micrite matrix. Dissolution of aragonite allochems has resulted in the development of secondary porosity, about half of which has been filled by sparry calcite cement.

At the base of the core is what appears to be a highly weathered lime mudstone, commonly with a faint pink tinge to it (see core photo 2; [Appendix 5](#)). In thin section, this turns out to be a generally quartz-rich, somewhat iron-stained packstone/wackestone. What makes it different from the one above is the presence of echinoid plates and spines which make up to 10% of the limestone. In places, quartz makes up as much as 30-35% of the grains (RD38, G-00165; [Appendix 7](#)). These two components, along with minor allochems, are embedded in a micrite/micospar cement which is discoloured as a result of iron-staining.

4.2.6.9 Core 276/62RD39

Holocene Section? (0-0.62 m): There is a great deal of ambiguity about this core; namely, the core description does not fit the thin section description. For example, the thin section from 12-13 cm is essentially a bafflestone, consisting of branching coralline algae (*Lithophyllum* sp.?) that forms an open network, whereas the core description for this interval describes a floatstone of coral gravel. Similarly a coral described in thin section from 35-36 cm gave a U-series age of $10,590 \pm 58$, but the core description is a boundstone. It does not appear that the samples have just been given the wrong

sampling depths because the thin section from 46-47 cm is described as a calcitic packstone, whereas there is no evidence of calcite in the core. However, the age is the oldest Holocene date so far, and suggests (no matter what core it comes from) that the timing of first reef growth at the end of the transgression was at about this time.

4.2.6.10 Core 276/63RD40

Pleistocene Section? (0-0.83 m): The upper 20 cm of the core is a framestone, consisting of iron-stained corals and coralline algae that have been bored and infilled with cemented lime mud. From 20-48 cm the core is comprised of unconsolidated corallgal gravel that is iron-stained in the upper part but becomes dark-grey towards the base. The lower 48-83 cm of the core is a reddish framestone, consisting of a framework of corals and coralline algae that have been infilled by cemented internal sediments. The iron-staining appears to be associated mainly with the matrix.

4.2.6.11 Core 276/65RD41

Pleistocene Section? (0-0.43 m): The entire core is a floatstone, comprised of broken coral fragments in a sandy matrix.

4.2.6.12 Core 276/67RD42

Pleistocene Section? (0-0.63 m): From 0-26 cm the core is a rudstone/grainstone consisting of sand-to pebble-sized skeletal fragments in a cemented sandy matrix, slightly iron-stained in the uppermost part. From 26 to 45 cm the core is a heavily iron-stained floatstone consisting of breccia-like, angular fragments of limestone. From 45 to 63 cm the core is a framestone consisting of corals and other skeletal fragments in a vuggy matrix.

4.2.6.13 Core 276/68RD43

Pleistocene Section? (0-0.83 m): This core was collected in 24 m water depth from the peak of a localised mound located on the northernmost limb of the platform reef. The upper 0-35 cm of the core comprises slightly iron-stained branching coral framework, bearing lithified crusts on some of the corals. From 35 – 50 cm the core is a greyish coloured, coral-sand floatstone, which overlies (50 – 83 cm) framestone, consisting of a single, small coral head thinly encrusted by coralline algae.

4.2.6.14 Discussion – Reef R5

A composite drill log for Reef R5 is shown in [Figure 4.12](#). Similar to Reef R4, the amount of Holocene material recovered in the cores is sparse, with only RD33 (0.86 m) and RD37 (0.58 m) indicating any significant reef growth. However, of the four Holocene ages for this reef two are relatively young, giving ages of 8000 ± 51 (RD33) and 7657 ± 47 (RD35) ([Tables 4.3](#)). This suggests that some reef growth continued here for up to 500 years after Reefs R1-R4.

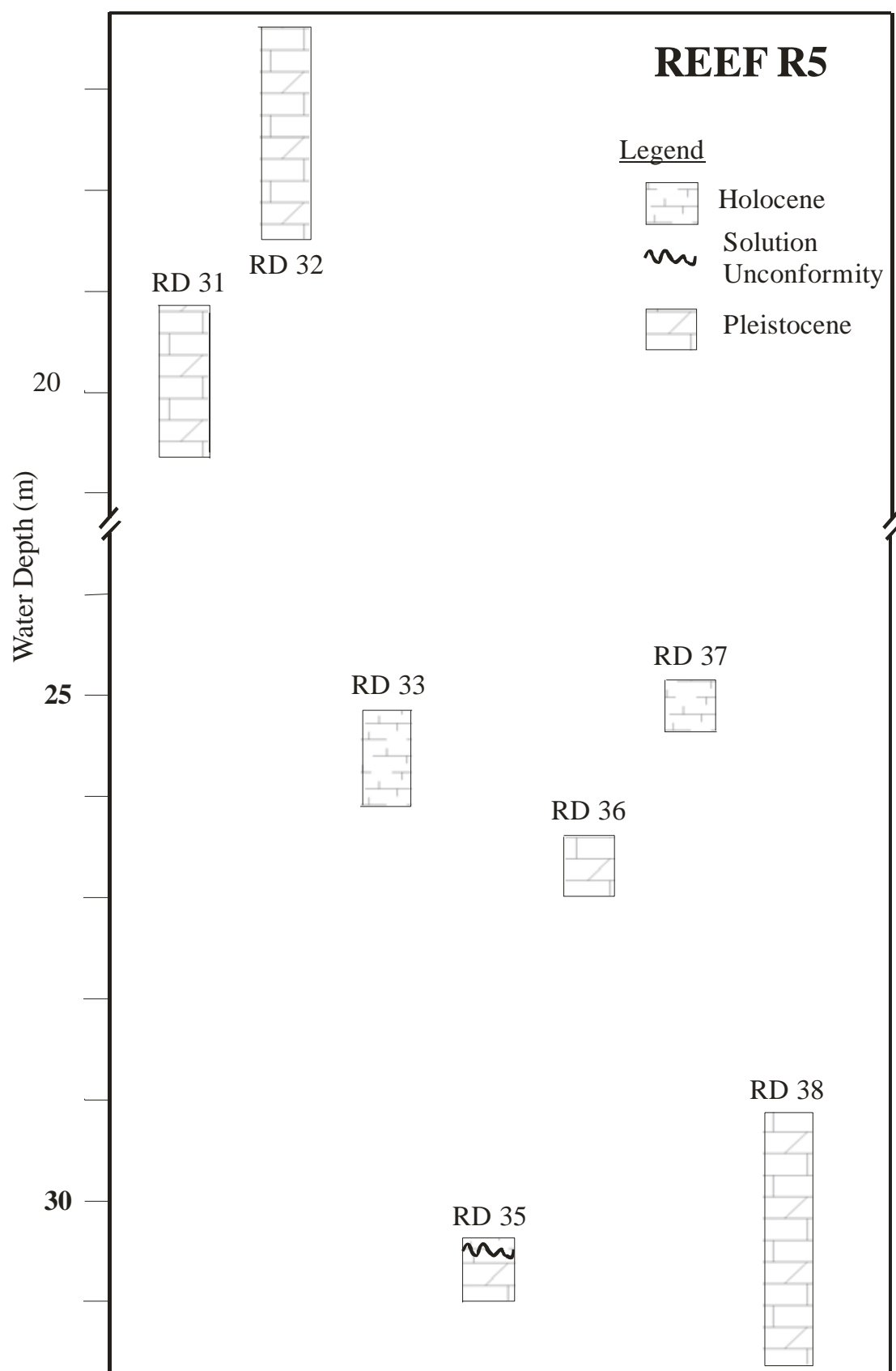


Figure 4.12. Composite core log for Reef R5 showing the position and lithology of drill holes in relation to water depth.

4.2.7 Reef R6

4.2.7.1 Core 276/34RD26

Holocene Section (0-1.25 m): The results of the U/Th dating ([Table 4.3](#)) shows that the entire core is Holocene. The top of the core (see core log; [Appendix 5](#)) consists of an *in situ*, fairly pristine coral (*Porites* sp.?), which has been bored at the top and base by the endolithic bivalve *Lithophaga* sp. Thin section examination shows that this aragonite coral has about 30% of its pores filled with cemented internal sediment. The XRD results indicate that the sample is 99% aragonite, which brings into question whether or not the pore fill is removed during cleaning or if all of the fill is aragonite.

The remainder of the section consists of a framestone that is dominated by large-size corals or broken coral fragments, which are somewhat bored (bivalves, polychaetes), but with very little fill. A fairly pristine coral, possibly *in situ*, occurs at the base.

The two ages of 2643 ± 28 and 3349 ± 37 ([Table 4.3](#)) come from near the top and bottom of this 1.25 m core, and indicate a growth rate of about 1.6 m kyr^{-1} . This appears to be at the very low end of reef growth rates, and this, together with rates of $1\text{--}4 \text{ m kyr}^{-1}$ for RD12, suggests that growth was too slow for the reefs to eventually reach sea level. In addition, the ages are much younger than the others from the region ([Table 4.3](#)). This could indicate that part of this reef has regenerated, while the others have not. The core is from a water depth of 19.2 m, making this reef the shallowest in the area ([Fig. 4.13](#)). It's possible that this had some bearing on its regrowth, but there is insufficient information to say this unequivocally. In fact the shallowest parts of other reefs have no Holocene growth at all.

4.2.7.2 Core 276/43RD27

Holocene Section (0-1.05 m): Results from XRD, dating, and thin section examination show that the entire core is Holocene. The top 44 cm of the core consists of a framestone (see core log; [Appendix 4](#)), consisting of corals that are encrusted by coralline algae and heavily bored by sponges polychaetes and bivalves. An age of 7270 ± 38 yrs was obtained from a coral from 15 cm below the top. This coral has been analysed by XRD as 100% aragonite, yet the thin section shows parts of it filled with cemented internal sediment. Again, it is assumed that the XRD piece is more pristine than the thin section slice. However, those parts of the thin section that show pristine coral do show fine fringes of aragonite lining the coral pores. This might explain the slightly younger age of this coral when compared to the majority of Holocene corals.

Parts of the framestone consist of thin (1 mm wide) stringers of crustose coralline algae, together with some encrusting bryozoans and foraminifera. Some mollusc fragments (mainly bivalves) and intact gastropods are also present. The coralline algae do not resemble the more nodular and branching *Lithophyllum* sp. described in other boundstones/bafflestones. The algae are more ribbon-like and have quite large conceptacles. Some semi-lithified lime mud is present partly filling cavities and conceptacles, while other conceptacles contain spherulitic aragonite (RD27, G-00179; [Appendix 7](#)).

The remainder of the core has been designated as a floatstone, although in essence it appears to be a broken down framework, with broken branching coral fragments in a pebbly/sandy matrix. There has been extensive infilling of cavities by silt- and sand-size internal sediments and some quartz (3%). The internal sediments consist of articulated coralline algae, forams and mollusc fragments in an Mg-calcite micrite cement.

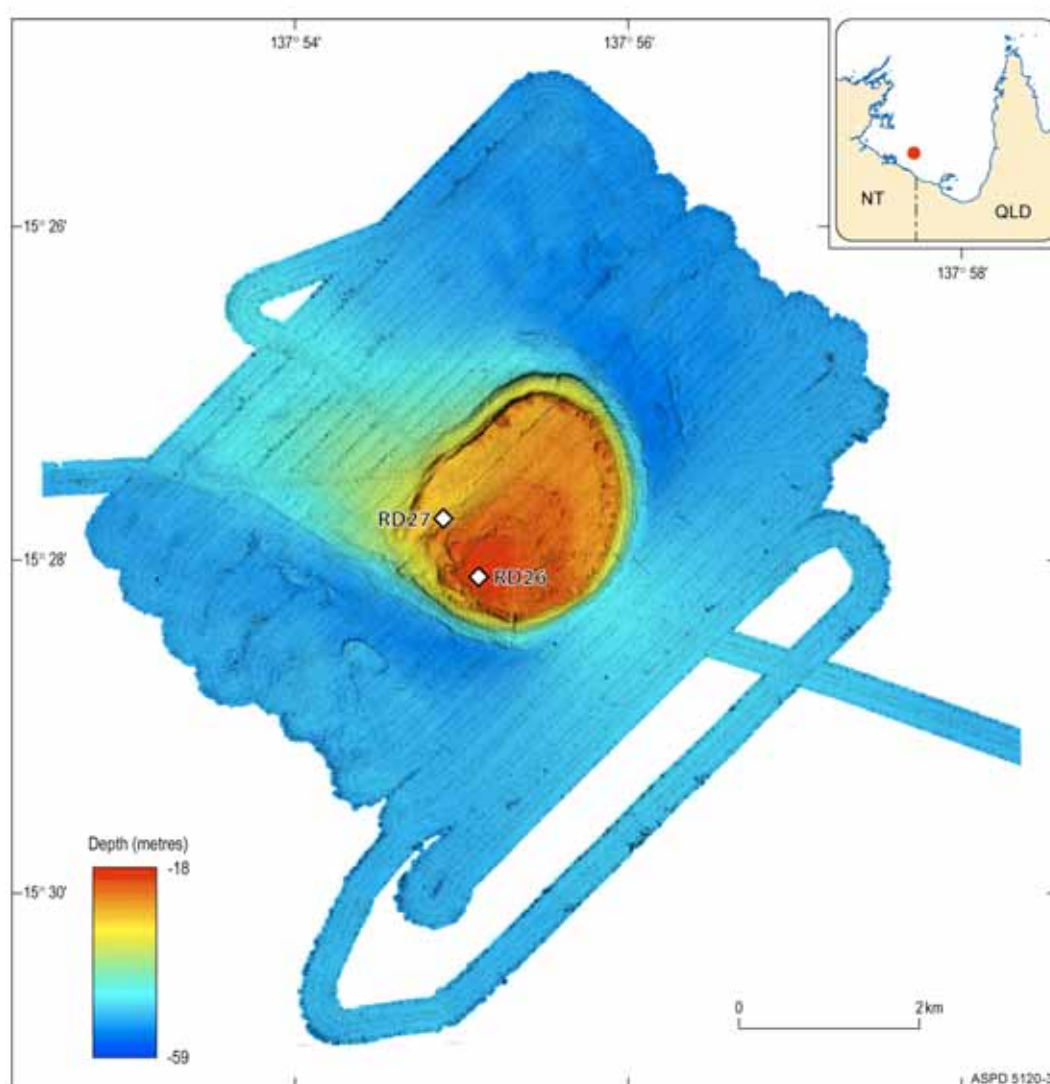


Figure 4.13. Locations of drill core sites on reef R6.

4.2.8 Reef R7

4.2.8.1 Core 276/45RD28 (length: 1.22 m; water depth: 29.2 m)

Holocene Section (0-0.55 m): The top 24 cm consists of a weathered and somewhat iron-stained framestone of slightly bored branching corals and crustose coralline algae (see core log; [Appendix 4](#)). The matrix consists of internal sediments and quartz in a micrite cement.

At the base of the Holocene section, the core consists of broken fragments of branching coral in a calcareous sandy matrix. XRD analysis of a coral at 0.45m shows it to be 100% aragonite, while in thin section it does show signs of leaching (mainly a patchy darkening of the trabeculae). This coral gave a U/Th age of 9661 ± 46 years.

Pleistocene Section (0.55-1.22 m): The solution unconformity occurs at 0.55m where the underlying unit changes to a weathered, iron-stained framestone that consists of corals, coralline algae and internal sediment (see core log; [Appendix 4](#)). In thin section the top part consists of an algal boundstone which appears to be unaltered, and even has fans of aragonite cement (RD28; Fig. G-00183). However, on closer inspection it shows evidence of mouldic porosity development and the

precipitation of fine sparry calcite cement. The two together (i.e. aragonite and calcite cements) is unusual for these reefs, although elsewhere this is often found at the solution unconformity.

The lower part of the Pleistocene section consists of a packstone showing abundant dissolution of skeletal particles (see core photo; [Appendix 5](#)). Iron-staining becomes more significant below 1 meter, mainly around the perimeter of larger (unfilled) cavities (see core photo; [Appendix 5](#)). The width of the iron-staining around the cavities is fairly uniform; about 2 mm (RD28, G-00181; [Appendix 7](#)). Elsewhere, there are “blebs” of iron stained micrite partly filling cavities (RD28, G-00182; [Appendix 7](#)). This suggests that the iron-staining was a relatively late event, presumably during the last glacial.

4.2.8.2 Core 276/46RD29

Pleistocene Section (0-0.84 m): The top half of the core consists of a highly weathered and iron-stained framestone with a large amount of cavity fill by reddish brown internal sediment (see core log; [Appendix 4](#)). The larger coral fragments have been replaced by neomorphic calcite. Micrite-cemented internal sediments and sparry calcite cement fill some of the coral pores. The interskeletal cavities are filled with a skeletal packstone that consists of larger fragments of coral and coralline algae (>2 mm), together with sand- and silt-size allochems (corals, algae, molluscs, forams) and quartz, together with primary(?) micrite, that has been cemented by sparry calcite. The rock has been subaerially exposed and aragonitic constituents have been converted to calcite or form mouldic porosity. The porosity (both primary and secondary) is variable, but, overall, it is about 30%. Some of the larger vugs or cavities (>5 mm) are now filled with a reddish clay that contains silt and sand size quartz grains. Quartz makes up about 5-10% of the limestone, but it tends to be more concentrated in cavities, and locally can be as high as 25-30%. The quartz is angular to rounded in shape and is poorly sorted. Grainsize varies from fine silt to fine sand (RD29, G-00055; [Appendix 7](#)).

Below this is a semi-consolidated, weathered grainstone and part of a coral (see core log; [Appendix 4](#)). This coral (*Platygyra* sp.?) is fairly pristine, with some micrite-cemented internal sediments (plus quartz) filling some pores. This coral gave an age of $78,900 \pm 1500$ years, and the original skeleton has been completely replaced by neomorphic calcite. Some very fine calcite cement lines several of the coral pores. This, in turn, is underlain by a small faviid which also has been neomorphosed to calcite.

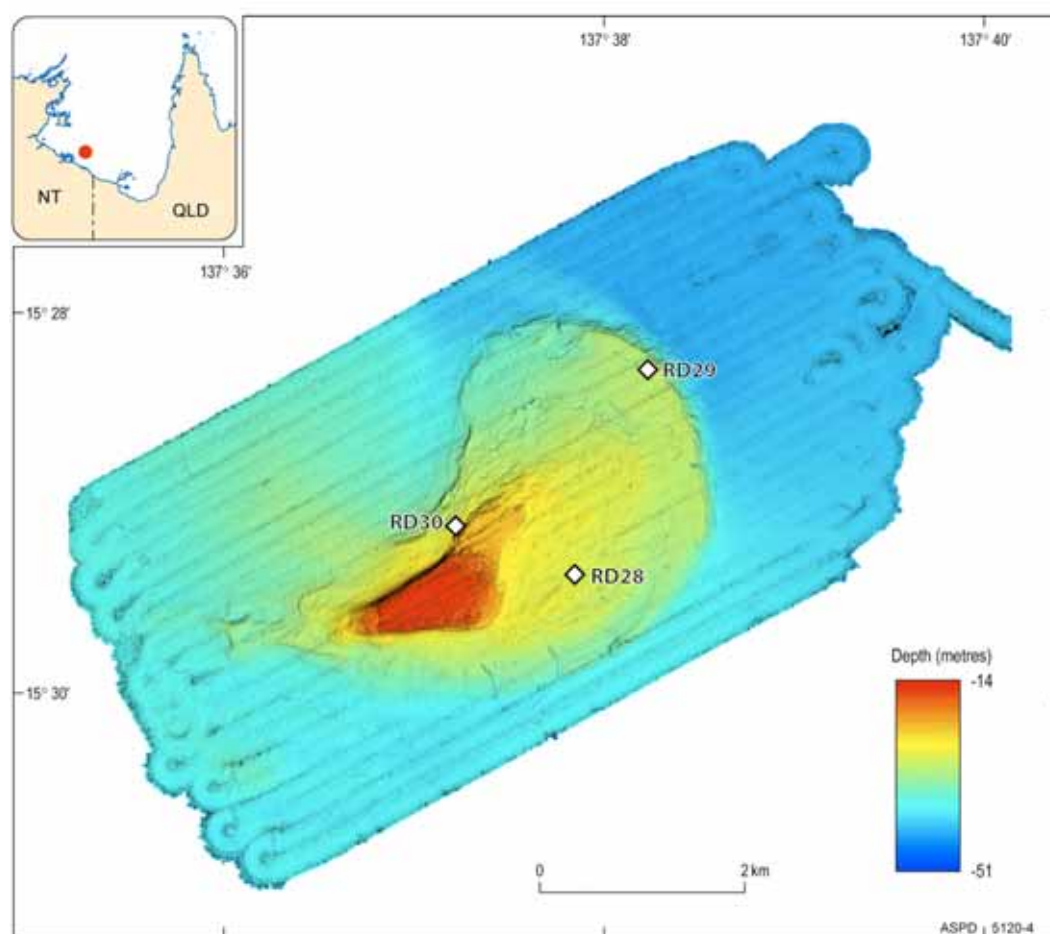


Figure 4.14. Locations of drill core sites on reef R7.

4.2.8.3 Core 276/49RD30

Holocene Section (0-0.78 m): This framestone (see core log; [Appendix 4](#)) consists of fragments of corals, with some encrustation by coralline algae and vermetids, and molluscs which appear to be mainly *in situ*. Corals are both branching and small heads. The coral has been bored, or in this case mainly excavated by barnacles. These borings have been filled by a variety of skeletal fragments (including silt-size aragonite) and two generations of lime mud/micrite, both of which are marine in origin, but only the latter appears to contain quartz. Fine fringes of aragonite cement are present lining some coral pores. The XRD results report 32% calcite, but no signs of low Mg-calcite were detected in thin section, and it would appear that it is Mg-calcite, presumably from coralline algae.

Towards the base of the core is a small *Porites* sp. head, which has some very fine fringes of aragonite cement, but is otherwise fine. The XRD results show 4.6% calcite, but nothing is apparent in thin section. It could be that this is related to a thin layer of coralline algae which occurs on the exterior of the coral. Because this would have been removed during the cleaning process, the age of 9892 ± 48 is considered to be reliable.

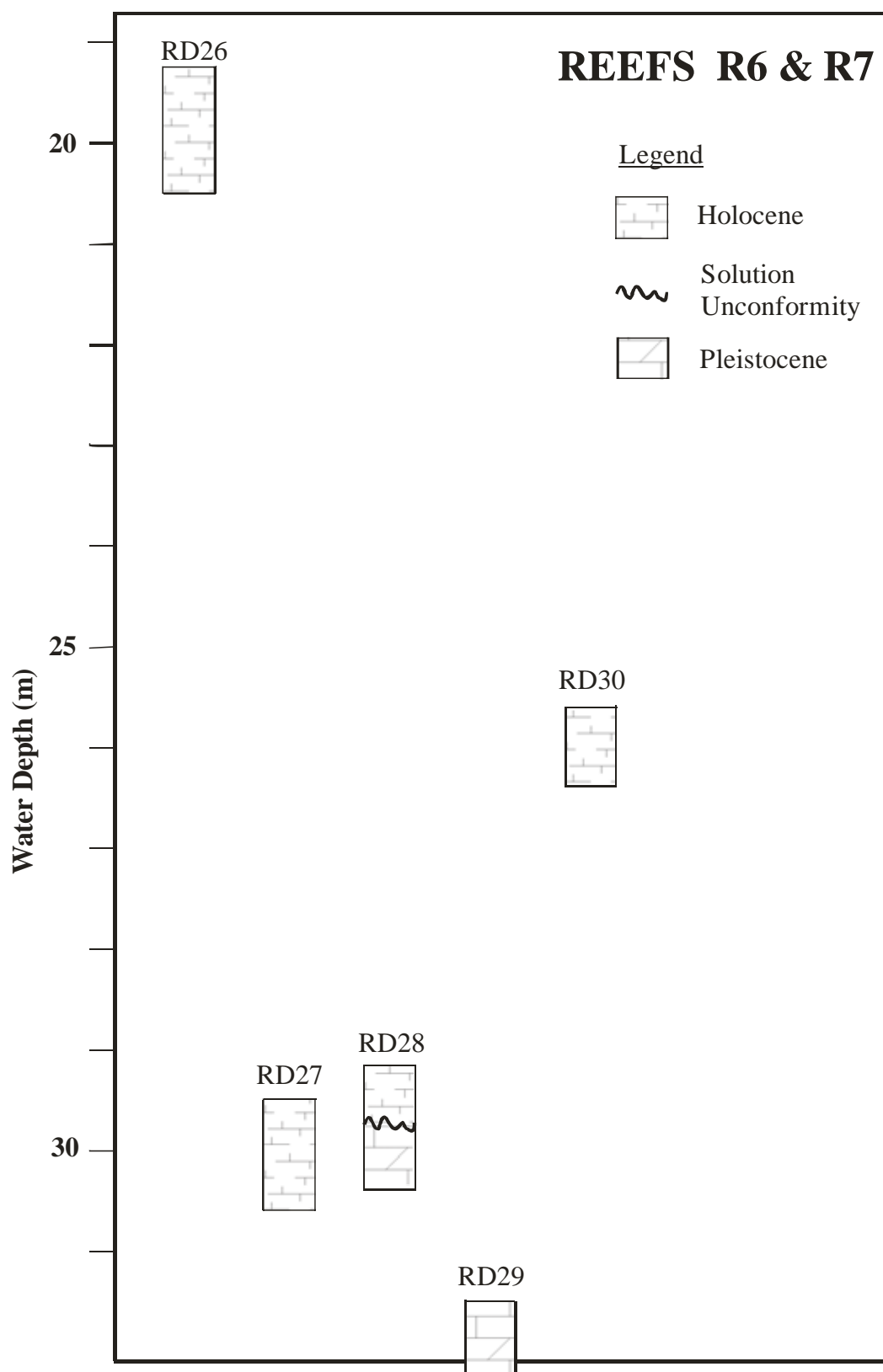


Figure 4.15. Composite core log for Reefs R6 and R7 showing the position and lithology of drill holes in relation to water depth.

4.3 DISCUSSION OF REEF DRILLING RESULTS

4.3.1 Hardground

The top 10-24 cm of four cores (1, 2, 4, 7) consists of an iron-stained, often heavily encrusted, and well lithified rudstone which is considered to represent a hardground. Because all these cores are Holocene, it is obvious that this lithology represents an hiatal surface that was formed after the demise of the coral reef; i.e. post \approx 9000 years. The interskeletal pores are cemented by Mg-calcite micrite, parts of which are often iron-stained. Up to three generations of borings by bivalves and sponges are present, and each generation later filled by micrite cement (RD01, G-00110; [Appendix 5](#)). The presence of banded iron and phosphate minerals in hole 2 (RD02, G-00113 & 114; [Appendix 5](#)) suggests slow growth of authigenic phases, possibly under slightly anoxic redox conditions. The significance of the hardground being so widespread on this reef is that it is obvious that no new phase of reef growth occurred after the short-lived, early Holocene phase. This suggests that conditions in the Gulf were no longer conducive to reef growth post \approx 9000 years.

While the tops of the two cores from Reef R2 have hardgrounds, those from Reef R3 do not. This is supported by video footage of the reef top, which shows a predominantly sandy bottom. The hardground lithologies are very similar to those from Reef R1, with heavily bored, infilled and cemented coral/algal floatstone or framestone that has been extensively iron stained. The presence of up to 8% quartz in Reef R2 hardgrounds is an indication of deposition of terrigenous material either by floods, cyclones or aeolian processes during the phase of consolidation. The presence of iron-stained ooids, although rare, is an indication of periodic growth of carbonate/iron oxide? phases.

Hardground: No hardground limestone was found at the tops of any of the cores, although two cores (RD 18 & 19) have a topping of iron-stained, uncemented rubble that is similar in character to the more indurated hardgrounds encountered in Reefs R1-R3.

4.3.2 Boundstone/Bafflestone

Five of the drill holes recovered limestone dominated by crustose coralline algae. In holes 1 and 2 the coralline algae form a true boundstone along with corals and other skeletal material, but in holes 3, 4, and 7 the coralline algae, along with vermetid gastropods and serpulid worm tubes, forms a distinctive lithology which is also noticeable because of the dark-coloured mud filling the interskeletal cavities (see core photos in the core logs for holes 3 and 4; [Appendix 5](#)). The dark matrix boundstone in holes 3, 4, and 7 can also be classified as a bafflestone because the coralline algae form an open, self supporting framework rather than encrusting other skeletal material. The crustose coralline algae are of a short, stubby, branching nature and appear to be mainly *Lithophyllum* sp. This open framework has trapped a dark, almost black, mud within its branches which in turn has become lithified to varying degrees. Other coarser skeletal elements (articulated coralline algae, forams and molluscs) and quartz grains (about 5%) have been also incorporated into the matrix of the bafflestone (RD04, G-00132; [Appendix 5](#)). There are at least two generations of interskeletal cavity fill; the second is only semi-lithified. While the fine matrix does appear to be carbonate, it is noticeable that it contains numerous small, black inclusions, which presumably imparts the darker colour too the hand specimen. The nature and origin of these inclusions has not been determined. It is apparent that the dark coloured bafflestone occurs below any of the dated corals, which suggests that it forms part of a latest Pleistocene/early Holocene transgressive facies. The dark matrix appears similar to modern day mangrove muds (this needs to be confirmed by ^{14}C dating and biomarker/palynology analysis). If correct, this suggests that pioneer mangrove communities colonised the upper platform soon after the initial transgression of the platform, along with crustose coralline algae. This presumably short lived facies was replaced by a reefal facies once sea level drowned the previously exposed platform.

The presence of rounded silt-size black grains, which occur as a late stage geopetal fill of vermetid gastropods, suggests that the coralline algal boundstone had already been constructed before it started to trap the silt-size matrix. The mineralogy of these grains is unknown, but it could suggest that it is these that are imparting the darker colour to the matrix. If the dark matrix is of mangrove origin (a premise that is not supported at this stage, other than by the black (anoxic?) colour), the boundstone was likely to have formed during the initial transgressive stage of the various reef top platforms (30 m, 27 m, and 21 m; see Harris et al., 2004), and it is possible that short-lived mangrove forests were established on them, but were quickly inundated by the rising sea level, after which corals were established.

4.3.3 Solution Unconformity and Framework

As mentioned above, the solution unconformity where it occurs in holes 1, 2, 4, and 7 occurs within a narrow depth range (26.7-27.3 m; Fig. 4.5). While the solution unconformity is usually marked by the first occurrence of calcite (either as a cement and/or replacing aragonite skeletons), in some holes the presence of calcrete is the diagnostic factor. Calcrete appears to be present in the top 10 cm of holes 1 and 2. In the former, it can be identified from the presence of alveolar structure and both microspar and needle calcite cements. In hole 2 it is the laminations and red iron-rich inclusions that point to a soil horizon. In the other holes in Reef R1 there is no indication of calcrete development, and it should be stressed here that it was not detected in most of the other drill holes from the southern Gulf. This could suggest that in the majority of reefs the presence of vegetation was sparse, and that the exposed reefs existed as bare mounds during subaerial exposure.

Some idea of what type of framework was capable of being constructed during this short phase of reef growth during the early Holocene can be discerned from core 12, which has the thickest Holocene section of all the cores drilled during the survey. Here, the framestone shows a variety of branching, platy and head corals, predominantly species of *Acropora*, *Pocillopora* and *Porites*, which have been encrusted by coralline algae and bored, mainly by bivalves and sponges, with filling of the larger borings by internal sediment (see photo core 12; Appendix 5). This variety of framework is typical of most healthy, offshore reefs and shows little evidence of stress. The three U-series ages from core 12 (Table 4.3) show that the reef was actively growing between 9500 and 8300 years ago at rates of up to 4m kyr⁻¹; another sign of healthy reef growth. However, if the rate of 0.95 m kyr⁻¹ was more typical it would be apparent that sea level rise between 9500 and 6000 would outstrip the rate of reef growth, and the reef would eventually drown.

In core 11 from Reef R3 is a pre-Holocene packstone that is distinctly red, suggesting a high amount of iron oxides (see photo core 11; Appendix 5), although in thin section the iron staining was not that apparent. One aspect of this limestone is the notable lack of skeletal material in both hand specimen and thin section, except for some scattered pieces of coral and coralline algae. This suggests that the depositional environment was proximal to the reef rather than being part of the reef itself. The position of the drillhole on the northern edge of the platform in over 30 m of water may be some indication that the main locus of growth was to the south (see RD12). While most of the aragonite allochems seem simply to have dissolved and not been filled with calcite cement, the absence of what would have been allochems with a Mg-calcite mineralogy (e.g. coralline algae, benthic forams, echinoids) is puzzling, but could suggest that acidic conditions concomitant with the deposition and remineralisation of the iron oxides during a prolonged period of subaerial exposure may have led to leaching of both aragonite and Mg-calcite allochems.

Most of the Holocene reef limestones described so far contain quartz grains that are mainly silt-size or, at most, fine sand-size. In one core from this reef (RD 20), the quartz grains are statistically much coarser (100-500 µm) and are associated with well-rounded intraclasts that have the appearance of being transported as bedload. This core, at a water depth of 29.6 m, is located towards the leeward

edge of the platform (see [Fig. 4.9](#) for location of core RD20), in deeper water than the Holocene sections of cores located on the platform ([Fig. 4.9](#)). The source of the quartz and intraclasts is difficult to determine, but presumably can only be derived from the surrounding seafloor (unlikely given the positive topography of the platform) or from the underlying carbonate platform. The position of the platform in the vicinity of Mornington Island may be another factor, but again the transport mechanism remains obscure.

Calcrete: Evidence of pedogenesis was found only in one drill hole (RD 17) on reef R4, where a floatstone showed numerous root moulds (core RD17; [Fig. 4.9](#); [Appendix 5](#)).

Pleistocene reef framework: The majority of the Pleistocene section consists of a framestone whose interskeletal cavities are commonly filled with iron-stained internal sediment. The two most common constituents are coral and coralline algae, together with molluscs, large benthic foraminifera and echinoid fragments. As well as the framestone, there are packstone and rudstone elements which contain most of the above allochems, but have a micrite matrix (generally) or a sparry calcite cement. Commonly the matrix is iron-stained, and the red colour of the cores is generally imparted by this iron-stained matrix. As well as quartz, which can make up to 15% of the limestone, there are numerous sand- to granule-size, usually well-rounded, intraclasts which consist either of skeletal fragments (e.g. coral) or sand size quartz in an iron-rich micrite. The origin of the non-skeletal, iron-rich intraclasts is not certain, but they are possibly the weathered remnants of Tertiary palaeosols.

Subaerial diagenesis: The principal form of subaerial diagenesis of the Pleistocene corals is neomorphism; the process whereby aragonite is converted to calcite in situ, by what is termed “thin film transformation”. This involves dissolution of aragonite on one side of a thin film of water and precipitation of low Mg-calcite on the other. This results quite often in the formation of relatively large calcite crystals (>100 µm), which retain the original structure of the skeleton. The other method of conversion to calcite is known as solution/precipitation, where the coral aragonite is almost always totally dissolved by meteoric water and the ensuing mould is later filled by sparry calcite cement.

A vadose environment of diagenesis is usually determined from fabric selective calcite mosaics, whereas a phreatic environment is determined by cross-cutting fabrics (Pingitore, 1976). An example of a vadose fabric in corals is where the coral has been converted to calcite by neomorphism, but without the calcite mosaic extending beyond the skeleton. Any void fill is usually calcite cement, which appears clear in plain polarised light as opposed to the rather murky appearance of the neomorphic calcite ([Fig. 4.16 A and B](#); G-00006; G-00025), and forms a typical fabric selective mosaic. On the other hand, the fabric in corals affected by freshwater phreatic diagenesis shows both skeleton and cement made up of a single crystal cutting both skeleton and cement ([Fig. 4.16 C and D](#); G-00174; G-00175).

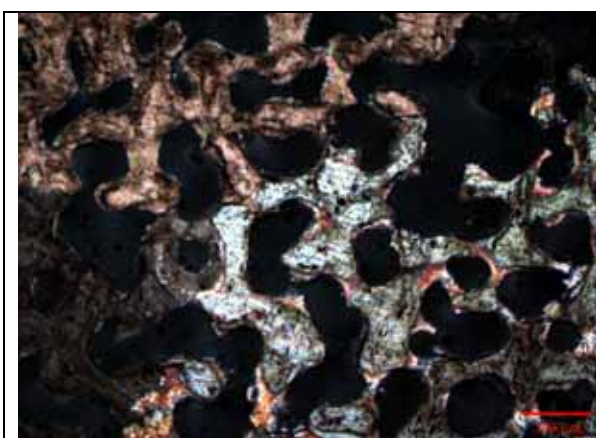


Fig. 4.16 (A) G-00006. Photomicrograph showing an example of vadosic diagenesis, with coral skeleton replaced by neomorphic calcite, but without any growth of crystals into the coral pores (Crossed polarisers; scale bar = 200 μm).

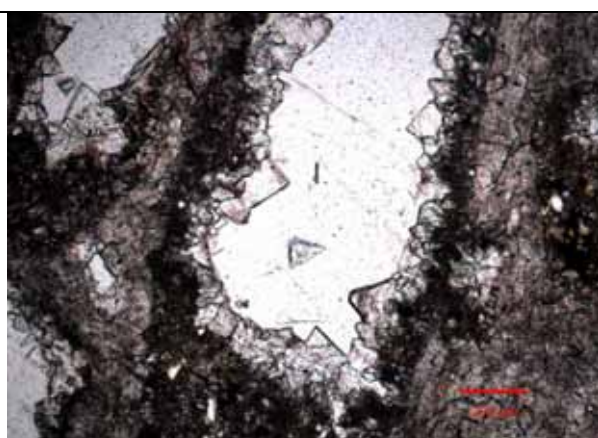


Fig. 4.16 (B) G-00025. Photomicrograph of clear, euhedral calcite cement lining coral pore. The coral (dark) has been neomorphosed to calcite (Plain polarised light; scale bar = 200 μm).

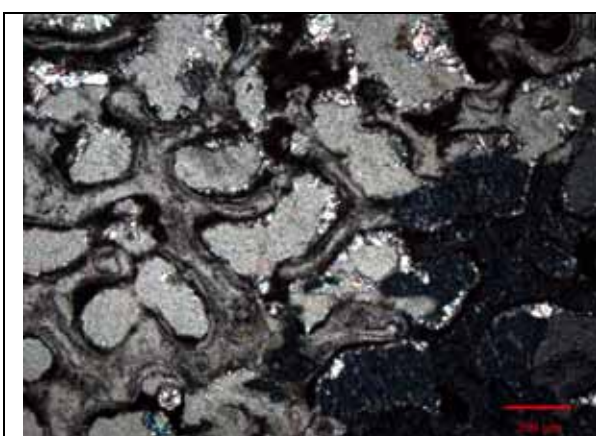


Fig. 4.16 (C) G-00174. Photomicrograph showing both coral and pores made up of a single crystal of calcite, indicative of phreatic diagenesis (Crossed polarisers; scale bar = 200 μm).



Fig. 4.16 (D) G-000175. Photomicrograph showing detail of G-000174. The two calcite crystals, whose boundary is marked by the dark line running from top left to lower right, show envelopment of both coral and pores (Crossed polarisers; scale bar = 100 μm).

4.4 BRYOMOL REEF – CORE 276/17RD13

One final note regarding the results of the Survey 276 drilling campaign relates to the Bryomol reef mapped during the earlier survey 238 on the eastern side of Mornington Island. A single rotary drill core was collected from the centre of this reef in 27.6 m water depth, upon the flat top surface of the bank. The core contains an upper 0-10 cm thick bed of well-lithified, iron-stained rudstone, overlying an unlithified wackstone comprised of sand-gravel sized skeletal fragments in a muddy sediment matrix. Iron staining is prevalent throughout the lower unit, with red mottles common in the lowermost 10 cm of the core.

The depositional environment represented by the lithology of this core, taken together with the morphology of the Bryomol bank, is unlike the coral reef platforms R1 to R7 discussed above. The

occurrence of an upper bed of lithified rudstone is of particular significance, as it is consistent with the broad-scale karst morphology of the bank top (doline solution erosion depressions and pock-mark features). The over-deepened channels flanking the bank on either side appear to have their origins in the tidal currents that are accelerated as the flow around the constriction formed between Mornington Island and the coast. Thus a picture is emerging of the formation of the Bryomol Bank less as a depositional feature and more of an erosional remnant that has been preserved by its protective upper layer of limestone. The dominant role played by current erosion is also manifest in the numerous scroll marks and elongate ridges which may be either protrusions of lithified beds or younger deposits that contain limestone beds.

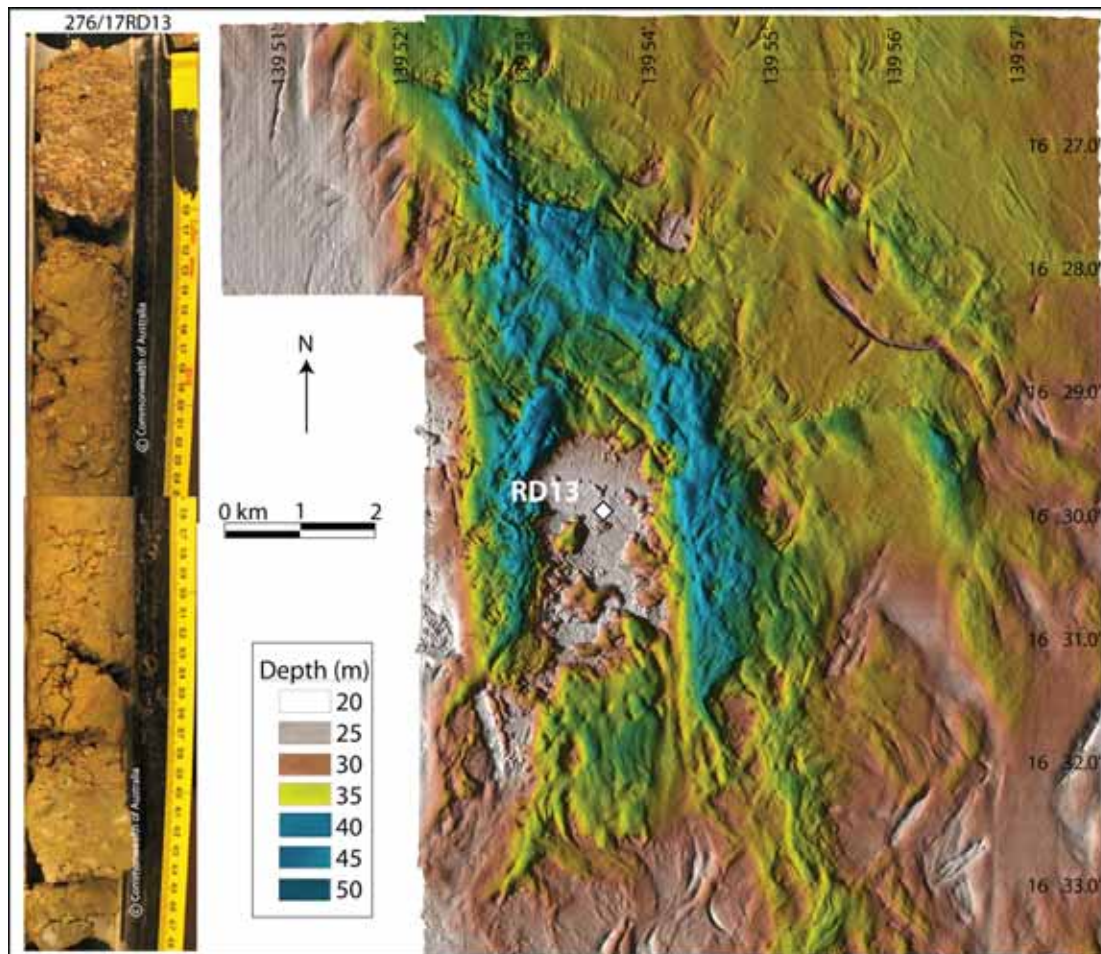


Figure 4.17. Multibeam image showing the Bryomol reef located on the eastern side of Mornington Island. Inset is a photograph of the split rotary drill core obtained on survey 276.

Chapter 5. Biological description of submerged reefs and benthic habitats

5.1 INTRODUCTION

The Gulf of Carpentaria is a shallow, tropical, shelf environment most commonly described through its association with fishing industries (e.g. Salini et al. 1990, Brewer et al. 1991, Pownall 1994, Somers 1994, Brewer et al. 1996, 1998, Salini et al. 2001, Stobutzki et al. 2001). However, other ecological habitats and issues have also been studied including some benthic environments (e.g. Long and Poiner 1994, Die et al. 2000), planktonic communities (e.g. Rothlisberg et al. 1994), demersal fish communities (e.g. Blaber et al. 1989, 1990, 1994 a&b and 1995, Brewer et al. 1994, Martin et al. 1995), elasmobranchs (Stevens and Wiley 1986, Stevens and Lyle 1998, Stevens and McLoughlin 1991, Salini et al. 1992), seasnakes (Wassenberg et al. 1994, Fry et al 2001, Milton 2001), turtles (Poiner et al. 1990, Poiner and Harris 1996), and seabirds (Blaber and Milton 1994). However, very little is known about the habitats commonly described by trawl operators as ‘untrawlable ground’. These have typically been described as ‘hard substrates’ due their ability to damage trawl nets (Die et al. 2000). The demersal fish communities on these ‘reef-associated habitats’ have been described broadly by Blaber et al. (1994a). However, the nature of the benthic habitats which form the basis of these communities remains undescribed.

The untrawlable areas of the Gulf of Carpentaria usually correspond to shallower features on the sea bed. A voyage on the *RV Southern Surveyor* in March/April 2005 (SS04/2005) aimed to characterise these features in this region and the preliminary results of the biological sampling are presented below.

5.2 MATERIALS AND METHODS

Six submerged features were studied during SS04_2005 (see [Figs. 2.1, 2.2 and 2.3](#)). Each reef feature was sampled at a variety of sites and usually by several sampling apparatus. At most sites a benthic dredge, underwater video camera and sediment grab were deployed to collect information to form the basis of the biological characterisation of these underwater features.

5.2.1 Benthic sled

The benthic sled ([Fig 2.1](#)) consisted of a rigid, rectangular, steel frame supporting a collection net consisting of an outer steel chain mesh ‘bag’ of 6 cm mesh (stretched knot to knot) lined with polyethylene trawl mesh with 3 cm mesh (knot to knot). This sled was towed slowly behind the vessel for an average of about 3.1 minutes ($SD \pm 1.07$) and over a distance of about 36.2 m ($SD \pm 11.22$), and was deployed to collect samples of the sedentary benthic organisms and material that characterised the surface of the sea bed features being studied. The data collected provides semi-quantitative information on the species that characterise the sedentary benthic habitats. Accurate biomass estimates of benthic species can not easily be calculated from this sampling device due to the difficulty in measuring the relatively short distance covered by each tow. More quantitative estimates of benthic habitats will be estimated from the underwater video transects.

The material collected by the sled was either (i) wholly sorted in the ships laboratory, or (ii) for large samples, partially sorted on the ships deck to collect most living organisms and the remainder, mainly coral rubble and shell rubble, was discarded. The retained part of the catch was sorted into broad taxonomic categories, and the weight and numbers within each category recorded. For the larger samples, a biologically representative subsample of the abundant species groups was taken for later processing. These were also weighed and counted before being stored for more detailed sorting and analyses at the CSIRO Marine Laboratory, Cleveland. Colonial organisms were weighed but not counted. Each stored sample was given a bar code to match the sample with the log data. Species

groups were either stored in 70% ethanol (soft corals, sea pens and most echinoderms), 10% formaldehyde (annelids, ascidians and plants) or frozen (sponges, crustaceans, molluscs, hard corals, fish and holothurians).



Figure 5.1 Photographs of the benthic sled used for sampling seabed biota.

5.2.2 Underwater Video Camera

The underwater video camera consisted of a Sony video camera within an underwater housing and mounted in a sled (Fig. 5.2). This rig was towed slowly behind the vessel usually for 15 or 20 minutes. The distance was not estimated due to the very slow speed of the vessel (often drifting with little if any lateral movement) during deployment of this device. The video data collected will provide an alternative source of information by which we will characterise the sedentary benthic organisms of the sea bed during this studied. The data collected should provide quantitative abundance estimates (relative percentage cover and/or numbers) of many of the species groups identified in the benthic sled. Following deployment the video rig, the video tapes were removed, backup up onto video tape and DVD for later analyses.



Figure 5.2 Underwater video camera being deployed from RV *Southern Surveyor*.

5.2.3 Sediment grab

A Smith-Macintyre sediment grab ([Fig 5.3](#)) was deployed at most sampling sites to collect one sample of the sea bed sediment and macro-infauna/epifauna from each site. Following the removal of the sediment sub-sample the remains of the material obtained from each grab was sieved through a 3 mm brass sieve to separate the macro-fauna. These organisms were then stored in either ethanol, formaldehyde or frozen (see above) in preparation for later sorting and identification.

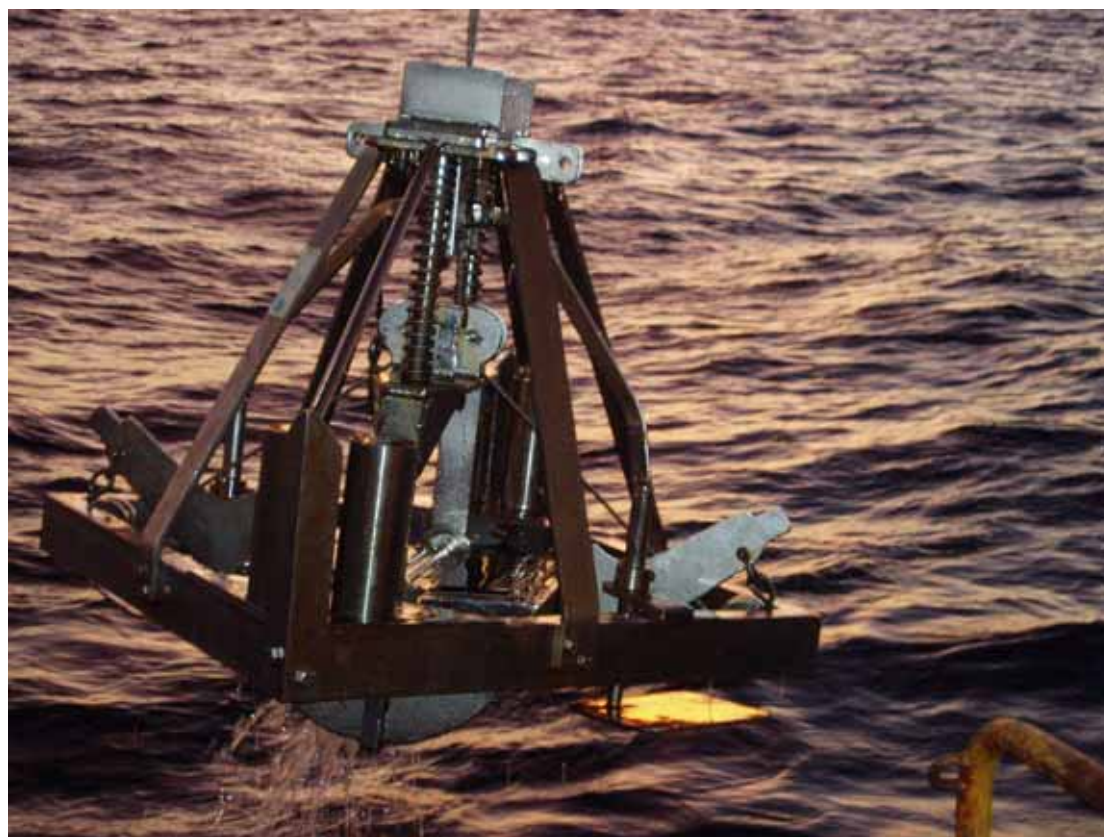


Fig. 5.3 *Smith-Macintyre benthic grab sampler used for sampling seabed sediments and biota.*

The CSIRO Division of Marine and Atmospheric Research has recently provided funding to process the samples from each of the devices and the subsequent project will commence in January 2006. This will provide a detailed description of the species, biodiversity and variability found within these reefs. A description of the data collected and processed on board the ship is presented below.

5.3 PRELIMINARY RESULTS

5.3.1 Benthic Sled

Benthic sled samples were taken from 43 different locations during the voyage. A total of 169.5 kg of material was processed from these samples and 66.6 kg were stored for detailed processing and analyses in the laboratory. Hard corals, sponges, crustaceans and molluscs occurred in more than 90% of these samples, with echinoderms, gorgonians and annelid worms occurring in more than half the samples ([Table 5.1](#)). The weight of the samples was dominated by hard corals, sponges and gorgonians, with sponges, molluscs, echinoderms and crustaceans the most numerically abundant of the non-colonial species groups.

Table 5.1. Summary of data collected from 43 benthic sled tows taken during SS04/2005. The data is summarised using 17 species groups. Total numbers of colonial organisms were not assessed.

SPECIES GROUP	TOTAL NUMBERS	FREQUENCY OF OCCURRENCE	TOTAL WEIGHT (G)	SUBSAMPLE WEIGHT (G)
Hard corals	-	0.98	88356.2	28920.2
Sponge	439	0.95	53298.9	20188.4
Crustaceans	215	0.95	183.2	183.1
Molluscs	277	0.91	7838.4	7838.4
Echinoderms	240	0.88	2233	1814
Gorgonians	-	0.74	9299.2	2004.8
Annelid worms	105	0.60	136.7	164.5
Alcyonarians	-	0.42	3101.8	1594.6
Ascidians	-	0.42	798.4	798.5
Hydroids	-	0.37	466.5	372.3
Algae	25	0.26	1375.1	1375.1
Teleost fish	12	0.23	23.2	23.2
Other plants	20	0.23	395.05	395.05
Bryozoans	-	0.16	460.8	135.8
Other cnidarians	-	0.16	1509.7	719.8
Sipunculid	3	0.07	9.21	3.81
Platyhelminthes	3	0.05	26.85	27.3
Total			169,512.2	66,558.9

5.3.2 Sediment grabs

Sediment grab samples were taken from 63 different locations during the voyage ([Appendix 2](#)). A total of 6.5 kg of material was processed from these samples and stored for detailed processing and analyses in the laboratory. No species group dominated these samples, with only sponges and hard corals occurring in more than 20% of the samples ([Table 2](#)). The weight of the samples was also dominated by these two species groups, with sponges, crustaceans and echinoderms the most numerically abundant of the non-colonial species groups.

5.3.3 Underwater Video

Underwater video transects were taken from 67 different locations during the voyage ([Appendix 2](#)). Although no detailed sampling of this video data has been completed, on-board observations confirmed that the sites sampled on the submerged reefs could be described as either: (i) predominantly bare substrate with a consistent, scattered coverage of sessile macro-fauna, including single soft corals (alcyonaceans), gorgonians, hard plate corals (e.g. *Turbinaria* sp) and sponges; or (ii) dominated by a diverse, complex, coral reef like coverage of macro-fauna, consisting of these same species groups, and often interspersed with small patches of barer substrate.

Although this second category comprised less than half of the sites sampled, they were numerous enough to confirm the presence of dense, diverse coral reefs throughout the raised sea bed habitats sampled during this voyage.

Table 5.2. Summary of data collected from 63 sediment grabs taken during SS04/2005. The data is summarised using 14 species groups. Total numbers of colonial organisms were not assessed.

SPECIES GROUP	TOTAL NUMBERS	FREQUENCY OF OCCURRENCE	TOTAL WEIGHT (G)	SUBSAMPLE WEIGHT (G)
Sponge	31	0.32	1980.2	1980.2
Hard corals	-	0.27	3123.4	3123.4
Echinoderms	18	0.20	106.7	106.7
Crustaceans	19	0.17	6.6	6.6
Annelid worms	11	0.15	10.0	10.0
Molluscs	7	0.12	31.6	31.6
Gorgonians	-	0.07	161.4	161.4
Teleost fish	4	0.05	3.3	3.3
Bryozoans	-	0.05	8.4	8.4
Alcyonarians	-	0.05	113	113
Other plants	2	0.03	302	302
Other cnidarians	-	0.03	68.4	68.4
Ascidians	-	0.03	25.6	25.6
Algae	1	0.02	521	521
Total			6461.6	6461.6

5.4 PROPOSED SAMPLE ANALYSES AND REPORTING

The laboratory analyses of the samples described above will provide a detailed description of the species composition, biological diversity and habitat classification of the submerged reef habitats in the Gulf of Carpentaria (as sampled during SS04/2005). The samples collected in the benthic dredge will allow identification of a wide range of species, including genetic identification of hard corals using tissues collected and preserved specifically for this purpose. Analyses of video data will provide a more quantitative assessment of the density of species groups. Both methods will also allow comparisons of biodiversity and species richness between regions and different topographical features.

The preliminary analyses of the biological sampling during SS04/2005 provides clear evidence that coral reef habitats are common on the raised sea bed features of the Gulf of Carpentaria. Both the benthic dredge and video transects provided evidence of hard corals, sponges, soft corals and related coral reef organisms at many of the sites sampled. Many of the video transects also recorded large fish in densities that appear to be similar to shallower, clearer water coral reef systems. This study provides the first description of these submerged reefs and will be analysed and described in detail in the ensuing study.

Chapter 6. Discussion

6.1 SUBMERGED CORAL REEFS IN NORTHERN AUSTRALIA

Survey 276 set out to achieve four main objectives:

1. To acquire drill core samples from suspected submerged coral reefs to confirm their coral composition and provide material suitable for radiometric dating;
2. To collect multibeam sonar and sub-bottom profile information from other bathymetric mounds in the southern Gulf to ascertain their geomorphic nature;
3. To collect biological samples and underwater video records of the seafloor in order to document the benthic communities and fauna associated with the submerged reef features; and
4. Collect data on water properties, currents and suspended sediments to document the modern reef habitats and their environments.

The survey was successful in meeting all four of these objectives. The drill operations were successful in recovering 39 m of core material from 43 sites. The drill cores document the existence of coral reef bioherms in 7 different locations in the southern Gulf. Preliminary U/Th dating of the preserved coral has so far yielded 22 ages, including 18 Holocene ages and 4 Late Pleistocene ages. These ages indicate that phases of reef growth have occurred over at least the last glacial cycle (the reefs are probably much older than last interglacial in age). Also, the ages document an early Holocene reef growth phase prior to 7 kyr BP that was followed by much reduced (or even zero) reef growth since that time.

Multibeam sonar data was collected from two elongate reef platforms, extending over 100 km westwards from Mornington Island plus from two smaller platform reefs around 2 km in width located in the southern Gulf. The reefal origin of these features is clearly indicated by their overall geomorphic expression. Also mapped during the survey were a deeply-incised shelf valley located off the northern end of the Wessel Islands as well as a further submerged reef in the Arafura Sea. The latter Arafura reef is significant because it implies the potential existence of numerous other submerged reefs on the continental shelf off northern Australia.

Biological samples and underwater video have shown conclusively that the submerged reefs are alive; many common reef species have been sampled and documented including hard corals, sponges, soft corals and related coral reef organisms. Thus the reefs are alive and locally flourishing but their vertical growth has been restricted to a handful of small locations on the reef crests. In short, their rate of carbonate production during the Holocene has been insufficient for the reef tops to reach present sea level.

Finally, the oceanographic information provides much vital evidence that characterises the environments in which the reefs occur. Of particular significance for reef growth is the observation of low suspended sediment concentrations in both surface and near-bed water samples obtained; surface samples range from 2.8 to 12.8 mg/l while deep samples range from 2.9 to 14.4 mg/l. These values are not significantly different from typical values obtained in the Great Barrier Reef (Harris and Baker, 1991) and casts doubt on suggestions that reef growth in the Gulf of Carpentaria is inhibited by high levels of turbidity. Similarly the temperature range for Gulf reefs in 29.8 to 30.6° C, which is well within the range normally associated with coral growth.

6.2 WATER DEPTHS OF SUBMERGED REEFS

If the level of the upper surfaces of submerged reefs reflects a phase of reef growth in relation to sea level, then hypsometric curves of individual reefs may provide some insights into the past sea levels when reef growth was most widespread. Hypsometric curves for all of the reefs mapped in the southern Gulf of Carpentaria illustrate that the upper surfaces of reefs fall within two very closely grouped depth intervals (Fig. 6.1). Reefs R1, R4 R6 and R8 have hypsometric peaks at 25.8 to 27.8 m and reefs R2, R3 and R7 have hypsometric peaks at between 30.4 to 30.9 m. Reef R2 exhibits bimodal hypsometric peaks at 27.2 and 30.8 m. The heights of these peaks reflects the amount of surface area focussed within a specified depth range, whereas the width of the peaks reflects the variability in depth. So Reef R1 has a large (area of $>7 \text{ km}^2$) and incredibly flat platform surface indicated by the sharp peak (narrow depth range of $<2 \text{ m}$). In contrast, the broad peak for Reef R4 indicates that the platform occurs at a more broad depth range, spanning 7-8 m.

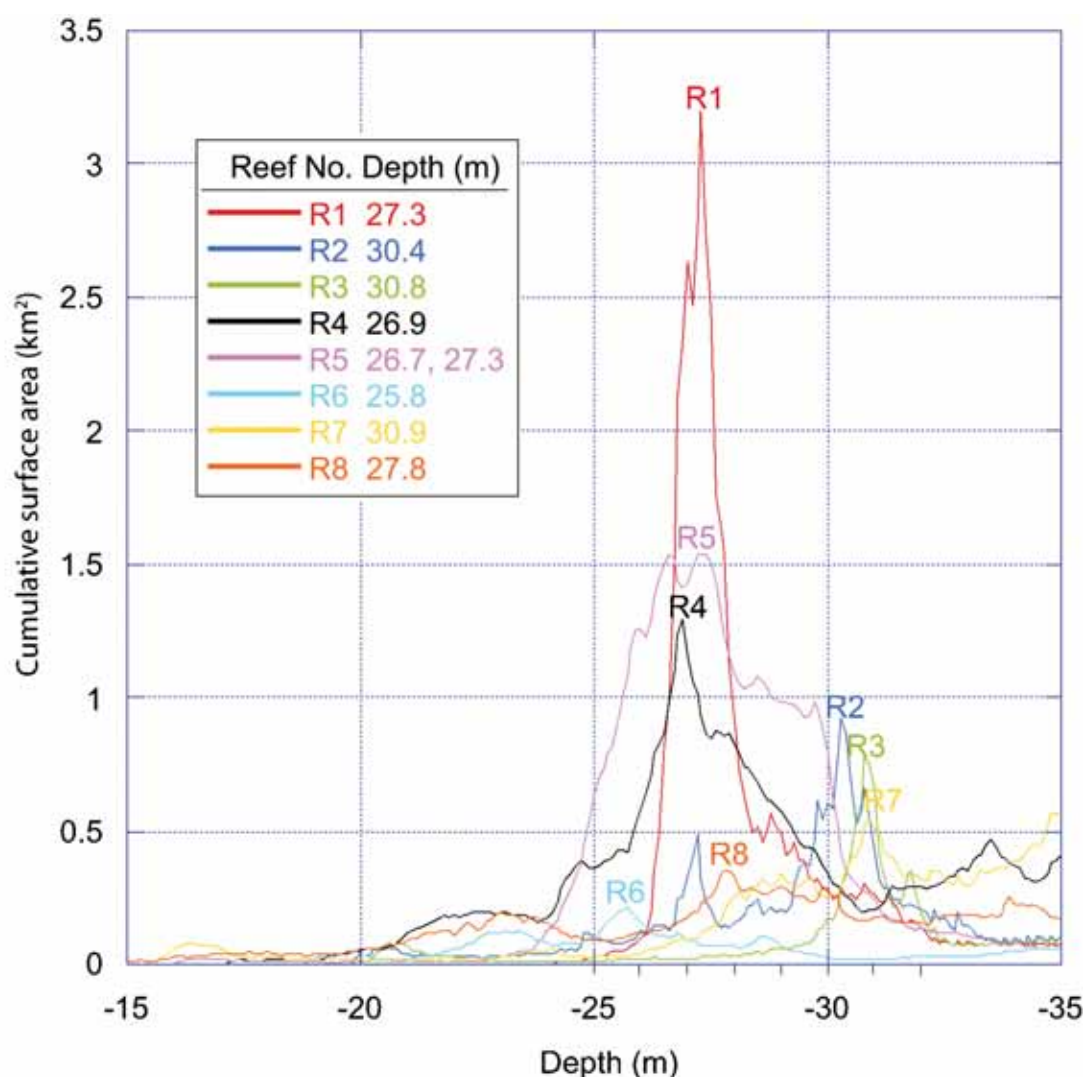


Fig. 6.1 Hypsometric curves for submerged reef platforms in the Gulf of Carpentaria (R1 to R7) and the Arafura Sea (R8). Water depths were binned at 10 cm intervals and total surface area within each bin summed to create the curves shown. The modal depths for major hypsometric peaks are listed for each separate reef.

The significance of these results for sea level reconstruction is in relation to our ability to accurately estimate the water depths corresponding to phases of previous reef growth over broad geographic areas. A regional signal is suggested by the close correspondence of surface elevations for reefs located many hundreds of km apart. For example, Reefs R2 and R3 are located some 270 km from

Reef R7, but they have mean surface elevations within 50 cm of each other. Reef R8 in the Arafura Sea is over 750 km from Reefs R1, R4 and R5 but they have hypsometric modal peaks within 1 m of each other. The similarity in these values suggests contemporaneous phases of reef growth over broad geographic regions corresponding to a particular water depth.

There are also implications in these results for the tectonic stability of the continental margin of northern Australia. Our results suggest that there has been little if any differential vertical displacement between the sites of these submerged reefs over the past ~120 kyr.

In summary, the hypsometric modal peaks of reef depths (Fig. 6.1) suggest that reef growth occurred in relation to sea level at two discrete positions at around 27 and 30 m below present mean sea level. These depths correspond with broad horizontal submerged reef surfaces, representing regionally significant phases of carbonate deposition during a prolonged Quaternary sea level still stand. Our U/Th dating proves that only a brief phase of reef growth occurred during the Holocene, post-glacial transgression of the continental shelf. We conclude that the reefs are therefore relict features, whose growth and development relates to an earlier, pre-Holocene sea level still stand.

6.3 FUTURE RESEARCH

While the present survey results represent a significant advance in our knowledge of Australia's coral reef system and its Quaternary history, it also raises some fascinating questions for future investigations to address. The question of the timing of reef growth has not been fully addressed by the results of the present study. Our drill cores did not produce an unaltered aragonite sample suitable for U/Th dating to allow us to estimate the exact age of the submerged platforms. Hence although the hypsometric analysis shows that reef growth appears to coincide with sea level still-stand positions of about 27 to 30 m below present sea level, we don't know at what time(s) in the past this occurred. Our U/Th ages only suggest minimum ages for some corals that have undergone varying degrees of diagenesis. Further drilling of these submerged reefs is needed to attempt to acquire unaltered Pleistocene corals.

A related question is the true distribution of Australia's northern reef province. Our preliminary results suggest that submerged reefs are pervasive and widespread in the Gulf of Carpentaria. We also identified (but did not have time to drill) another submerged reef in the Arafura Sea. Existing nautical charts suggest that there are numerous shoals and banks along the northern coastline of the Northern Territory. Unanswered questions are: how many of these bathymetric shoals are submerged coral reefs? How many of them support extant reef fauna and are they actively growing? What is their age and history and how does this compare with the Carpentaria reefs? Answering these questions will be the aim of future surveys planned by Geoscience Australia and its partners in the years ahead.

References Cited

- Agrawal, Y.C., and Pottsmith, H. C. (2000) Instruments for particles size and settling velocity observations in sediment transport. *Marine Geology*, 168, 89-114.
- Blaber, S.J.M., D.T. Brewer and J.P. Salini, 1989. Species composition and biomasses of fishes in different habitats of a tropical northern Australian estuary: Their occurrence in the adjoining sea and estuarine dependence. *Estuarine, Coastal and Shelf Science*, 29: 509-531.
- Blaber, S. J. M., D. T. Brewer, J. P. Salini, and J. Kerr, 1990. Biomasses, catch rates and abundances of demersal fishes, particularly predators of, prawns in a tropical bay in the Gulf of Carpentaria, Australia. *Marine Biology*, 107: 397-408
- Blaber, S. J. M., D. T. Brewer, and A. N. Harris, 1994a. The distribution, biomass and community structure of fishes of the Gulf of Carpentaria. *Australian Journal of Marine and Freshwater Research*, 45: 375-396.
- Blaber, S. J. M., D. T. Brewer, and J. P. Salini, 1994b. Comparisons of the fish communities of tropical estuarine and in-shore habitats in the Gulf of Carpentaria, northern Australia. In: Dyer, K. R. and Orth, R. J. (Eds.) *Changes in Fluxes in Estuaries. International Symposium Series* (Olsen & Olsen, Denmark) p. 363-372
- Blaber, S. J. M., D. T. Brewer, J. P. and Salini, 1995. Fish communities and the nursery role of the shallow inshore waters of a tropical bay in the Gulf of Carpentaria. *Estuarine, Coastal and Shelf Science*. 40: 177-193
- Blaber, S. J. M and D. A. Milton, 1994. Distribution of seabirds at sea in the Gulf of Carpentaria, Australia. *Australian Journal of Marine and Freshwater Research*, 45(3): 445-454.
- Brewer, D. T., S. J. M., Blaber, J. P. Salini, and D. A. Milton, 1994. Aspects of the biology of *Caranx bucculentus* (Teleostei: Carangidae) from the Gulf of Carpentaria, Australia. *Australian Journal of Marine and Freshwater Research*, 45: 413-428.
- Brewer, David T., Steve Eayrs, Richard P. Mounsey, and You-Gan Wang, 1996. Assessment of an environmentally friendly, semi-pelagic fish trawl. *Fisheries Research*, 26:225-237.
- Brewer, D. T., N. Rawlinson, S. Eayrs, and C. Y. Burridge. 1998. An assessment of Bycatch Reduction Devices in a tropical Australian prawn trawl fishery. *Fisheries Research*, 36: 195-215
- Brewer, D. T., S. M. Blaber and J. P. Salini. 1991. Predation on penaeid prawns by fishes in Albatross Bay, Gulf of Carpentaria. *Marine Biology*, 109: 231-240
- Brown, C.B. (1950) In Rouse, H (Ed.), Engineering Hydraulics. Wiley, New York, 1039pp.
- Burford, M.A., Long, B.G. and Rothlisberg, P.C., 1994. Sedimentary pigments and organic carbon in relation to microalgal and benthic faunal abundance in the Gulf of Carpentaria. *Marine Ecology Progress Series.*, 103: 111-117.
- Chappell, J. and Shackleton, N.J., 1986. Oxygen isotopes and sea level. *Nature*, 324: 137-140.
- Chivas A.R., Garcia, A., van der Kaars, S., et al., (2001). Sea-level and environmental changes since the last interglacial in the Gulf of Carpentaria, Australia: an overview. *Quaternary International*, 83-85: 19-46.
- Collins, L.B., Zhu, Z.R. and Wyrwoll, K.H., 1996. The structure of the Easter Platform, Houtman Abrolhos Reefs: Pleistocene foundations and Holocene reef growth. *Marine Geology*, 135: 1-13.
- Damuth, J.E., 1980. Use of high-frequency (3.5 - 12 kHz) echograms in the study of near bottom sedimentation processes in the deep sea. *Marine Geology*, 38: 51-75.
- De Dekker, P., Chivas, A.R., Shelly, J.M.G., Torgersen, T. (1988). Ostracod shell chemistry: a new palaeoenvironmental indicator applied to a regressive/transgressive record from the Gulf of Carpentaria, Australia. *Palaeogeography, Palaeoclimatology, Palaeoecology*, 66, 231-241.
- Die, D, Loneragan, NR, Haywood, MDE, Vance, DJ, Manson, FJ, Taylor, B, Bishop, J. (1995). *Indices of recruitment and effective spawning stocks in the Northern Prawn Fishery*. Final report FRDC project FRDC 95/014.

- Die, D., Loneragan, N., Haywood, M., Vance, D., Manson, F., Taylor, B. and Bishop, J., (2000). *Indices of recruitment and effective spawning for tiger prawn stocks in the Northern Prawn Fishery*. FRDC 1995/014 Final Report.
- Doyle, L.J. and Roberts, H.H. (Editors), 1988. *Carbonate-Clastic Transitions*. Developments in Sedimentology, 42. Elsevier, Amsterdam, 304 pp.
- Dunham, R.J., 1962. Classification of carbonate rocks according to depositional texture. In: W.E. Ham (Editor), *Classification of Carbonate Rocks*. Amer. Assoc. Petrol. Geol., Tulsa, Oklahoma, pp. 108-121.
- Edgar, N.T., Cecil, C.B., Mattick, R. Chivas, A.R., De Dekker, P., Djajadihardja, Y., (in press). A modern analogue for tectonic, eustatic, and climatic processes in cratonic basins: Gulf of Carpentaria, northern Australia. In: Cecil, C.B., Edgar, N.T. (Eds), *Allocyclic Controls on Stratigraphy and Sedimentation*. Special Publication, Society of Economic Paleontologists and Mineralogists.
- Embry, A.F. and Klován, J.E., 1971. A late Devonian reef tract on northeastern Banks Island, Northwest Territories. *Bulletin of Canadian Petroleum Geology*, 19: 730-781.
- Engelund, F., and Hansen, E. (1967) *A monograph on sediment transport in alluvial streams*. Teknisk Vorlag, Copenhagen, Denmark, 62pp.
- Fry, G. C., D. A. Milton, T. J. Wassenberg, 2001. The reproductive biology and diet of sea snake bycatch of prawn trawling in northern Australia: characteristics important for assessing the impacts on populations. *Pacific Conservation Biology*, 7: 55-73.
- Gadd, P. E., Lavelle, J. W., and Swift, D.J. P. (1978) Estimates of sand transport on the New York Shelf using near-bottom current-meter observations. *Journal of Sedimentary Petrology* 48, 239-252.
- Gordon, L., 1996, *Principles of operation - A practical primer*. RD Instruments publication number 951-6069-00, second ed.
- Hardisty, J. (1983) An assessment and calibration of formulations for Bagnold's bedload equation. *Journal of Sedimentary Petrology*, 53, 1007-1010.
- Harris, P.T., (1994). Comparison of tropical, carbonate and temperate, siliciclastic tidally dominated sedimentary deposits: examples from the Australian continental shelf. *Australian Journal of Earth Science*, 41: 241-254.
- Harris, P.T., 2003. *Sources and sinks of terrigenous sediments in the southern Gulf of Carpentaria*, Geoscience Australia, Canberra, Report to National Facility Steering Committee. 23pp.
- Harris, P.T., and Baker, E.K., 1991, The nature of sediments forming the Torres Strait turbidity maximum. *Aust. J. Earth Sci.*, 38: 65-78.
- Harris, P.T. and Davies, P.J., 1989. Submerged reefs and terraces on the shelf edge of the Great Barrier Reef, Australia: morphology, occurrence and implications for reef evolution. *Coral Reefs*, 8: 87-98.
- Harris, P.T., Heap, A.D., Passlow, V., Scaffi, L., Fellows, M., Porter-Smith, R.N., Buchanan, C., and Daniell, J., 2003, *Geomorphic Features of the Continental Margin of Australia: Report to the National Oceans Office on production of a consistent, high quality bathymetric data grid and delineation and description of geomorphic units for Australia's EEZ*: Canberra, Geoscience Australia Record 2003/30, 141pp.
- Harris, P.T., Heap, A.D., Wassenberg, T. and Passlow, V., 2004. Submerged coral reefs in the Gulf of Carpentaria, Australia. *Marine Geology*, 207: 185-191.
- Haywood, M. D. E., Vance, D. J., & Loneragan, N. R. (1995). Seagrass and algal beds as nursery habitats for tiger prawns (*Penaeus semisulcatus* and *P. esculentus*) in a tropical Australian estuary. *Marine Biology*, 122, 213-223.
- Heap, A.D., Daniell, J., Mazon, D., Harris, P.T., Scaffi, L., Fellows, M., and Passlow, V., 2004, *Geomorphology and sedimentology of the northern marine planning area of Australia: Review and synthesis of relevant literature in support of regional marine planning*: Canberra, Geoscience Australia Record 2004/11, p. 68.

- Hill BJ, Haywood M, Venables B, Gordon S, Condie S, Ellis N, R Tyre A, Vance D, Dunn J, Mansbridge J, Moeseneder C, Bustamante R., Pantus F. (2002). Surrogates I – Predictors, impacts, management and conservation of the benthic biodiversity of the Northern Prawn Fishery. Final report to FRDC Project 2000/160, CSIRO Marine Research, 437 pp.
- Jones, M.R. (1987). Surficial sediments of the western Gulf of Carpentaria, Australia. *Australian Journal of Marine and Freshwater Research*, 38, 151-167.
- Jones, M.R., Torgersen, T. (1988). Late Quaternary evolution of Lake Carpentaria on the Australian-New Guinea continental shelf. *Australian Journal of Earth Sciences*, 35, 313-324.
- Li, M.Z., and Amos, C. L. (2001) SEDTRANS96: the upgraded and better calibrated sediment-transport model for continental shelves. *Computers and Geosciences*, 27, 619-645.
- Long, B. G. and I. R. Poiner, 1994. Infaunal benthic community structure and function in the Gulf of Carpentaria, northern Australia. *Australian Journal of Marine and Freshwater Research*, 45(3): 293-316.
- Macintyre, I.G., 1972. Submerged reefs of the eastern Caribbean. *American Association of Petroleum Geologists Bulletin*, 5: 49-53.
- Martin, T. J., D. T. Brewer and S. J. M. Blaber. 1995. Factors affecting distribution and abundance of small demersal fishes in the Gulf of Carpentaria. *Marine and Freshwater Research*, 46: 909-920.
- Miller, M.C., McCave, I.N. and Komar, P.D. (1977) Threshold of sediment motion under unidirectional currents. *Sedimentology*, 24, 507-527.
- Neumann, A.C. and Macintyre, I.G., 1985. Reef response to sea level rise: keep-up, catch-up or give-up, *5th International Coral Reef Congress*, Tahiti, pp. 105-110.
- Milton, D. A., 2001. Assessing the susceptibility to fishing of populations of rare trawl bycatch: sea snakes caught by Australia's Northern Prawn Fishery. *Biological Conservation*, 101: 281-290.
- Nortek, 2000. *Vector Operations Manual*, 1 November 2000. <http://www.nortek-as.com>
- Pawlowicz, R., Beardsley, B. and Lentz, S. (2002) Classical tidal harmonic analysis including error estimates in MATLAB using T_TIDE. *Computers and Geosciences*, 28, 929-937.
- Poiner, I. R., R. C. Buckworth, and A. N. M. Harris, 1990. Incidental capture and mortality of sea turtles in Australia's northern prawn fishery. *Australian Journal of Marine and Freshwater Research*, 41(1): 97-110.
- Poiner, I. R., and A. N. M. Harris, 1996. Incidental capture, direct mortality and delayed mortality of sea turtles in Australia's Northern Prawn Fishery. *Marine Biology*, 125: 813-825.
- Pond, S. and G. L. Pickard (2000) *Introductory Dynamical Oceanography*, 2nd Edition. Butterworth Heinemann, Oxford. 329pp.
- Pownall, P.C. (Ed.), 1994. *Australia's Northern Prawn Fishery: the first 25 years*. NPF25, Cleveland, Australia.
- Rivett, D., Wannan, B., Weston, N., Pitts, D., Thorogood, J., Conacher, C., Sutcliffe, K., Northgate, J., Cleland, D., Collins, N., & Cummings, B. (1999). *Multiple use strategic plan for the southern Gulf of Carpentaria, report prepared for the Queensland Department of State Development: Report 3: The MUSP Strategy*. Environment North and Associated Consultants, 150 pp.
- Rothlisberg PC, Pollard PC, Nichols PD, Moriarty DJW, Forbes AMG, Jackson CJ and Vaudrey D (1994). Phytoplankton community structure and productivity in relation to the hydrological regime of the Gulf of Carpentaria in summer. *Australian Journal of Marine and Freshwater Research* 45: 265-82
- Salini, J. P., S. J. M. Blaber, and D. T. Brewer. 1990. Diets of piscivorous fishes in a tropical Australian estuary with special reference to predation on penaeid prawns. *Marine Biology*, 105: 363-374.
- Salini, J., D. Brewer, M. Farmer, and P. Jones, 2001. Lunar periodicity of prawns and bycatch in trawls from the Gulf of Carpentaria, northern Australia. *Marine Biology*, 138: 975-983

- Salini, J. P., S. J. M. Blaber, and D. T. Brewer, 1992. Diets of sharks from estuaries and near-shore waters of the north-eastern Gulf of Carpentaria. *Australian Journal of Marine and Freshwater Research*, 43: 87-96.
- Somers, I. F. (1987). Sediment type as a factor in the distribution of commercial prawn species in the western Gulf of Carpentaria, Australia. *Aust. J. Mar. Freshw. Res.*, 38, 133-149.
- Somers, I. F., 1994. Species composition and distribution of commercial penaeid prawn catches in the Gulf of Carpentaria, Australia, in relation to depth and sediment type. *Australian Journal of Marine and Freshwater Research*, 45(3): 317-336.
- Stevens, J. D. and P. D. Wiley, 1986. Biology of two commercially important carcharhinid sharks from northern Australia. *Australian Journal of Marine and Freshwater Research*, 37: 671-688.
- Stevens, J. D. and J. M. Lyle, 1898. Biology of three hammerhead sharks (*Eusphyra blochii*, *Sphyrna mokarran* and *S. lewini*) from northern Australia. *Australian Journal of Marine and Freshwater Research*, 40 (2): 129-146.
- Stevens, J. D. and K. J. McLoughlin, 1991. Distribution, size and sex composition, reproductive biology and diet of sharks from northern Australia. *Australian Journal of Marine and Freshwater Research*, 42 (2): 151-199.
- Stobutzki, I. C., M. J. Miller, D. H. Heales, and D. T. Brewer, 2002. Sustainability of elasmobranchs caught as bycatch in a tropical prawn (shrimp) trawl fishery. *Fishery Bulletin*. 100: 800-821.
- Stobutzki, I. C., M. J. Miller, P. Jones, and J. P. Salini, 2001. Bycatch diversity and variation in a tropical Australian penaeid fishery; the implications for monitoring. *Fisheries Research*, 53(3): 283-301.
- Torgersen, T., Luly, J., De Dekker, P., Jones, M.R., Searle, D.E., Chivas, A.R., Ullman, W.J. (1983). Late Quaternary environments of the Carpentaria Basin, Australia. *Palaeogeography, Palaeoclimatology, Palaeoecology*, 67, 245-261.
- Torgersen, T., Hutchinson, M.F., Searle, D.E., Nix, H.A. (1988). General bathymetry of the Gulf of Carpentaria and the Quaternary physiography of Lake Carpentaria. *Palaeogeography, Palaeoclimatology, Palaeoecology*, 41, 207-225.
- Tucker, M.J. and Pitt, E.G., 2001. *Waves in Ocean Engineering*. Elsevier Ocean Engineering Book Series, 5. Elsevier, 521 pp.
- Wassenberg, T. J., Salini, J. P., Heatwole, H., Kerr, J. D. 1994. Incidental capture of sea snakes (Hydrophidae) by prawn trawlers in the Gulf of Carpentaria, Australia. *Australian Journal of Marine and Freshwater Research*, 45: 429-43.
- Xu, Z. (2002) *Ellipse Parameters Conversion and Velocity Profiles for Tidal Currents in Matlab*. Maurice-Lamontagne Institute, Ocean Science Division, Fisheries and Ocean Canada. 24pp.
- Yalin, M.S. (1963) An expression for bedload transportation. *Journal of Hydraulics Division, Proceedings ASCE* 90 (HY5), 105-119.

Appendix 1. Scientific Party

1. Dr. Peter Harris (GA)	Cruise Leader
2. Dr Andrew Heap (GA)	Co-Cruise Leader
3. Dr. Mark Hemer (GA)	Oceanography
4. Mr. David Brewer (CSIRO)	Biological sampling
5. Mr Don Heales (CSIRO)	Biological sampling
6. Mr James Daniell (GA)	Computer support; swath bathymetry
7. Ms. Alison Hancock (GA)	Technician (sediment sampling, database)
8. Mr Cameron Buchanan (GA)	Computer support; swath bathymetry
9. Mr John Stratton (GA)	Technician (sediment sampling, drill operation)
10. Mr Andrew Hislop (GA)	Technician (sediment sampling, drill operation)
11. Mr Craig Wintle (GA)	Technician (sediment sampling, drill operation)
12. Mr. Jack Pittar (GA)	Electronics Technician
13. Mr. David Holdway (GA)	Electronics Technician
14. Mr. H. Kippo (CSIRO)	Computer Technician
15. Mr. Stephen Thomas (CSIRO)	Electronics Technician

Crew

16. Ian Taylor	Master
17. Samantha Durnian	1 st Mate
18. Rob Ferries	2 nd Mate
19. John Morton	Chief Engineer
20. S. Mason	1 st Engineer
21. C. Heap	2 nd Engineer
22. Mal McDougall	Bosun
23. P. Chamberlaine	IR
24. Graham McDougall	IR
25. P. French	IR
26. M. McRae	IR
27. P. Wainwright	Chief Cook
28. Angie Zutt	2 nd Cook
29. C. Aylett	Steward

Appendix 2. List of stations and activities completed on Survey 276.

StationNo	SampleName	SampleType	Start latdeg	Start latMin	Start longdeg	Start longMin	Start Water Depth
01	276/01CAM01	CAMERA	-15	17.72	140	19.47	26.80
01	276/01CAM02	CAMERA	-15	17.772	140	19.504	26.40
01	276/01CTD01	CTD	-15	17.72	140	19.47	26.80
01	276/01DR01	DREDGE CHAINBAG	-15	17.73	140	19.503	26.40
01	276/01GR01	GRAB SMITH MCINTYRE	-15	17.74	140	19.475	26.80
01	276/01RD01	CORE ROTARY DRILL	-15	17.74	140	19.475	26.80
02	276/02CAM03	CAMERA	-15	16.501	140	20.152	26.40
02	276/02CAM04	CAMERA	-15	16.516	140	20.122	26.40
02	276/02CTD02	CTD	-15	16.491	140	20.129	26.80
02	276/02DR02	DREDGE CHAINBAG	-15	16.47	140	20.102	26.40
02	276/02GR02	GRAB SMITH MCINTYRE	-15	16.506	140	20.136	26.80
02	276/02RD02	CORE ROTARY DRILL	-15	16.522	140	20.143	26.40
03	276/03CAM05	CAMERA	-15	15.143	140	18.495	30.80
03	276/03CAM06	CAMERA	-15	15.157	140	18.527	31.20
03	276/03CTD03	CTD	-15	15.149	140	18.5	30.40
03	276/03DR03	DREDGE CHAINBAG	-15	15.187	140	18.493	31.20
03	276/03GR03	GRAB SMITH MCINTYRE	-15	15.144	140	18.501	30.40
03	276/03RD03	CORE ROTARY DRILL	-15	15.146	140	18.484	30.80
04	276/04CAM07	CAMERA	-15	19.507	140	18.687	26.00
04	276/04CTD04	CTD	-15	19.481	140	18.676	26.00
04	276/04DR04	DREDGE CHAINBAG	-15	19.59	140	18.643	26.00
04	276/04GR04	GRAB SMITH MCINTYRE	-15	19.487	140	18.475	26.00
05	276/05CAM08	CAMERA	-15	19.28	140	17.471	26.40
05	276/05CTD05	CTD	-15	19.291	140	17.446	26.40
05	276/05GR05	GRAB SMITH MCINTYRE	-15	19.289	140	17.45	26.40
05	276/05GR06	GRAB SMITH MCINTYRE	-15	19.253	140	17.428	26.40
06	276/06CAM09	CAMERA	-15	19.836	140	18.282	26.40
06	276/06CTD06	CTD	-15	19.86	140	18.27	26.40
06	276/06DR05	DREDGE CHAINBAG	-15	19.74	140	18.192	26.40
06	276/06GR07	GRAB SMITH MCINTYRE	-15	19.849	140	18.279	26.40

StationNo	SampleName	SampleType	Start latdeg	Start latMin	Start longdeg	Start longMin	Start Water Depth
07	276/07CAM10	CAMERA	-15	18.012	140	21.522	27.20
07	276/07CTD07	CTD	-15	18.01	140	21.532	27.60
07	276/07DR06	DREDGE CHAINBAG	-15	18.013	140	21.509	27.20
07	276/07GR08	GRAB SMITH MCINTYRE	-15	18.007	140	21.523	27.60
07	276/07GR09	GRAB SMITH MCINTYRE	-15	18.005	140	21.516	27.20
08	276/08CAM11	CAMERA	-15	18.992	140	21.108	27.60
08	276/08CTD08	CTD	-15	19.157	140	21.144	28.40
08	276/08DR07	DREDGE CHAINBAG	-15	19.029	140	21.105	28.40
08	276/08GR10	GRAB SMITH MCINTYRE	-15	19.007	140	21.011	27.60
09	276/09CAM12	CAMERA	-15	19.001	140	19.496	27.20
09	276/09CTD09	CTD	-15	18.987	140	19.466	27.20
09	276/09DR08	DREDGE CHAINBAG	-15	18.989	140	19.475	27.20
09	276/09GR11	GRAB SMITH MCINTYRE	-15	18.988	140	19.479	27.20
09	276/09GR12	GRAB SMITH MCINTYRE	-15	18.994	140	19.494	27.20
10	276/10RD04	CORE ROTARY DRILL	-15	19.247	140	17.45	26.40
11	276/11RD05	CORE ROTARY DRILL	-15	19.365	140	18.572	23.20
11	276/11RD06	CORE ROTARY DRILL	-15	19.332	140	18.604	23.20
12	276/12RD07	CORE ROTARY DRILL	-15	19.758	140	18.231	26.40
13	276/13CAM13	CAMERA	-15	26.347	140	9.976	29.20
13	276/13CAM14	CAMERA	-15	26.341	140	9.974	29.20
13	276/13CTD10	CTD	-15	26.358	140	9.967	29.20
13	276/13DR09	DREDGE CHAINBAG	-15	26.433	140	9.757	29.20
13	276/13GR13	GRAB SMITH MCINTYRE	-15	26.358	140	9.967	29.20
13	276/13RD08	CORE ROTARY DRILL	-15	26.358	140	9.967	29.20
14	276/14CAM15	CAMERA	-15	26.86	140	10.185	26.40
14	276/14CAM16	CAMERA	-15	26.87	140	10.191	26.40
14	276/14CTD11	CTD	-15	26.863	140	10.168	26.40
14	276/14DR10	DREDGE CHAINBAG	-15	27.127	140	10.229	26.40
14	276/14GR14	GRAB SMITH MCINTYRE	-15	26.863	140	10.189	26.40
14	276/14RD09	CORE ROTARY DRILL	-15	26.874	140	10.185	26.40
15	276/15CAM17	CAMERA	-15	30.864	140	6.627	30.40
15	276/15CAM18	CAMERA	-15	30.859	140	6.658	30.40
15	276/15CTD12	CTD	-15	30.879	140	6.63	30.40

StationNo	SampleName	SampleType	Start latdeg	Start latMin	Start longdeg	Start longMin	Start Water Depth
15	276/15DR11	DREDGE CHAINBAG	-15	30.854	140	6.61	32.80
15	276/15GR15	GRAB SMITH MCINTYRE	-15	30.879	140	6.629	30.80
15	276/15RD10	CORE ROTARY DRILL	-15	30.879	140	6.629	30.80
15	276/15RD11	CORE ROTARY DRILL	-15	30.879	140	6.629	30.40
16	276/16CAM19	CAMERA	-15	31.387	140	6.842	20.60
16	276/16CTD13	CTD	-15	31.401	140	6.846	20.80
16	276/16GR16	GRAB SMITH MCINTYRE	-15	31.401	140	6.846	20.20
16	276/16RD12	CORE ROTARY DRILL	-15	31.401	140	6.846	20.20
17	276/17CAM20	CAMERA	-16	30.132	139	53.659	27.60
17	276/17CTD14	CTD	-16	30.164	139	53.662	27.60
17	276/17DR12	DREDGE CHAINBAG	-16	30.021	139	53.614	28.80
17	276/17GR17	GRAB SMITH MCINTYRE	-16	30.163	139	53.663	27.60
17	276/17RD13	CORE ROTARY DRILL	-16	30.163	139	53.663	27.60
18	276/18CM01	CURRENT METER	-16	5.748	139	2.374	41.20
19	276/19CM02	CURRENT METER	-15	41.992	138	51.947	26.00
20	276/20CM03	CURRENT METER	-16	5.7	139	2.4	41.20
20	276/20CTD15	CTD	-16	5.7	139	2.4	41.20
21	276/21CAM21	CAMERA	-16	2.188	139	8.064	44.80
21	276/21CM04	CURRENT METER	-16	2.213	139	8.031	44.80
21	276/21CTD16	CTD	-16	2.222	139	8.022	44.80
21	276/21GR18	GRAB SMITH MCINTYRE	-16	2.221	139	8.021	44.80
22	276/22CAM22	CAMERA	-16	0.008	139	5.812	23.60
22	276/22CTD17	CTD	-16	0.055	139	5.799	23.60
22	276/22DR13	DREDGE CHAINBAG	-15	59.73	139	5.543	22.00
22	276/22GR19	GRAB SMITH MCINTYRE	-16	0.053	139	5.798	23.60
22	276/22RD14	CORE ROTARY DRILL	-16	0.053	139	5.799	23.60
23	276/23CAM25	CAMERA	-15	59.631	139	5.579	22.00
23	276/23CTD18	CTD	-15	59.653	139	5.495	22.00
23	276/23DR14	DREDGE CHAINBAG	-15	59.56	139	5.63	21.20
23	276/23GR20	GRAB SMITH MCINTYRE	-15	59.654	139	5.495	22.00
23	276/23RD15	CORE ROTARY DRILL	-15	59.653	139	5.495	22.00
24	276/24CAM24	CAMERA	-15	58.777	139	6.481	19.60
24	276/24CTD19	CTD	-15	58.777	139	6.496	20.40

StationNo	SampleName	SampleType	Start latdeg	Start latMin	Start longdeg	Start longMin	Start Water Depth
24	276/24GR21	GRAB SMITH MCINTYRE	-15	58.777	139	6.496	20.40
24	276/24RD16	CORE ROTARY DRILL	-15	58.777	139	6.496	19.60
25	276/25CAM25	CAMERA	-15	59.289	139	5.102	23.60
25	276/25CTD20	CTD	-15	59.241	139	5.067	23.60
25	276/25DR15	DREDGE CHAINBAG	-15	59.299	139	5.161	23.60
25	276/25GR22	GRAB SMITH MCINTYRE	-15	59.292	139	5.114	23.60
25	276/25RD17	CORE ROTARY DRILL	-15	59.299	139	5.093	23.60
26	276/26CAM26	CAMERA	-16	1.008	139	7.425	25.60
26	276/26CTD21	CTD	-16	1.004	139	7.413	26.00
26	276/26DR16	DREDGE CHAINBAG	-16	0.885	139	7.367	26.80
26	276/26GR23	GRAB SMITH MCINTYRE	-16	1.009	139	7.423	26.00
26	276/26RD18	CORE ROTARY DRILL	-16	1.002	139	7.44	25.60
27	276/27CAM27	CAMERA	-16	0.515	139	7.447	25.20
27	276/27CTD22	CTD	-16	0.518	139	7.446	25.20
27	276/27DR17	DREDGE CHAINBAG	-16	0.375	139	7.505	26.00
27	276/27GR24	GRAB SMITH MCINTYRE	-16	0.058	139	7.447	25.20
27	276/27RD19	CORE ROTARY DRILL	-16	0.518	139	7.447	25.20
28	276/28CAM28	CAMERA	-15	57.81	139	8.44	29.60
28	276/28CTD23	CTD	-15	57.799	139	8.102	29.60
28	276/28DR18	DREDGE CHAINBAG	-15	57.936	139	8.332	29.60
28	276/28GR25	GRAB SMITH MCINTYRE	-15	57.801	139	8.101	29.60
28	276/28RD20	CORE ROTARY DRILL	-15	57.8	139	8.101	29.60
29	276/29CAM29	CAMERA	-16	3.04	139	1.867	18.40
29	276/29CTD24	CTD	-16	3.034	139	1.884	16.80
29	276/29DR19	DREDGE CHAINBAG	-16	3.081	139	1.86	17.20
29	276/29GR26	GRAB SMITH MCINTYRE	-16	3.061	139	1.949	16.80
29	276/29RD21	CORE ROTARY DRILL	-16	3.037	139	1.883	18.40
30	276/30CAM30	CAMERA	-16	3.28	139	1.444	20.00
30	276/30CTD25	CTD	-16	3.273	139	1.433	20.00
30	276/30DR20	DREDGE CHAINBAG	-16	3.577	139	1.424	24.00
30	276/30GR27	GRAB SMITH MCINTYRE	-16	3.282	139	1.431	20.00
30	276/30RD22	CORE ROTARY DRILL	-16	3.28	139	1.458	20.00
31	276/31CTD26	CTD	-16	4.022	139	1.88	27.20

StationNo	SampleName	SampleType	Start latdeg	Start latMin	Start longdeg	Start longMin	Start Water Depth
31	276/31GR28	GRAB SMITH MCINTYRE	-16	4.027	139	4.027	27.30
31	276/31RD23	CORE ROTARY DRILL	-16	4.027	139	4.027	27.20
32	276/32CAM31	CAMERA	-16	2.89	139	3.092	26.40
32	276/32CTD27	CTD	-16	2.855	139	3.044	26.40
32	276/32DR21	DREDGE CHAINBAG	-16	2.896	139	3.199	26.40
32	276/32GR29	GRAB SMITH MCINTYRE	-16	2.885	139	3.094	26.40
32	276/32RD24	CORE ROTARY DRILL	-16	2.897	139	3.102	26.40
33	276/33CAM32	CAMERA	-15	57.106	139	10.141	38.00
33	276/33CTD28	CTD	-15	57.052	139	10.094	37.60
33	276/33DR22	DREDGE CHAINBAG	-15	56.126	139	10.154	38.00
33	276/33GR30	GRAB SMITH MCINTYRE	-15	57.052	139	10.082	37.60
33	276/33RD25	CORE ROTARY DRILL	-15	57.085	139	10.112	38.00
34	276/34CAM33	CAMERA	-15	28.107	137	55.109	18.20
34	276/34CTD29	CTD	-15	28.067	137	55.106	19.60
34	276/34GR31	GRAB SMITH MCINTYRE	-15	28.105	137	55.123	19.20
34	276/34RD26	CORE ROTARY DRILL	-15	28.105	137	55.123	19.20
35	276/35CAM34	CAMERA	-15	27.786	137	55.509	24.00
35	276/35CTD30	CTD	-15	27.798	137	55.495	23.20
35	276/35GR32	GRAB SMITH MCINTYRE	-15	27.777	137	55.521	23.20
36	276/36CAM35	CAMERA	-15	27.467	137	55.72	25.20
36	276/36CTD31	CTD	-15	27.461	137	55.698	25.60
37	276/37CAM36	CAMERA	-15	27.32	137	55.833	22.40
37	276/37CTD32	CTD	-15	27.315	137	55.84	22.40
37	276/37GR33	GRAB SMITH MCINTYRE	-15	27.315	137	55.84	22.40
38	276/38CAM37	CAMERA	-15	27.074	137	55.601	23.20
38	276/38CTD33	CTD	-15	27.066	137	55.603	26.40
38	276/38GR34	GRAB SMITH MCINTYRE	-15	27.067	137	55.597	26.40
39	276/39CAM38	CAMERA	-15	27.365	137	55.117	28.80
39	276/39CTD34	CTD	-15	27.37	137	27.37	28.80
39	276/39GR35	GRAB SMITH MCINTYRE	-15	27.37	137	55.132	28.80
40	276/40CAM39	CAMERA	-15	27.817	137	55.523	23.60
41	276/41CAM40	CAMERA	-15	27.852	137	55.373	23.60
42	276/42CAM41	CAMERA	-15	27.757	137	54.92	29.60

StationNo	SampleName	SampleType	Start latdeg	Start latMin	Start longdeg	Start longMin	Start Water Depth
43	276/43DR23	DREDGE CHAINBAG	-15	27.76	137	54.891	28.00
43	276/43DR24	DREDGE CHAINBAG	-15	27.303	137	55.13	28.00
43	276/43RD27	CORE ROTARY DRILL	-15	27.77	137	54.885	29.60
44	276/44CAM42	CAMERA	-15	29.507	137	37.093	16.00
44	276/44CTD35	CTD	-15	29.489	137	37.115	15.60
44	276/44DR25	DREDGE CHAINBAG	-15	26.667	137	37.947	16.00
44	276/44GR36	GRAB SMITH MCINTYRE	-15	29.489	137	37.115	15.60
45	276/45CAM43	CAMERA	-15	29.372	137	37.854	29.20
45	276/45CTD36	CTD	-15	29.358	137	37.863	28.80
45	276/45DR26	DREDGE CHAINBAG	-15	29.365	137	37.743	29.20
45	276/45GR37	GRAB SMITH MCINTYRE	-15	29.358	137	37.863	28.80
45	276/45RD28	CORE ROTARY DRILL	-15	29.36	137	37.885	29.20
46	276/46CAM44	CAMERA	-15	28.303	137	38.21	31.60
46	276/46CTD37	CTD	-15	28.321	137	38.214	31.60
46	276/46DR27	DREDGE CHAINBAG	-15	28.297	137	38.208	31.60
46	276/46GR38	GRAB SMITH MCINTYRE	-15	28.312	137	38.19	31.60
46	276/46RD29	CORE ROTARY DRILL	-15	28.303	137	38.234	31.60
47	276/47CAM45	CAMERA	-15	28.501	137	37.616	33.60
47	276/47CTD38	CTD	-15	28.518	137	37.646	33.60
47	276/47GR39	GRAB SMITH MCINTYRE	-15	28.52	137	37.647	33.60
48	276/48CAM46	CAMERA	-15	28.781	137	38.7	41.60
48	276/48CTD39	CTD	-15	28.821	137	38.709	41.60
48	276/48DR28	DREDGE CHAINBAG	-15	28.639	137	38.415	31.00
48	276/48GR40	GRAB SMITH MCINTYRE	-15	28.818	137	38.712	41.60
49	276/49CAM47	CAMERA	-15	29.134	137	37.224	24.00
49	276/49CTD40	CTD	-15	29.157	137	37.378	24.40
49	276/49DR29	DREDGE CHAINBAG	-15	29.159	137	37.387	25.60
49	276/49GR41	GRAB SMITH MCINTYRE	-15	29.169	137	37.361	24.00
49	276/49RD30	CORE ROTARY DRILL	-15	29.139	137	37.416	25.60
50	276/50CAM48	CAMERA	-15	43.429	138	82.767	18.00
50	276/50CTD41	CTD	-15	43.405	138	52.755	18.00
50	276/50DR30	DREDGE CHAINBAG	-15	43.56	138	52.903	18.00
50	276/50GR42	GRAB SMITH MCINTYRE	-15	43.425	138	52.762	18.00

StationNo	SampleName	SampleType	Start latdeg	Start latMin	Start longdeg	Start longMin	Start Water Depth
50	276/50RD31	CORE ROTARY DRILL	-15	43.408	138	52.722	19.20
51	276/51CAM49	CAMERA	-15	43.242	138	53.16	17.60
51	276/51CTD42	CTD	-15	43.273	138	53.091	17.20
51	276/51DR31	DREDGE CHAINBAG	-15	43.249	138	53.224	17.60
51	276/51GR43	GRAB SMITH MCINTYRE	-15	43.264	138	53.089	17.20
52	276/52CAM50	CAMERA	-15	43.3	138	53.071	16.40
52	276/52RD32	CORE ROTARY DRILL	-15	43.312	138	53.037	16.40
53	276/53CAM51	CAMERA	-15	41.937	138	53.952	24.80
53	276/53CTD43	CTD	-15	41.925	138	53.958	25.20
53	276/53DR32	DREDGE CHAINBAG	-15	41.869	138	54.064	24.80
53	276/53GR44	GRAB SMITH MCINTYRE	-15	41.925	138	53.958	25.20
53	276/53RD33	CORE ROTARY DRILL	-15	41.929	138	53.953	25.20
54	276/54CAM52	CAMERA	-16	5.842	139	2.318	41.60
54	276/54CM05	CURRENT METER	-16	5.731	139	2.429	42.00
54	276/54CTD44	CTD	-16	5.81	139	2.361	41.60
54	276/54GR45	GRAB SMITH MCINTYRE	-16	5.828	139	2.349	41.60
55	276/55CM06	CURRENT METER	-16	2.235	139	8.052	45.20
55	276/55CTD45	CTD	-16	2.332	139	8.222	39.00
56	276/56CAM53	CAMERA	-15	41.318	138	54.391	27.60
56	276/56CTD46	CTD	-15	41.302	138	54.391	27.60
56	276/56DR33	DREDGE CHAINBAG	-15	41.226	138	54.235	30.00
56	276/56GR46	GRAB SMITH MCINTYRE	-15	41.302	138	54.392	27.60
56	276/56GR47	GRAB SMITH MCINTYRE	-15	41.302	138	54.391	27.60
57	276/57CAM54	CAMERA	-15	40.924	138	54.903	44.00
57	276/57CTD47	CTD	-15	40.962	138	54.901	44.00
57	276/57DR34	DREDGE CHAINBAG	-15	40.767	138	54.972	44.00
57	276/57GR48	GRAB SMITH MCINTYRE	-15	40.954	138	54.907	44.00
57	276/57RD34	CORE ROTARY DRILL	-15	40.952	138	54.923	44.00
58	276/58CAM55	CAMERA	-15	39.806	138	53.707	22.00
58	276/58CTD48	CTD	-15	39.801	138	53.73	22.00
58	276/58DR35	DREDGE CHAINBAG	-15	39.854	138	53.674	22.00
58	276/58GR49	GRAB SMITH MCINTYRE	-15	39.836	138	53.691	22.00
58	276/58RD35	CORE ROTARY DRILL	-15	39.836	138	53.679	30.40

StationNo	SampleName	SampleType	Start latdeg	Start latMin	Start longdeg	Start longMin	Start Water Depth
59	276/59CAM56	CAMERA	-15	39.993	138	52.725	24.40
59	276/59CTD49	CTD	-15	39.994	138	52.918	26.80
59	276/59DR36	DREDGE CHAINBAG	-15	40.087	138	52.705	24.40
59	276/59GR50	GRAB SMITH MCINTYRE	-15	39.996	138	52.906	26.80
59	276/59RD36	CORE ROTARY DRILL	-15	40.017	138	52.829	26.40
60	276/60CAM57	CAMERA	-15	41.632	138	51.693	24.00
60	276/60CTD50	CTD	-15	41.631	138	51.674	24.00
60	276/60DR37	DREDGE CHAINBAG	-15	41.64	138	51.69	24.00
60	276/60GR51	GRAB SMITH MCINTYRE	-15	41.643	138	51.676	24.00
60	276/60RD37	CORE ROTARY DRILL	-15	41.645	138	51.665	24.80
61	276/61CAM58	CAMERA	-15	39.111	138	49.684	29.20
61	276/61CTD51	CTD	-15	39.082	138	49.693	29.20
61	276/61DR38	DREDGE CHAINBAG	-15	39.323	138	49.679	29.20
61	276/61GR52	GRAB SMITH MCINTYRE	-15	39.067	138	49.717	29.20
61	276/61RD38	CORE ROTARY DRILL	-15	39.088	138	49.729	29.20
62	276/62CAM59	CAMERA	-15	37.868	138	51.22	27.60
62	276/62CTD52	CTD	-15	37.897	138	51.216	28.00
62	276/62DR39	DREDGE CHAINBAG	-15	37.831	138	51.265	27.60
62	276/62GR53	GRAB SMITH MCINTYRE	-15	37.892	138	51.199	28.00
62	276/62RD39	CORE ROTARY DRILL	-15	37.803	138	51.237	27.60
63	276/63CAM60	CAMERA	-15	37.392	138	51.771	30.80
63	276/63CTD53	CTD	-15	37.185	138	51.805	30.80
63	276/63DR40	DREDGE CHAINBAG	-15	37.315	138	51.771	30.80
63	276/63GR54	GRAB SMITH MCINTYRE	-15	37.186	138	51.856	30.80
63	276/63RD40	CORE ROTARY DRILL	-15	37.14	138	51.815	30.80
64	276/64CAM61	CAMERA	-15	36.293	138	49.998	20.00
64	276/64CTD54	CTD	-15	36.284	138	50.041	20.80
64	276/64GR55	GRAB SMITH MCINTYRE	-15	36.297	138	50.012	20.80
65	276/65CAM62	CAMERA	-15	36.108	138	49.008	26.40
65	276/65CTD55	CTD	-15	36.133	138	49.019	26.40
65	276/65DR41	DREDGE CHAINBAG	-15	36.13	138	48.937	26.40
65	276/65GR56	GRAB SMITH MCINTYRE	-15	36.111	138	49.008	26.40
65	276/65RD41	CORE ROTARY DRILL	-15	36.119	138	49.031	26.00

StationNo	SampleName	SampleType	Start latdeg	Start latMin	Start longdeg	Start longMin	Start Water Depth
66	276/66CTD56	CTD	-15	33.15	138	46.93	59.20
66	276/66GR57	GRAB SMITH MCINTYRE	-15	33.199	138	46.936	59.20
67	276/67CAM63	CAMERA	-15	36.153	138	46.834	29.60
67	276/67CTD57	CTD	-15	36.126	138	46.885	29.60
67	276/67DR42	DREDGE CHAINBAG	-15	36.188	138	46.676	29.60
67	276/67GR58	GRAB SMITH MCINTYRE	-15	36.132	138	46.828	29.60
67	276/67RD42	CORE ROTARY DRILL	-15	36.117	138	46.949	29.60
68	276/68CAM64	CAMERA	-15	35.128	138	47.045	22.80
68	276/68CTD58	CTD	-15	35.021	138	47.112	22.80
68	276/68DR43	DREDGE CHAINBAG	-15	35.128	138	47.039	22.80
68	276/68GR59	GRAB SMITH MCINTYRE	-15	35.033	138	47.118	22.80
68	276/68RD43	CORE ROTARY DRILL	-15	35.009	138	47.119	24.00
69	276/69CAM65	CAMERA	-10	57.888	136	47.912	112.00
69	276/69CTD59	CTD	-10	57.914	136	47.923	112.00
69	276/69GR60	GRAB SMITH MCINTYRE	-10	57.915	136	47.923	112.00
70	276/70CTD60	CTD	-11	12.435	134	44.423	42.00
70	276/70GR61	GRAB SMITH MCINTYRE	-11	12.43	134	44.438	42.00
71	276/71CAM66	CAMERA	-11	13.41	134	44.582	18.80
71	276/71GR62	GRAB SMITH MCINTYRE	-11	13.436	134	44.553	18.80
72	276/72CAM67	CAMERA	-11	13.952	134	44.522	22.00
72	276/72GR63	GRAB SMITH MCINTYRE	-11	13.896	134	44.564	22.00

Appendix 3. Voyage Narrative

22-3-05 Tuesday. Loading and stowage of scientific equipment was completed @1700. The new drill rig was assembled and a trial-test run carried out along side the jetty. The drill penetrated about 1.5 m into hard-packed clay. The drill-core sample was retained. The Reson swath mapping equipment was installed and made ready for testing at sea.

23-3-05 Wednesday. *Southern Surveyor* sailed from Weipa @ 1000 hrs to conduct a patch test using the Reson 8101. Had to leave one member of the science party (Andrew Hislop) ashore because the ship is only allowed to carry 29 persons at sea. The patch test was completed @1530 hrs and the boat called from shore to take off the Reson technician and return Mr. Hislop. However, @1545 hrs the Reson system unexpectedly shut-down and could not be restarted. The ship anchored @ 2000 hrs and repair work was attempted all night by the Reson Technician but to no avail – he had not brought any spares from Singapore. An outline of the survey plan was presented @1800 hrs by the Chief Scientist to the ships crew and science party.

24-3-05 Thursday. The Reson technician was put ashore @ 0630 and the ship was underway by 0700. The Scientific party were taken on a tour of the ship by the first mate Samantha Durnian and a fire/lifeboat drill was conducted @1030 hrs. Transit to first sample stations arriving @2230 hrs. It has been agreed that Reson will send another technician, this time with spares, to attempt to repair the 8101 system on board. We will pick him up from Mornington Island. There is no replacement Reson unit available to the company in Singapore. If the repairs are not successful, the science plan will have to be altered to focus more on deep-water areas where the ship's EM-300 system will be effective.

25-3-05 Good Friday. The first drill core was recovered @0015 on reef R1, 2.3 m long, comprised of reefal limestone. This core confirms our hypothesis that the reef structure is indeed comprised of coral and associated reef material. Two further drill-cores were collected, but at Station 3 the ship was blown off station by a gust of wind. The drill was recovered but with some damage sustained. Electric wires had to be replaced and some mechanical parts rebuilt. Station work continued through the day collecting CTD, grab, camera and dredge samples while the drill was being repaired. Station 9 was completed @2230 hrs by which time the drill repairs were nearly completed.

26-3-05 Saturday. Stations 10 to 16 were completed, with 8 successful rotary drill cores collected. Drill core lengths ranged from 17 cm to 206 cm and confirm that the reef rims are comprised of coral

framework material. The drill has performed very well and it has proved to be moderately easy to deploy and operate. There was a minor incident when Craig Wintle cut his hand on the sharp metal edge of a control panel. One negative issue associated with *Southern Surveyor* is that the stench of sewage is episodically pumped through the ship via the air conditioning system, and is also encountered frequently while working on deck. It is most unpleasant and I am concerned that there may be health risks associated with it, the least of which is increasing the likelihood of seasickness in some people. The sewage situation has not improved since my last voyage on *Southern Surveyor* in 2003, when the entire forward hold (Green Room) was flooded with raw sewage on one occasion.

27-3-05 Easter Sunday. Station 17 was completed @ 0700 hrs, on the surface of a Karst limestone bank located in the tidal channel east of Mornington Island. The drill core penetrated 3 m, but only a 50 cm core was obtained, comprised of compact clay with Caliche nodules. The drill core catcher seems to be unable to retain non-lithified material, even hard clay. Another safety incident occurred when the main winch was being used to raise the drill tower – it surged in causing a wire to part and a heavy metal sheave fell to the deck from the A-frame. Luckily no one was injured. As a result the drill tower will henceforth be raised using the main ships wire and movement using the A-frame to raise-lower the tower. Transit to recover the ADCP mooring, completed @ 1100 hrs; BRUCE was recovered @ 1330 hrs. A regional survey was commenced along zig-zag lines that crossed the shallow bank top, to seek the best place to commence swath mapping, and to test the overall performance of the EM-300 system. The EM-300 has been found to give acceptable results in shallow water depths of around 20 to 30 m, albeit with a narrower swath width and coarser resolution than would be expected from the Reson 8101. The sub-bottom profiler is giving excellent results, and has been providing detailed sub-seafloor images to 30 ms depth, of fluvial cut/fill processes as well as some images of faulted and folded units that crop-out at the seabed. One issue is that there is no hard-copy printer that generates a paper trace with time-stamps (the printer we have does not add time stamps). A hard copy record with time stamps is needed for station selection and interpretation and I recommend we purchase an EPS recorder that does this job.

28-3-05 Easter Monday. Swath mapping of a channel and platform/barrier margin proceeded using the EM-300. Water depths are from 45 to 17 m and 20 lines, each 20 km in length, were completed by 2400 hrs. The ADCP and BRUCE instrument frames were re-deployed, the ADCP in its original location and the BRUCE frame located in the deepest section of the valley, in about 44 m water depth. On interrogation, the ADCP was found to have recorded data but the lead weight was not installed on its gimbaled mounting, which seems to have caused a few minor artifacts in the data. In the BRUCE package the Nortek CM seems to have recorded data, along with the OBS sensors, but the LISST and

Seacat CTD sensors failed to record any data. The LISST laser particle size analyzer is suspect and it was not included on the frame when BRUCE was redeployed.

29-3-05 Tuesday. Guido the Reson Technician was received aboard @0730 and Jon Stratton went ashore; one of the science party had to go ashore because the ship is only allowed to carry 29 persons at sea. Guido will spend 24 hrs on board and attempt to repair the 8101 system. Swath mapping during the night has revealed more of the submerged platform feature which exhibits spur and groove, parallel ridges and abundant erosion features. The platform is looking more like a heavily eroded submerged barrier reef, but further swath mapping and sampling will be required to reveal its true identity.

30-3-05 Wednesday. Swath mapping of Area A continues. Both the EM-300 and Reson systems are now fully functional and we are starting to make comparisons in the quality of data generated by the two machines. The nature and origin of the platform is still ambiguous. There are elongate ridges, spur and groove platform margins and Karst doline features, but the overall appearance is one of widespread erosion and the features all appear rounded and muted, in comparison with the 3 platform reefs. This may be due to the closer proximity of land and therefore the greater influence of fluvial processes.

31-3-05 Thursday. Swath mapping of Area A completed @ 1030 hrs. Heap and Harris selected 12 stations in Area A based on geomorphology and seismic characteristics, targeting rocky-reef type features, Karst features, rim features and the highest peaks of mound-shaped features. Drilling completed at the five locations by 2400 hrs.

1-4-05 Friday. Drilling at 12 locations has proven the elevated portions of the platforms are calcareous and of coral reef origin. Cores have penetrated 3m but maximum recovery has been only up to about 1.5 m; this is attributed to gravel and unconsolidated material falling out of the drill core during pull-out. The new system of raising and lowering the drill tower using the A-frame is working safely. The cores recovered so far have included an upper lithified limestone unit about 30 to 50 cm thick, which overlies an unconsolidated gravel comprised of reefal carbonate material. In some cores two lithified units and two rubble units or compact clayey limestone units have been encountered. Work was stopped @1430 hrs to take the 2nd cook to Mornington Island (5 hrs 30 mins return trip); she is going home due to a death in the family.

2-4-05 Saturday. Station work was completed @ 0200 hrs and transit to Area C, a small bathymetric mound 60 miles west of Mornington Island. The ship was again subjected to inundation by strong sewage stench between 0230 and 0400 hrs that caused the operations room to be evacuated. People reported feeling nauseous and had headache, sinus and eye irritation. People who were off-watch were woken up by the smell. The ship has no equipment installed to determine the gas's composition and it is a potential health risk. I have written a letter of complaint to Capt. Fred Stein. Arrived at the bathymetric mound and commenced swath mapping @0900 hrs. The mound (R4) exhibits the same patch reef geomorphology as the other three patch reefs we have mapped. Swath mapping completed by 2230 hrs and commenced sampling @ 2300.

3-4-05 Sunday. At the first sampling station on Reef R4 the drill was damaged during recovery. Nevertheless a 1.2 m core was obtained at this site comprised of coral. Six stations were occupied without the drill until it was repaired @1000 hrs. The underwater video revealed the reef is host to the most dense and diverse coral cover we have seen in the Gulf to date. Staghorn, brain and plate corals are present. Another drill was obtained @1200 hrs, penetrated around 1 m into limestone comprised of coral and associated reef fauna. Three attempts to dredge the reef top resulted in a small sample being obtained and the ship departed for Area D, arriving @1400 hrs. Swath mapping of this small bathymetric mound located 60 miles northeast of the Edward Pellew group of islands, again revealed it to exhibit the same patch reef geomorphology as the other reefs previously mapped. Harris and Heap selected six stations based on the swath image for sampling.

4-4-05 Monday. Swath mapping of Area D was completed @0300 hrs and sampling began at six stations using CTD, grab and camera. Drill cores from three locations encountered limestone comprised of coral and other reef fauna. Transit to Area B, arriving @ 2330 hrs and began swath mapping. Sewage smell incidents continue to occur.

5-4-05 Tuesday. Swath mapping of Area B continues. Wind speed up to 18 knots today and some choppy seas but mostly calm weather.

6-4-05 Wednesday. Swath mapping of Area B continues. At 2330 hrs a terrible pungent sewage smell was emitted from the toilet outside of the Operations Room. One sailor (G. McDougal) was overcome by the gas causing him to gag. The Operations Room was evacuated. The gas seemed to have entered one single toilet, bubbling up through the bowl. The toilet door was sealed and the gas eventually dispersed. Staff were able to reenter the Operations Room @2400 hrs to resume work. I told the staff that if any of them felt unable to continue working under these conditions I will cancel

the rest of the survey and request the Captain to head for the nearest port. We have only 3 full work days remaining until we are scheduled to depart for Darwin.

7-4-05 Thursday Swath mapping of Area B was completed @1700 hrs. The sparker system was deployed to run 3 lines over the reef front, normal to isobaths, but the results were not very informative. The ship speed was kept at 5 knots and the seas were calm, and we attribute the lack of penetration to the properties of the rocks and sediments. No significant sub-surface reflectors were seen in the data. Station work commenced @2230 hrs.

8-4-05 Friday Three stations were completed by 0645 hrs, including 3 drill cores. The longest drill core of the 3 was 1.95 m at station 51. The seabed is rocky-reef with some corals, but not overly abundant. No “coral gardens”. The ship transited to Man O’War Island where we picked up a gas detector unit @0945 hrs to measure the gas content in the sewage smell. To minimize the disruption of this diversion to our program, I have decided to collect the current meters today (1 day early) as we are passing nearby them. Arrived at the first (ADCP) mooring @ 1130 hrs and completed recovery of BRUCE @1430 hrs. Transit back to Area B arriving @ 1700 hrs and start sampling. A 1.5 m core taken from station 57 in 44 m water depth contained >1 m of lithified carbonate gravelly sand overlying compact clay.

9-4-05 Saturday. Alas the opposite shift has taken the record for the longest core – 2.5 m penetrated into limestone overlying siltstone. This information will be crucial to determining the basement composition of the platform. Station work progressed through the day, with station 67 (drill #42) completed @2400 hrs.

10-4-05 Sunday. Station 68 was completed @0330 hrs on a submerged reef-top in 20 m water depth and a short drill core obtained. This concluded the sampling work in Area B. Started transit to Darwin. At 0930 hrs I was advised by the Captain that an extra 16 hrs was available for work due to an error in his transit time estimate. Andrew Heap and I devised a program to map a >100 m deep incised valley north of the Wessel Islands and also to map a submerged reef in the Arafura Sea. Watches will continue until 12-4-05.

11-4-05 Monday Mapping of the “Wessel Deep” was completed @0700 hrs, with a CTD, grab and camera station completed at the centre of the deep in 107 m water depth. The water was turbid and the seabed composed of mobile coarse sand and gravel. Arrived at the position of a shallow sounding (Little Reef?) @1700 but 3 passes over the region of this chart sounding showed it to be a false depth.

Arrived at the “Big Reef” location @1900 hrs and commenced swath mapping. The feature is indeed a submerged reef, but its western half is draped by a thick sediment blanket, that streams away to the WNW. Mapping continued through the night.

12-4-05 Tuesday. Completed 3 grabs, 1 CTD and 2 camera operations at the “Big Reef” site. The reef supports some live corals (*Turbinaria*) and abundant fish, but turbid water restricted visibility. Work was completed by 0650 and we resumed our transit to Darwin.

13-4-05 Wednesday. Arrive Darwin. Gear unloading commenced @ 0900. Scientific party departed for airport @1100 hrs.

Appendices 4 to 8